Lawrence Berkeley National Laboratory
Recent Work

Title

BUNDLE SHEATH AND MESOPHYLL CHLOROPLASTS OP C4 PLANTS: AN IN SITU COMPARISON OF THEIR ROOM TEMPERATURE FLUORESCENCE

Permalink

https://escholarship.org/uc/item/7kz2s8p8

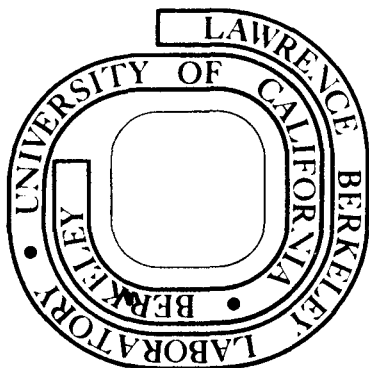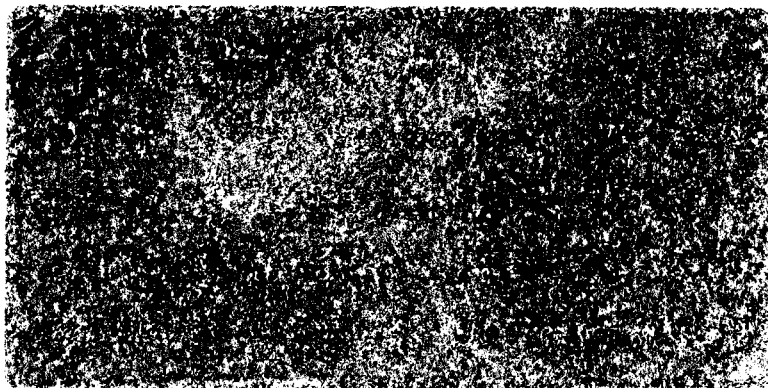**Author**

Elkin, Lynne.

Publication Date

1973-06-01

BUNDLE SHEATH AND MESOPHYLL CHLOROPLASTS OF C4 PLANTS: AN IN SITU COMPARISON OF THEIR ROOM TEMPERATURE FLUORESCENCE

Lynne Elkin
(Ph. D. thesis)

June 1973

DISCLAIMER

TO

E. L. E. and V. L. W.

Contents

Acknowledgments

I am grateful for the continued interest and support of Drs. Park and Laetsch throughout the experimental portion of this study, and to Dr. Sauer for his careful reading of the manuscript. I appreciated the advice and technical assistance of my husband, Berah McSwain, William Nolan, Albert Pfeifhofer and Vicki Whitman.

Bundle Sheath and Mesophyll Chloroplasts of C_4 Plants:
An _in situ_ Comparison of Their Room Temperature Fluorescence

Abstract   Lynne Elkin

High resolution studies of chloroplast fluorescence can
be performed _in situ_ with the aid of a fluorescence microscope
and infrared film. A technique is described for quantifying
this photographic data. Both the fluorescence yield and fluores-
cence spectra of C_4 chloroplasts are affected by the buffer
used and by the ionic composition of the isolating medium.

The fluorescence properties of agranal bundle sheath chloro-
plasts are strikingly different from those of mesophyll and other
chloroplasts. The ratio of fluorescence emission above 700 nm/
below 700 nm is approximately twice as great in bundle sheath
as in mesophyll chloroplasts. The fluorescence yield of bundle
sheath chloroplasts is approximately half that of mesophyll
chloroplasts.

The fluorescence patterns and ultrastructure of C_4 chloro-
plasts are correlated. Lamellar appression is associated with
an enrichment of the far-red component of fluorescence. Un-
appressed lamellae have a higher proportion of the infrared
component.

Tris treatment is used to eliminate the variable component of fluorescence. This variable component of chloroplast fluorescence is interpreted as evidence for a functional photosystem II in agranal bundle sheath chloroplasts. <u>Dichanthium annulatum</u> bundle sheath chloroplasts have a variable component of fluorescence equal to that of mesophyll chloroplasts. In both types of chloroplasts this variable fluorescence has a strong infrared component, in addition to the expected far-red component. The fluorescence emission spectra of untreated and Tris-treated <u>Dichanthium annulatum</u> chloroplasts are very similar.

February 7, 1973

ABBREVIATIONS

ATP   adenosine triphosphate

chl a   chlorophyll a

chl b   chlorophyll b

CMU   [3(p-chlorophenyl)-1,1-dimethylurea]

DCIP,   2,6-dichlorophenolindophenol
DCPIP

DCMU   [3,(3,4-dichlorophenyl)-1,1-dimethylurea]

DPC   1,5-diphenylcarbazide

EDTA   ethylenediaminetetraacetate

F 685,   fluorescence emission with peaks at designated
F 695,   wavelengths
F 735

F_o background fluorescence

F   steady state fluorescence

HA   hydroxylamine

HEPES   N-2-hydroxyethylpiperazine-N'-2-ethanesulfonic acid

k   1000 X gravity

ug   micrograms

um   micrometers

MES   [2-(N-morpholino) ethanesulfonic acid)]

nm   nanometer

$NADP(H_2)$ nicotinamide adenine dinucleotide phosphate,
               (reduced)

NBT	nitro-blue tetrazolium chloride
OD	optical density
PEP	Phosphoenolpyruvate
PMS	phenazine methosulphate
PS I	photosystem I
PS II	photosystem II
SDS	sodium dodecyl sulfate
TNBT	tetranitro-blue tetrazolium chloride
TRIS	tris (hydroxymethyl) amino-methane
TES	N-tris (hydroxymethyl)methyl-2-aminoethanesulfonic acid

I. Introduction

A. Preface

Tropical grass leaves characteristically possess parallel vascular bundles surrounded by large sheathing cells. In cross section these leaves display a row of vascular bundles, each with its own concentric ring of bundle sheath cells. The chloroplasts found in these bundle sheath cells are typically larger than those found in the adjacent mesophyll cells. This form of anatomy is characteristic of a group of plants known as C_4 plants because C_4 acids are their initial carbon dioxide fixation products.

Mesophyll and bundle sheath chloroplasts in sugar cane leaves appear to have similar chlorophyll concentrations when viewed under bright field microscopy. However, under fluorescence microscopy, only the mesophyll chloroplast fluorescence is detectable by the human eye. These bundle sheath chloroplasts have either a drastically reduced fluorescence yield, a predominance of fluorescence in the infrared region of the spectrum to which the human eye is relatively insensitive, or a combination of both. This thesis relates the altered fluorescence patterns of sugar cane bundle sheath chloroplasts, as well as those of other C_4 plants, with their structure and function.

B. Photosynthesis in Eucaryotic Cells

Photosynthesis is the biological process by which solar energy is converted into chemical energy. In green plants, the

process is often considered to consist of three parts; a two-reaction photochemical phase, an electron transport phase, and a carbohydrate synthesis phase. This thesis is primarily concerned with the first two phases.

The light reactions of photosynthesis commence with the absorption of light by a pigment molecule. Figure 1 presents the structure and absorption spectra of chlorophyll a and chlorophyll b, two important forms of the major pigment involved in the photochemistry of photosynthesis in eucaryotic cells. Both chlorophylls a and b are tetrapyrroles with a fifth carbon ring and a phytol chain. In chlorophyll b, a formyl group replaces the methyl group on ring 3 of chlorophyll a. Whereas chlorophyll a exists in all oxygen evolving photosynthetic plant cells, chlorophyll b is an additional pigment found in green algae and in all green land plants.

Chlorophyll a and chlorophyll b differ in their absorption spectra. In addition, the absorption spectra of chlorophyll molecules are slightly altered by a number of factors, the most important being the nature of the solvent, the state of aggregation of the molecules, and the specific interactions with lipid and protein molecules (44). Various _in vivo_ spectral species of chlorophyll a, e.g., chlorophyll a_{672} and chlorophyll a_{683}, are the same pigment molecule associated with different micro-environments. These species are designated by the wavelength of their respective red absorption maxima. One of these, P700,
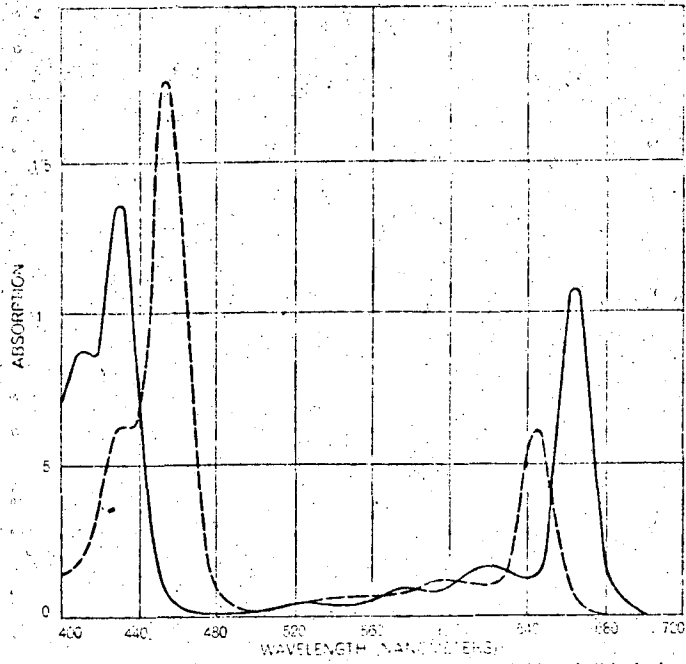
ABSORPTION SPECTRA show that chlorophyll *a* (*solid line*) and chlorophyll *b* (*broken line*) strongly absorb blue and far red light. The green, yellow and orange wavelengths lying between the peaks are reflected and give both pigments their familiar green color.
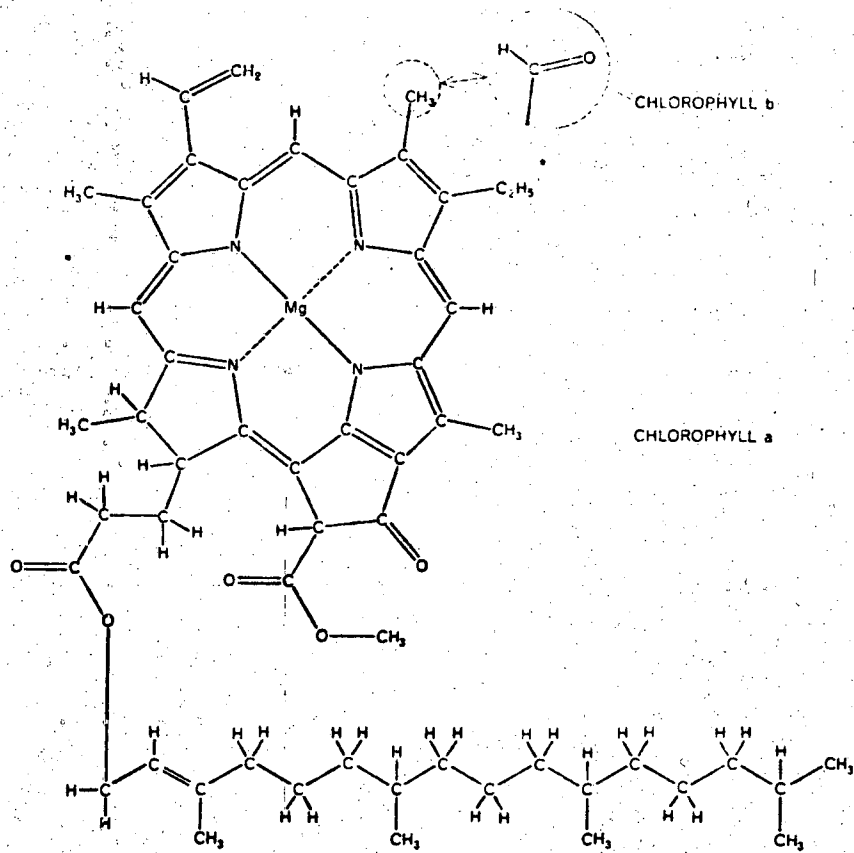
Fig. 1.   after Levine (178).

a special form of chlorophyll a absorbing maximally at 700 nm, appears to be the reaction center of light reaction I (164). It is found in unusually high concentrations in agranal bundle sheath chloroplasts of C_4 plants (191). Spinach stroma lamellae also have a high P700 content (241).

Isolated PS I contains a greater ratio of chlorophyll a molecules than isolated PS II (4). Consequently, the chlorophyll a/ chlorophyll b ratio is commonly used to indicate the relative proportions of PS I and PS II in any given membrane, in any given species, although this relationship is only established for fragments of chloroplasts from C_3 plants. C_4 plant chloroplasts may not conform to this pattern.

Chlorophyll a is the key photosynthetic pigment, and directly absorbs much of the light used to drive the photosynthetic reactions. _In vivo_, chlorophyll b and other pigment molecules transfer their excitation energy by resonance transfer to chlorophyll a which undergoes a photoexcitation leading to electron transport. Consequently, chlorophyll b is referred to as an accessory pigment. Strong evidence for the key role of chlorophyll a comes from the fluorescence spectra which show that it is always chlorophyll a that fluoresces, no matter which accessory pigment is excited.

In this thesis, the chlorophyll fluorescence associated with the light reactions is used to help characterize electron

transport in C_4 plants. It is a valuable tool because it is a non-destructive means of monitoring photochemical reactions, and its yield at a given incident intensity is often inversely related to the capacity of PS I for electron transport (68, 77, 116, 202). Consequently, it is indicative of processes competing for de-excitation to the ground state.

Fluorescence of the photochemically excited chlorophyll generally increases in the presence of metabolic inhibitors of photosynthesis; non-fluorescence means of dissipating energy act as quenchers of the fluorescence (76, 77). Consequently, when photosynthesis is chemically blocked at moderate light intensities, the fluorescence rises. Photosynthesis involves two sequential photochemical reactions in which electrons are transferred from water to NADP. The first photochemical reaction, light reaction I, oxidizes the intermediate electron transport chain and reduces NADP; the second, light reaction II, oxidizes water with the release of oxygen and reduces the electron transport chain. A widely accepted scheme of the electron transport process which accompanies this quantum conversion is represented in Figure 2. There are two (possibly connected) pigment complexes associated with the two light reactions. The molecules in the pigment complexes act as funnels or antennae to concentrate the absorbed light energy into a reaction center (light trap) where the actual photochemical events occur (Fig. 3).
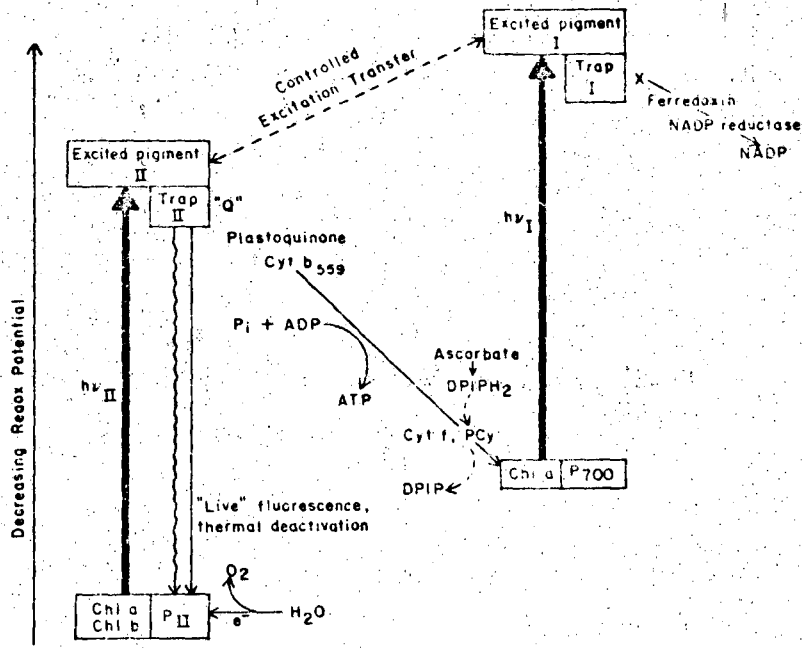
Fig. 13. Electron transport scheme for the two light reaction mechanism in chloroplasts. Pcy plastocyanin

Fig. 2. after Sun and Sauer (268).

PIGMENT SYSTEM **II**   PIGMENT SYSTEM **I**

LIGHT REACTION **II**   LIGHT REACTION **I**

Fig. 2

A working hypothesis for the distribution of the chlorophylls in the two pigment systems in the higher plants and the green algae. The two systems seem to contain both chlorophyll a (Chl a) and chlorophyll b(Chl b) but in different proportions. (In the red and blue-green algae, the phycobilins replace Chl b). It is suggested that most of the long wave-length forms of chlorophyll a (Chl a 685 - 705) are present only in pigment system I. The two major "bulk" Chl a (Chl a 670 and Chl a 680) are almost equally distributed in the two systems--System II having relatively more Chl a 670. (In red and blue-green algae, a very large proportion of Chl a is in pigment system I.) The energy trap of system I is P700, and that of system II is P680 - 690. The possible source of all the emission bands is also depicted in the diagram. (Modified after Govindjee, G. Papageorgiou and Rabinowitch "Chlorophyll Fluorescence and Photosynthesis". In G. G. Builbault (editor): Fluorescence, Theory, Instrumentation and Practice, Marcel Dekker, Inc., New York, 1967, pp. 511 - 564.) (For a review on the relation of "light reactions" of photosynthesis to chlorophyll fluorescence, see Govindjee and G. Papageorgiou "Chlorophyll Fluorescence and Photosynthesis:Fluorescence Transients", In A.C.Giese(editor): Photophysiology, Current Topics in Photobiology and Photochemistry, Academic Press, New York, 1971, pp.1-46

Fig. 3. after Govindjee (113).

Unequal sharing of absorbed light quanta between the two photosystems is moderated by spillover, and occurs due to the different spectral absorption and spatial separation of their pigment complexes. This spillover is less important at wavelengths greater than 670 nm. The higher proportion of long-wavelength-absorbing chl a molecules in system I enables it to absorb a majority of light in the far red and near infrared. PS II is incapable of using these wavelengths as effectively and therefore may become the rate-limiting photoreaction.

The physically distinctive pigment packages can interchange excitation energy, thereby providing a means for balanced and efficient excitation of the two photosystems. This "controlled spillover model" (as opposed to a "separate package model") of pigment systems I and II is supported by the quantum requirement measurements for the two light reactions of spinach chloroplasts (268). The factors which control the transfer of energy between the two photosystems are not yet totally characterized. The difference in quantum requirement between the two light reactions might be caused by an unsymmetrical spatial distribution of the two light reaction centers with respect to the antennae pigments.

Photosynthesis in the green plant is totally associated with a cell organelle called the chloroplast (148, 272). Chloroplasts are approximately the shape of oblate spheroids, usually ranging from 4-10 um in diameter and 1-2 um thick. Their

characteristic green color is caused by the chlorophylls and they are surrounded by a double membrane. Chloroplasts isolated with intact outer envelopes are called class I, while those with broken limiting membranes are called class II (267). The isolated chloroplasts examined in this study are primarily class I.

During chloroplast development, the prolamellar bodies proliferate membranes and pinch off flattened membrane sacs called thylakoids. Small thylakoids frequently occur in stacks called grana. These grana stacks are joined by a series of membranous channels which serve to interconnect the internal space of the thylakoids (230). The grana membranes are collectively called the grana lamellae. The interconnecting membranes traverse the stroma matrix and are called the stroma lamellae. The bundle sheath chloroplasts of several C_4 plants are agranal and contain only membranes which resemble stroma lamellae. This thesis investigates the nature of this resemblence.

The lamellae are the sites of the photochemical and electron transport reactions (229). The freeze fracture procedure reveals that chloroplast lamaellae contain an internal membrane substructure which may have functional significance (225). The two classes of internal particles which are exposed by fracturing might correlate with the presence of the two light reactions (241).

The soluble non-membranous stroma matrix inside the chloroplast contains the enzymes of the reductive carbon cycle. These

reactions are also known as the dark reactions, the Calvin cycle, or the C_3 cycle. This thesis investigates the photochemistry of a group of plants which incorporate carbon dioxide into C_4 compounds before utilizing the Calvin cycle. It was the unusual carbon fixation patterns in these plants which first inspired my interest in them.

C. Fluorescence

1. Fluoresence Artifacts

Self-absorption of fluorescent light within the sample (even within a single chloroplast) can cause distortion of spectral shapes and relative peak heights (60). Assuming a homogeneous distribution of pigments, the high pigment concentrations of in- tact leaves cause strong self-absorption, a resultant apparent fluorescence yield decrease, and a spectral emission shift toward longer wavelengths (105). In order to avoid this problem, the sample must be dilute enough to withstand a doubling of concentra- tion without altering fluorescence spectra or yield (60).

Unfortunately, it is impossible to dilute the concentrations of a single intact chloroplast. This problem may be avoided by using chloroplast fragments, although rupturing of the chloroplast membranes produces other artifacts. It is a contention of this study that chloroplasts of C_4 plants must be intact for the most meaningful fluorescence studies, and that this potential artifact must be investigated. The relative contribution of self-absorption must then be estimated.

Since low temperature fluorescence spectra ($77^{o}K$) are more sharply resolved than room temperature spectra, they are commonly used to study photosynthesis (4). Because the use of the fluorescence microscope necessitates working at room temperature, it is difficult to relate this work to many of the low temperature studies.

2. Q and Variable Fluorescence Yield

In this study, variable fluorescence is used as a measure of PS II. Duysens and Sweers designate a certain molecule which affects the electron acceptor of PS II as Q, quencher of chl a_2 fluorescence (94). Only the oxidized form of Q serves as the quencher. The reduced form, QH, cannot function in this capacity. In the presence of Q, transfer of excitation can occur from chl a_2 to the reaction center. Excitation of system II results in the formation of QH which decreases quenching.

The addition of a strong reductant like sodium dithionite will also cause the formation of QH, thereby resulting in increased fluorescence yield (no quenching). Whereas PS II light enhances fluorescence (QH does not quench), PS I light has the antagonistic effect of decreasing fluorescence yields (94, 105, 116). Excitation of PS I can oxidize QH to Q, thereby quenching fluorescence. Q must therefore be situated between PS I and PS II. DCMU increases fluorescence because it prevents the reoxidation of QH by system I light (105). After prolonged

darkness, chloroplast fluorescence rises from a low initial level, F_0, to a steady state value, F_∞, which is three to four times higher (138). When Q is kept oxidized, fluorescence remains at F_0 (45).

During their studies, Yamashita and Butler made the following observations which involve the phenomenon of variable fluorescence (288, 289, 290, 291, 292, 293).

a) Low light intensity causes a moderate level of non-variable background fluorescence. In the absence of electron acceptors, irradiation with white light increases the fluorescence-yield approximately three-fold. Presumably the light causes PS II mediated formation of the non-quencher QH (288,291).

b) Similar irradiation of Tris-washed chloroplasts with low light results in only a 20% increase in fluorescence-yield. This minimal light-induced fluorescence-yield increase implies a lack of electrons to reduce Q (288, 291).

c) Chemical reductants, like sodium dithionite, can decrease fluorescence quenching, presumably by donating electrons to reestablish QH (291).

d) Tris-washed chloroplasts lack Hill reaction activity (288).

e) Hill reaction activity can be restored to Tris-washed chloroplasts by thorough rewashing with a combination of reductants and/or standard media. The ease with which the damage is repaired implies that Tris treatment causes only a mild, reversible denaturation,

since no irreplaceable components of the oxygen evolution system are lost (292).

f) Tris washing reduces Mn^{++} concentration, but reactivation is possible without the addition of Mn^{++} (292).

g) DCMU restores the variable yield of fluorescence in Tris-washed chloroplasts. Presumably there are enough endogenous donors to produce QH provided loss of electrons by QH is blocked (291). In this study, Tris-treated chloroplasts are examined after DCMU treatment.

h) Hydroxylamine can inactivate oxygen evolution, but at higher concentrations it can donate electrons to PS II (198). Consequently, hydroxylamine can restore some of the variable fluorescence lost by Tris-washed plastids (289, 291).

i) Irradiation of Tris-washed chloroplasts irreversibly prevents the restoration of variable fluorescence with electron donors. Tris-washed chloroplasts appear to be especially sensitive to photobleaching (290).

On the basis of the above observations, Yamashita and Butler conclude the following (288-291):

a) Duysens and Sweers' hypothesized quencher, Q, is a useful concept for studying the photochemistry of PS II.

b) Tris blocks the PS II mediated donation of electrons from water to trap II.

c) Certain electron donors like hydroxylamine can substitute for water as the electron donor to PS II.

d) Variable fluorescence is indicative of PS II activity. In this study, variable fluorescence is used as a measure of PS II.

3. Fluorescence of Photosystems I and II

Although fluorescence is used to characterize the photo-chemistry of photosynthesis, opinion varies as to the precise correlation between fluorescence and the two light reactions. Duysens' hypothesis of two forms of chlorophyll a, strongly fluorescent chlorophyll a_2 and weakly fluorescent chlorophyll a_1 is widely accepted (105, 236). Since low temperature fluorescence spectra reveal the presence of F695 and F735, in addition to F685, many attempts are being made to correlate these peaks with chl a_1 and chl a_2. The different chlorophyll a fluorescence emission spectra obtained with 400 nm (preferential chl a absorption) versus 470 nm (preferential chl b absorption) constitutes strong evidence for light assigning the bulk of F685 to PS II and the bulk of F735 to PS I (116, 117, 202, 206, 236).

Anderson and Boardman (4), pioneers in the field of deter-gent fractionation of membranes, use digitonin and density gradients to obtain a separation of small system I particles from larger system II enriched particles. They sediment at 144,000 g and 10,000 g, respectively. Room temperature fluorescence studies of these particles reveal a relative fluorescence-yield for that of the 144,000 g particles equal to only 20% that of the10,000g particles (44,53).

The 77°K spectra of the two particles differed markedly, although the two room temperature spectra were similar (Fig. 4) (44, 53). F735 corresponds to 75% of intact chloroplast fluorescence, 60% of 10,000 g particle fluorescence, and 97% of 144,000 g particle fluorescence at 77°K. Anderson and Boardman concluded that most of the F735 is associated with system I, although some is present in system II. They observed that F695 is predominantly associated with PS II. The association between F685 and F695 is confirmed by many others (116, 117, 135, 206, 236); however, Goedheer claims that F695 is associated with system I (105).

Govindjee reported that at room temperature, F695 belongs to PS I, but at 77°K, F695 originates in both PS I and PS II (113). Furthermore, he suggested that it is inaccurate to correlate F735 exclusively with PS I and F685 exclusively with PS II; it is more accurate to state that the ratio F735/F685 is higher in PS I and lower in PS II (113). Assuming that all variable fluorescence (cf. Sections I. C2 and I. C3) originates in PS II, 65-70% of F735 belongs to PS I (113).

Mohanty et al. also conducted fluorescence studies of system I and system II particles (197). At both room temperature and at 77°K they found the system I spectra to be significantly richer in the long wavelength component than the system II spectra. On the basis of these data they concluded that multiple peaks are characteristic of each particle. They did, however, attach importance to the relative peak heights. They detected substantial short wavelength components in system I particles and
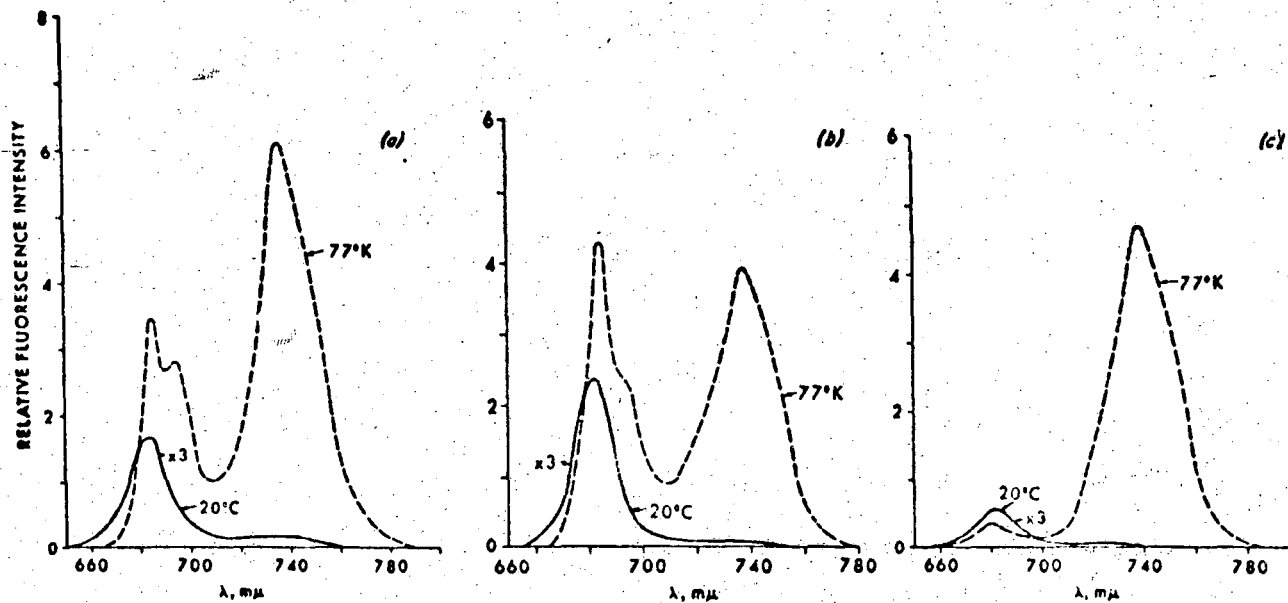
Fig. 8. Fluorescence emission spectra of chloroplast fractions at 20°C (solid lines) and 77°K (broken lines) (39). The fluorescence intensities at 20°C have been multiplied by a factor of 3. (a) Chloroplasts, (b) 10,000y fraction, (c) 144,000g fraction.

Fig. 4. after Boardman (44).

long wavelength components in system II particles.

4. Lamellar Organization and Fluorescence

This thesis investigates the correlation between lamellar organization (cf. Appendix A) and fluorescence in the chloroplasts of C_4 plants. In greening pea seedlings, the development of system II activity accompanies the formation of grana and a decline in the chlorophyll a/b ratio (48). For the first five hours of illumination there is minimal lamellar appression or Hill reaction activity. PS I activity develops within an hour, although system II requires six to eight hours for significant activity (48). After two hours F685 predominates although system I is fully developed and system II activity is practically non-existent. The increase in system II activity 6 hours after the first illumination is concomitant with F735 development.

5. Ions and Fluorescence

Since the fluorescence of C_4 plant chloroplasts is unusually sensitive to the ionic environment of the tissue (cf. Section II. A), it is appropriate to explore the basis for this sensitivity. The ionic environment strongly influences the fluorescence-yield of isolated chloroplasts (139, 203, 204, 205). At $77^O K$, Mg^{++} increases F685 and F695 yields, but decreases F735 (203, 204). The Mg^{++} only affects those fluorescence components dependent upon the redox state of Q, i.e., F_∞, F_{DCMU}, F_{red}, but not F_o (139). The divalent cations of strontium, barium, and manganese, and the monovalent cations of sodium, lithium, potassium, rubidium,

and cesium (205) act similarly. Murata interprets the differential ionic effect on F685 and F735 as a suppression of bulk excitation transfer from chl a_2 to chl a_1 (202, 207).

Ions also stabilize the inter-lamellar association in chloroplasts. Izawa and Good isolated chloroplasts in low salt media and obtained plastids with swollen grana (146). The grana membranes stay loosely attached near the edge of the thylakoids, although the chlorophyll is not lost. This lack of appression did not disrupt Hill reaction or electron transport activity (oxygen evolution, ferricyanide reduction). The introduction of salts caused a re-cementing of lamellae, often in a grana-like conformation. Consequently, Izawa and Good suggested that a rigid distinction between grana and stroma might be unwarranted.

D. Correlation Between Lamellar Structure and Function

One of the objects of this study is to correlate lamellar structure and function with the aid of the fluorescence microscope. There are several possible approaches to this problem. Lintilhac and Park used fluorescence and electron microscopy to demonstrate the potential photochemical importance of stroma lamellae (181). They found fluorescing chlorophyll to be uniformly present in all chloroplast membranes. A single sample was first examined in a fluorescence microscope and then in the electron microscope. The fluorescence intensity increased only when lamellae overlapped. "Careful examination shows that the intensity of fluorescence is fairly constant and that variations can usually be correlated with

variations in the number of superposed membranes (181).

Tetrazolium and ditetrazolium salts are superior to silver ions for the localization of Hill reaction reducing sites (256). In the presence of light the salts that are inside the chloroplasts are reduced to insoluble formazans or diformazans. Shumway and Park detected delocalized precipitation of the reduced salts and concluded that this technique does not provide adequate resolution to localize PS II within sites on individual lamellae (256). It is difficult to apply this technique to C_4 monocot plants because bundle sheath cells are surrounded by a suberized layer which limits penetration of the dyes (cf. Section I. E).

Hall used the Hill oxidant, ferricyanide, which was reduced in the presence of Cu^{++} (123). Since the Hill reaction-mediated precipitate formed on both grana and stroma lamellae, Hall et al. concluded that all chloroplast lamellae have a functional PS II (123). Unfortunately the resolution is insufficient for localizing reaction centers in lamellae.

The complex problem of studying the light reactions of photosynthesis may be simplified by physically separating the two photosystems prior to the recording of data. The use of isolated C_4 bundle sheath chloroplasts is an alternative method for pursuing the same objective. Many studies, however, involve separated photosystems. Incubating chloroplasts with the non-ionic detergent digitonin non-randomly disrupts their membranes (4, 44, 45). Subsequent differential centrifugation separates small system I

particles from larger system II enriched particles. The frag-
ments centrifuge down at 144,000 g and 10,000 g, respectively.

Michel and Michel-Wolwertz object to detergent separation
techniques because they result in modified absorption spectra and
disrupted orientation of chlorophyll molecules (194, 195). Mechan-
ical shearing with a French press avoids these problems yet pro-
motes the separation of PS I and PS II. In my thesis, the sus-
ceptibility of C_4 chloroplasts to chemical damage is noted (cf.
Sections II. A and III. B4). It would therefore be safest to substi-
tute physical treatment for chemical treatment whenever possible.
Sane et al. (241) improved upon the techniques of Michel et al.
by using a relatively mild French press treatment (Table 1).

The separation of photosystems I and II with the French press
preserves morphological structure (241). Electron microscope
studies of French press treated spinach indicated that the 160K,
PS I fraction originates from unappressed stroma lamellae and end
membranes of grana stacks (241). In my thesis, it was initially
assumed that C_4 bundle sheath chloroplast lamellae are analogous
to stroma lamellae. Therefore, an investigation of the light
reactions in bundle sheath chloroplasts would provide data
possibly applicable to the study of stroma lamellae.

Developmental and mutant studies provide additional infor-
mation about grana and stroma lamellae. The immature chloroplasts
in the basal portion of a spinach leaf have a higher proportion of
stroma lamellae and a higher chl a/chl b ratio than those found

Table 1. Photochemical Activity of French Press Treated Spinach
Chloroplast Fractions Obtained by Sane et al. (241)

	Band 1	Broken chloroplasts	Band 2	Band 3
Chl a/b	6.0		2.6	2.6
$\dfrac{\text{Chl a + b}}{P_{700}}$	350,337	535,560	950,123	825,840
$\dfrac{\text{NADP reduction}}{\text{DCPIP Hill reaction activity}}$	247	8.4	0.43	0.15
fluorescence yield	low		high	high
variable fluorescence	absent	present	present	present

in the mature plastids of the leaf tip (110). However, additional
work by Park and Sane indicates that the chl a/chl b ratio
does not necessarily indicate the ratio of PS I/PS II activity
(223). Stroma lamellae do consistently have a higher chl a/chl b
ratio than grana.

Park and Sane (223), using romaine lettuce in their study,
divided the leaves into three groups: pale inner leaves (I),
yellow middle leaves (M), and outer green leaves (O). As ex-
pected, chloroplasts (I) had a higher proportion of stroma to
grana lamellae, a higher chl a/chl b ratio, and an enriched
PS I activity in comparison to (O) chloroplasts. Surprisingly,
(M) chloroplasts had a high chl a/chl b ratio of 7.0 in spite of
substantial grana development. Both (M) and (O) chloroplasts
had similar PS II rates and variable fluorescence.

An unusual situation, however, exists with mutant NC 95 (140).
The variegated regions of this mutant completely lack lamellar
appression, are inactive in the Hill reaction, and display negli-
gible natural photosynthetic activity. They do have a normal
manganese content and appear to have an inactive PS II pigment
assembly. System I, however, is functional, as evidenced by NADP
photoreduction with ascorbate-DCPIP and by PMS-mediated photophos-
phorylation. Consequently, Homann and Schmid hypothesize a corre-
lation between PS II and appressed lamellae (140). There appears
to be at least one normal or mutant plant to match every possible
hypothesized correlation between lamellar appression and the photo-
chemistry of photosynthesis.

E. The C_4 Phenomenon

The work of Calvin and Benson on carbon fixation established phosphoglycerate, a 3-carbon compound, as the initial stable storage product of photosynthesis (69). In 1965, Hatch and Slack (128) startled the complacent field of carbon fixation by confirming an earlier report by Kortschak, Hartt, and Burr (165); both reports identified C_4 dicarboxylic acids as the initial product of CO_2 fixation in sugar cane.

Since the confirmation of the startling "C_4 phenomenon," great attention has been paid to the photosynthesis of C_4 plants. Additional differences in C_4 photosynthesis have been discovered which inspired the work in this thesis. The C_4 phenomenon has been sufficiently studied so that it is now more appropriate to refer to the C_4 syndrome, the symptoms of which are outlined below.

1. Leaf Anatomy - Kranz

All C_4 plants have a Kranz type leaf anatomy, or a minor modification of it (172). The correlation between leaf anatomy and C_4 photosynthesis appears pivotal to the current visualization of the carbon fixation scheme. The anatomy also presents special, practical problems in the isolation of chloroplasts as discussed below.

Kranz anatomy indicates a well developed bundle sheath (parenchyma sheath) layer around the vasculature (Fig. 5).
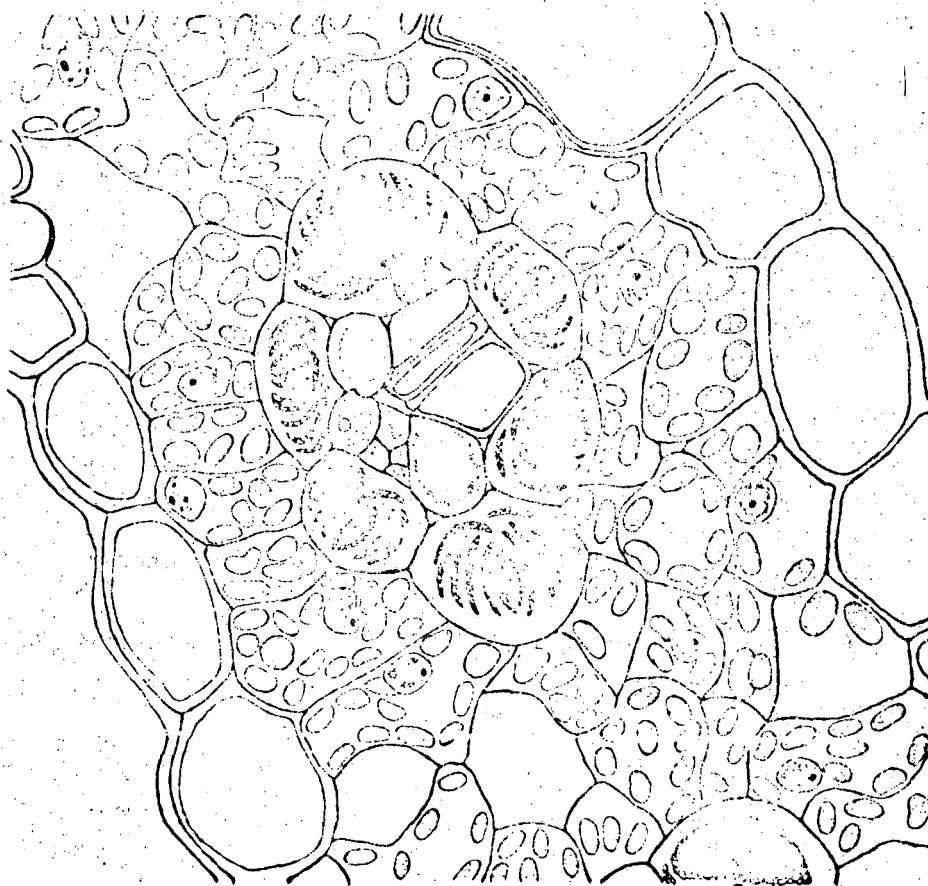
Fig. 5. Cross section of a corn leaf; (bs) bundle sheath,
(m) mesophyll, (vb) vascular bundle. after Rhoades (239).

The bundle sheath walls of monocots contain a suberized layer which is reminiscent of an endodermis, and which might help regulate water loss from the plant (209). This suberized layer is not formed in C_4 dicots (172). In sugar cane, the suberized layer is located in the bundle sheath walls adjacent to mesophyll cells; however, in older tissue, it can surround entire bundle sheath cells (172). In either case it can hinder diffusion across the cell walls of the bundle sheath to the mesophyll. However, the suberized walls are penetrated by numerous plasmodesmata which might facilitate diffusion across the walls. This suberized layer increases the difficulty of in situ chemical treatments of bundle sheath chloroplasts because of penetration problems.

Laetsch (172) used light microscopy while Edwards and Black (96) used scanning electron microscopy to visualize the internal topology of C_4 leaves. Both reported large, smooth-walled bundle sheath cells tightly packed against the parallel vascular bundles. In Digitaria, bundle sheath cells usually have angular edges; they are tightly packed with organelles, the most prominent of which are the chloroplasts (96). In contrast, the mesophyll cells have rounded edges and a scattered distribution of organelles. There is usually a size differential (172), and frequently a difference in shape. Often, the bundle sheath chloroplasts will appear a paler green than those of mesophyll, although alternatives do exist in Atriplex lentiformis and others. Most characteristically, the bundle

sheath chloroplasts are packed with numerous large starch grains while mesophyll plastids are usually devoid of them.

2. Chloroplast Ultrastructure

The most unique feature of C_4 chloroplast ultrastructure is the peripheral reticulum (172). However, the chloroplast lamellar configuration is the ultrastructural feature most relevant to this study. The correlation between lamellar appression and fluorescence as detected by infrared film is the core of this work. Consequently, an extensive series of Laetsch's electron micrographs is provided as a reference in Appendix A.

Briefly, mesophyll and bundle sheath chloroplasts often show dimorphic lamellar configurations, however there is no consistent pattern. Sugar cane represents one extreme with its agranal bundle sheath plastids and conventional mesophyll chloroplasts. In contrast, Atriplex bundle sheath chloroplasts contain a normal complement of grana while the mesophyll chloroplasts exhibit limited thylakoid appression. Spartina, and other C_4 plants, have equal grana development in both the mesophyll and bundle sheath chloroplasts. Bundle sheath lamellae are often distended by large numbers of swollen starch grains.

Chloroplast lamellar development is fairly consistent within a given species. Laetsch reports that appression of membranes in sugar cane is not affected by light intensity, but is affected by temperature (172). In contrast, Goodchild reports that light intensity can affect the number of grana (108).

The developmental sequence can also involve lamellar changes. Laetsch's work on sugar cane reveals that bundle sheath and mesophyll proplastids are indistinguishable; both initially form small grana which the bundle sheath chloroplasts subsequently lose (174).

3. Chloroplast Isolation and Separation

Chloroplast isolation and separation are crucial to the investigation of C_4 photosynthesis, and involve the separation of bundle sheath from mesophyll chloroplasts. Unfortunately, isolation and separation of these chloroplasts is difficult because of the delicacy of chloroplast membranes relative to bundle sheath cell walls. Mesophyll chloroplasts are more easily released, but preparations are still contaminated with bundle sheath chloroplasts. Separation of the two types of intact isolated chloroplasts from a mixture of the two is not yet possible. It is also difficult to distinguish between the two types under the light microscope. The original thesis observation with the fluorescence microscope was made because grana are easily seen with this instrument. Initial attempts at separation involved sucrose density gradients and were based on the assumption that the high starch content of bundle sheath chloroplasts relative to mesophyll chloroplasts would cause a density differential. Recently, a successful isolation of mesophyll and bundle sheath cells has been accomplished

by Edwards and Black (95). The revised technique of Anderson
et al. (5) appears to yield the first good bundle sheath chloro-
plast preparation, although it is questionable whether they are
intact. Other C_4 chloroplast isolation procedures resulted in
fragmented bundle sheath chloroplasts and/or impure preparations.
Table 2 outlines various chloroplast isolation and separation
procedures applied to C_4 plants. Until a method is perfected,
it is preferable to study C_4 chloroplasts in situ, whenever
possible.

Recent developments in the field of C_3 chloroplast isola-
tion might be applied to C_4 chloroplast isolation and separation.
The buffers developed by Jensen and Bassham can be used to isolate
consistently high yields of Class I spinach chloroplasts (148).
These chloroplasts fix carbon dioxide at rates of up to 60% of
those recorded in vivo. Light and electron microscopy confirm
the integrity of the outer membrane.

Takebe (1967) used macerozyme, a crude polygalacturonase,
to isolate intact tobacco cells. He then used cellulose to
dissolve the cell wall and free the protoplasts (270). Since
bundle sheath and mesophyll cells differ greatly in size and
density, their separation is much easier than separating fragile
chloroplasts. Unfortunately, C_4 monocots appear to be impervious
to these enzymes (147). Hopefully, this approach can be
successfully adapted in the near future.

Table 2. Summary of C$_4$ Chloroplast Isolation and Separation Techniques

Reference	Buffer	Centrifugation	Isolation	Separation	Results/Plant
Baldry (19) 1968	pyrophosphate sorbitol	4,000g	Waring Blender	discontinuous sucrose gradient	Class II 50% B.S. sugar cane
Slack et al. (262) 1969	non-aqueous	5,000g 12,000g	tissue homogenizer	density gradient	distorted & swollen, broken chloroplasts sugar cane
Bjorkman et al. (40) 1969			Waring Blender, mortar & pestle & glass beads	differential grinding	Atriplex Amaranthus corn
Berry et al. (34) 1970	Tris		mortar & pestle & glass beads	differential grinding	corn
Woo et al. (286) 1970	TES sorbital	200g 1,000g 10,000g	sorvall omnimixer, T.B. homogenizer	differential grinding	B.S. strands & fragments Sorghum
Bucke et al. 1971	HEPES sucrose		mortar & pestle & glass beads	differential grinding	variable, 60-75% B.S. corn and sugar cane
Brangeon (54) 1971	Tris	1,000g	Waring Blender	differential grinding	Class II mesophyll 80% B.S. 75% corn
Anderson et al. (5) 1971	TES sorbital	300g 1,000g	sorvall omnimixer +razor	differential grinding & chopping	Class I? 90% B.S. 85% M. Sorghum
Edwards et al. (95) 1971	tricine sorbital	1,000g	mortar & pestle, T.B. homgenizer	nylon net, stainless steel sieve	90% purity, 93% intact M cells, 70% intact B.S. cells Digitaria
Waygood (279) 1971	mannitol	2,000g	laceration with 5 scalpels		corn

Andersen et al. - see Woo et al. A153 1970
(2)
1972

Lyttleton (1970) used Ludox, a colloidal silica, as a substitute for sucrose in a discontinuous density gradient (187). Non-toxic Ludox has a high density, a low viscosity, and a negligible osmotic potential which allows the separation of 80% of the chloroplasts as class I. The increased density of starch-ladened bundle sheath chloroplasts increases the potential application of this method to C_4 plants.

Karlstam and Albertson (1972) used countercurrent distribution to separate class I from class II spinach chloroplasts; this technique is normally applied to whole cells. The consistent application of an appropriate phase system standardizes the distribution of organelles in the dextran - polyethylene-glycol mixture (154). Mesophyll and bundle sheath chloroplasts might respond differentially to this method.

4. CO_2 Fixation - the C_4 Pathway

Hatch and Slack postulate the existence of two linked carbon fixation cycles (126). The mesophyll enzyme, phosphoenolpyruvate carboxylase, is the initial carbon fixing enzyme. The product of this fixation, oxaloacetate, is converted to the more stable malate or aspartate. Malate or aspartate then donates its fourth carbon atom to an acceptor molecule. The second cycle occurs in the bundle sheath and incorporates most of the reactions of the C_3 pathway.

Investigation of this C_4 pathway indicates the convergent evolution of C_4 plants with respect to factors involving CO_2

fixation. Downton and Tregunna hypothesize a further correlation between CO_2 fixation, the degree of appression of chloroplast lamellae, and the presence of PS II in C_4 plants (90).

5. Evidence of a Possible Photosystem II Deficiency
   in Bundle Sheath Chloroplasts

Initial investigations of C_4 photosynthesis indicated a possible PS II deficiency in the bundle sheath chloroplasts. The high chl a/b ratio, characteristic of PS I, is observed in the agranal bundle sheath plastids of Sorghum bicolor, and in the nearly agranal bundle sheath plastids of Zea mays (6, 71, 235).

Woo et al. detected enriched F735 and greatly diminished F685 and F695 in $77^{O}K$ fluorescence emission spectra of Sorghum bicolor bundle sheath fragments (Fig. 6) (286). They emphasized the similarity between the $77^{O}K$ fluorescence emission spectra of digitonin-photosystem I particles and their bundle sheath fragments. Woo et al. reported the quantum yield of fluorescence as 0.13 for the mesophyll and 0.19 for the bundle sheath. The Dichanthium fluorescence data obtained in this study indicate a higher (2:1) M/BS relative fluorescence yield. Bazzaz and Govindjee reported that mesophyll fluorescence is stronger than bundle sheath fluorescence in corn (29).

Woo et al. extended their investigations to other PS II parameters. They failed to detect measurable Hill reaction
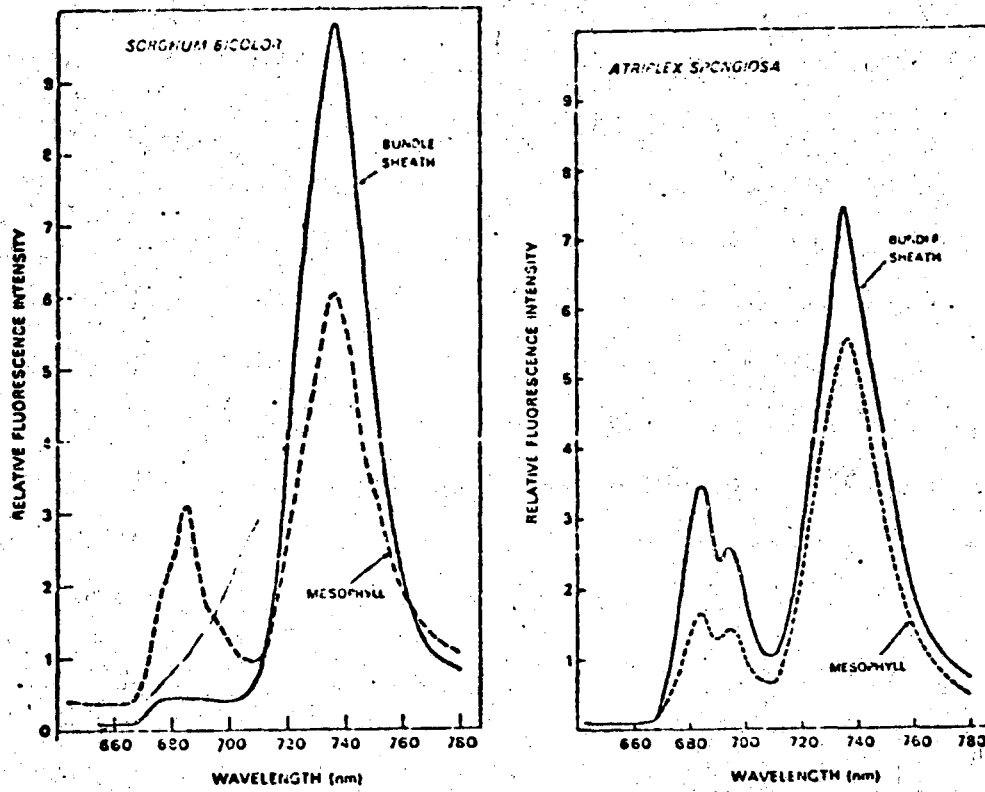
Fig. 6. after Woo, Pyliotis, and Downton (286).

activity (NADP photoreduction, or O_2 evolution) in the bundle
sheath chloroplast fragments of either Sorghum bicolor or
Zea mays. In contrast, the mesophyll chloroplasts exhibit
high Hill reaction activity. All chloroplasts tested show strong
photoreduction of NADP in the presence of ascorbate-DCIP (PS I).

Normally, cyt f is oxidized by excitation of PS I and reduced
by excitation of PS II. The Sorghum bicolor and Zea mays meso-
phyll chloroplasts exhibit this expected wavelength dependence
for the oxidation of cyt f, in contrast to the wavelength inde-
pendent photooxidation observed in bundle sheath chloroplast
fragments (286). DCMU-treated chloroplasts lose PS II activity,
and oxidize cyt f independently of wavelength, in a manner remini-
scent of bundle sheath chloroplast fragments.

The PS II electron carrier, cytochrome b_{559} appeared
to be missing in bundle sheath chloroplast fragments (286). Woo
et al. claim to have confirmed their chlorophyll fluorescence
and cyt b_{559} data on intact bundle sheath cells, although they
performed their experiments on chloroplast fragments. Since their
bundle sheath cells were in fact bundle sheath strands, it is
difficult to visualize how they could have measured a fluorescence
emission spectrum without encountering serious problems with
self-absorption. Specimen condition, therefore, remains a potential
source of error in this experiment.

Woo et al. concluded that agranal bundle sheath chloroplasts
are deficient in PS II pigment assemblies. Related work by

Anderson et al. and by others involved similar results and conclusions (3, 5, 6, 47, 233). Anderson et al. observed a similarity between the pigment composition of bundle sheath fragments and digitonin-photosystem I particles (6). The action of digitonin on mesophyll chloroplasts paralleled that on spinach. In contrast, bundle-sheath chloroplast digitonin fractions were almost uniform in composition and activity (6).

Anderson et al. confirmed the work of Woo et al. on a preparation of relatively intact bundle sheath chloroplasts in an attempt to eliminate the possibility of selective PS II destruction during isolation (5). Although these chloroplasts showed internal structure and lacked the highly refractile appearance characteristics of class I chloroplasts under phase contrast microscopy, the chloroplasts were reported to swell on the microscope slide. Anderson et al. interpreted this as indicating the presence of an outer membrane. Anderson claimed this is another form of class I chloroplasts, but conceded that some components may be missing (3).

Anderson et al.'s carefully isolated bundle sheath chloroplasts were still only capable of between 5-15% of the mesophyll PS II activity. Agranal Sorghum chloroplasts were half as active as the nearly agranal corn chloroplasts. Anderson et al. concluded that the former harsh isolation procedure did not artificially inactivate PS II. The young age of the experimental material (2-3 weeks) is the only obvious potential

weakness of this work, since at least sugar cane bundle sheath chloroplasts develop grana before becoming agranal (174).

These studies, which show a deficiency of PS II in bundle sheath chloroplasts, are now being questioned by many researchers in light of the evidence presented below. Chloroplast isolation damage, once again, appears to be the possible nemesis of investigations involving C_4 photosynthesis. However, the discrepancy between the evidence for and against the existence of PS II in the bundle sheath chloroplasts is not well understood. The data obtained in this in situ study compliments the data obtained with chloroplast fragments, thereby increasing our understanding of the general phenomenon.

G. Evidence Favoring Photosystem II Activity in Bundle Sheath Chloroplasts

Recent discoveries indicate the presence of an easily damaged PS II in bundle sheath chloroplasts (2, 38). Using corn bundle sheath fragments, Bishop, Smillie and Andersen detected DCMU-sensitive Hill reaction activity equal to 70-80% that of the mesophyll provided that either DCPIP, cyt c or potassium ferri-cyanide is available as an electron acceptor (2, 38, 39, 264, 265).

However, in agreement with earlier work, they could detect neither NADP-mediated Hill reaction activity, nor wavelength dependent photooxidation of cyt f (2). Addition of plastocyanin permit-ed them to achieve NADP photoreduction by agranal Sorghum bicolor

chloroplasts (265). This need for plastocyanin was inversely related to the integrity of the specimen. The modified gentle isolation technique of Anderson and Boardman decreased the need for plastocyanin, while sonication increased this need (265).

Anderson claimed that Bishop et al.'s plastocyanin-induced NADP-reduction results from the small quantities of PS II present, and not from a well developed PS II (3). Bishop et al. claimed that this NADP photoreduction originated in PS II be- cause it is light dependent and susceptible to DCMU. Consequent- ly, Bishop et al. hypothesized the presence of both photosystems I and II in agranal plastids; however, they suggested that the normal link between the two photosystems is missing (38). Iso- lation might have disrupted soluble linking protein similar or identical to plastocyanin (264).

A related observation was the naturally occurring wavelength dependent photooxidation of cyt f by intact bundle sheath cells (39). This photooxidation revealed the unusual susceptibility of bundle sheath chloroplasts to isolation damage, since Bishop et al. confirmed that isolated bundle sheath chloroplast frag- ments do not have this wavelength dependence.

Anderson et al. criticize the work of Bishop, Smillie, and Andersen for obtaining very low mesophyll reaction rates (5). It is also unusual that their chl a/b ratios were low and were always between 1.6 and 2.6 for both mesophyll and bundle sheath plastids. The chl a/b ratios of the two plastid

types differed by only 0.6. This small difference might have been a function of the very young age of their experimental material (2 weeks), although Bishop et al. claimed to obtain similar results on mature tissue. In either case, because of the prolonged ontogeny of bundle sheath chloroplasts, it would seem safer to experiment upon mature plants.

Adequate support for the above work was supplied by Mayne and Black (41, 191, 192) who worked on mature tissue with higher chl a/b ratios. They isolated intact mesophyll and bundle sheath cells from Digitaria for experiments which provided extensive evidence for the existence of PS II in nearly agranal C_4 bundle sheath chloroplasts. Their careful specimen preparation procedure was the key to their success, and conferred upon their study a high degree of credibility. They documented complete electron transport from water to NADP in both types of chloroplasts, although the ratio of PS II to PS I was 2-3 times higher in mesophyll chloroplasts (191). Table 3 and Figure 7 summarize the data from their work. The work of Karpilov (155), in the USSR, is also in agreement with Mayne and Black's data (191).

Bazzaz and Govindjee detected approximately equal PS II activity in the mesophyll and bundle sheath chloroplasts of Zea mays, although their fluorescence induction data and spectra agreed with Boardman's (Fig. 8) (113). The bundle sheath chloroplasts were more active than the mesophyll chloroplasts

Table 3. Summary of spectral and electron transport characteristics
of mesophyll cells and bundle sheath cells from _Digitaria_
sanguinalis. after Mayne, et al. (191).

Characteristic	Mesophyll:bundle sheath
Absorption at 700 nm	1:2
P-700 change	1:2
Ratio of f730:f685	1:3
Chlorophyll a:b ratio	3:4.5
Delayed light emission	2:1
Variable fluorescence yield	2 or 3:1
Ferredoxin NADP-reductase	3 or 4:1
Hill reaction activity	2:1
Glyceraldehyde 3-P dehydrogenase	1:1
Malic enzyme	1:20
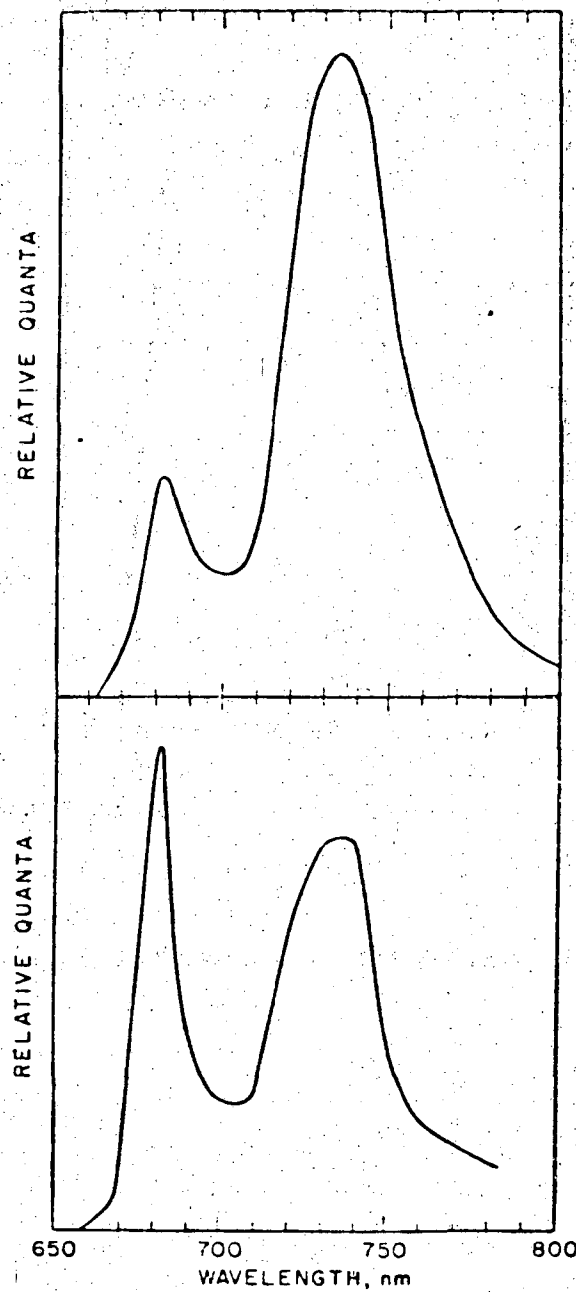
FIG. 3. Fluorescence emission spectra of cell extracts at liquid nitrogen temperature. Upper trace is an extract of bundle sheath cells. Lower trace is an extract of mesophyll cells. Both samples were adjusted to an equal absorption at 675 nm.

Fig. 7. after Mayne, Edwards and Black (192).

Fig. 8

Emission spectra of mesophyll and bundle sheath chloroplasts of *Zea mays*, excited at 440 nm, at 77°K. Absorbance at 678 nm for 1 mm pathlength, 0.001. (After Maarib Bazzaz, unpublished results.)

Fig. 8. after Govindjee (113).

in the reduction of methyl viologen using reduced DCPIP as donor
in the presence of DCMU; this might have resulted from the meso-
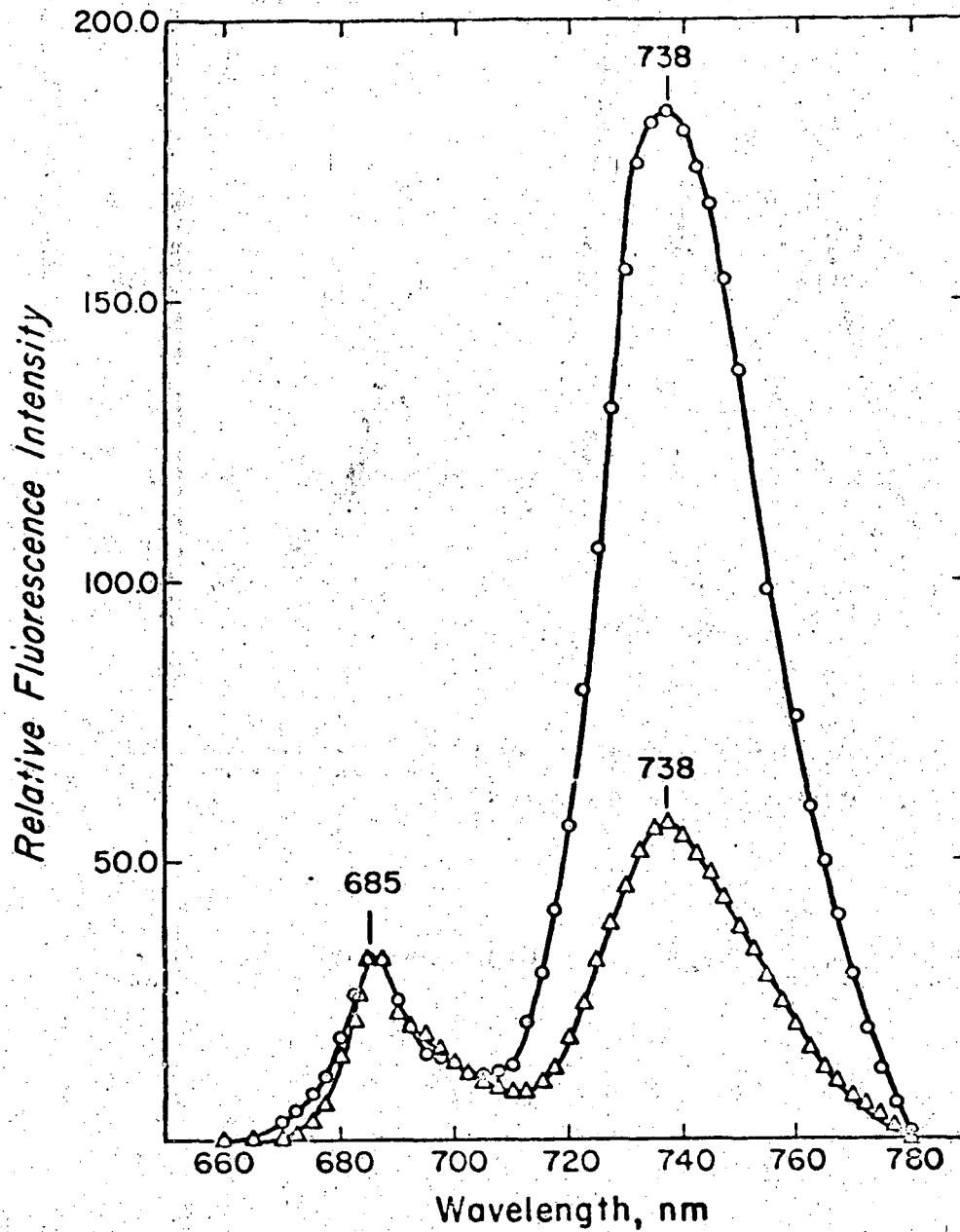phyll's reduced ability to use water as a donor for DCIP reduction
(113). When DPC was used as donor, the mesophyll did have a
higher PS II activity than the bundle sheath (113).

Bailey et al. treated Sorghum bicolor with SDS and then
separated the protein complexes by electrophoresis on a poly-
acrylamide gel (16). Sorghum mesophyll chloroplasts and spinach
chloroplasts both yielded a PS I - protein complex / PS II -
protein complex ratio of approximately 1:2.2. In contrast,
the ratio was 1:0.7 in bundle sheath chloroplasts. This large
quantity of PS II protein, however, appeared to be somewhat
pigment deficient. Nevertheless, the existence of the protein
supports the potential presence of PS II in bundle sheath
chloroplasts.

Therefore, most investigations of C_4 plants indicate the
presence of PS II activity in the studied agranal bundle sheath
chloroplasts. This correlates well with the measurements of
variable fluorescence recorded in this study.

F. Thesis Proposal

Initially I investigated the observed difference in appear-
ance of mesophyll and bundle sheath chloroplasts under the
fluorescence microscope, hoping that it would elucidate the
distribution of the two light reactions of photosynthesis be-
tween the two types of chloroplasts. First, I confirmed this

observation on a variety of C_4 plants besides sugar cane, and analyzed the cause of this phenomenon using infrared color film, and infrared black and white film. These photographic data indicate the extent to which the apparent low fluorescence yield of bundle sheath chloroplasts is actually a decrease in yield, a shift toward longer wavelengths, or a combination of both phenomena.

To characterize the bundle sheath lamellae using fluorescence techniques, it is preferable to design a technique for studying chloroplast fluorescence in situ because fluorescence characteristics change rapidly upon isolation. In situ study with the fluorescence photomicroscope avoids the special problems of physical and chemical damage associated with the isolation and separation of C_4 chloroplasts.

The unusual fluorescence patterns in agranal bundle sheath chloroplasts imply a possible PS II deficiency. This possibility is investigated by using variable fluorescence as a measure of PS II.

Initially it was assumed that unappressed C_4 bundle sheath chloroplast lamellae were analogous to spinach stroma lamellae. Consequently, isolated agranal bundle sheath chloroplasts might constitute an isolated PS I, analogous to spinach stroma lamellae, which could be observed in situ. It is now apparent that the situation is more complex, and some PS II activity exists in these membranes. Therefore, unappressed C_4 bundle sheath chloroplast

lamellae might be analogous to developing C_3 chloroplasts which have not yet acquired appressed membranes; to reduced chloroplasts which have secondarily lost their grana; to dissociated C_3 chloroplasts analogous to the chloroplasts isolated by Izawa and Good in low salt media; to structural chloroplast mutants; or to a combined structural and functional chloroplast mutant. Chloroplast fluorescence patterns in C_4 plants are compared with the degree of lamellar appression as depicted in the electron micrographs of W.M. Laetsch, as well as other published data.

II. Materials and Methods

A. Experimental Materials

Table 4 lists the growth locations of the experimental
plants used in this investigation. Table 5 outlines the rele-
vant growth conditions. All plants are soil grown and propa-
gated from seed, with the exception of the sugar cane, which is
propagated in vermiculite from a portion of the cane stem. The
young plants are transferred to soil after they attain a height
of 12-16 inches.

Only mature, dark green, healthy portions of leaves are used
in experiments. White (spider-mite damaged areas) and red
spotted areas are avoided. The red spots are a reaction of
cane leaves to artificial light conditions, and can be almost
completely eliminated by lowering the photoperiod to nine hours
or less (18).

The experimental leaves which are scheduled to be photo-
graphed with high-speed black and white infrared film, are
freshly picked the day of each experiment. They are temporar-
ily stored in plastic bags at $4^{O}C$. The leaves, scheduled to be
photographed with infrared color film, are cut prior to use
and are also stored in plastic bags at $4^{O}C$. Most leaves may
be stored in this manner for three days, although leaves were
typically sectioned within two hours of being detached.

Table 4. Growth Locations of Experimental Plants

Plant Species	Outdoors	Greenhouse	Growth Chamber
Amaranthus edulis Michx. ex Moq.			
mature		G	
cotyledon		G	
Atriplex lentiformis (Torr.) Wats.		G	
Cenchrus sativa		G	
Cynodon dactylon (L.) Pers.	UCBL		
Digitaria sanguinalis (L.) Scop.	UCBL	G	
Dichanthium annulatum (Forssk.) Stapf		G	
Echinochloa colonum (L.) Link.		G	
Euphorbia maculata L.		G	S
Euphorbia serphyllifolia Pers.		G	S
Euphorbia splendens Bojer		G	
Froelichia gracilis (Hook.) Moq.		G	S
Mollugo cerviana Ser.		G	S
Mollugo verticillata L.		G	
Portulaca oleracea Linn.		G	S

Plant Species	Outdoors	Greenhouse	Growth Chamber
<u>Sorghum caffrorum</u> Beauv.		G	S
<u>Spartina foliosa</u>	FG		
<u>Spinacia oleracea</u> Linn.	F		
<u>Saccharum officinarum</u> Linn.			L

(UCBL)   Plants grown on a U.C. Berkeley lawn.

(FG)   Field grown plants.

(F)   Farm grown plants.

(G)   Greenhouse grown plants.

(S)   Plants grown in a small growth chamber.

(L)   Plants grown in a large growth chamber.

Table 5. Growth Conditions of Experimental Plants

Growth Conditions	Outdoors	Greenhouse	Growth Chambers: 58"Large	24"Small
Photoperiod	seasonal	seasonal	9 hours	16 hours
light intensity	seasonal	60% seasonal	1800 f-c top 1100 f-c bottom	1800 f-c
temperature	seasonal	minimum 63°F, maximum seasonal	80°F	
water	minimum once/week	daily	daily	
fertilizer	once/year Nitro foam	once/week 15-8-4	Hoaglands concentrated, weekly	Hoaglands daily - 1X
insect pests	none critical	spider mites	spider mites	spider mites
insect control	none	pentac once/10 days, except Dichanthium	non- chemical	Ortho Home & Garden Spray

B. Preparation of Experimental Material for
    Observation

Unless otherwise indicated, all experimental material is

obtained from fresh, untreated pieces of leaves. Table 6

lists the ingredients of the three buffers used to suspend the

leaf material. The isoascorbate and pyrophosphate are added

just prior to the start of each experiment. Completed buffers

A and C are discarded after 16 hours. Completed buffer E may

be used for approximately one week. Incomplete buffers can be

stored for months in the freezer. Either substitution of NaOH

for KOH, or the presence of Tris buffer tends to alter the

fluorescence from that naturally observable in leaf sections

floating in H_2O. Consequently, these ingredients are avoided

in the standard buffers. The effects of Tris buffer and ions

on chloroplast fluorescence are discussed in sections I. C2 and I. C5.

A sharp stainless steel razor blade and a dry pith stick

are used to cut fresh cross sections of sugar cane leaves.

Softer leaves are sectioned on a Lab Line/Hooker Plant

Microtome #1225 (Fig. 9a). This microtome is specifically

designed to section fresh material. A sharp razor blade,

mounted at the end of a circularly rotating arm, comes in

contact with the leaf once each 360° rotation (Fig. 9b).

The frail leaf is supported from below by a rectangular piece

of carrot tissue. A manually operated stage holds the carrot-

supported leaf. Each notch of the manual advance control

Table 6. Composition of Experimental Buffers

	Jensen-Bassham Solution A-modified	Jensen-Bassham Solution C-modified	Solution E
Buffer	0.05M MES**	0.05M HEPES***	0.055M PO_4
pH	6.1 with KOH*	7.2 with KOH*	7.2 with KOH*
Sorbitol	0.33M	0.33M	0.33M
$NaNO_3$	0.002M	0.002M	0.002M
EDTA dipotassium	0.002M	0.002M	0.002M
$MnCl_2$	0.001M	0.001M	0.001M
$MgCl_2$	0.001M	0.001M	0.001M
NaCl	0.02M		
K_2HPO_4	0.005M	0.005M	buffer
Pyrophosphate* $Na_4P_2O_7 \cdot 10\ H_2O$	0.005M	0.005M	0.01M
Sodium isoascorbate* (reductant)	0.002M	0.002M	no reductant

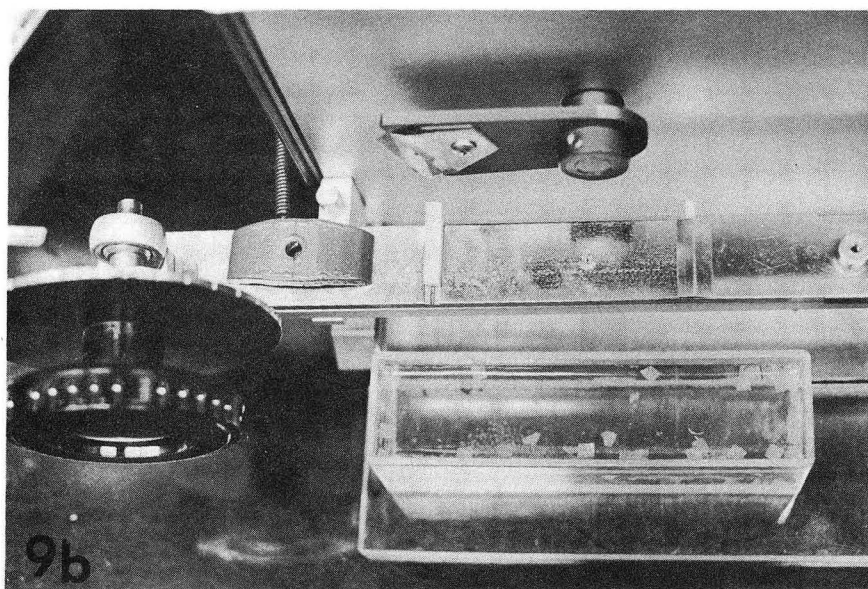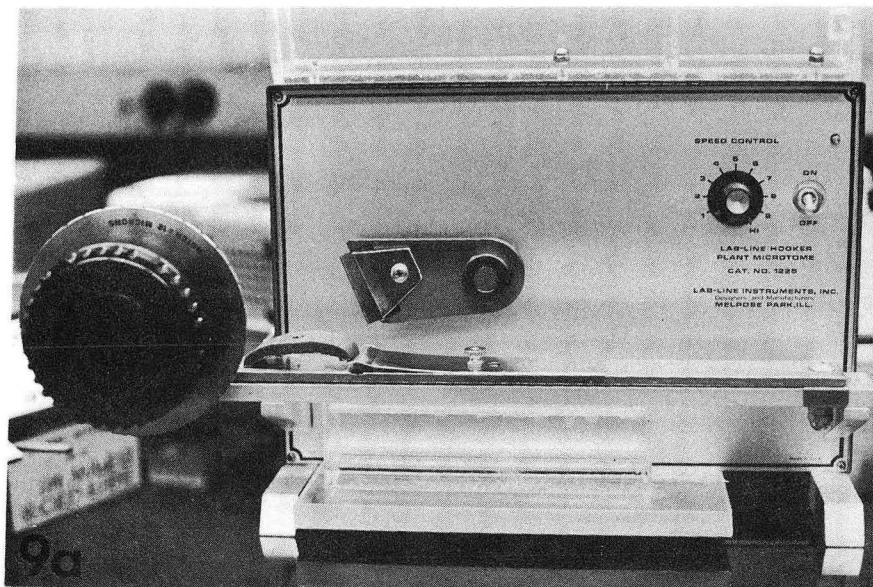* Stored separately - added just prior to use.

** [2-(N-morpholino) ethanesulfonic acid)]

*** (N-2-hydroxyethylpiperazine-n -2-ethanesulfonic acid)

Fig. 9a. Lab Line / Hooker Plant Microtome

#1225

Fig. 9b. A view, from above, looking down upon

the cutting mechanism of the microtome. The metal

plate which holds the carrot in place is removed.

XBB 7310-6165

pulls the specimen approximately 12 microns closer to the knife. Consequently, the thinnest possible section is 12 microns. Multiple advances resulting in sections approximately 24 to 36 microns thick can be made between knife rotations.

Chloroplasts are isolated into solutions A and C, according to the procedure of Jensen and Bassham (148). During the isolation of sugar cane chloroplasts, it is frequently necessary to remove excess starch grains and cell debris by a preliminary 5-minute centrifugation at 200 g. This cell debris also contains a small number of isolated cells.

Only fresh (unfixed), untreated leaf sections are photographed in color. Approximately one-half of the experiments involving high-speed black and white infrared film involve experimental chemical treatment of fresh (unfixed) leaf sections. Table 7 outlines these procedures.

Prior to microscopic examination, the specimens are covered with #1 1/2 cover glasses (0.16-0.19mm). Most objective lenses are corrected optically for this thickness in order to minimize spherical aberration (158). Beeswax is used to seal the cover glasses on those specimens destined to be photographed for periods longer than 10 minutes, after excess buffer is first removed with absorbent paper.

Specimens for electron microscopy are fixed according to the current fixation schedule of Laetsch et al. (Table 8).

Table 7. Chemical Treatments of Experimental Plants

	Final Concentration in Moles/liter	Solvent	Vacuum Infiltration	Minimum Time of Incubation In Minutes	Special Conditions	Removal of Chemical Treatment
NBT	10^{-4}	Buffer E	No	15	15°C strong light	No
DCMU	10^{-5}	Buffer E	No	5	4°C	No
DCMU	10^{-5}	Buffer E		5	4°C	No
followed by the addition			No		strong light	
of NBT	10^{-4}	Buffer E		15	15°C	Yes
Tris, pH 8.0	0.8	H_2O	Yes	60	4°C	Yes: substitute Solution E
Tris, pH 8.0	0.8	H_2O	Yes	60	4°C	Yes: substitute Solution E
transferred to						
HA	3×10^{-3}	Buffer E	No	5	4°C	No
Tris, pH 8.0	0.8	H_2O	Yes	60	4°C	Yes: substitute Solution E
transferred to NBT	10^{-4}	Buffer E	No	15	4°C	No

Table 8. W.M. Laetsch - <u>Current Electron Microscope Fixation</u>
<u>and Embedding Procedures</u>, Dec. 1970

Day 1

2% glutaraldehyde in 0.1M. Na Cacodylate buffer - 3 hrs. room temp.
    rinse in 0.1M. Na Cacodylate buffer 20 min. 3 times at room temp.

2% O_sO_4 in 0.1M. Na Cacodylate buffer - 1-2 hours at 4°C

30% Acetone   30 min. at 4°C
50%   "   30 min. "   "
70%   " & 1% Uranyl Nitrate   overnight "   "

Day 2

90% Acetone   15 mins. at 4°C
95%   "   15   "   "   "
100%   "   20 mins. 4°C warm to room temp.
100%   "   30 mins. 2 times at room temp.
Propylene oxide   30 mins. 2 times "   "   "

To 1 ml Propylene oxide add 5 drops Coulter Epon   15 mins.
                                1.5A /1.0B + 1 1/2% Vol. DMP
"   "   "   "   "   " 5 more drops Coulter Epon 15 mins.
"   "   "   "   "   " 10 more   "   "   "   60 mins.
"   "   "   "   "   " equal volume   "   "   2 hours

Pure Epon -------------------------------overnight room temp.

Embed in moulds. After 8 hours, transfer to 45°C. After 15
additional hours, transfer to 60°C. Let the moulds harden for
2 days at 60°C and for 1 day at 95°C.

C. Fluorescence Photomicroscopy

The following is a list of microscope equipment used throughout this investigation (Fig. 10):

1. Zeiss Fluorescence Photomicroscope

2. High-Pressure Mercury Vapor Lamp, HBO 200 W/4 (Fig. 11).

3. KG1 Heat-Absorbing Filter (Zeiss #46-78-30, Fig. 12b).

4. BG38 Red Suppressing Filter (Zeiss #46-78-85, Fig. 12a).

5. BG 12 Exciter Filter (Zeiss #46-78-89, Fig. 12c).

6. Heat Reflecting Filter (Zeiss #46-78-32, Fig. 12b) or one centimeter path of 7% $CuSO_4$.

7. Achromatic - aplanatic phase contrast fluorescence condenser (NA - 1.4).

8. Objective lenses: Planapochromat 25/0.65; Apochromat 40/1.0 oil with iris diaphragm; and Phase 100/1.3 oil.

9. #53 Barrier Filter (Zeiss #46-78-66, Fig. 12d).

The adjustment of the above equipment to conditions optimal for observation of fluorescence is critical for fluorescence photomicroscopy. The optics must be carefully aligned, while all diaphragms must be open. The condenser and lenses used must be of the highest possible numerical aperture. The condenser is coated with oil and set on its bright-field position in order to maximize the collection of light.

Fig. 10

Spectral emission of HBO 200 W super-pressure mercury lamp
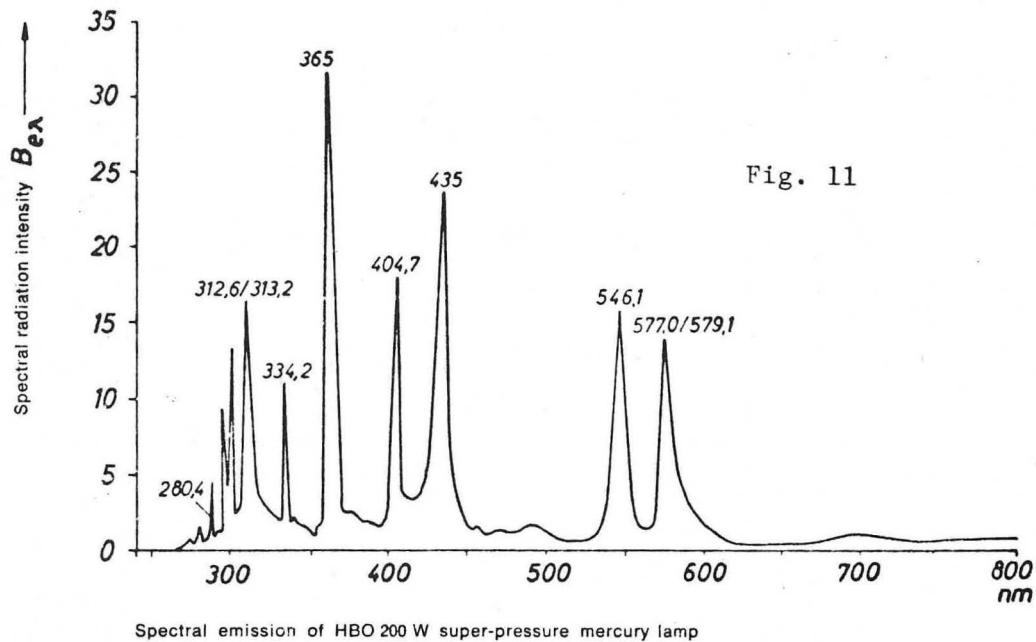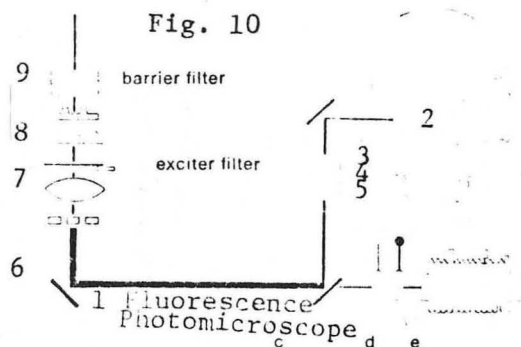
Fig. 10. The path of light in the fluorescence photomicroscope. after (298).

Fig. 11. Spectral emission of HBO 200 W super-pressure mercury lamps. after (298).

a

Diagram 9:
46 78 85
BG 38 minus red filter, 32 mm dia.,
2.5 mm thick

b

Diagram 6:
46 78 30
KG 1 heat-absorbing filter, 32 mm dia.,
2 mm thick
46 78 32
heat-reflecting filter, 32 mm dia.,
2 mm thick

c

Diagram 7:
Exciter filters for reflected-light
fluorescence microscopy:
46 78 86
UG 5 exciter filter, 32 mm dia.,
2 mm thick
46 78 87
UG 1 exciter filter, 32 mm dia.,
1.5 mm thick
46 78 88
GB 3 exciter filter, 32 mm dia.,
2.5 mm thick
46 78 89
BG 12 exciter filter, 32 mm dia.,
3 mm thick

d

Diagram 10:
46 78 67
barrier filter −65, 18 mm dia.,
0.9 mm thick
46 78 66
barrier filter 53, 18 mm dia.,
2 mm thick
46 78 65
barrier filter 50, 18 mm dia.,
2.2 mm thick
The barrier filters −65 and 53 are
mounted in the upper.
the barrier filter 50 in the central slide
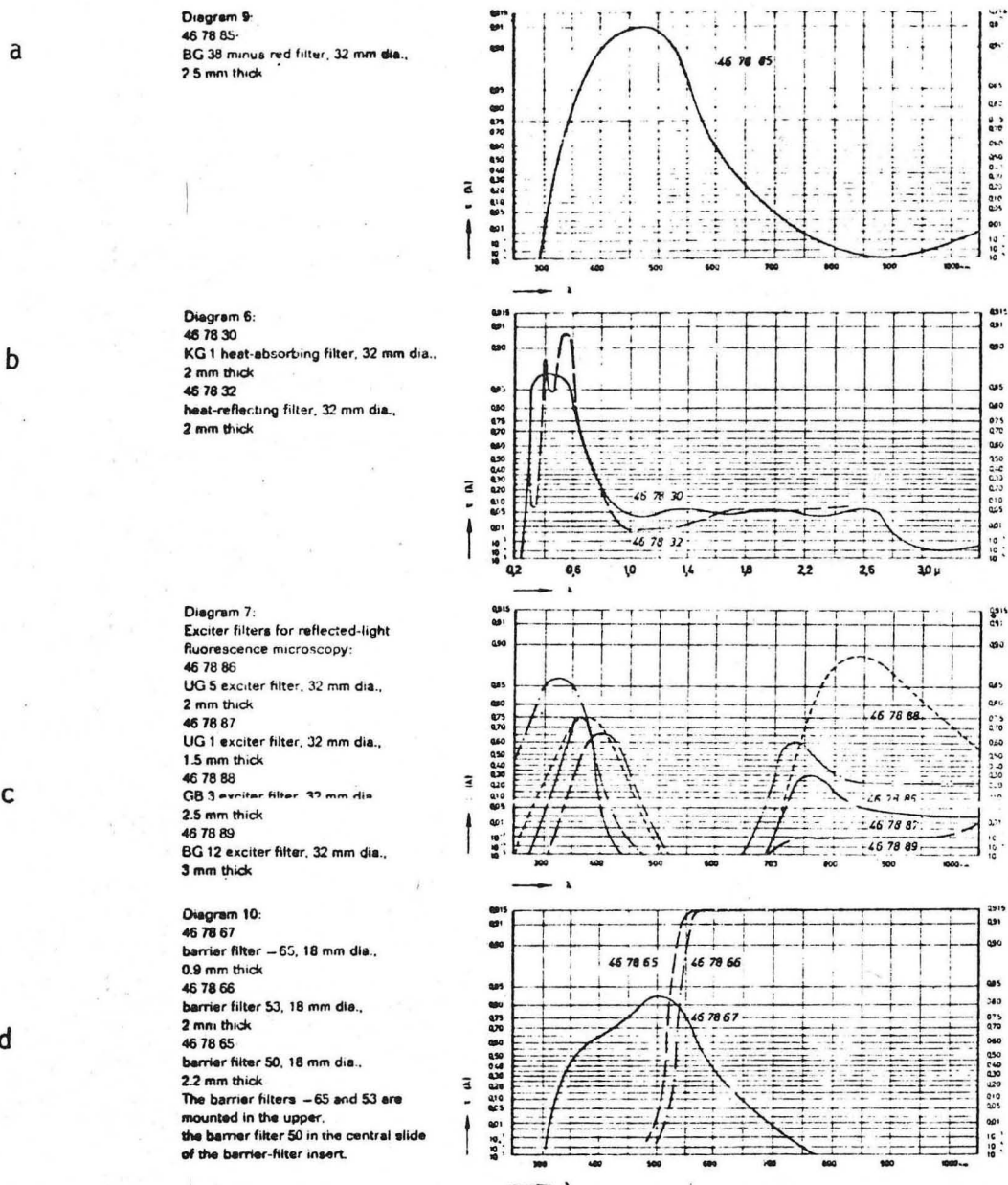of the barrier-filter insert.

Fig. 12. Spectral properties of Zeiss filters.
after (296).

For color photography, the condenser is adjusted to attain the most intense, visible, even fluorescence possible. Since it is desirable to have a uniform actinic light intensity for all quantitative high-speed black and white infrared photographic work, the need for a uniform condenser setting becomes critical. This setting is standardized by adjusting the condenser for Kohler illumination prior to switching to fluorescence.

Although the Zeiss photomicroscope contains a built-in automatic camera, it is not suitable for fluorescence photomicroscopy. Even under ideal conditions, the fluorescence intensity is very weak, while the indirect optical path between the specimen and the film results in a loss of nearly 90% of the potential luminous intensity (65). Although this does not interfere with transmitted light photomicroscopy, the loss is quite unacceptable for fluorescence photomicroscopy. This intensity loss is supposedly eliminated on the newer model Zeiss microscopes because the camera is located directly above the objective lens. Further problems arise from the insensitivity of the built-in light meter to wavelengths of light above 650 nanometers (295). Since almost all chloroplast fluorescence occurs at wavelengths above 650 nanometers, the cesium-antimony photocell is not an appropriate light detector.

The best results are obtained by mounting a camera back on the microscope top, in direct line with the specimen (Fig. 13a).

Fig. 13a. Zeiss fluorescence photomicroscope with Besseler Topcon camera back mounted on top.

    camera back   (c)

    straight mounting tube (t)
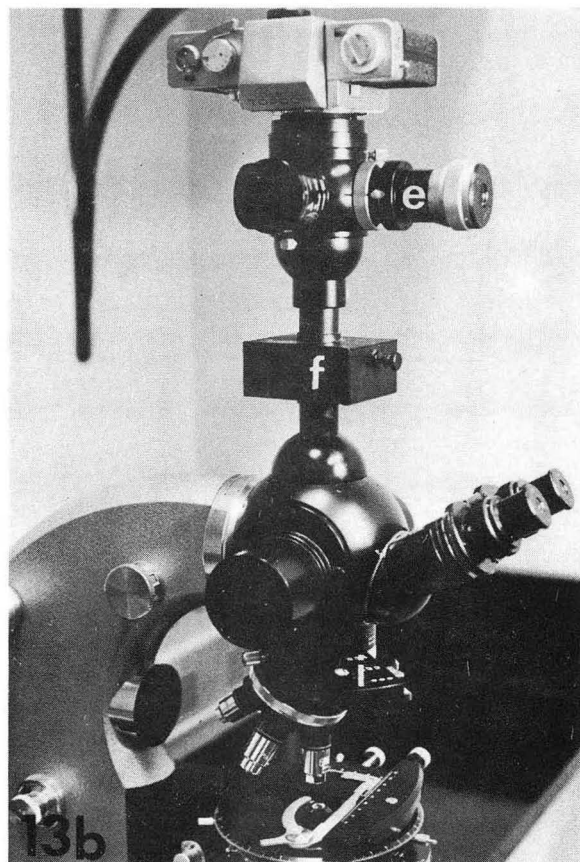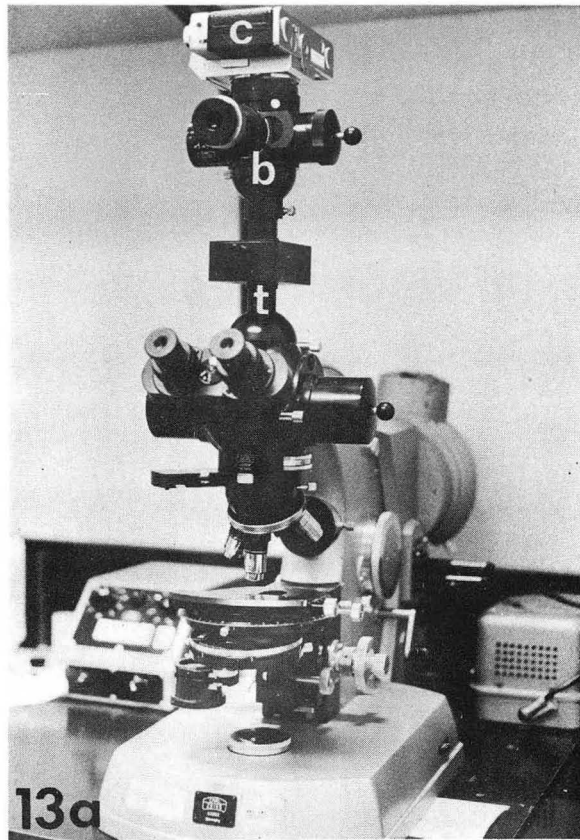
    basic body II   (b)

Fig. 13b. Another view of the microscope showing the optical equipment between the specimen and the film.

    custom made filter box   (f)

    insert for barrier filters (i)

    focusing eyepiece   (e)

XBB 7310-6164

This is made possible by a straight mounting tube (Zeiss #47-39-20), and a Basic Body II (Zeiss #47-60-11). An adapter is also necessary for commercial cameras. The Basic Body II incorporates a rotatable prism which can vary the direction of the light beam between the camera and the focusing eyepiece (Zeiss #47-60-25).

The straight mounting tube includes a custom-made filter box (Fig. 13b) which permits the insertion of 2" x 2" glass filters between the specimen and the camera.

A Wratten 88A filter transmits infrared radiation while blocking visible radiation (Fig. 14a). A Corning 2-63 Filter cuts off all wavelengths below 580 nm, while transmitting 85% of all wavelengths above 630 nm (Fig. 14b). This filter, while not interfering with chloroplast fluorescence, effectively eliminates the fluorescence of lignin which can interfere with the quantitative analysis of high-speed black and white infrared film.

Both Wratten and Corning filters can be cut to a size easily inserted into the microscope column. Since interference filters cannot easily be cut, the use of a series of Baird-Atomic interference filters necessitated the construction of the filter box shown in Fig. 13b.
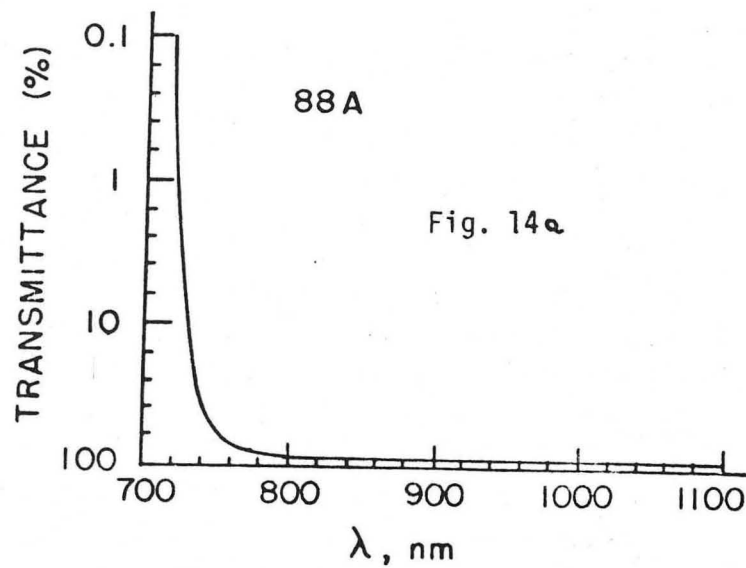
Twelve of the thirteen Baird Atomic Interference Filters belong to the B-1 series, and consequently have a half band

Fig. 14a. Spectral properties of Wratten 88A filter. after (159).

Fig. 14b. Spectral properties of Corning glass filters. Starting at the left: 2-63, 2-62, 2-61, 2-60, 2-59, 2-58, 2-64. after (80).
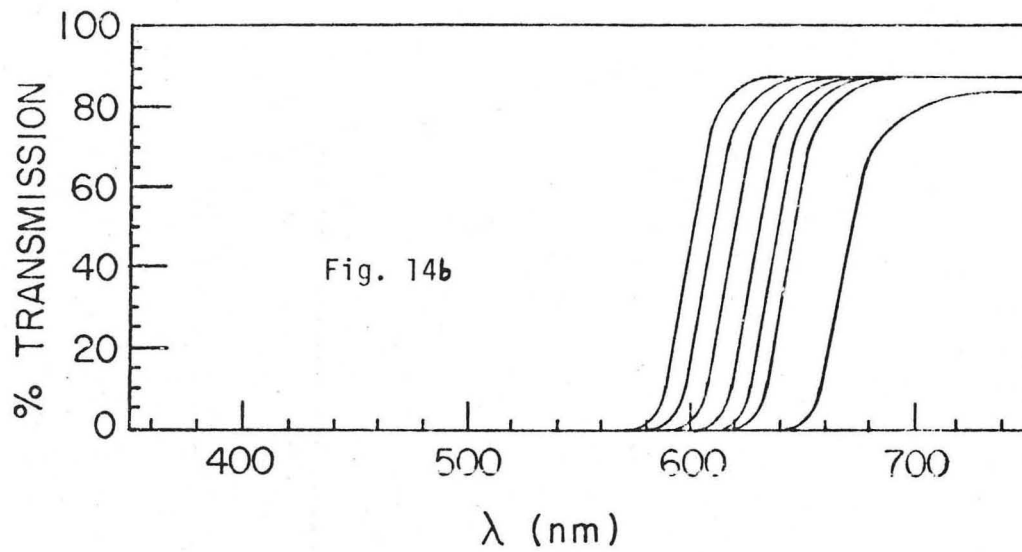
XBL718-5288

width of 10 nm (Fig. 15 and 16). The 709 nm interference filter belongs to the BA-1 series and has a half band width of 5 nm (Fig. 16). We have checked that all of the interference filters are blocked against secondary transmissions. The total transmission outside the transmission band region is less than 0.1% (17). This percentage was confirmed as described below.

The percentage transmission of each filter is measured from the spectra obtained on a Cary Model 14 spectrophotometer equipped with a "%T slidewire" (Fig. 15 and 16). Perpendicular positioning of the filter is critical, and is most easily attained with the "Cary Standard Transmission Accessory".

The area under the Percentage Transmission Curve of a filter is a measure of its total percentage transmission (Table 9). Since the filters are used for a quantitative analysis of fluorescence emission, it is necessary to correct for this varied transmission. The proper filter correction factor is determined by comparing the area under the % transmission curve for one filter with the corresponding area for the filter with the maximum transmission (cf. section IV.F).

D. Film

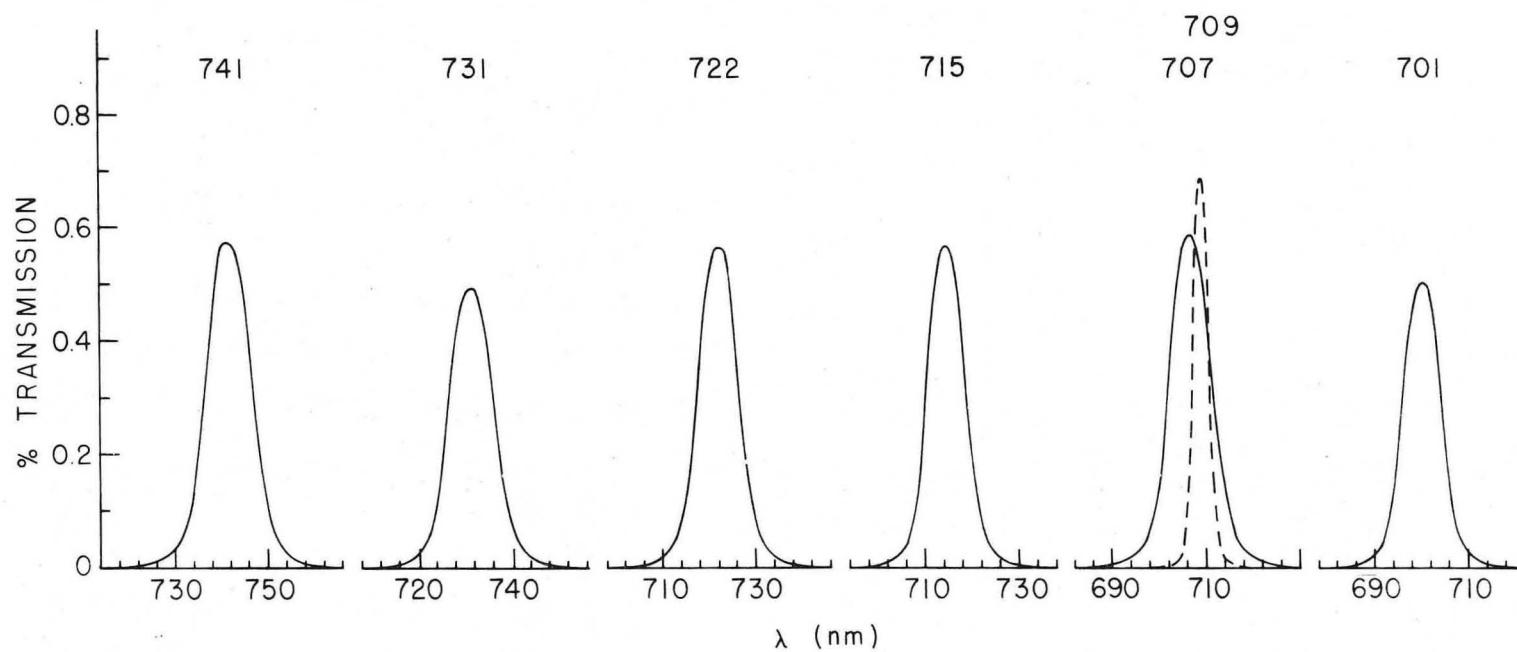### 1. Analysis of Emulsion Characteristics

When quantitatively analyzing film exposed to different wavelengths of light, it is necessary to correct for the

Fig. 15. Spectral properties of Baird Atomic interference filters.
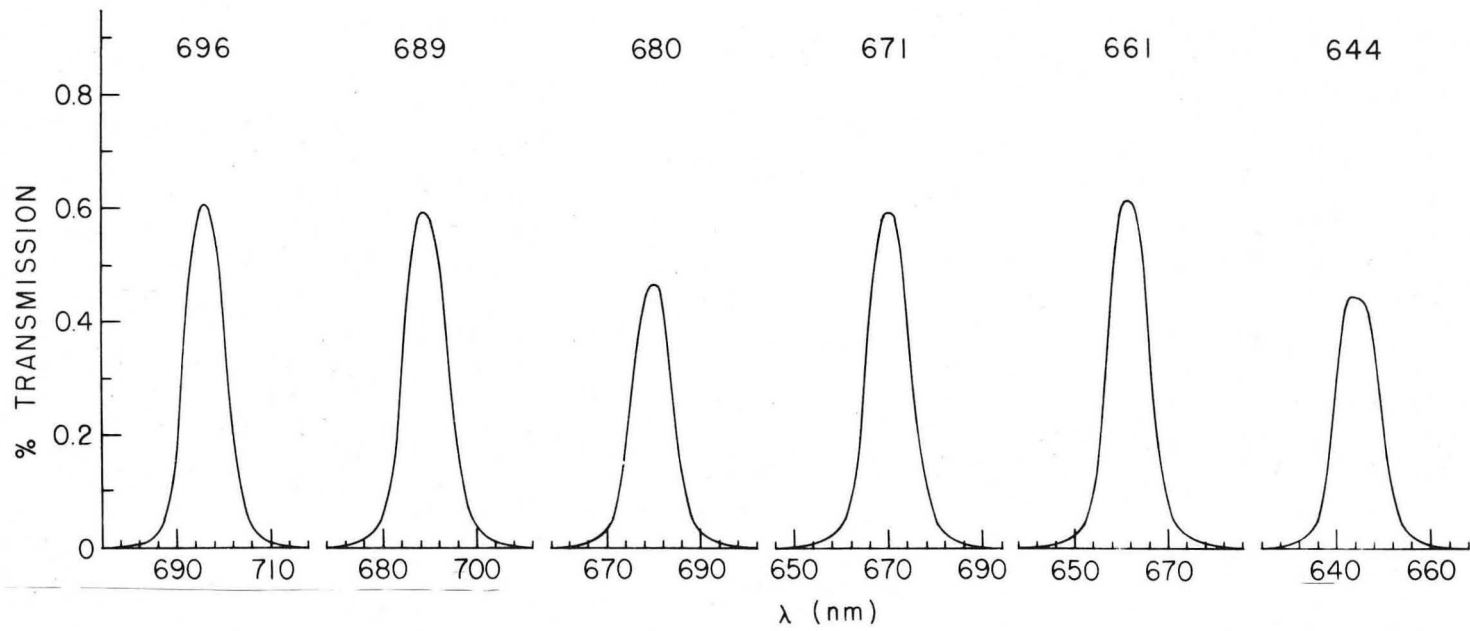
Fig. 16. Spectral properties of Baird Atomic interference filters.

XBL 718-5287

Table 9.   Relative Spectral Sensitivity of High Speed Black and
White Infrared Film and Interference Filters

Peak Wavelength of 20 nm band	Relative Diffuse Film Density*	Relative Area Under Percentage Transmission Curves
644	11.24	0.22
661	10.61	0.29
671	10.90	0.28
680	11.03	0.21
689	11.89	0.29
696	12.65	0.28
701	12.52	0.22
707	12.90	0.28
709	12.90	0.12
715	13.20	0.24
722	12.99	0.26
731	12.91	0.23
741	13.23	0.30

*as measured on the Joyce-Loebl Double Beam Recording Microdensito-
meter (cf. II. E).

spectral sensitivity of the film emulsion. A 35-mm camera loaded with the film under investigation, is placed in front of the exit slit of a Bausch and Lomb 500 nm grating monochrometer. For an accurate comparison, the film must be exposed to equal numbers of quanta of different wavelengths of light. A calibrated silicon photocell (92) is substituted for the camera that was in the path of the exit rays of the monochrometer so that the number of quanta may be adjusted. The 3mm slit width setting corresponds to a half band width of 10 nm.

Therefore, it is now possible to expose the film to approximately equal numbers of quanta of 20 nm wide bands of light centered at different wavelengths. An analysis of the density of the exposed film determines the spectral sensitivity of the film in that region (Table 9). In a manner analagous to that used to compute the filter factor, the film correction factor is obtained by comparing the relative diffuse densities of the film exposed to 20 nm bands of light centered at different wavelengths.

2. Infrared Color Films

With the exception of the photographs shown in Figures 21a and 22, Infrared Aero Ektachrome 8443 is the infrared color film exclusively used in this investigation. Since the film quality differs between emulsion batches, it is advisable to purchase large quantities of film of a single emulsion for a given

experiment. During the two-year course of this investigation, eighty rolls of infrared color film, corresponding to four separate emulsion batches, were used. The spectral response of each film emulsion is tested before the film is accepted for experimental use. The spectral responses of the four separate film emulsions accepted were uniform enough for qualitative color analysis. A fifth emulsion batch proved unacceptable.

Since infrared color film is especially sensitive to emulsion deterioration, the film must be obtained fresh and immediately stored at $-10^{o}C$ until its actual use. A "frozen" 35mm film cassette requires about four hours of thawing to return to room temperature. The film must be processed or refrozen (in the presence of a desiccant) immediately after it is exposed.

For proper development, infrared color film requires strict E-3 processing. The resultant positive image film (commonly referred to as "slides"), maintains a very precise spectral response. Figure 17 illustrates the response of the film to monochromatic light. Internegatives must be prepared from the slides in order to obtain these positive prints. The film is exposed according to the procedure outlined in Section II D; however, the monochrometer slit width is now set at 1 mm to provide greater spectral resolution.

As illustrated in Figure 17, infrared color film 8443, a false color film, records wavelengths between 660 and 690

Fig. 17a-c. Spectral response of Infrared Aero Ektachrome
film to monochromatic light. Starting at the top, the wave-
lengths are: 660, 690, 696, 698, 700, 702, 704, 706, 708, 710,
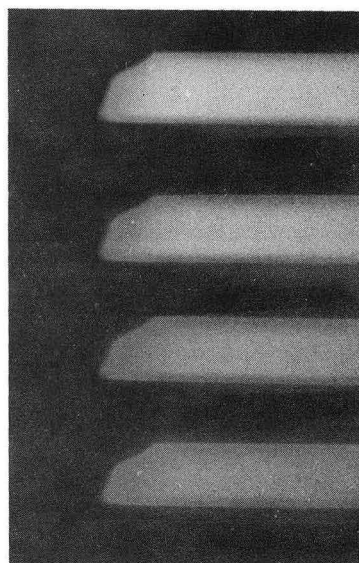715, 730, 750, 780.

Fig. 17d. Spectral response of Infrared Aero Ektachrome film
to double exposures of limiting amounts of 680 and 730 light.
The ratios of 680 : 730 starting at the top are as follows:
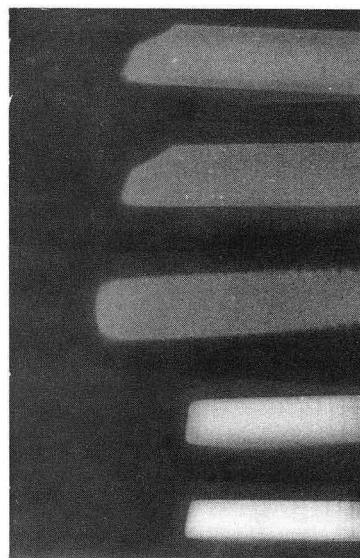2:1, 1:1, 1:2, 1:4, 1:8, 1:16, 1:32.

17a

17b

17c

17d
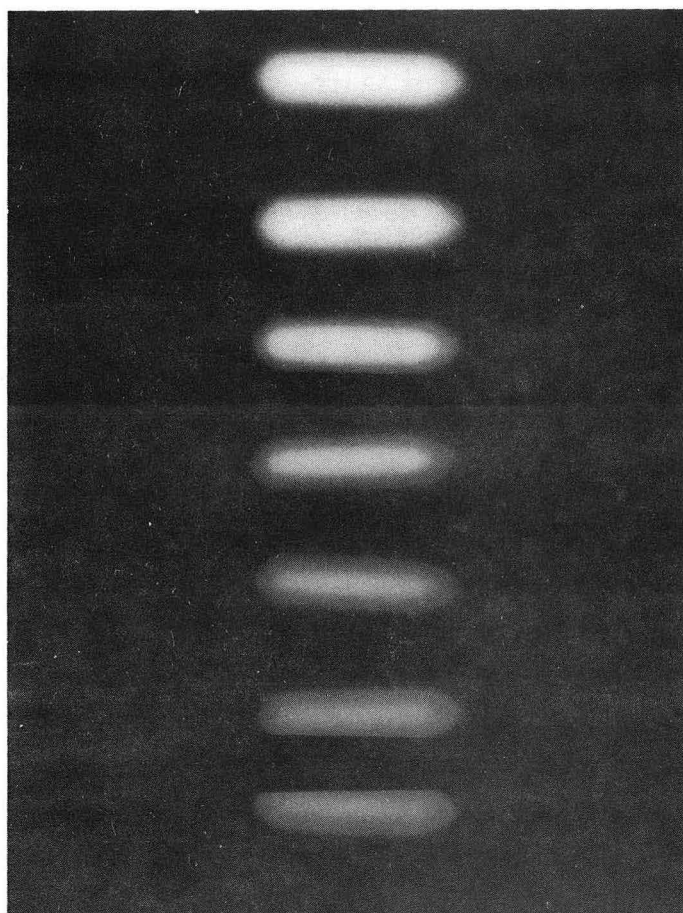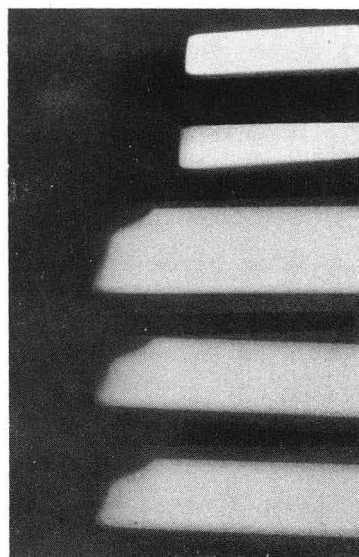
nm as yellow, wavelengths between 696 and 700 nm as gold, wavelengths between 702 and 706 nm as orange, wavelengths between 708 and 730 nm as red, and wavelengths between 750 and 780 nm as violet. Note the subtle, but distinct difference between yellow and gold. The film is therefore capable of registering unique responses to wavelengths in this region of the spectrum.

This very precise pattern of spectral response, is achieved as follows. Infrared color film 8443 contains separate cyan-forming, yellow-forming, and magenta-forming dye layers, each with a different spectral sensitivity (Fig. 18). The process of image formation in infrared color film, as in other positive image film, is one of bleaching, rather than of deposition. The spectral sensitivity of the cyan-forming layer refers to its loss of cyan dye at the stated wavelength of light. Figure 19 indicates the coordinated reactions of the three dye layers in infrared color film 8443 which produce its characteristic color formation. For example, only the cyan-forming layer is sensitive to 730 nm light. Consequently, a strong exposure to 730 nm light will cause the complete loss of cyan dye. In contrast, the yellow and magenta dyes will not be affected. These remaining yellow and magenta dyes blend to form the red color which is observed.

Similarly, exposure to 680 nm light equally bleaches the cyan and magenta-forming layers. Consequently,

Fig. 18. Spectral sensitivity of the three dye layers of Infrared Aero Ektachrome film, type 8443; cyan-forming layer (a), yellow-forming layer (b), magenta-forming layer (c). after (160).
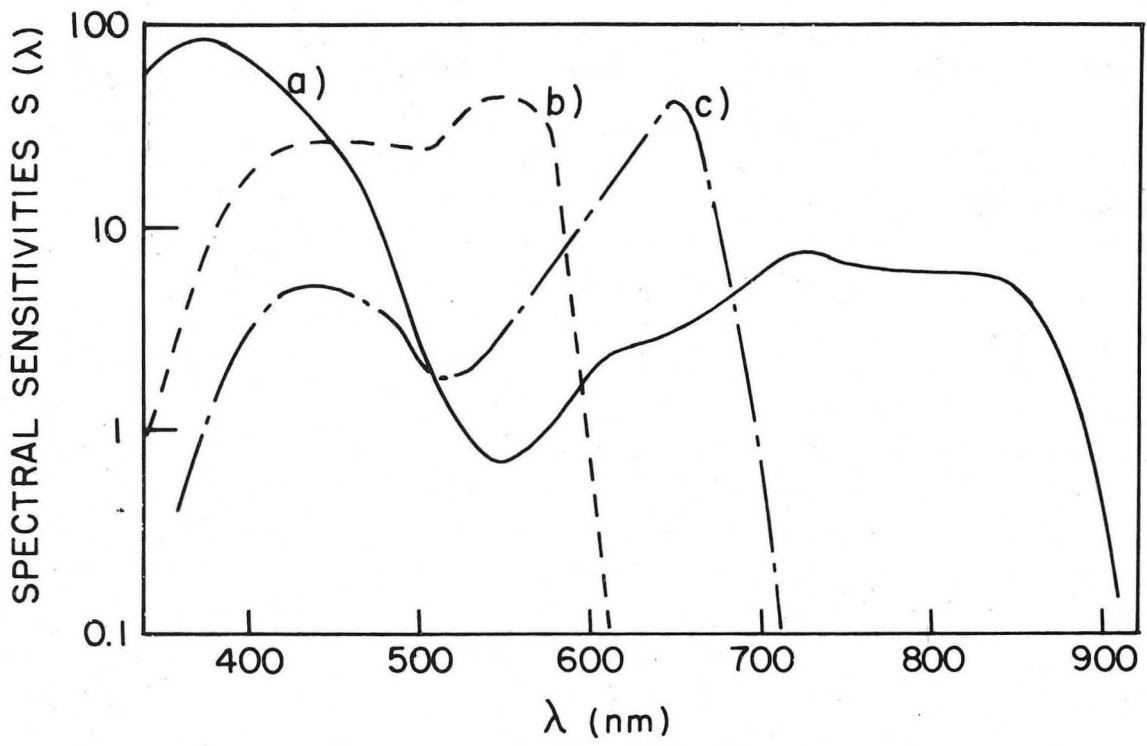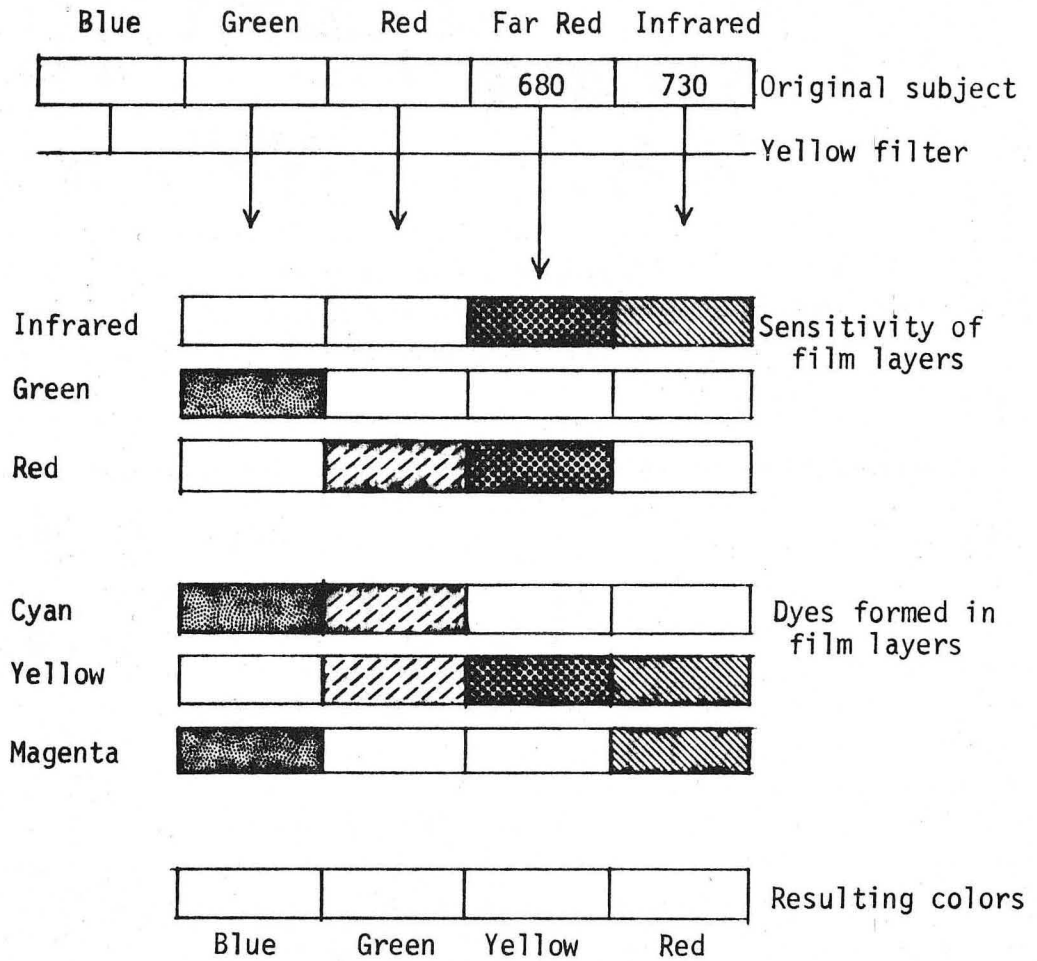

XBL717-5269

Fig. 19. Development of color in Infrared Aero Ektachrome film. Adapted from (160).

680 nm light of strong intensity will remove all cyan and magenta dyes from the film, leaving only the yellow dye to remain as the response to this wavelength.

Natural chloroplast fluorescence is not monochromatic in that it contains both far-red and infrared components. The boundary between far-red and infrared light occurs at 700 nm. Although the film records far-red light as yellow, and infrared light as red, the response to simultaneous exposure of both far-red and infrared radiation is complex. As explained above, since dye-layer sensitivity is equivalent to dye bleaching, the action of infrared light on the cyan layer is redundant with the action of intense far-red light. Far-red light of sufficient intensity will cause the loss of the cyan as well as the magenta dye. Concomitant infrared light obviously need not bleach cyan dye if the far-red light is capable of bleach-ing it all. Therefore, the addition of infrared radiation to far-red radiation can only affect the film when the far-red radiation is too weak to bleach the cyan layer completely. Conversely, once the film is exposed to sufficient amounts of far-red light to have lost its magenta dye, it will no longer be capable of forming the red color indicative of infrared exposures.

Figure 17d explores the response of infrared color film 8443 to double exposures of limited amounts of far-red and infrared light. The film turns red-orange, instead of red,

with as little as a 1:4 incident ratio of far-red to infrared
light. A true orange color develops when the ratio is 1:2.
A true gold color is attained when the ratio is 1:1. A pure
yellow is obtained when the ratio is 2:1. Therefore, when as
little as one-fifth of the incident light is from the far-red,
formation of a true red color is no longer possible. When at
least half of the incident light is from the far-red, formation
of a true orange color is no longer possible. The gold color
resulting from an equal mixture of far-red and infrared light
is readily distinguishable from orange. A yellow color is not
attained unless 60% or more of the light is from the far-red.

Consequently, a yellow color on the film could either be in-
dicative of exposure to far-red light, or of a predominance of
far-red over infrared light. Similarly, a gold color results
either from light between 696 and 700 nm, or from simultan-
eous exposure to approximately equal quantum fluxes of red
and far-red light. An orange color indicates incident wave-
lengths between 701 and 704 nm, or else a predominance of
at least 66% of infrared relative to far-red light quanta.
A true red color is indicative of at least 80% infrared
light, and a maximum of 20% far-red light.

Infrared Aero Ektachrome film 8443 is therefore an ideal tool
for studying chloroplast fluorescence because of its innate
ability to distinguish between far-red and infrared components
of fluorescence. Some of this precision is lost in making

prints from different slides, thereby diminishing the distinction between red, red-orange, and orange, as originally recorded on the film.

Although underexposure or overexposure can affect the colors recorded by infrared color film 8443, the dye response to infrared versus far-red light still remains different. In the case of underexposure, the distinction is maintained by the orange color which results from far-red exposure, versus the deep red color development resulting from infrared exposure (Fig. 20a). Overexposed film maintains the distinction between far-red and infrared by showing yellow-white versus orange color development, respectively (Fig. 20b).

During the summer of 1971, the Eastman Kodak Company ceased producing Infrared Aero Ektachrome Film 8443, and started to produce Ektachrome Infrared Film in its place. Although fresh Ektachrome Infrared Film, when processed by the readily available E-4 development process, supposedly responds similarly to Film 8443, it is not well suited to a scientific investigation of chloroplast fluorescence. Its most serious disadvantage is an unpreventable, relatively rapid emulsion deterioration. In contrast to the Infrared Ektachrome Aero Film used in this investigation, and stored without resultant deterioration for as long as a year at $-10^{\circ}C$, the 3 separate batches of Ektachrome Infrared Film purchased deteriorated within a month at $-10^{\circ}C$. In addition, although fresh Ektachrome Infrared Film can also distinguish between far-red

Fig. 20a. Underexposed (4 seconds) infrared fluorescence photograph of a cross section of a leaf of <u>Dichanthium</u> <u>annulatum</u> (77-5), buffer C, pH 7.1. X 250.

Fig. 20b. Overexposed photograph (60 seconds) of the same leaf section. X 375.

Fig. 20c. Fluorescence photomicrograph of glutaraldehyde-fixed sugar cane chloroplasts (15b-35a) separated on a sucrose density gradient and recorded on High Speed Ektachrome film. Although the chloroplasts have been damaged by harsh treatment, the bundle sheath chloroplast fluorescence appears to be a purple red, as opposed to the scarlet red color characteristic of the mesophyll chloroplast fluorescence. X 1600.
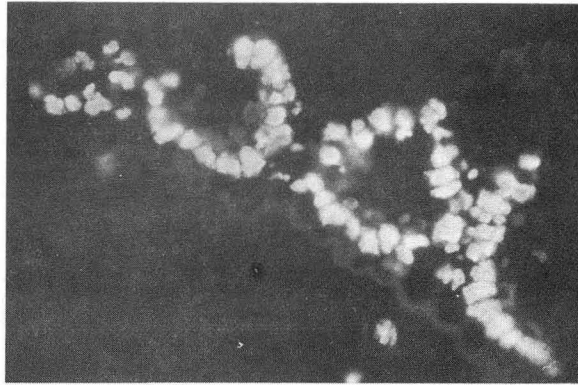
20a
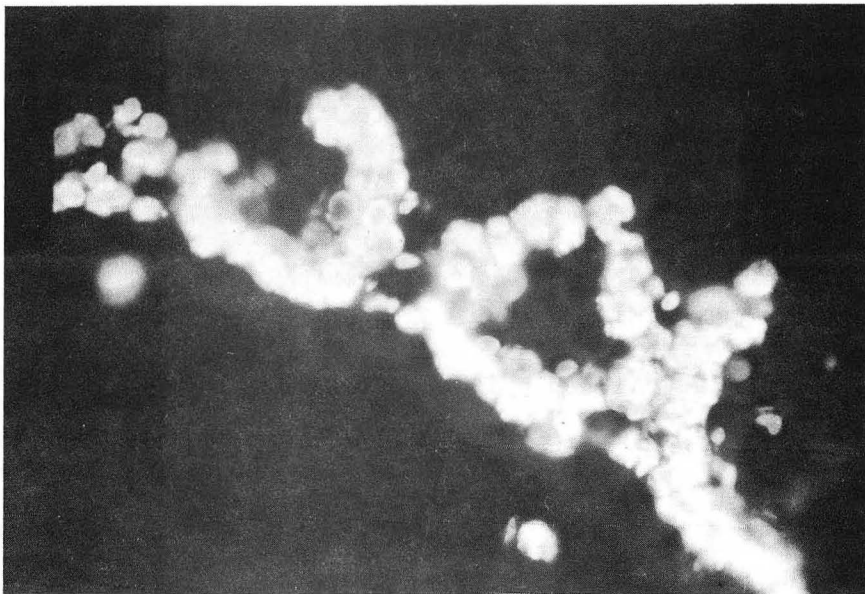
20b
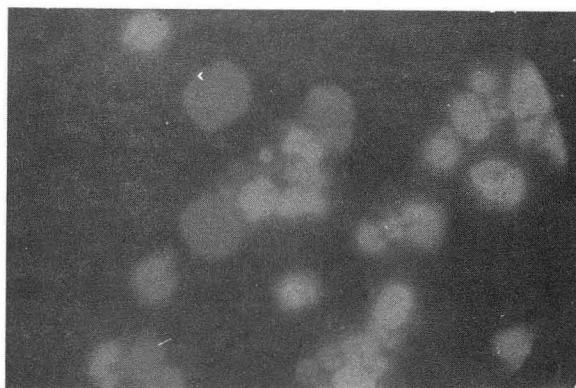
20c

XBB 7310-6125

and infrared radiation (Fig. 21a), the resulting colors are
not nearly as distinctive as those recorded on Infrared Aero
Ektachrome Film (Fig. 21b). The colors associated with Ekta-
chrome Color film developed according to the E-4 process
(Fig. 21a) can be sharpened by changing the development proce-
dure to the E-3 process (Fig. 22) (124). The resulting colors
are not too different from those developed with Infrared Aero
Ektachrome 8443 (Fig. 22).

3. Control Films

Both High-Speed Ektachrome (daylight) and Kodak Infrared
(black and white) film are used for control photographs. Since
the spectral sensitivity of the High Speed Ektachrome film is
similar to that of the human eye, the photographs record those
components of fluorescence within the visible portion of the
spectrum. A chloroplast with a strong far-red component of
fluorescence appears as a rich scarlet red, while a chloroplast
with a strong infrared component of fluorescence is barely
visible as a deep purple (Fig. 20c).

Kodak Infrared (black and white) film is sensitive
throughout the entire visible, as well as most of the infra-
red, portion of the spectrum (Fig. 23a). Since the response
is fairly uniform to wavelengths between 640 and 740 nm,
the density of the resulting photographic negative can
be used to approximate relative fluorescence intensities,
after applying a minor correction factor.

Fig. 21a. Fluorescence photomicrograph of a cross section
of a leaf of Euphorbia serphyllifolia (64-3a) recorded on
Kodak's new Ektachrome Infrared film, processed as directed,
buffer C, pH 7.3. X 375.

Fig. 21b. Same as above recorded on Infrared Aero Ektachrome
Film X. 250.

Fig. 21c. Same as above, recorded infrared black and white
film (66-1A). X 325.

Fig. 22. Fluorescence Photomicrograph of a cross section of
a leaf of Dichanthium annulatum recorded on Kodak's new
Ektachrome Infrared film, processed with the E3 process
in order to change the characteristics of the film, buffer C,
pH 7.0 X 625.
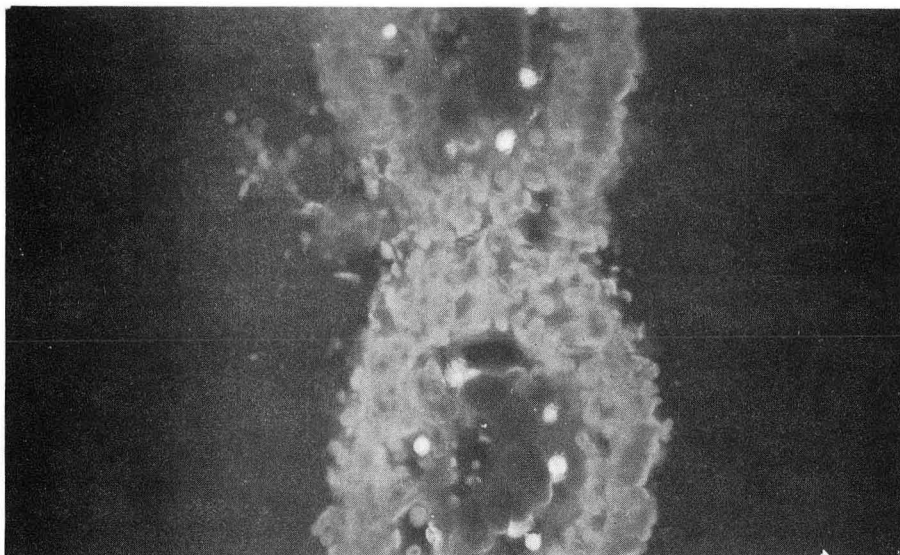
21a
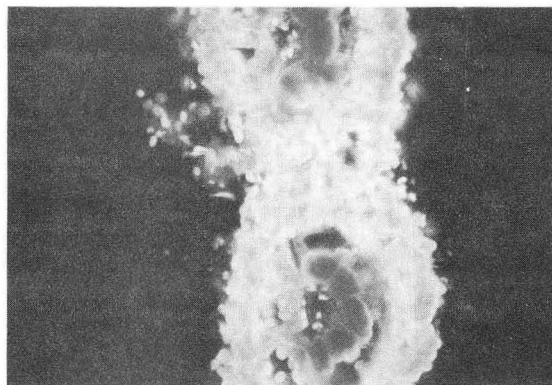
21b
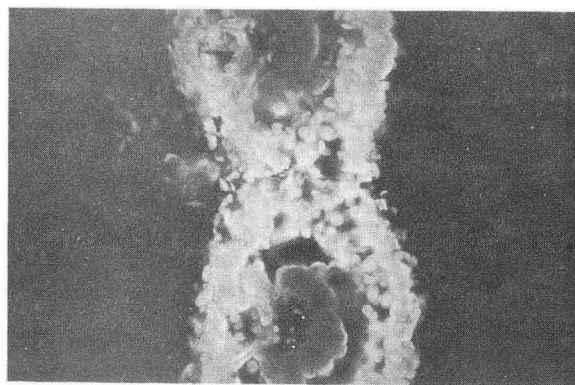
21c

XBB 7310-6124
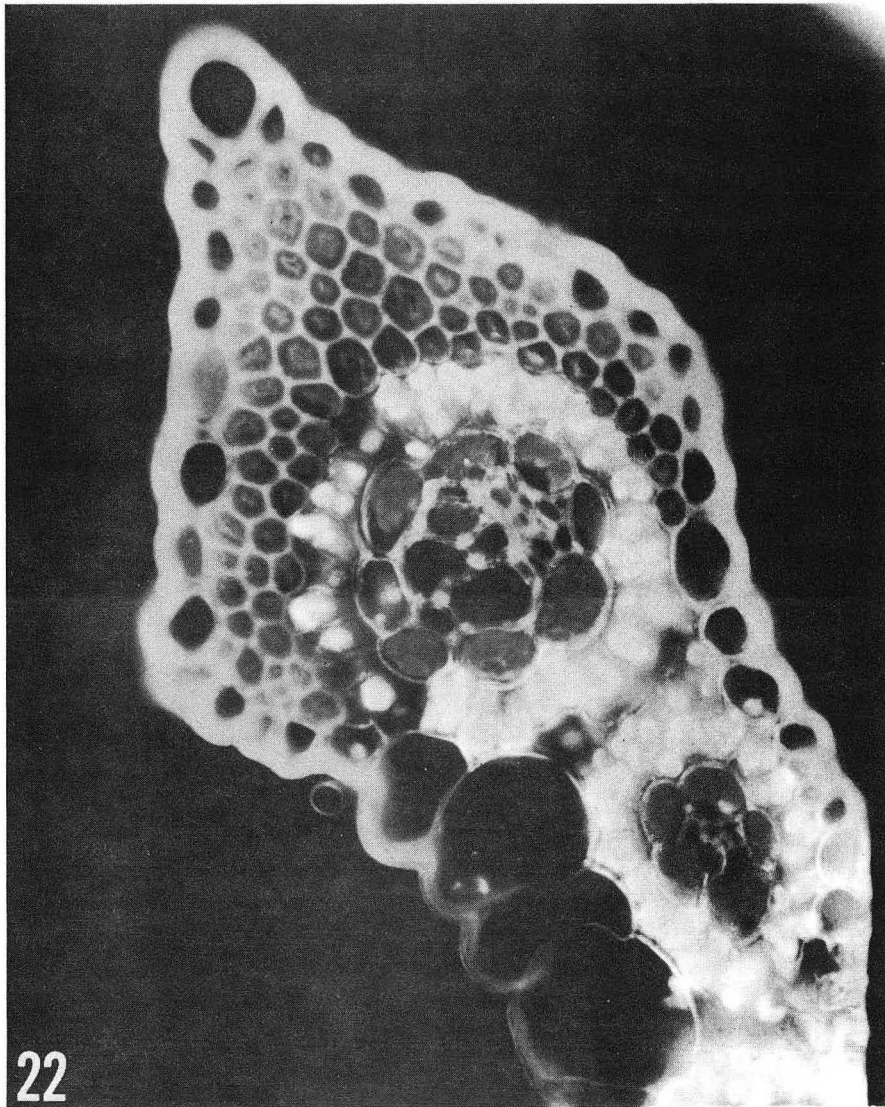
22

XBB 7310-6123

SENSITOMETRIC DATA

Spectral Sensitivity* Curves

Developed 12 minutes in KODAK Developer D-76 at 68 F
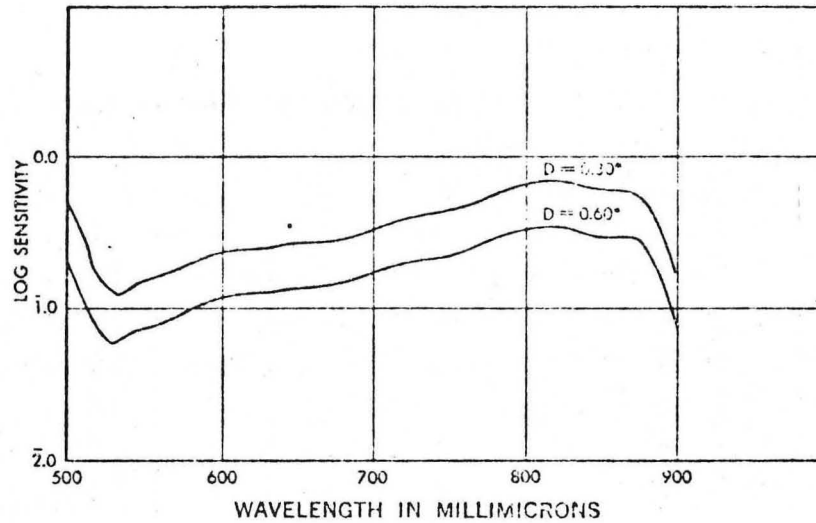
*Sensitivity = reciprocal of exposure (ergs/cm²) required to produce specified density above density of base plus fog.

Spectral Sensitivity Curve
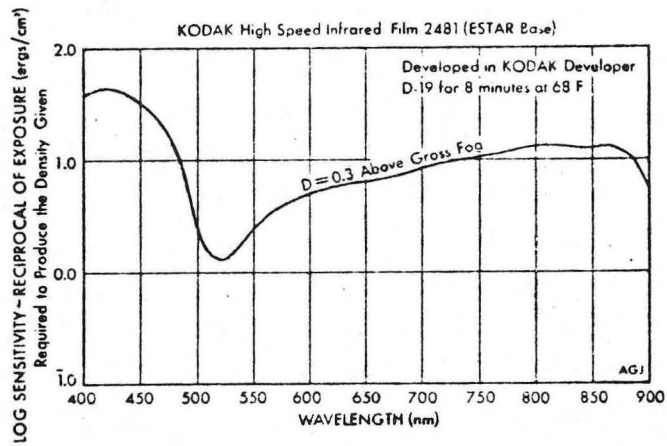
Fig. 23a. after (162).

Fig. 23b. after (163).

4. High-Speed Black and White Infrared Film.

High-speed black and white infrared film maintains approx-
imately the same spectral response as Kodak Infrared (black and
white) film (Fig. 23b). However, the high-speed film is approxi-
mately ten times as sensitive to light. Consequently, this film
must remain in total darkness, until development is complete,
except during photographic exposures.

High-speed black and white infrared film, like its color
counterpart, is very sensitive to temperature, and should be
stored at $-10^{\circ}C$ with a desiccant. Similarly, the development
procedures are equally critical to both films. For uniform
results it is necessary to develop the film at $20^{\circ} \pm 0.3^{\circ}C$ for
12 ± 0.05 minutes. This critical development period is followed
by a sequence of procedures with less critical time and tem-
perature controls. These include a thirty-second "stop-bath",
a seven-minute fixation, a two-minute "hypo-clear", and a six-
minute water rinse. When dry, the unnumbered film is labeled
with a rapidograph pen.

Aspects concerned with the quantitative analysis of this
film are discussed in Section IV-C.

E. Microdensitometry

The Joyce, Loebl Double-Beam Recording Microdensitometer
is used to analyze the density of photographic negatives
(Fig. 24). This instrument compares the density of a circular

Fig. 24a. Joyce Loebl Double Beam Recording
Microdensitometer.

Fig. 24b. Scanning stage of the microdensitometer showing
the photographic negative to be scanned in place.

Scanning specimen stage   (s)

graph paper support   (g)

arm connecting "g" and "s"   (a)

case that holds the grey wedge
and carriage which attaches it
to the recording pen   (c)

photographic negative   (n)

Fig. 25. Densitometer tracing of a photograph (2.3 second
exposure) of Tris-treated Dichanthium annulatum bundle sheath
chloroplasts (131 T - F - 36). Each peak is a result of two
or more scans across a single chloroplast. The maximum rela-
tive density, as indicated by the uppermost mark of the
recording pen, is written above each peak.
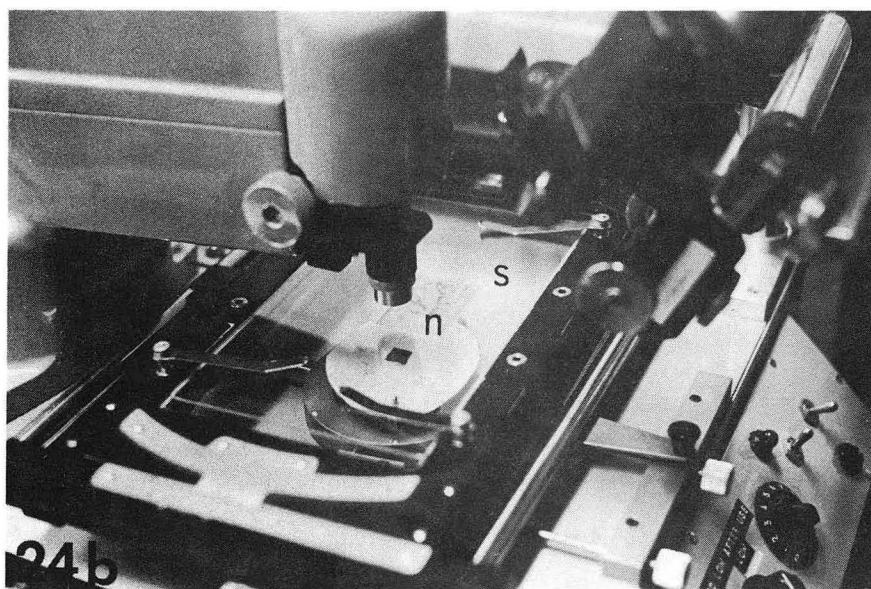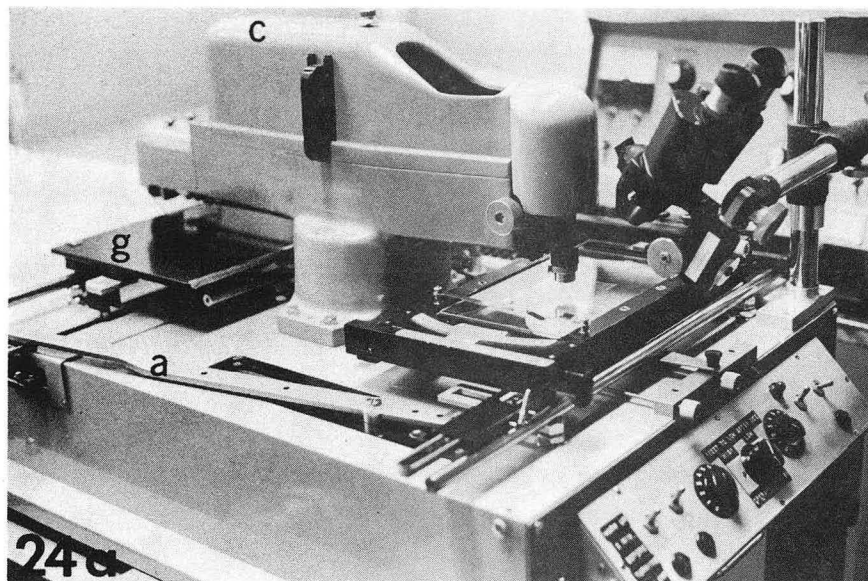
XBB 7310-6163
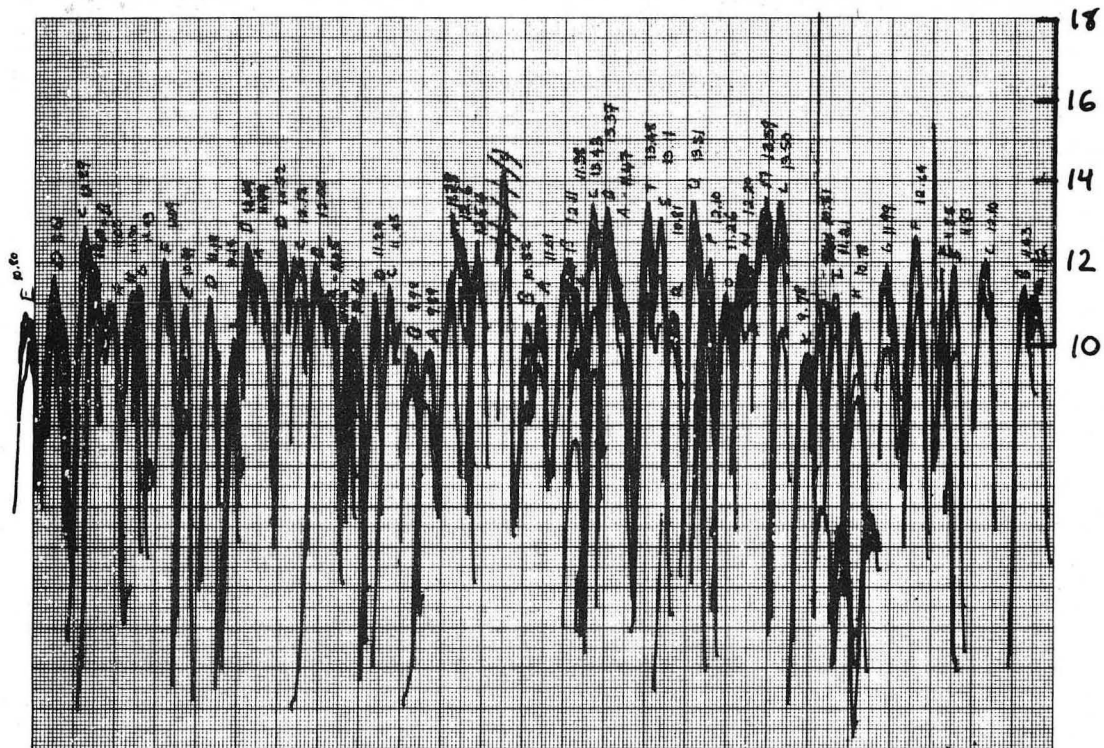
Fig. 25. Densitometer tracing of a photograph (2.3 second exposure) of Tris-treated <u>Dichanthium annulatum</u> bundle sheath chloroplasts (131 T - F - 36). Each peak is a result of two or more scans across a single chloroplast. The maximum relative density, as indicated by the uppermost mark of the recording pen, is written above each peak.

area approximately 0.1 mm with that of a standard grey wedge. A recording pen is attached to the carriage which scans the wedge in search of the equivalent density. As the carriage moves, the pen marks the graph paper. Since the graph paper used has a vertical axis of 18mm, the maximum relative density is approximately 18. The photographic negative to be scanned is placed on a stage whose movement is coordinated with that of the sheet of graph paper held on a separate stage. Both the scan speed and the density range of the grey wedges are variable. The relative density units between 9.0 and 18.5, recorded with the medium grey wedge, correspond to an O.D. of between 0.3 and 1.2. Since the measured density varies with the size of the measuring beam, only one size measuring beam is used throughout this investigation. The resultant bias in measurement is therefore constant and eliminated by the use of relative density units.

Perhaps the greatest error results from faulty alignment of the instrument. Before a given photographic negative is scanned, the densitometer optics must be aligned in a manner similar to adjusting a microscope for Kohler illumination. Any incorrect adjustment results in an inaccurate zeroing of the recording pen relative to the background density of the film.

Although constant checking can keep alignment error to a minimum, irregular film emulsions increase the difficulty

of setting the background density of the film at zero. It therefore becomes necessary to scan the background of the film for a minimum density, instead of arbitrarily choosing a blank area as the standard background.

In this investigation, the densitometer is used to record the maximum relative density of chloroplasts in fluorescence photomicrographs of cross sections of leaves. Since the chloroplast is an irregular emitting body, it is necessary to scan its entire surface in order to find the maximum relative density. This involves from three to eight horizontal scans of the densitometer per chloroplast. Figure 25 illustrates the densitometer tracing corresponding to one leaf cross section. The fifty-three peaks correspond to the fifty-three chloroplasts in clear focus in that section. Each peak is superimposed on the one to seven smaller peaks resulting from scans through less dense areas of that chloroplast.

In those cases where a single leaf section is photographed several times under varying conditions, it is most efficient to make a positive print of the first photographic negative. Then the chloroplasts, and the order in which they are scanned, can be written on the print. This "chloroplast map" is then used to systematically guide the scan pattern across subsequent photographs of the same leaf section.

F. Statistical Analysis

The mean diffuse density, $\bar{D}$, standard deviation, σ, and standard error of the mean, E, are obtained using a standard program for the "Olivetti Programma 101." The standard error is then used to compute the 0.05 confidence limit of that statistic. Since the sample size is small (less than 100), it is necessary to assume a "t" distribution instead of a normal distribution. For a given statistical mean, the 0.05 confidence limits are defined by the points $\bar{D} \pm L$, where

$$L = [E]\ [t_{0.05}]_{(n-1)}$$

E is the standard error of the mean, and "t" is the critical value of "t" in Students' t-distribution, corresponding to a probability P = 0.05, and n-1 degrees of freedom.

In this investigation, these statistics are applied to the analysis of the average density of chloroplasts on a single photographic negative. Consequently if D_i (i = 1, 2, ...N) represents the relative density of one of the N chloroplasts on a given photographic negative, then the probability is 0.95 that the interval $\bar{D}_S \pm L$ will cover the population mean where $\bar{D}_S$ is the sample mean.

III. Qualitative Comparison of Mesophyll
and Bundle Sheath Chloroplast
Fluorescence in C_4 Plants

A. Initial Observations

The large pale green bundle sheath chloroplasts of sugar
cane (Fig. 26a), so readily visible with a transmitting light
microscope, seem to disappear when viewed by fluorescence
microscopy (Fig. 26b). This visual observation does not permit
a distinction between a lack of bundle sheath fluorescence or
its shift into the infrared. Ektachrome film mimics the eye's
insensitivity to infrared radiation, and therefore accurately
records the fluorescence as it appears to the eye through the
microscope (Fig. 26b).

Infrared color film, a false color film sensitive from 500 -
900 nm, is capable of distinguishing between visible and infra-
red radiation (cf. II. D2). The infrared photograph in Figure 26c
records the mesophyll fluorescence in yellow-gold. This color
is characteristic of a predominance of far-red relative to infra-
red radiation. The bundle sheath is recorded in the red color
characteristic of a predominance of infrared relative to far-red
radiation. Infrared black and white film detects the relative
fluorescence intensities, but does not distinguish between wave-
lengths.

B. Experimental Observations

1. Wratten 88A Filter

The presence of a small infrared component of mesophyll
fluorescence is easily demonstrated by using a Kodak Wratten 88A

Fig. 26a. Ektachrome photograph of a cross section of a
sugar cane leaf (18-15a) showing 1/4 of a vascular bundle
(v), 3 bundle sheath cells, (b) and several mesophyll cells
(m). X 1280.

Fig. 26b. Ektachrome fluorescence photograph of a cross
section of a different sugar cane leaf (9a-2), exposure time
15 seconds. X 650.

Fig. 26c. Infrared black and white fluorescence photograph
(8-00) of the same leaf section, exposure time 15 seconds. X 650.
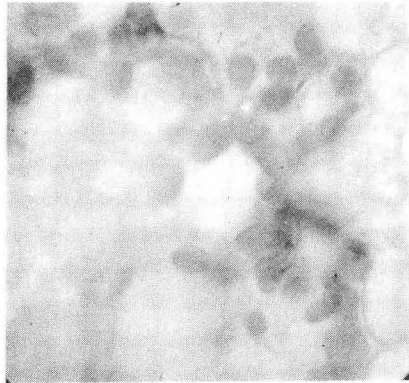
26a

26b
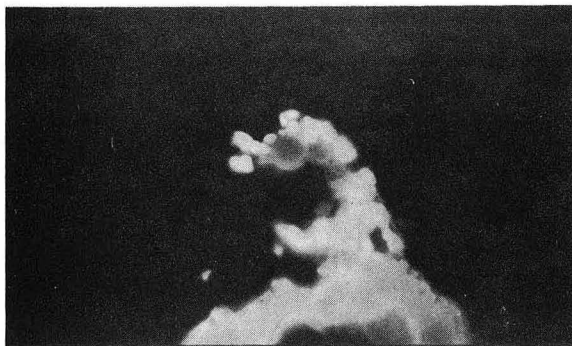
26c

XBB 7310-6122

filter to prevent wavelengths below 700 nm from striking the film. Infrared film bleaches the magenta dye of the film leaving the cyan and yellow layers intact. Intense far-red light bleaches both the cyan and magenta components. Therefore, in the presence of intense far-red light, the film cannot react uniquely to infrared light. Consequently, the presence of intense far-red light masks the film's characteristic response to infrared light (Fig. 27a). The use of the 88A filter prevents this concealment (Fig. 27b). This phenomenon occurs in every plant examined in this study.

2. Isolated Chloroplasts

The photographic red and yellow distinction is maintained in very thin cross sections and in isolated chloroplasts (Fig. 27c). In contrast, photographs of spinach cross sections and chloroplasts are characteristically yellow (Fig. 27d).

3. Self-Absorption

The phenomenon of self-absorption is discussed in Section I. C2. Self-absorption usually results in a shift of the emission spectrum toward longer wavelengths, resulting from absorption of the shorter wavelengths by chlorophyll. Thick sections of any green leaf will have enough self-absorption to produce irregular red patterns on the film. This, however, is easily distinguished from the regular limitation of the red color to the bundle sheath region.

Fig. 27a. Infrared fluorescence photomicrograph of a cross
section of a sugar cane leaf (34-00) suspended in two day old
buffer A. The slight green color associated with some of the
mesophyll chloroplasts might be due to inadequate specimen
protection by the buffer. X 250.

Fig. 27b. Infrared fluorescence photomicrograph of a cross
section of a sugar cane leaf (26-11) photographed through a
Wratten 88A filter which effectively eliminates all visible
wavelengths of light. X 660.

Fig. 27c. Infrared fluorescence photomicrograph of sugar
cane chloroplasts (25-15a) isolated in buffer C, pH 7.0.
X 1280.

Fig. 27d. Infrared fluorescence photomicrograph of spinach
chloroplasts (38-19a) isolated in buffer C, pH 7.5. X 320.
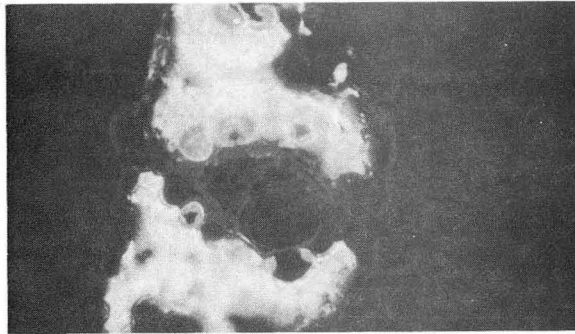
27a
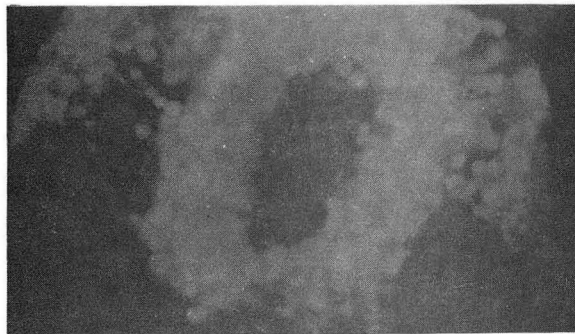
27b
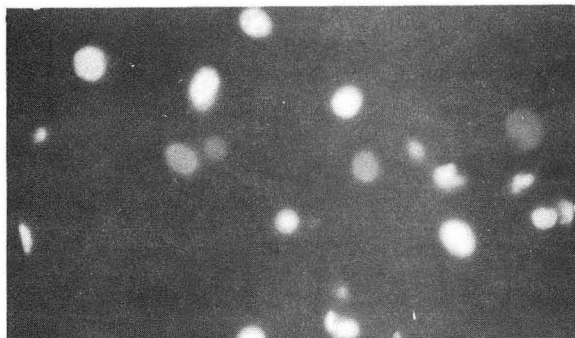
27c
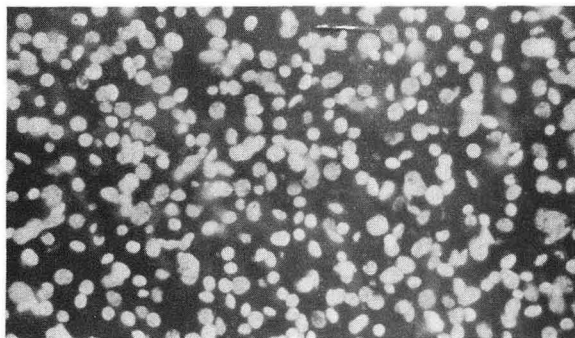
27d

XBB 7310-6121

Although in the case of thin leaf cross sections the thickness of the specimen obviously causes some degree of self-absorption, the following indicates that this is not significant enough to shift the color of the film. Although a microscope slide of isolated chloroplasts is much denser than the "ideal dilute solution," it is less dense than the more commonly used cuvette of chloroplast suspension. Photographs of microscope slides with only one or two chloroplasts in the entire 25x field of view still maintain the same red versus yellow distinction.

However, it is also necessary to consider the contribution of self-absorption to the fluorescence measurements of a single chloroplast. Since this thesis concerns the relative mesophyll to bundle sheath chloroplast fluorescence, it is perhaps most significant to consider the contributions of self-absorption to the relative fluorescence measurements of the two plastid types.

In _Digitaria_, Edwards and Black measure the chlorophyll content of mesophyll and bundle sheath cells as 3.5×10^{-5} ug and 9.9×10^{-5} ug chl per cell, respectively (96). Light and scanning electron microscope photographs of these cells show that bundle sheath cells are approximately twice as large as mesophyll cells (95). Although the bundle sheath chloroplasts are larger than mesophyll chloroplasts, they are more tightly packed in the cell (95). Therefore, the bundle sheath cells appear to hold 1.5-3.0 fold the number of chloroplasts as the mesophyll cells. Consequently,

the chlorophyll content is either approximately equal in the
two plastid types, or twice as high in the bundle sheath
plastids. Although the larger plastid size and the less dense
arrangement of thylakoids in the bundle sheath relative to
the mesophyll chloroplasts might also effect self-absorption,
it appears that there is no significant difference in the
contribution of self-absorption to the fluorescence measure-
ments of the two plastid types.

The distinction between mesophyll and bundle sheath can
also be observed with an epi-illuminator. This device
greatly reduces self-absorption by illuminating from above.
Unfortunately, the magnification and intensity are too low for
useful fluorescence photomicroscopy of the leaf sections used
in this study.

Additional evidence may be obtained by photographing single
intact bundle sheath cells. These can be found in the cell
debris obtained by grinding sugar cane in a mortar. Figure 28a
shows two isolated bundle sheath cells adjacent to two isolated
bundle sheath chloroplasts. The rectangular shape of the cell
walls and the high concentration of chloroplasts indicate that it
is a bundle sheath cell. Little color distinction can be made
between the chloroplasts in the cell and those that are released,
although the potential for self-absorption is much greater for
those still inside the cell.

99

Fig. 28a. Infrared fluorescence photomicrograph of two isolated sugar cane bundle sheath cells and two isolated bundle sheath chloroplasts (56-15). Although the thickness of the fluorescing specimen inside the cell is much greater than that of the fluorescing single chloroplasts outside the cell, the resulting increase in self-absorption has not altered the photographic appearance of the chloroplasts. X 225.

Fig. 28b. Infrared fluorescence photomicrograph of a cross section of a glutaraldehyde-fixed sugar cane leaf (56-5a). The red versus yellow distinction is minimally maintained in the presence of glutaraldehyde. X 225.

Fig. 28c. Infrared fluorescence photomicrograph of a cross section of a sugar cane leaf (26-12a) suspended in two day old buffer A, exposure time 18 seconds. The green color associated with certain portions of the mesophyll region might be due to inadequate specimen protection by the buffer. X 660.

Fig. 28d. Infrared fluorescence photomicrograph of a cross section of a sugar cane leaf (8-16a) showing approximately 1/4 of a vascular bundle, buffer A, 30 second exposure. X 1625.
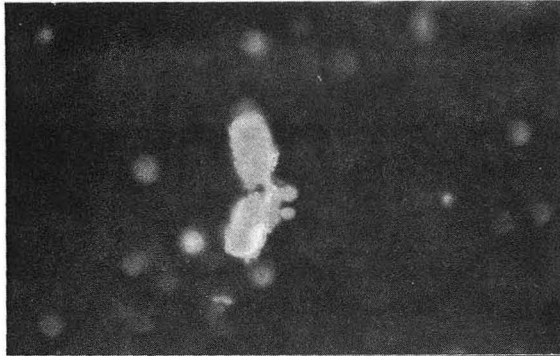
28a
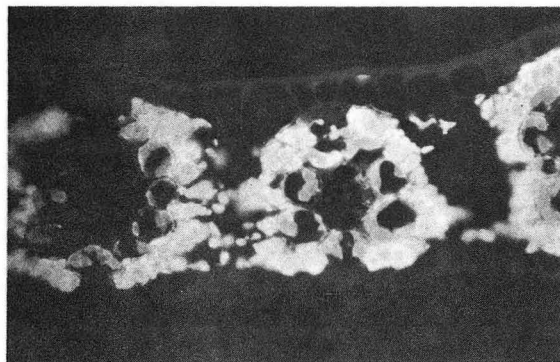
28b
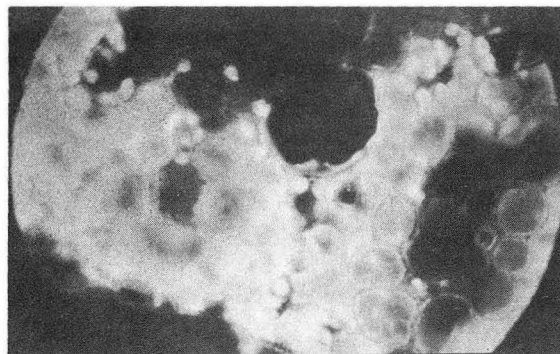
28c
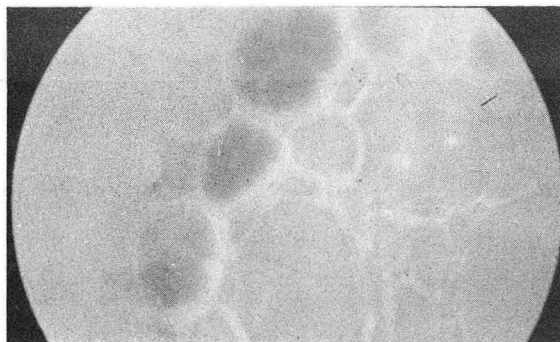
28d

XBB 7310-6120

4. <u>Effect of Isolating Medium on Fluorescence</u>

The fluoresence properties of damaged chloroplasts are different from those of intact plastids. A mixed suspension of mesophyll and bundle sheath chloroplasts suspended in H_2O rupture osmotically and lose the photographic red versus yellow distinction. Similarly, the color distinctions of very thin sections suspended in H_2O deteriorate within minutes, in contrast to thin sections immersed in Jensen-Bassham buffer which are stable for hours. Isolated sugar cane chloroplasts in this buffer retain the red versus yellow distinction for approximately an hour.

This disruption can be partially halted by fixation in glutaraldehyde (Fig. 28b). Since the use of buffer eliminates the need for this artificial procedure, virtually all experiments are performed on fresh, unfixed leaves. When NaOH is used to adjust the pH of the buffer, instead of KOH, the fluorescence recorded on the film shifts. The normally yellow mesophyll region turns greenish-yellow while the normally red bundle sheath becomes more orange (Fig. 28c). Thicker sections appear more immune to this effect, presumably because the cells are still intact (Fig. 28d). This phenomenon might result from the effects of ions on fluorescence as discussed in Section I. C5.

5. <u>Variation in Bundle Sheath Fluorescence with Species</u>

Infrared color fluorescence photomicrographs of C_4 plants fall largely into two major groups, I and II (Table 10). Group I

Table 10. Relative Long Wavelength Fluorescence in Bundle Sheath
Chloroplasts as Assayed by Infrared Color Film*

	I		II
A.	Saccharum officinarum	A.	Spartina foliosa
	Dichanthium annulatum		Cynodon dactylon
			Mollugo verticillata
B.	Zea mays		Spinacia oleracea (C_3)
	Sorghum caffrorum		Euphorbia splendens
C.	Digitaria sanguinalis	B.	Amaranthus edulis
			(cotyledon)
D.	Cenchrus sativa		Mollugo cerviana
	Echinochloa colonum		Portulaca oleracea
	Euphorbia maculata		Atriplex lentiformis
	Euphorbia serphyllifolia		Amaranthus edulis
			(mature leaves)

*See text for explanation of subgroupings

consists of those C_4 plants tested which display the red versus yellow distinction on the film. Photographs of Group II plants are completely yellow. Further subdivision of the two major groups is possible, but more difficult to document as photographic prints because of the difficulty in making color prints from slides. Slight variations in film, film processing, and in specimens also tend to obscure the distinction (Fig. 29c and 29d).

6. Qualitative Analysis of Chloroplast Fluorescence

While immersed in buffer, isolated chloroplasts of plants in Group IA (Table 10) maintain their red versus yellow fluorescence photographic distinction for approximately one hour (Fig. 28 and 29). The fluorescence distinction between chloroplasts of plants in Group IB (Table 10) is not maintained in buffer, although freshly released plastids or thin sections clearly maintain the distinction (Fig. 30). Infrared fluoresence photographs of Group IA and IB bundle sheath chloroplasts have enough specimen and/or film variation to vary in color between deep red to orange red (Fig. 29c,d). Digitaria is separated into a special group, IC, because it is more extreme in this variation (Fig. 31, 32). The four species in Group ID are grouped because their bundle sheath cells sometimes photograph with yellowish edges (Fig. 33, 34,35). They are included in group I because freshly released chloroplasts maintain the red versus yellow distinction when photographed.

Fig. 29a. Infrared fluorescence photomicrograph of a cross
section of a leaf of <u>Dichanthium annulatum</u> (68-6a). buffer C,
pH 7.2, 17 second exposure. X 250.

Fig. 29b. Same as above, infrared black and white film, show-
ing that the fluorescence yield is lower in the bundle sheath
chloroplasts relative to the mesophyll chloroplasts. X 300.

Fig. 29c. Infrared fluorescence photomicrograph of <u>Dichanthium
annulatum</u> chloroplasts (28-14a) isolated in buffer C, pH 7.0,
exposure time 22 seconds. X 1280.

Fig. 29d. Same as above (10-14a), isolated in buffer A, exposure
time 22 seconds. The difference in appearance is caused by the
difference in film emulsion batches, and possibly also by
slightly different development procedures. X 1600.

29a

29b

29c

29d

XBB 7310-6119
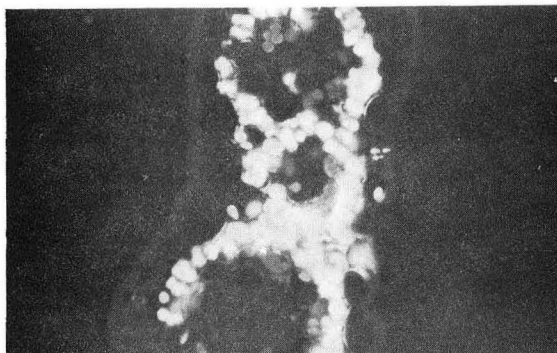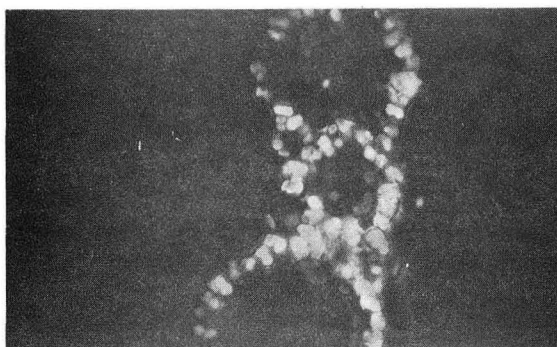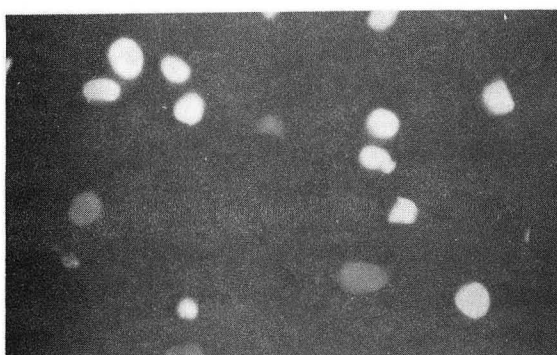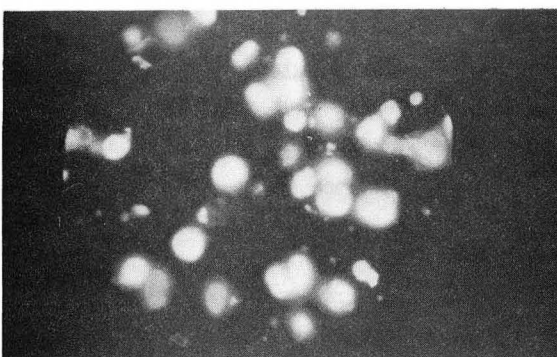
Fig. 30a. Infrared fluorescence photomicrograph of a cross section of a corn leaf (48-12), buffer C, pH 7.1. X 200.

Fig. 30b. Same as above, infrared black and white film (44-13a), showing the lower fluorescence yield in the bundle sheath chloroplasts. X 275.

Fig. 30c. Infrared fluorescence photomicrograph of a cross section of a leaf of Sorghum caffrorum (42-18a), solution C, pH 7.1. Note the difference in the two freshly released chloroplasts adjacent to the section. X 200.

Fig. 30d. Infrared fluorescence photomicrograph of a cross section of a corn leaf (48-10a), buffer C, pH 7.1. X 200.

30a

30b

30c

30d

XBB 7310-6118
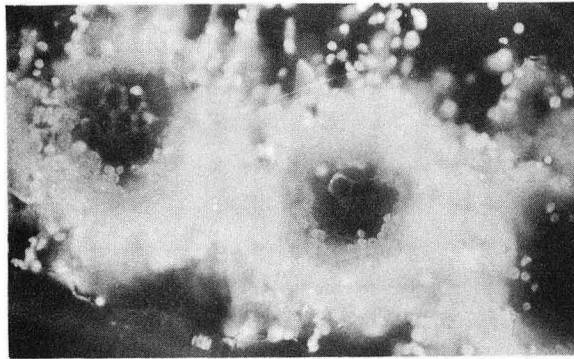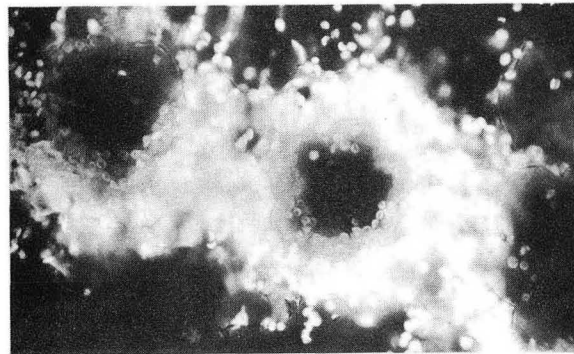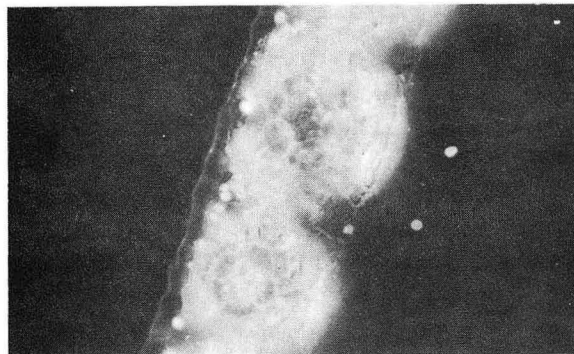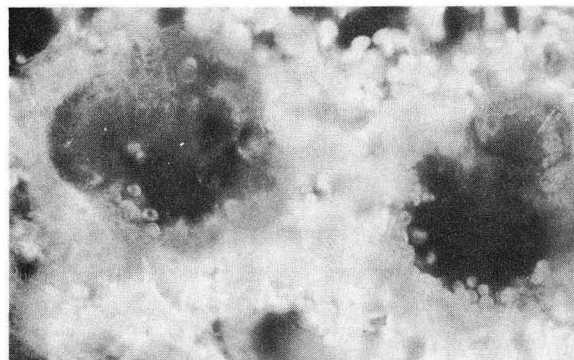
Fig. 31a. Infrared fluorescence photomicrograph of a cross section of a field grown leaf of _Digitaria sanguinalis_ (42-8a), buffer C, pH 7.1. X 320.

Fig. 31b. Black and white infrared fluorescence photomicrograph of an area adjacent to that shown in 31a (42-7a). X 400.

Fig. 31c. Similar to 31a. X 320.

Fig. 31d. Infrared fluorescence photomicrograph of a cross section of a greenhouse grown leaf of _Digitaria sanguinalis_ (81-0), buffer C, pH 7.1, 23 second exposure. The unusually vibrant color of the bundle sheath chloroplasts might be associated with the lower light intensity of the greenhouse. X 250.

31a

31b

31c

31d

XBB 7310-6117
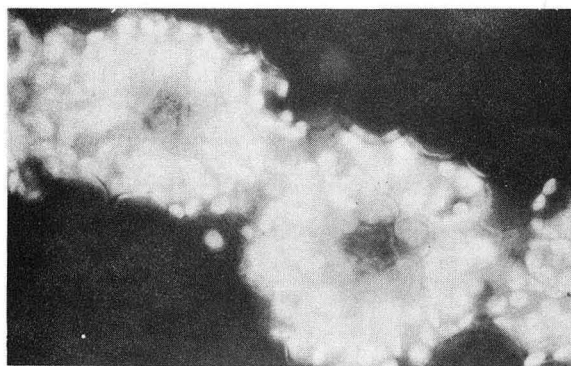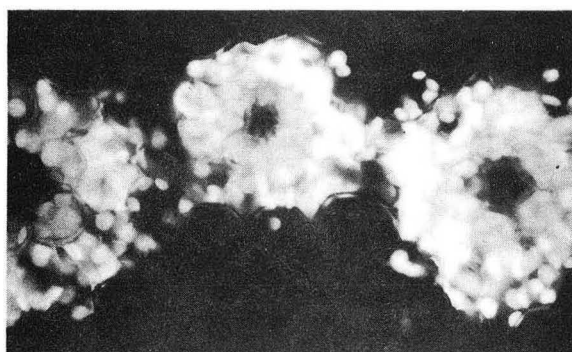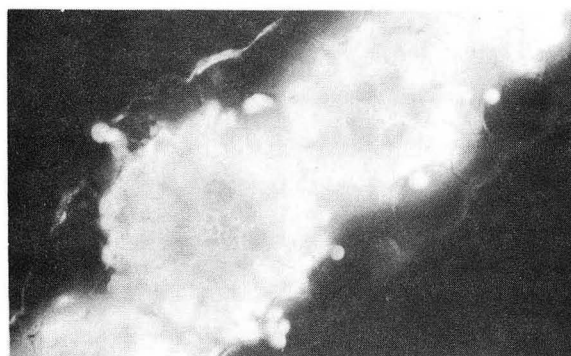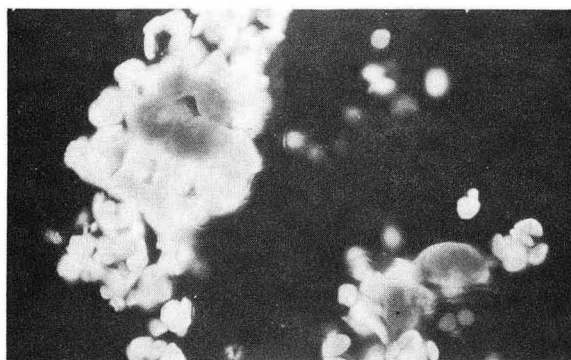
Fig. 32. Fluorescence photomicrographs of thick leaf sections of field grown _Digitaria sanguinalis_. X 1000.

Fig. 32a. High Speed Ektachrome film (23a-2), cross section.

Fig. 32b. Infrared film (22-0), same section as 32a.

Fig. 32c. High Speed Ektachrome film (23a-4), longitudinal section.

Fig. 32d. Infrared film (22-1), same section as 32c.

Fig. 33a. Infrared fluorescence photomicrograph of a cross section of a leaf of _Echinochloa colonum_ (72-00), buffer C, pH 7.1, exposure 25 seconds. X 250.

Fig. 33b. Infrared fluorescence photomicrograph of _Echinochloa colonum_ chloroplasts freshly released into buffer C, pH 7.1, exposure 15 seconds. X 250.

Fig. 33c. Infrared fluorescence photomicrograph of a cross section of a leaf of _Cenchrus sativa_ (72-15a), buffer C, pH 7.1, exposure 22 seconds. X 250.

Fig. 33d. Same as 33c, infrared black and white film (74-1), exposure 18 seconds. X 250.
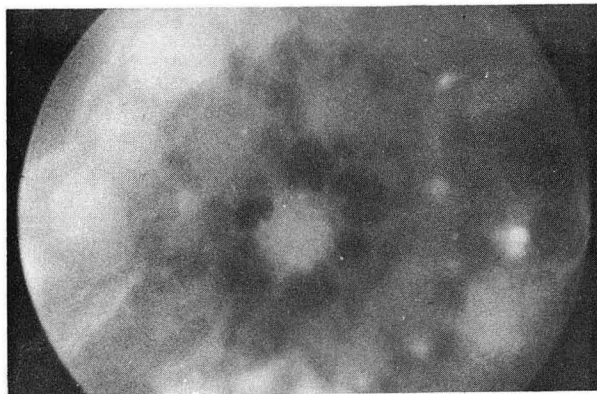
32a
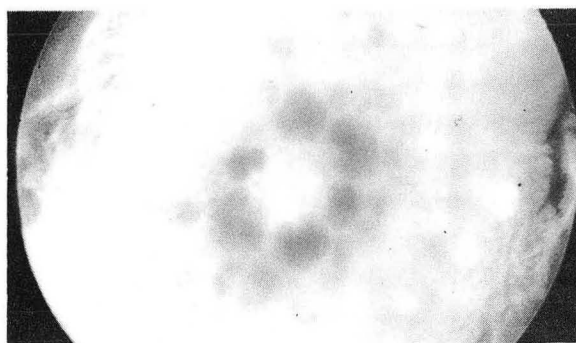
32b

32c

32d

XBB 7310-6116

112

33a

33b

33c

33d

XBB 7310-6115
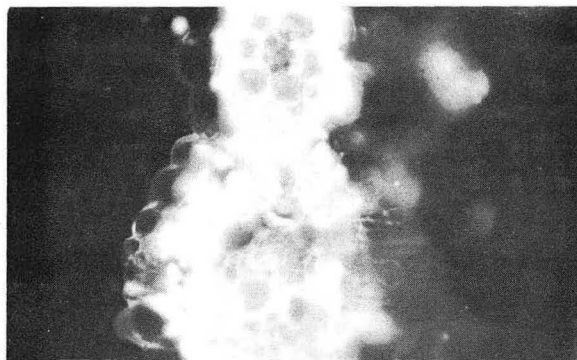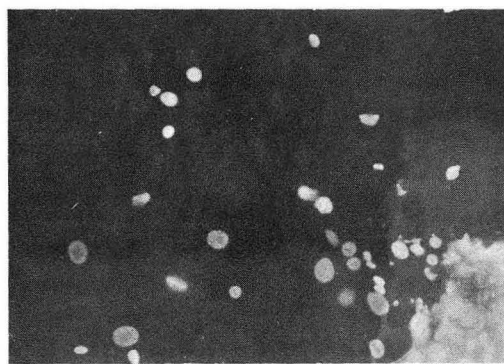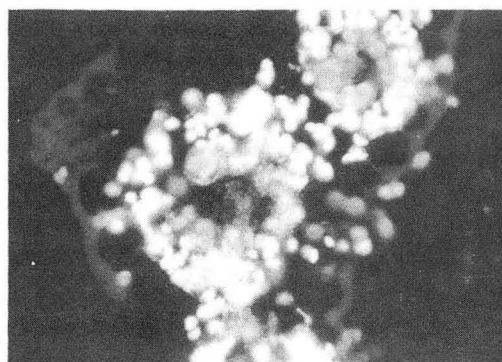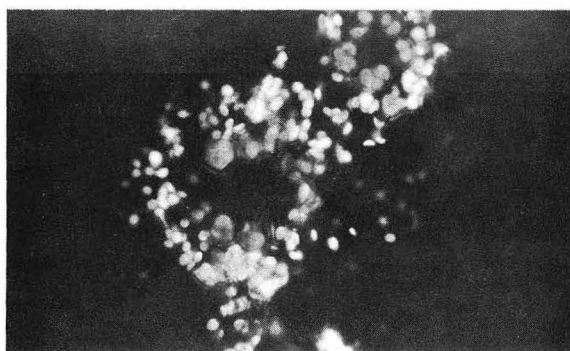
Fig. 34a. Infrared fluorescence photomicrograph of a cross section of a leaf of _Euphorbia_ _serphyllifolia_ (64-15a), buffer C, pH 7.3. X 125.

Fig. 34b. Same as above, infrared black and white film (66-4a). X 175. ·

Fig. 34c. Infrared fluorescence photomicrograph of _Euphorbia_ _maculata_ chloroplasts (78-7&8), freshly released into buffer C, pH 7.1, exposure 18 seconds. X 400.

Fig. 34d. Infrared fluorescence photomicrograph of a cross section of a leaf of _Euphorbia maculata_, buffer C, pH 7.1. X 150.

Fig. 35a. Infrared fluorescence photomicrograph of a cross section of a leaf of _Euphorbia serphyllifolia_ (51-000) buffer C, pH 7.1. X 320.

Fig. 35b. Same as above, infrared black and white film (44-19). X 480.

Fig. 35c. Similar to 35a (31-2a). X 175.

34a

34b

34c

34d
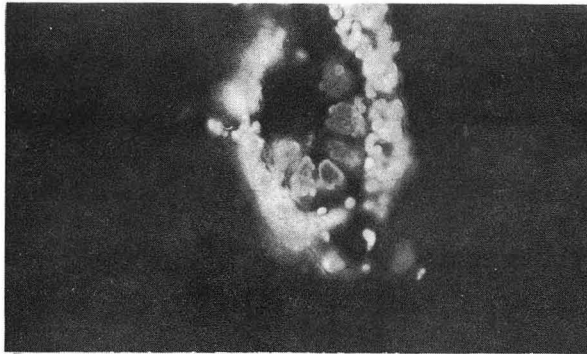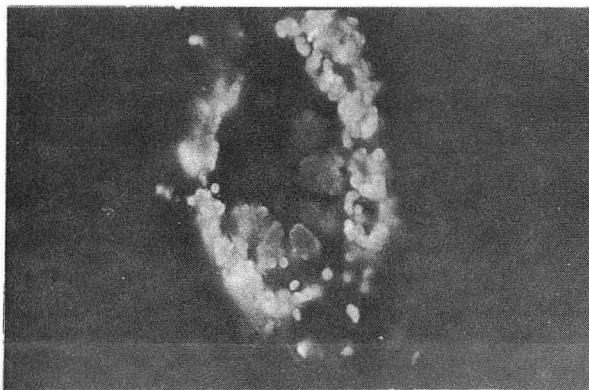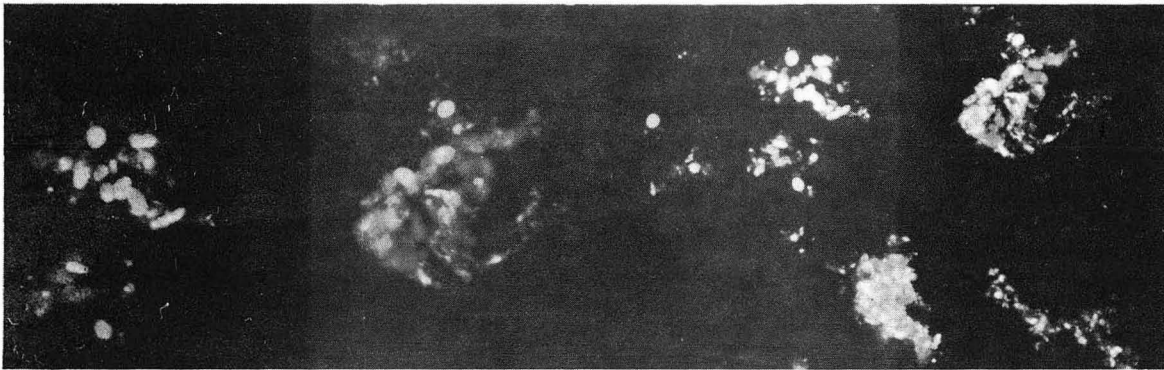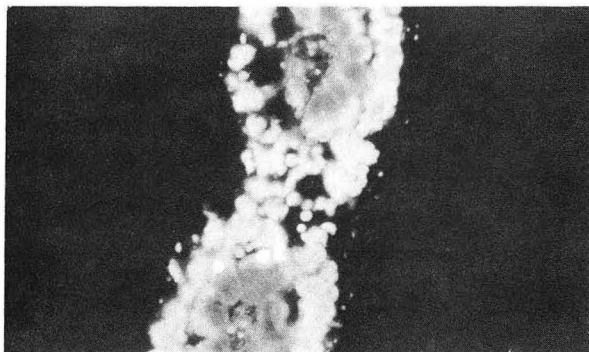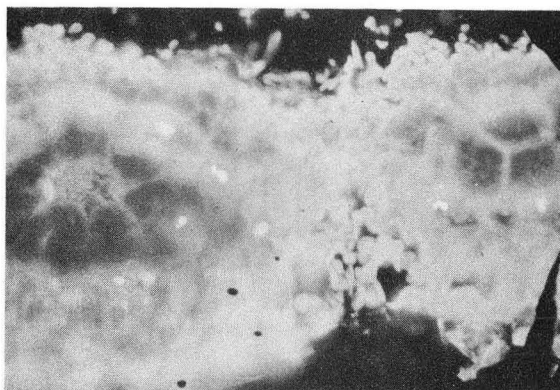
XBB 7310-6114

35a
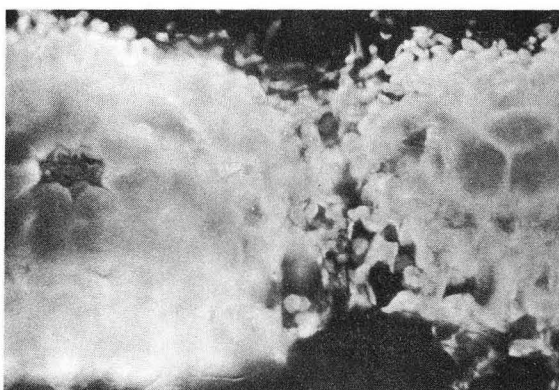
35b
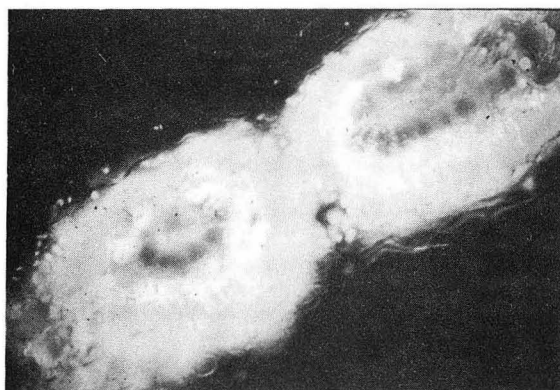
35c

XBB 7310-6113

Group II can similarly be subdivided. Group IIA consists of those plants with only (photographically) yellow chloroplast fluorescence (Fig. 36). Isolated chloroplasts and thin sections of Group IIB plants photograph in a similar manner to those in Group IIA; however, thick sections show red areas in the bundle sheath region possibly due to self-absorption (Fig. 37, 38, 39, 40a and b).

This phenomenon is most noticeable in <u>Mollugo cerviana</u>, <u>Amaranthus edulis</u> cotyledons, and <u>Portulaca oleracea</u>. This intensification is probably caused by the unusual bunching of chloroplasts along the innermost cell walls of these three species.

<u>Atriplex lentiformis</u> may also be a special case since the mesophyll region is a much paler green than the bundle sheath region (Fig. 37). If one concludes that in <u>Atriplex</u> the bundle sheath region has much more chlorophyll than the mesophyll region, it is logical that the bundle sheath cells might have significantly more self-absorption than the mesophyll cells.

7. <u>Cell Size; Plastid Arrangement, Size and Number</u>.

Any anatomical arrangement which increases the density of chlorophyll in the light path of the microscope will tend to increase the selective subtraction of emission due to self-absorption of fluorescence. Table 11 lists several factors which could increase self-absorption. It is for this reason that the distinction between Groups I and II is based predominantly on the photo-

Fig. 36a. Infrared fluorescence photomicrograph of a cross section of a leaf of field grown <u>Spartina foliosa</u> (81-11), buffer C, pH 7.1, 22 second exposure. X 280.

Fig. 36b. Infrared fluorescence photomicrograph of a cross section of a spinach leaf (50-16a) buffer C, pH 7.1. X 220.

Fig. 36c. Infrared fluorescence photomicrograph of a cross section of a leaf of <u>Cynodon dactylon</u> (68-14), buffer C, pH 7.2, second exposure. X 250.

Fig. 37a. Infrared fluorescence photomicrograph of a glutaral-dehyde-fixed leaf of <u>Atriplex lentiformis</u> (68-000), buffer C, pH 7.2. X 275.

Fig. 37b. Same as 37a, black and white infrared film (66-9). X 300.

Fig. 37c. Similar to 37b but thicker (50-10). X 200.

Fig. 37d. Same as 38c. X 350.
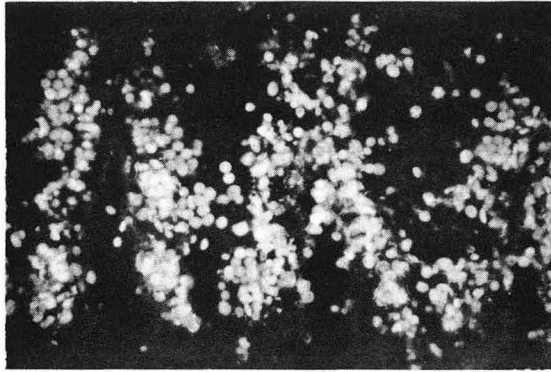
36a
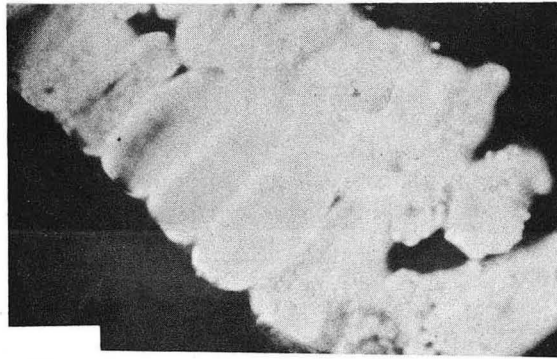
36b
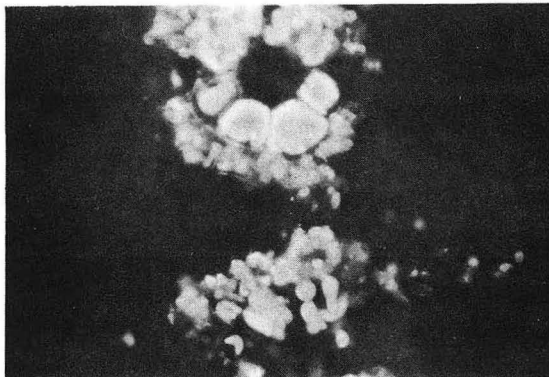
36c

XBB 7310-6112

37a

37b

37c

37d

XBB 7310-6111
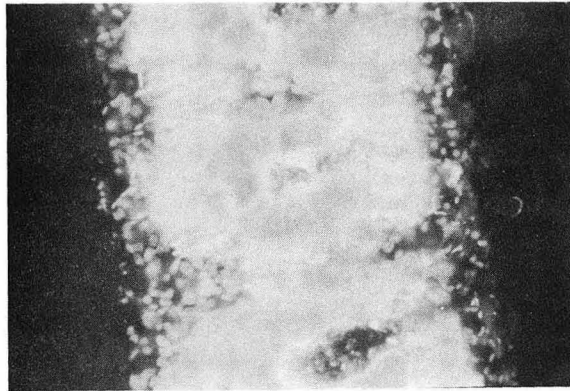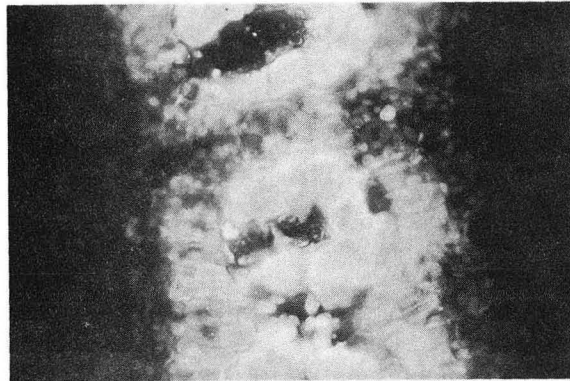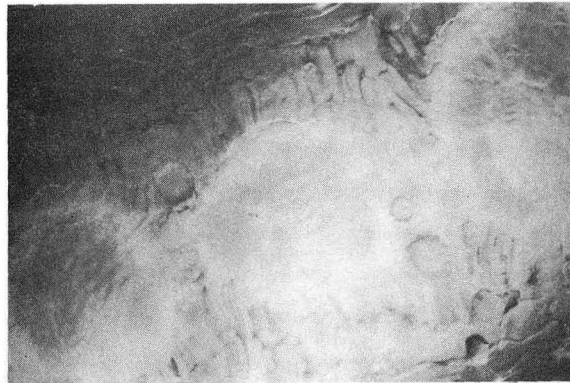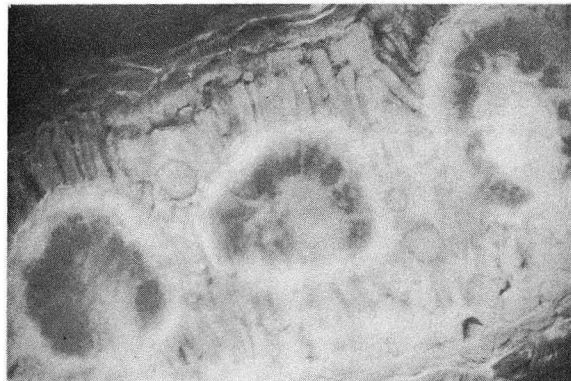
Fig. 38a. Infrared fluorescence photomicrograph of a thin cross section of a leaf of <u>Atriplex lentiformis</u> (50-8) buffer C, pH 7.1. X 200.

Fig. 38b. Infrared fluorescence photomicrograph of a thin cross section of a mature leaf of <u>Amaranthus edulis</u> (46-15), buffer C, pH 7.1. X 150.

Fig. 38c. Similar to 37b, but a thicker section (42-4a). Note the preferential fluorescence shift in the region of the bundle sheath. X 500.

Fig. 38d. Infrared fluorescence photomicrograph of a cross section of a leaf of <u>Froelichia gracilis</u> (31-1), buffer C, pH 7.0 adjusted with NaOH. Note the preferential fluorescence shift in the region of the bundle sheath. The green color associated with some of the mesophyll chloroplasts may be due to the use of NaOH. X 400.

38a

38b

38c

38d

XBB 7310-6110
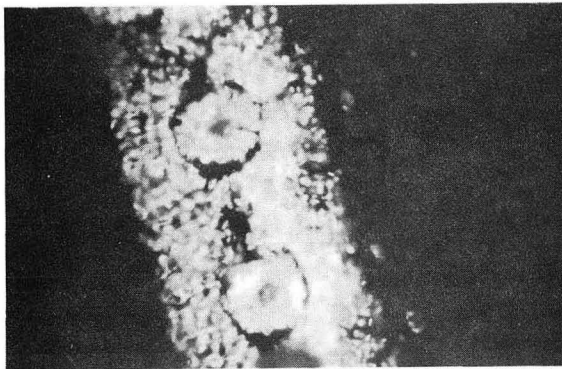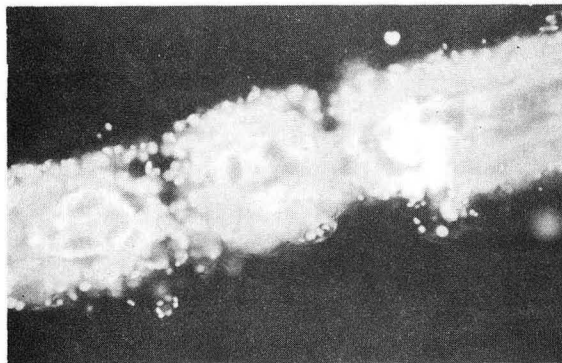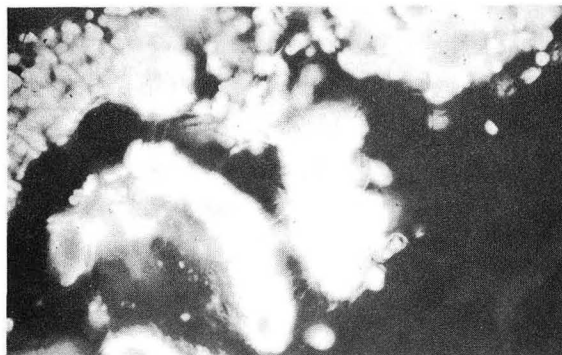
Fig. 39a. Infrared fluorescence photomicrograph of a cross section of a glutaraldehyde-fixed cotyledon of Amaranthus edulis (68-13a), buffer C, pH 7.2, 30 second exposure. X 250.

Fig. 39b. Infrared fluorescence photomicrograph of a cross section of a cotyledon of Amaranthus edulis (30-17a), buffer C, pH 7.0 adjusted with NaOH, exposure 25 seconds. The greenish color associated with part of the mesophyll may be caused by the NaOH. There is an unusually rich red color associated with the bundle sheath region for this species. X 300.

Fig. 39c. Black and white infrared fluorescence photomicrograph of a cross section of a leaf of Mollugo cerviana (70-1a), buffer C, pH 7.15, exposure 22 seconds. X 250.

Fig. 39d. Same as 39c, infrared color film. X 350.

Fig. 40a. Infrared fluorescence photomicrograph of Mollugo cerviana chloroplasts isolated in buffer C.

40b. Infrared fluorescence photomicrograph of a cross section of a leaf of Portulaca oleracea (81-16), buffer C, pH 7.1, 18 second exposure. X 275.

Fig. 40c. Ektachrome photograph of a cross section of a sugar cane leaf (18-12a) showing both bundle sheath and mesophyll chloroplasts. X 1280.

Fig. 40d. Similar to 40c (18-19a).
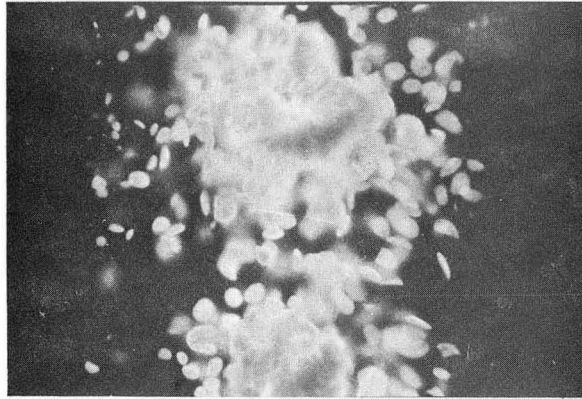
39a
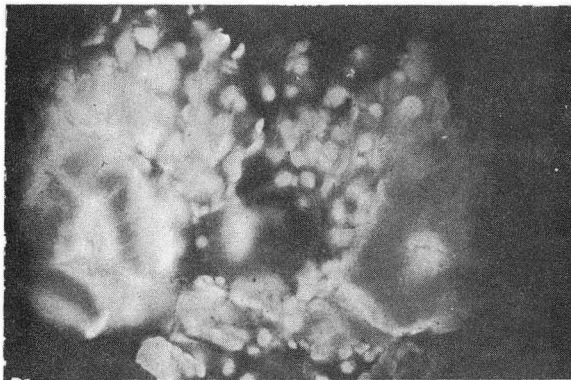
39b
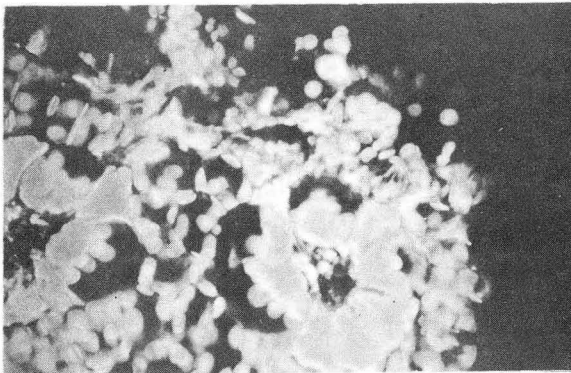
39c

39d

40a

40b

40c

40d

XBB 7310-6108
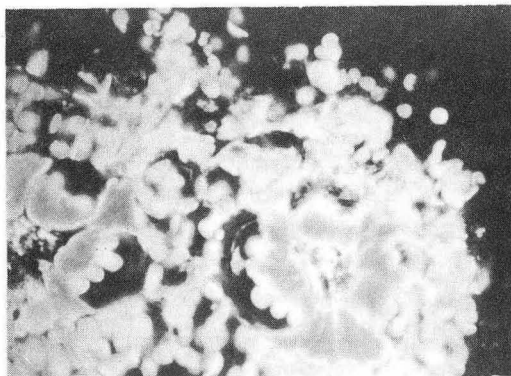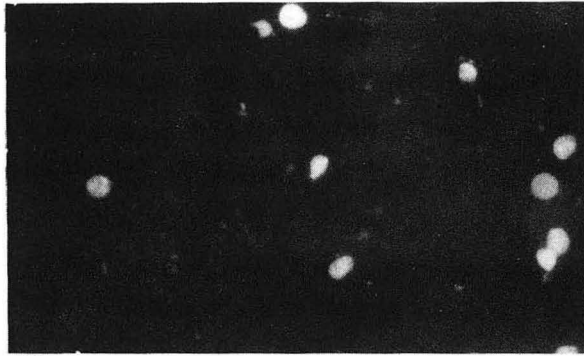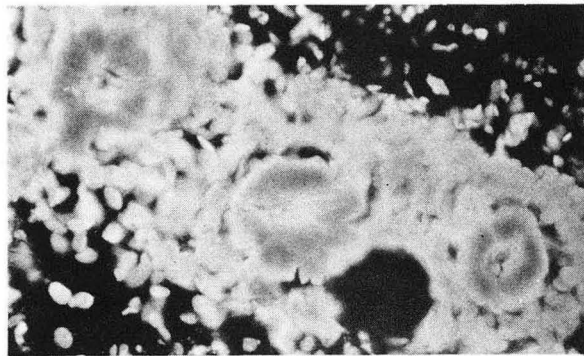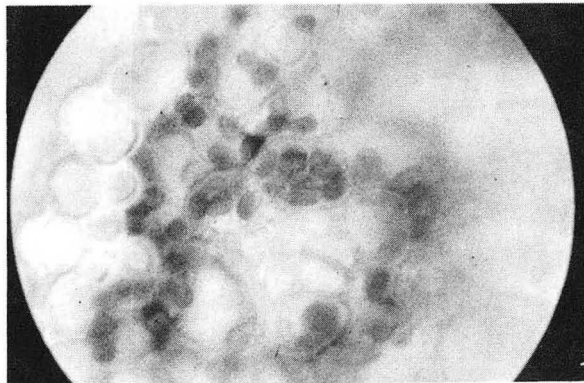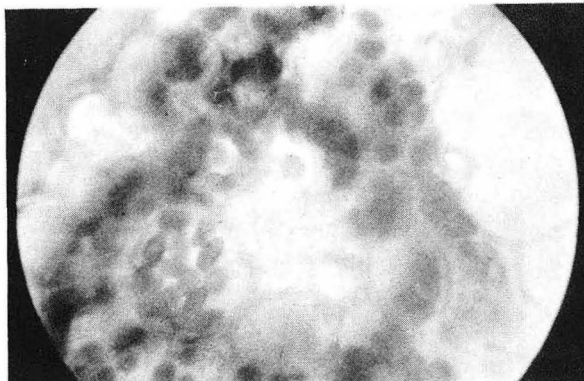
Cell and chloroplast relationships in C_3 and C_4 leaves (M, mesophyll; BS, bundle sheath).

Species	Cell size (μ)	Cell ratio M/BS	Plastids per cell	Plastids per cm^{-2} leaf	ratio M/BS	Chlorophyll* μg mg^{-1}	ratio a/b
Nicotiana tabacum	62×20	–	93.3	4.67	–	2.67	3.06
Euphorbia maculata							
M	29×10	1.7	12.9	4.42	1.19	3.03	2.45
BS	28×26		18.7				
Amaranthus edulis							
M	38×8	11.3	10.5	3.08	2.29	1.56	3.90
BS	40×24		38.7				
Saccharum officinarum							
M	58×16	5.1	30.7	1.63	3.70	2.73	3.56
BS	113×18		41.9				

Table 11. Cell and Chloroplast Relationships. after Laetsch (172).

graphic appearance of isolated chloroplasts. The separation of Group IIA from IIB might be due to these artifactual factors. At present, it is difficult to estimate the contribution of plastid size to self-absorption and to the possible concomitantly altered fluorescence emission pattern.

8. Relative Fluorescence Yield

Since black and white infrared film is equally sensitive to far-red and infrared radiation, the density of each photographic negative will be positively correlated with the fluorescence striking the film. It is necessary to insert a Corning 2-63 filter above the specimen to prevent the natural lignin fluorescence from exposing the film.

Figures 29, 30, 31, 33, 34, 35, 37, 39 illustrate the high correlation between a red color on the infrared color film and a significantly lower fluorescence intensity as shown on the infrared black and white film. This phenomenon is treated in depth in section IV.

9. Photochemistry and Chloroplast Ultrastructure

In Table 10, fluorescence is used to classify 18 C_4 and 2 C_3 plants into two groups (6 subgroups). The significance of these groupings would be reinforced if they were correlated with another physiological parameter. Because of the difficulty in separating bundle sheath and mesophyll chloroplasts, the procedures usually used to localize photosystems I and II have

not been applied to many C_4 plants. Cytochemical localization is still controversial. These data are urgently needed for a thorough understanding of photosynthesis in C_4 plants.

Fortunately, an extensive survey of C_4 chloroplast ultra-structure is being performed by Dr. W.M. Laetsch at the University of California, Berkeley. When these electron micrographs are grouped according to Table 10, a definite pattern emerges (cf. Appendix A). The bundle sheath chloroplast profiles of Group IA plants usually totally lack lamellar appression, while those of the plants in Group IB have only small numbers of tiny grana at the periphery of their plastids. Often no distinction can be made between the two groups.

Digitaria (Group IC) is unique in that its bundle sheath chloroplast profiles lack a consistent ultrastructural pattern. A single plant may contain chloroplast profiles which range from agranal to significantly granal (Fig. A 7-10). The variation in Digitaria fluorescence was documented before the variation in ultrastructure. The strongly infrared fluorescing bundle sheath chloroplasts came from mature leaves of young plants grown under greenhouse conditions (Fig. 31d). The other extreme was observed in growth chamber plants which were in the process of flowering (Fig. 31a, b, c). Mature leaves of young field grown material also appeared enriched in the long wavelength component of fluorescence (Fig. 32).

These observations on Digitaria were never extensively correlated with ultrastructure. It is significant that the agranal bundle sheath chloroplast profiles in Figure A 7 were obtained within a day from the same plant used to photograph Figure 31d. The intensity of the red color associated with with the bundle sheath chloroplasts is striking, and only begins to capture the intensity of the original slide.

The ultrastructure of Group ID chloroplast profiles differ from those in Groups IA, B and C. Cenchrus and rice grass (Echinochloa colonum) have larger numbers of small grana, although they maintain a predominance of unappressed lamellae. The two tested C_4 species of Euphorbia also have a predominance of unappressed lamellae, but in this case the lamellae are so numerous that there are several regions of appression.

In contrast to Group I bundle sheath chloroplasts, those in Group II display extensive lamellar appression. The absence of unappressed lamellae appears more important than the numbers of thylakoids in each stack. Froelichia gracilis accentuates this point because its stacking is almost exclusively restricted to double layers. Chloroplasts of Group IIA plants do appear to have a higher percentage of lamellar appression than those in Group IIB, however, the difference is not very striking.

C. Summary and Tentative Conclusions

The precise spectral response of infrared color film permits a qualitative evaluation of the fluorescence properties of C_4 chloroplasts. The photographs do not appear to be significantly altered by underexposure or overexposure; however, the buffers listed in Table 6 are necessary for specimen stability.

Experiments with a Kodak Wratten 88A filter reveal that in fluorescence photography, the long wavelength tail of chloroplast fluorescence can be masked by the predominant shorter wavelength component. Double exposures of the film are used to estimate that a shorter wavelength chloroplast fluorescence component of 30% or more can mask the film's characteristic response to infrared radiation, thereby concealing its presence.

Similarly, an infrared fluorescence component of 80% or more can mask the film's response to up to 20% far-red light. An orange color could indicate up to 30% far-red radiation.

The red or yellow color of bundle sheath chloroplast photographs can be used to classify C_4 plants into two basic groups. A coordinated examination of Laetsch's C_4 chloroplast electron micrographs and chloroplast fluorescence photomicrographs reveals a strong positive correlation between lamellar appression and the ratio of far-red to infrared fluorescence.

Since it is theorized that far-red chloroplast fluorescence might be associated with PS II, while infrared chloroplast fluorescence might be associated with PS I (cf. Section I. C3), the above

correlation might indicate an increased ratio of PS I to PS II in agranal C_4 chloroplasts. Quantitative work with infrared black and white film will be necessary to confirm this tentative hypothesis. Meanwhile, infrared color film appears to be a rapid and simple technique for surveying chloroplast fluorescence. The accuracy of this technique is tested in Section IV and discussed in Section V.

IV. Quantitative Comparison of Mesophyll
and Bundle Sheath Chloroplast
Fluorescence of <u>Dichanthium</u> <u>annulatum</u>

A. <u>Suitability for Quantitative Applications</u>

The relationship between film darkening and exposure is
expressed by a "Characteristic Curve." The "Characteristic
Curve", of a given film is defined as a graph of the diffuse
density of the photographic negative against the logarithm of
the exposure. Exposure is a function of both time and intensity.
Often the intensity is held constant and the logarithm of the
exposure time is used. This curve is a function of the parti-
cular film type as well as the applied development process.

Figure 41 shows the degree to which the slope of the "Character-
istic Curve", designated gamma, varies with the time of develop-
ment for high speed infrared film. Analogous changes are
possible with altered temperature of development. Theoretically,
the "Characteristic Curve" is stable for a given film type (e.g.,
Kodak High-Speed Infrared Film 2481) and an optimum development
procedure (12 minutes, 68°F). In practice, however, equally
important variations may be caused by different emulsion batches
of film, or by non-uniform attempts at performing the optimal pro-
cedure. Therefore, the "Characteristic Curve" is actually only
stable for rolls of film derived from the same emulsion batch,
and processed together. For this reason, all experiments in
this investigation are performed on a single emulsion batch
of Kodak High-Speed Infrared Film 2481.

Characteristic Curve

KODAK High Speed Infrared Film 2481 (ESTAR Base)

Exposure:
Infrared Daylight with a KODAK WRATTEN No. 25 Filter

Development:
KODAK Developer D-19 at 68 F

Time of Development (in minutes)

Gamma

DIFFUSE DENSITY

LOG EXPOSURE
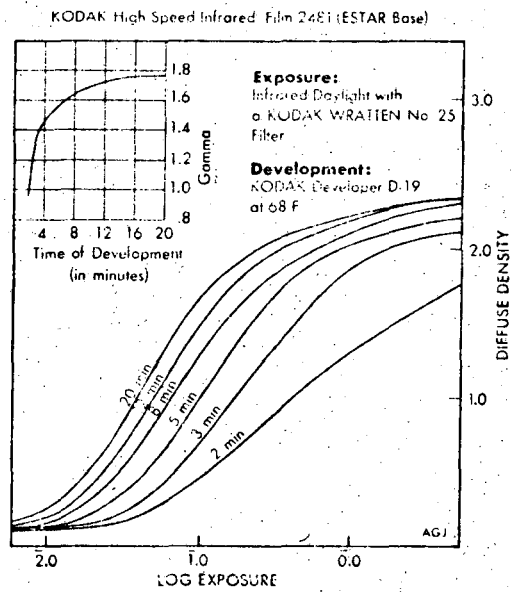
Fig. 41. after (163).

The use of a dual capacity development tank permits the development of two rolls of film (86 frames) simultaneously. The film from one experiment consists of the one or two rolls of film exposed within a 16-hour period and developed immediately thereafter in a single development tank. Therefore, uniformly shaped "Characteristic Curves" characterize the film used in a single experiment, and will always be similar, but never identical, to those of another experiment.

The "Characteristic Curve" for the high-speed black and white infrared film used in a single sub-experiment calibrates that film for quantitative analysis. The curve is obtained by plotting the density versus the logarithm of the exposure for a series of photographs of a single, uniformly emitting object. In this case, exposure is directly proportional to exposure time because the intensity is constant. For example, in the optical system used here, the eight sequential exposure times between 1/16 second and eight seconds, used to photograph a small fluorescing cell-wall fragment or bundle-sheath chloroplast, constitute a suitable photographic series for calibration.

Uniformly shaped (parallel) "Characteristic Curves" obtained by repeating this procedure on a single roll of film indicate that the photographic density is directly proportional to the logarithm of the exposure whenever the diffuse density of the film falls between 9.0 and 18.5 relative density units, as recorded by the microdensitometer (Fig. 49). The s-shaped curve

indicates that at relative densities below 9.0 there is a lag
phase, while at relative densities above 18.5 there is a saturation phase. Consequently, the "Characteristic Curve" is linear
over only approximately one-third of its relative density range.
Only photographic negatives depicting objects with relative densities in the range of 9.0-18.5 are suitable for quantitative
analysis.

Both the exposure time and the intensity of the incident
light determine the exposure of the film, when photographing
fluorescing objects of varying intensities. Equal exposures
are achieved when the product of intensity and exposure time is
kept constant. Therefore, when dealing with photographic
negatives whose densities fall within the linear region of the
"Characteristic Curve," the film is adaptable as a sensitive
mechanism for recording the magnitude of fluorescence.

If photographs of two fluorescent objects, A and B, have the
same diffuse density, and the exposure times are designated T_A and
T_B, respectively, then the fluorescence of object A relative
to object B is T_B/T_A. If photographs of two fluorescing objects,
C and D, have slightly different diffuse densities, then the
exposure times corresponding to a mutually selected adjusted
density can be read from the "Characteristic Curves," and used
to calculate the relative fluorescence of C with respect to D.
The relative densities of several series of high-speed infra-
red photographs are graphed as a set of related "Characteristic

Curves." These related curves indicate the exposure times necessary to give the same adjusted diffuse density for each object photographed. These relative exposure times are indicative of the magnitude of the fluorescence striking the film because the product of exposure time and intensity is constant for a given density.

High-speed black and white infrared film 2481 is more suited to this type of quantitative analysis than infrared black and white film IR-135. The former's higher ASA rating permits significantly shorter exposure times. This is an important asset during experiments which require multiple exposures of fluorescing objects susceptible to photobleaching.

B. Rationale for Recording Fluorescence Emission Spectra Photographically

A spectrofluorometer with sufficient spatial resolution and sensitivity to record the emission spectrum of a single chloroplast *in situ* would be ideal for these experiments. The electronic components are readily available for the construction of spectrofluorometers with the requisite sensitivity, although the sensitivities of commercially available spectrofluorometers are too low for this task. Unfortunately, the spatial resolution of spectrofluorometers which do not incorporate microscopes is inadequate for *in situ* studies of a single chloroplast.

A single chloroplast, subjected to the required intense actinic irradiation, is susceptible to fluorescence fading, especially when the chloroplast is isolated. Under the microscope, it is apparent that the fluorescence of isolated chloroplasts becomes totally lost within a matter of minutes, while chloroplasts within wholly or partially intact cells maintain visible fluorescence integrity for approximately one hour. The specimen integrity would therefore be a limiting factor in a single-chloroplast experiment. It would also be necessary to repeat the experiment numerous times to overcome sampling error. However, if the apparatus were assembled and working, the required number of experiments could probably be completed in a single day. Throughout this entire investigation, the combination of a microscope (M), optical filters (OF), and film (F) substitutes for the ideal, but unavailable microspectrofluorometer. Film is one of the most sensitive light detectors available. The spatial resolution afforded by the microscope provides an alternative to the nemesis of most C_4 light-reaction work, i.e., the separation of mesophyll from bundle-sheath chloroplasts. As of this time, no research group has succeeded in separating a preparation of intact, isolated, bundle-sheath chloroplasts contaminated with less than 10% mesophyll chloroplasts. (cf. Table 2). The results of this thesis reveal the magnitude of the effects of chloroplast damage and mesophyll contamination.

The equipment used in the MOFF procedure is more available and more versatile than that needed for custom-made spectrofluorometry; however, the time and labor associated with the data analysis probably renders this procedure equally high in cost. In addition, the spectral resolution resulting from the large half-band width (5 or 10 nm) restriction of MOFF is poor in comparison with the high speed spectral resolution (1nm or less) available in most spectrofluorometers. Therefore, the lack of suitable alternatives is the main reason for using the MOFF technique exclusively.

C. Analysis of the Photographic Negative

The high spatial resolution inherent in the MOFF technique imposes a statistical complication on the data analysis. The raw data of each experiment are recorded on photographs of the cross-sections of leaves. A single photographic negative records the data from 20-90 different chloroplasts. Since the density of each chloroplast must be analyzed individually on the densitometer, the data requires extensive (statistical) analysis.

Of the hundreds of chloroplasts present in each leaf section, only those in focus and free of underlying material are suitable for measurement. Figure 42 illustrates the densitometer tracing of an infrared photograph of a single cross-section containing 49 usable chloroplasts (N = 49). Each peak on the

138
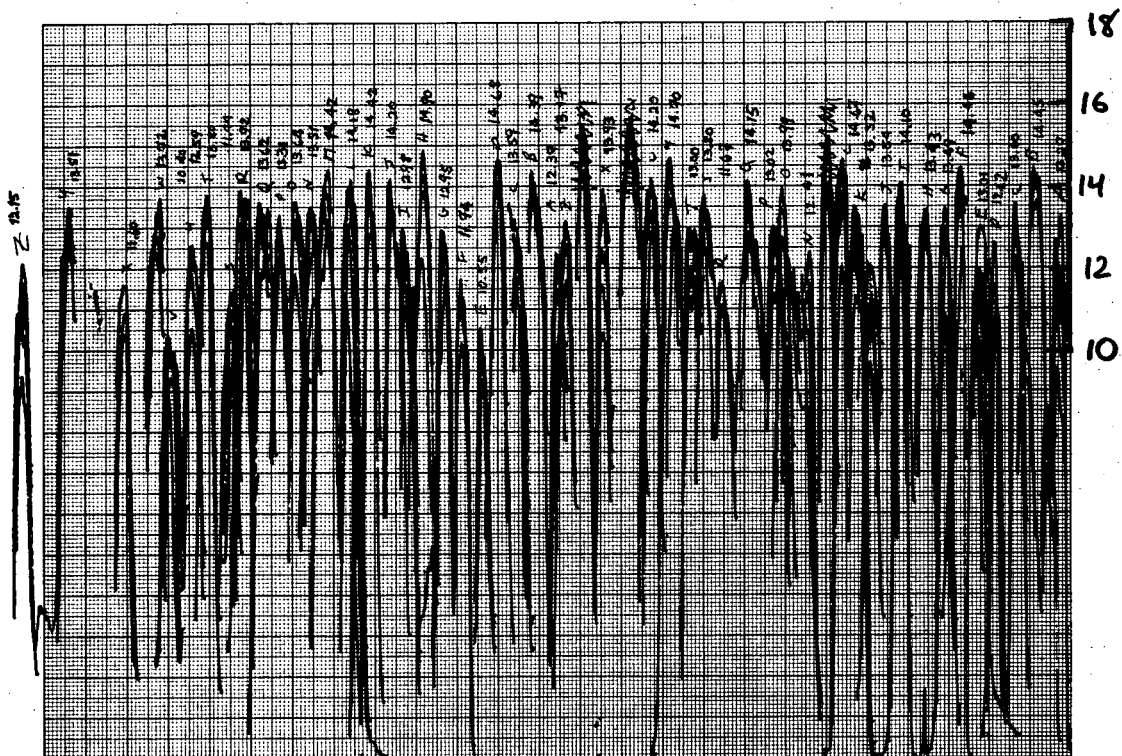
XBL 7310-1350

Fig. 42. Densitometer tracing of the 49 usable mesophyll
chloroplasts of a single photographic negative from experiment
131T-F (frame 35, 1.1 second exposure).

densitometer tracing records the relative density of a single

chloroplast. Subsequently, the relative density of each chloro-

plast of the leaf section is used to compute the statistical

relative mean density of the chloroplasts ($\bar{D}$).

The relative mean chloroplast density, $\bar{D}$, when graphed against

the logarithm of the exposure time, determines one point of a

"Characteristic Curve." Consequently, the data resulting from

a single photograph are summarized by a single point on a

"Characteristic Curve." Therefore, throughout this investigation,

relative mean density, ($\bar{D}$), is used in the same sense as diffuse

density.

The raw data from a single experiment consists of as many

as 86 photographs. The measured relative mean densities, ($\bar{D}$), of

these photographs can be used to determine the linear portion of

up to 40 uniformly shaped (parallel) "Characteristic Curves."

Since the two rolls of film, derived from the same emulsion batch,

are processed simultaneously, the gammas (slopes) of these re-

lated "Characteristic Curves" are assumed to be equal.

If the fluorescence intensities of the objects photographed

are identical, then the "Characteristic Curves" are identical.

However, whenever the luminous intensities of the objects being

photographed vary, the "Characteristic Curves" are displaced

laterally from each other along the abscissa or "Log Exposure"

axis. The amount of lateral displacement for a given density is

equal to the logarithm of the fluorescence intensity difference.

Since the gammas (slopes) of the linear portions of each
"Characteristic Curve" are parallel, the lines can be determined
in one of two ways. Two or more points determine the line, or a
single point plus the slope determine the line. In this case,
the slope is derived from other related "Characteristic Curves"
of the same experiment.

The "Characteristic Curves" of a single experiment can be
grouped into sub-experiments. The sub-experiment data consist
of either two or ten characteristic curves, depending upon the
number of times compared.

D. The Total Fluorescence Intensity of Mesophyll
    Relative to Bundle Sheath Chloroplasts

1. The Interpretation of a Series of "Characteristic Curves"

Tables 12 and 13 present the actual data and related statis-
tics derived from the series of gamma curves drawn in Figure 43.
Experiment 119-120 contains four sub-experiments, labeled A, B,
C, and D. Sub-experiment 119A involves five photographic nega-
tives of a single leaf cross-section taken at exposure times of
0.28, 0.55, 1.10, 2.00 and 2.60 seconds. Of these five, only
three negatives contained chloroplasts of densities between
9.0 and 18.5 relative density units (Fig. 44). Since the meso-
phyll chloroplasts are analyzed separately from the bundle sheath
chloroplasts, sub-experiment 119A contains four useful pieces of
data:

Table 12. Data for Experiment 119-120.

Experiment 119-120

Sub-experiment 119A

Specimen	T_e	$LogT_e$	$\bar{D}$	σ	N	$t_{.05}$	E	L	$\bar{D}_A$	Q	T_Q	F
M/P-119A	0.55	-0.2596	11.77	1.60	38	2.027	0.258	0.52				
M/P-119A	1.10	0.0414	16.57	1.72	34	2.036	0.294	0.60	13.75	-0.134	0.740	
BS/P-119A	1.10	0.0414	11.18	1.34	28	2.052	0.253	0.52	13.75	-0.190	1.549	2.09
BS/P-119A	2.00	0.3010	15.70	1.40	32	2.040	0.247	0.50				

Sub-experiment 119B

Specimen	T_e	$LogT_e$	$\bar{D}$	σ	N	$t_{.05}$	E	L	$\bar{D}_A$	Q	T_Q	F
M/P-119B	0.55	-0.2596	10.85	1.46	28	2.052	0.276	0.57				
M/P-119B	1.10	0.0414	15.54	1.74	29	2.048	0.323	0.66	15.00	0.006	1.015	1.73
BS/P-119B	1.60	0.2041	14.48	1.74	35	2.034	0.293	0.60	15.00	0.244	1.754	
BS/P-119B	2.60	0.4150	17.57	1.75	28	2.052	0.330	0.68				

Sub-experiment 120C

Specimen	T_e	$LogT_e$	$\bar{D}$	σ	N	$t_{.05}$	E	L	$\bar{D}_A$	Q	T_Q	F
M/P-120C	0.55	-0.2596	10.00	1.38	27	2.056	0.266	0.55				
M/P-120C	1.10	0.0414	15.21	1.71	34	2.036	0.293	0.60	14.25	-0.008	0.980	2.26
BS/P-120C	1.85	0.2672	13.57	1.17	14	2.160	0.313	0.68	14.25	+0.346	2.218	
BS/P-120C	2.70	0.4314	14.98	0.77	13	2.179	0.214	0.47				

Sub-experiment 120D

Specimen	T_e	$LogT_e$	$\bar{D}$	σ	N	$t_{.05}$	E	L	$\bar{D}_A$	Q	T_Q	F
M/P-120D	0.55	-0.2596	11.89	1.44	88	1.990	0.150	0.30	13.25	-0.174	0.670	2.38
BS/P-120D	1.95	0.2900	14.63	1.68	29	2.045	0.310	0.63	13.25	+0.203	1.596	

Table 13. Data for Experiment 119-120.

Specimen	$\bar{L}$	$\bar{\delta}_A \cdot \bar{L}$	Q+	T_{Q+}	$\bar{\delta}_A \cdot \bar{L}$	Q-	T_{Q-}	D_{MAX}	D_{MIN}
			Experiment 119-120 Sub-experiment 119A						
M/P-119A	0.56	14.31	-0.100	0.794	13.19	-0.176	0.667		
								$\frac{1.671}{0.667}=2.51$	$\frac{1.439}{0.794}=1.81$
BS/P-119A	0.51	14.26	0.223	1.671	13.24	0.158	1.439		
			Sub-experiment 119B						
M/P-119B	0.61	15.61	0.045	1.109	14.39	-0.033	0.927		
								$\frac{1.919}{0.927}=2.07$	$\frac{1.599}{1.109}=1.44$
BS/P-119B	0.64	15.64	0.283	1.919	14.36	0.204	1.599		
			Sub-experiment 129C						
M/P-120C	0.57	14.82	0.027	1.064	13.68	-0.043	0.906		
								$\frac{2.410}{0.906}=2.66$	$\frac{2.046}{1.064}=1.92$
BS/P	0.57	14.82	0.382	2.410	13.68	0.311	2.046		
			Sub-experiment 120D						
M/P-120D	0.30	13.55	-0.156	0.698	12.95	-0.193	0.641		
								$\frac{1.750}{0.641}=2.73$	$\frac{1.455}{0.698}=2.08$
BS/P-120D	0.63	13.88	0.243	1.75	12.62	+0.163	1.455		
			Experiment 121-122 Sub-experiment P-122						
M/P-122	0.58	14.83	0.097	1.25	13.67	0.002	1.000		
								$\frac{3.251}{1.000}=3.25$	$\frac{2.239}{1.250}=1.79$
BS/P-122	0.98	15.23	0.512	3.251	13.27	0.350	2.239		
			Sub-experiment T-121						
M/T	0.52	15.27	0.045	1.109	14.23	-0.040	0.912		
								$\frac{2.488}{0.912}=2.73$	$\frac{1.950}{1.109}=1.76$
BS?T-121	0.64	15.39	0.396	2.488	14.11	0.290	1.950		
			Sub-experiment H-122						
M/H-122	0.49	14.74	-0.067	0.857	13.76	-0.146	0.714		
								$\frac{2.871}{0.714}=4.02$	$\frac{2.529}{0.857}=2.59$
BS/H-122	0.34	14.59	0.458	2.871	13.91	0.403	2.529		
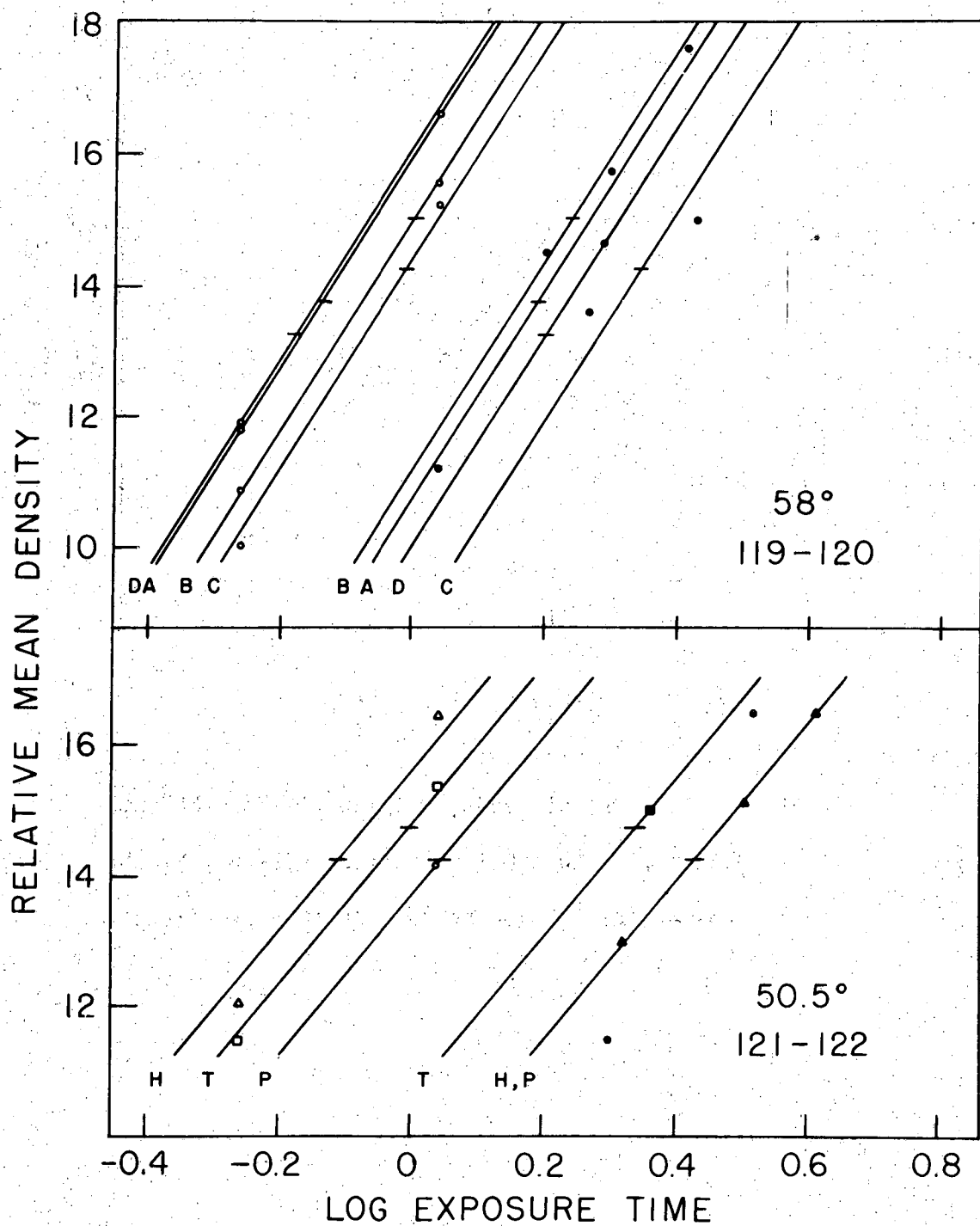
XBL 719-5361

Fig. 43. Characteristic curves for experiments 119-120 and
121-122; A/119A, B/119B, C/120C, D/120D, H/122H, T/121T, P/122P.
Cross lines indicate the adjusted relative mean densities.

Fig. 44. Infrared black and white photographs of two of the leaf sections used in experiment 119-120.

Fig. 44a. Sub-experiment 119A, frame 119A-4, 2.0 second exposure.

Fig. 44b. Sub-experiment 120C, frame 120C-4, 1.85 second exposure.

Fig. 44c. Sub-experiment 119A, frame 119A-3, 1.1 second exposure.

Fig. 44d. Sub-experiment 120C, frame 120C-3, 1.1 second exposure.
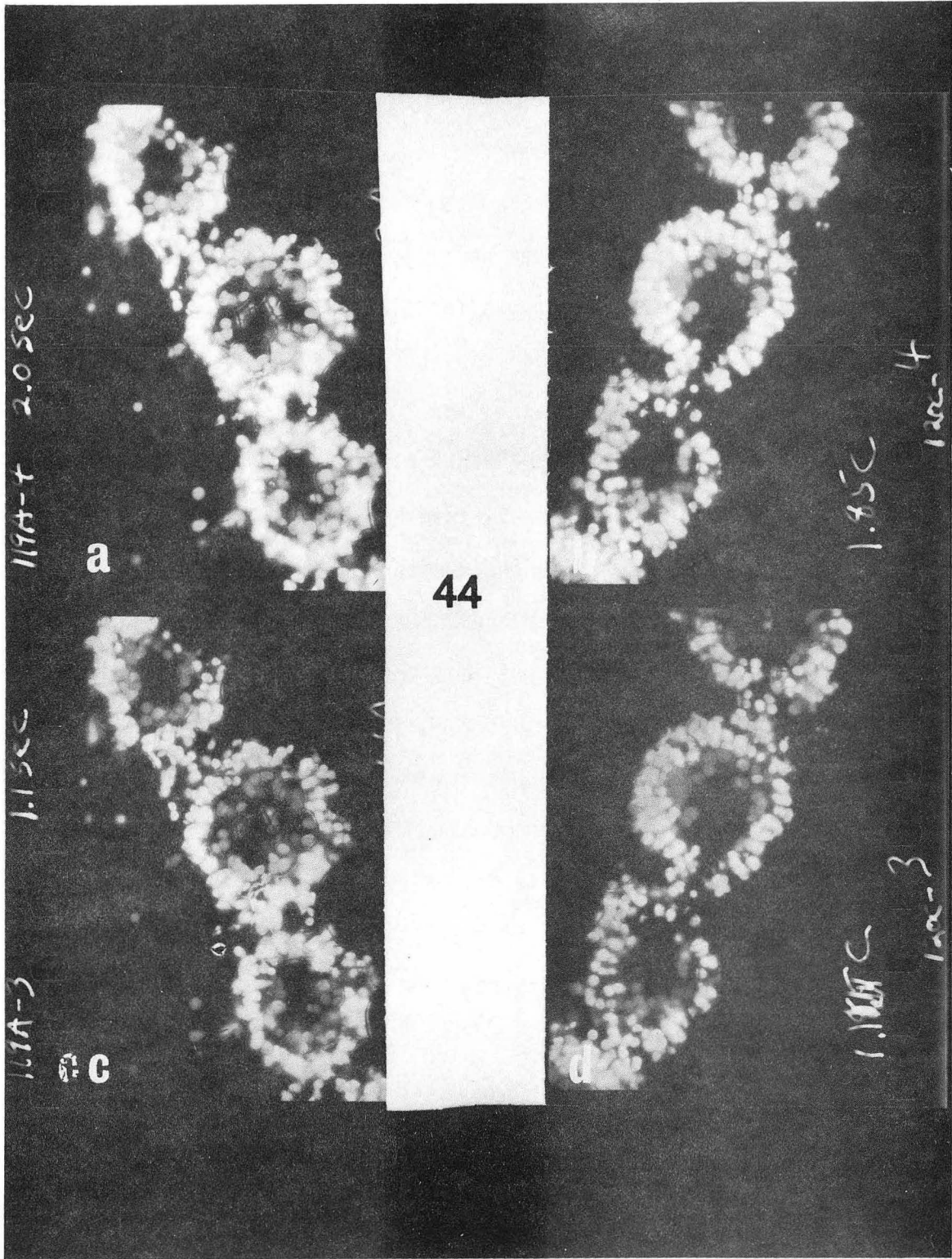
(1) The relative mean density, $\bar{D}$, of mesophyll chloro-
plasts photographed for 0.55 seconds equals 11.77.

(2) The relative mean density, $\bar{D}$, of mesophyll chloro-
plasts photographed for 1.10 seconds equals 16.57.

(3) The relative mean density, $\bar{D}$, of bundle sheath chloro-
plasts photographed for 1.10 seconds equals 11.18.

(4) The relative mean density, $\bar{D}$, of bundle sheath chloro-
plasts photographed for 2.00 seconds equals 15.70.

An examination of these four relative mean densities, or of
the three useful photographic negatives from which they were
derived (Fig. 44), shows the greater fluorescence intensity of
the mesophyll relative to the bundle sheath. This difference
in fluorescence intensity is analyzed quantitatively as follows.
Sub-experiment 119A provides the data for determining the linear
portion of two related "Characteristic Curves" -- one for the
mesophyll, and one for the bundle sheath (Fig. 43). The
difference in fluorescence intensity is analyzed by selecting
a density close to the average of the four mean densities of
sub-experiment 119A. This adjusted mean relative density, $(\bar{D}_A)$,
is chosen as 13.75 for sub-experiment 119A. The relative
fluorescence intensity of mesophyll to bundle sheath chloroplasts
is calculated by determining the exposure times which would
result in a relative mean density of 13.75 for both the mesophyll
and bundle sheath chloroplasts of sub-experiment 119A. The
"Characteristic Curves" for the mesophyll and bundle sheath

chloroplasts yield the logarithms of the exposure times (designated Q in Table 12) corresponding to the chosen adjusted relative mean relative density, $(\bar{D}_A)$, of 13.75. The antilogarithms of Q (designated T_Q in Table 12) give the exposure times which correspond to the value of the adjusted relative mean density for the sub-experiment. F, the ratio of mesophyll to bundle sheath chloroplast fluorescence intensity, is obtained by dividing T_Q mesophyll by T_Q bundle sheath (cf. Section V-B).

Tables 12 and 13 also include the information needed to estimate the standard experimental error in computing the ratio F. The standard error of the mean, (E), is used to compute the 0.05 confidence limit for the adjusted relative mean density $(\bar{D}_A)$. Statistically, for an estimated adjusted relative mean density, $(\bar{D}_A)$, of 13.75 (mesophyll chloroplasts - sub-experiment 119A), and an N of 36, the probability is 95% that the adjusted relative mean density $(\bar{D}_A)$ can vary by an average error factor of ± 0.56, (L). Therefore the probability is 95% that $\bar{D}_A$ falls in the range 13.19-14.31 $(\bar{D}_A \pm L)$. Correspondingly, the probability is 95% that the antilogarithms of the exposure times of the chloroplasts will fall in the range from -0.176 to -0.100. These values define upper and lower bounds of 0.677 and 0.794 seconds, respectively, for the range of exposure times. The maximum relative mesophyll to bundle sheath fluorescence is computed by dividing the larger possible bundle sheath exposure time by the smaller possible mesophyll exposure time (Table 13).

The minimum mesophyll to bundle sheath fluorescence ratio is obtained by dividing the smaller possible bundle sheath exposure time by the larger possible mesophyll exposure time. Consequently, the probability is 95% (0.05 confidence limit) that the actual mean relative mesophyll to bundle sheath chloroplast fluorescence intensity ratio falls between 1.81 and 2.51, while the sample mean ratio is 2.09.

Numerous sources of error can contribute to this statistical variation. Individual chloroplasts can vary in their fluorescence intensity. Alternatively, their apparent intensity can vary because they are slightly out of focus on the film. Similarly, an entire leaf cross section could become slightly out of focus during the course of an experiment as a result of a gradual drying of the specimen. Since exposures greater than one second are timed by hand with the aid of a stopwatch, there is an additional degree of uncertainty in the measurement of long exposure times.

Finally, the measurement of density could vary either from an uneven film emulsion, or from improper alignment of the densitometer. Consequently, when interpreting these experimental results, the summation of these errors is expressed in the confidence limits.

2. Experimental Results.

The raw data used to analyze the relative fluorescence intensities of the experimental photographs are located in

Appendices B and C. The organizational format is identical to that used for experiment 119-120. The "Characteristic Curves" of Figures 45 and 46 summarize the remaining raw data used to compute the ratio of mesophyll to bundle sheath fluorescence intensity (cf. Section IV.D). The degree to which the experimental points yield parallel "Characteristic Curves" is one indication of the precision of a given experiment.

In experiment 130-131, the gammas of the "Characteristic Curves" spread in three patterns between 57-73 degrees, and probably result from improper agitation during development, or from an unevenness of the film emulsion. It is unlikely that random error could result in such uniformity.

Tables 14, 15, 16 and 17 summarize the experimental ratios obtained from plain (untreated), Tris-treated, Tris-hydroxyla-mine-treated, and DCMU-treated leaf sections of Dichanthium annulatum, respectively. Surprisingly, with the exception of sub-experiment H-122, the mesophyll to bundle sheath fluorescence intensity ratios are approximately equal. There is a slight, non-statistically significant variation, with DCMU showing the lowest ratio, and Tris showing a higher ratio than the untreated material.

3. Discussion

The data summarized in these Tables should give some indi-cation of the relative contributions of Photosystems I and II
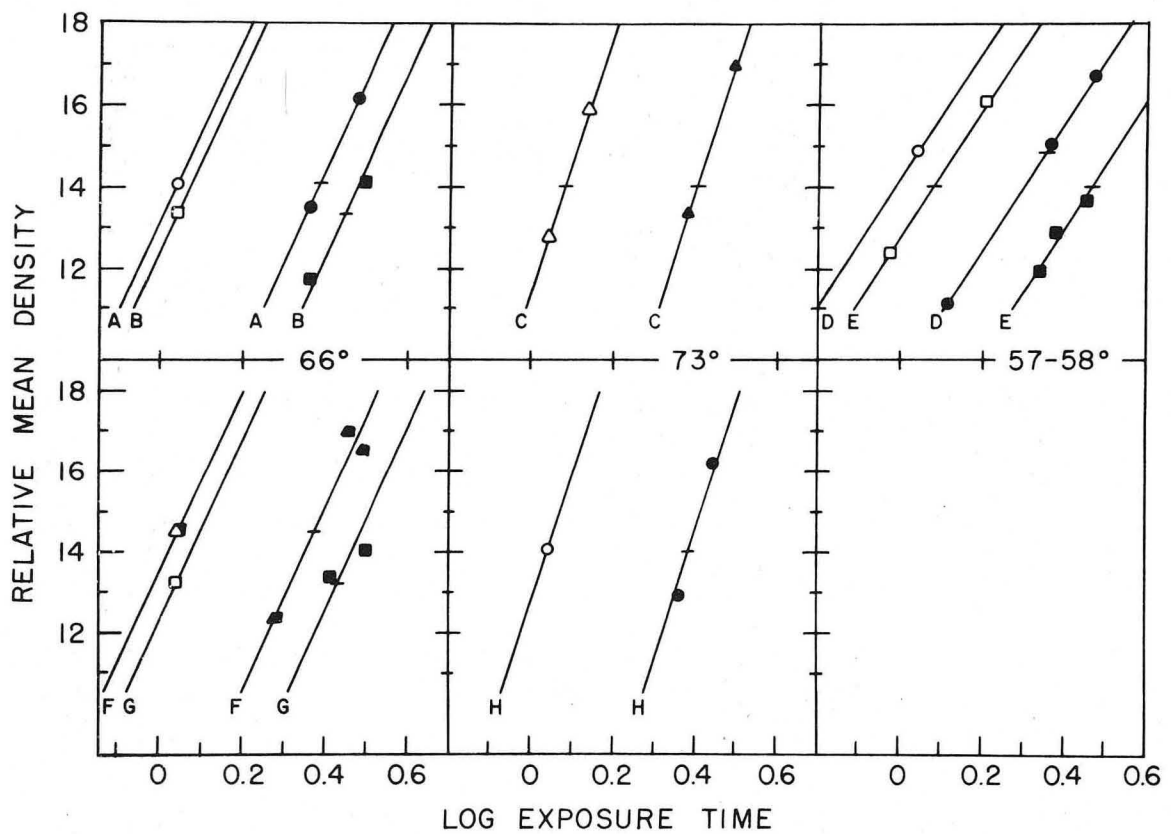
XBL717-5272

Fig. 45. Characteristic curves for experiment 130-131 (o) untreated,
(■) Tris treated, (▲) H. A. treated; open symbols, mesophyll; closed
symbols, bundle sheath; A/P-131D, B/T-131F, C/H-131, D/P-131E,
E/T-130, F/T-130T, G/T-131G, H/P-131C. Cross lines indicate the
adjusted relative mean densities.
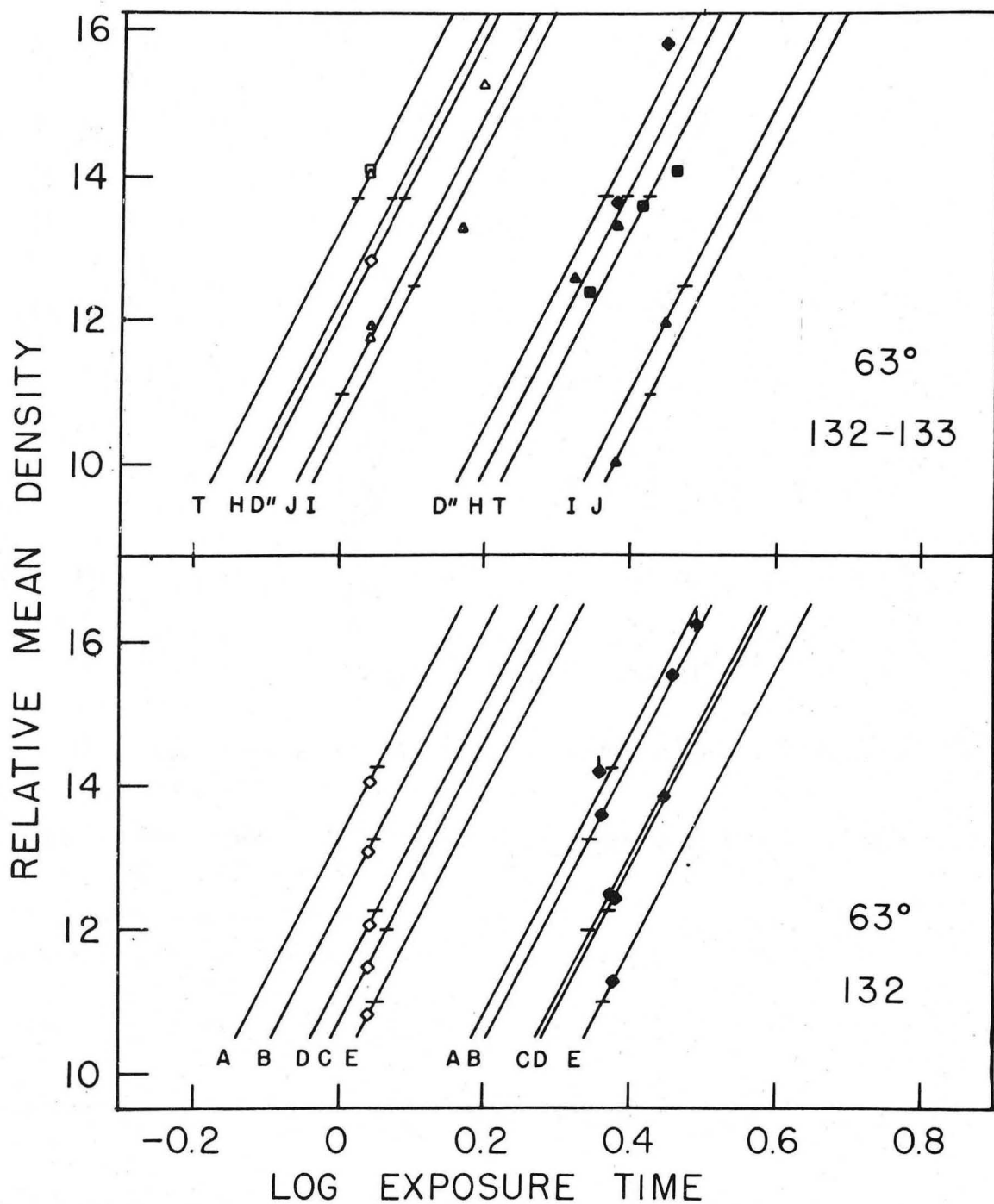
Fig. 46. Characteristic curves for experiments 132-133: (◊) XBL 719-5362
DCMU, (o) untreated, (▫) Tris-treated, (△) hydroxylamine-
treated; open symbols, mesophyll; closed symbols, bundle sheath;
A/D-132A, B/D-132B, C/D-132C, D/D-132D, D"/D-132DD, E/D-132E,
H/H-133A, I/H-133C, J/H-133D, T/T132. Cross lines indicate the
adjusted relative mean densities.

Table 14. Relative M/BS Chloroplast Fluorescence Yields of Untreated _Dichanthium annulatum_ leaf sections. F is the ratio of Mesophyll to Bundle Sheath Chloroplast Fluorescence.

PLAIN

Specimen	F_{MIN}	F	F_{MAX}
P-119A	1.81	2.09	2.51
P-119B	1.44	1.73	2.07
P-120C	1.92	2.26	2.26
P-120D	2.08	2.38	2.73
P-122	1.79	2.40	3.25
P-131C	2.04	2.21	2.36
P-131D	1.99	2.22	2.47
P-131E	1.81	2.21	2.30
Mean	1.86	2.19	2.49
σ	0.20	0.21	0.36

Table 15. Relative M/BS Chloroplast Fluorescence Yields of
Tris-treated <u>Dichanthium annulatum</u> Leaf Sections.

TRIS

Specimen	F_{MIN}	F	F_{MAX}
T-121	1.76	2.20	2.73
T-130	1.66	2.42	2.79
T-130T	1.86	2.14	2.79
T-131F	1.99	2.56	2.30
T-131G	2.24	2.45	2.70
T-132	2.19	2.52	2.93
Mean	1.98	2.38	2.71
σ	0.19	0.07	0.09

Table 16. Relative M/BS Chloroplast Fluorescence Yields of
DCMU-treated <u>Dichanthium annulatum</u> Leaf Sections.

		DCMU	
<u>Specimen</u>	F_{MIN}	$\underline{F}$	F_{MAX}
D-132A	1.89	2.11	2.36
D-132B	1.80	1.97	2.18
D-132C	1.75	1.91	2.08
D-132D	1.86	2.07	2.30
D-132DD	1.68	1.88	2.11
D-132E	1.91	2.05	2.20
Mean	1.82	2.00	2.21
σ	0.09	0.09	0.11

Table 17. Relative M/BS Chloroplast Fluorescence Yields of
Hydroxylamine-treated _Dichanthium annulatum_
Leaf Sections.

	HYDROXYLAMINE		
Specimen	F_{MIN}	F	F_{MAX}
H-122	2.95	3.45	4.02
H-131	1.94	2.09	2.25
H-133A	1.86	2.09	2.34
H-133C	2.08	2.37	2.62
H-133D	2.49	2.69	2.85
Statistical Mean and	2.09	2.31	2.52
without H-122	0.28	0.29	0.27
Same with H-122	2.26	2.54	2.82
σ	0.45	0.57	0.71

within mesophyll and bundle sheath chloroplasts. The total fluorescence from an untreated chloroplast includes the fluorescence from both Photosystems I and II, although most fluorescence probably stems from PS II. Tris treatment should decrease fluorescence by diminishing the variable fluorescence component of PS II (cf. Section I. C2). Initially, it was assumed that far-red fluorescence originated predominantly in PS II. If the bundle sheath chloroplasts lacked PS II, as was inferred from the infrared color data, then for Tris-treated material, the total fluorescence from mesophyll chloroplasts should decrease, while that from the bundle sheath should remain unchanged. This would result in a decreased mesophyll to bundle sheath fluorescence intensity ratio.

The mesophyll to bundle sheath ratio of 2.38 observed for Tris-treated material implies that the bundle sheath chloroplasts are at least as much affected by Tris treatment as are the mesophyll chloroplasts. Three independent sources of evidence indicate that the chloroplasts contained in the leaf cross-sections are, in fact, affected by the Tris treatment. Tris-treated leaf sections display no System II-dependent tetrazolium precipitate, whereas the untreated controls heavily precipitated the dye (Fig. 47 and 48). Secondly, there is a visible decrease in fluorescence intensity of Tris-treated leaf sections. Finally, the spectral distribution of the fluorescence emission shifts more toward the orange-red than is characteristic of the untreated material.

Fig. 47. Untreated _Dichanthium_ _annulatum_ (142-7A) with heavy precipitate of tetrazolium dye (10^{-4} M NBT, 15 minutes) after exposure to light. X 550.

Fig. 48. Tris-treated (1 hour, 0.8M, pH 8.0) _Dichanthium_ _annulatum_ (142-21A) does not precipitate tetrazolium dye (10^{-4}M NBT, 15 minutes) after exposure to light. X 550.

47

XBB 718-3562

48
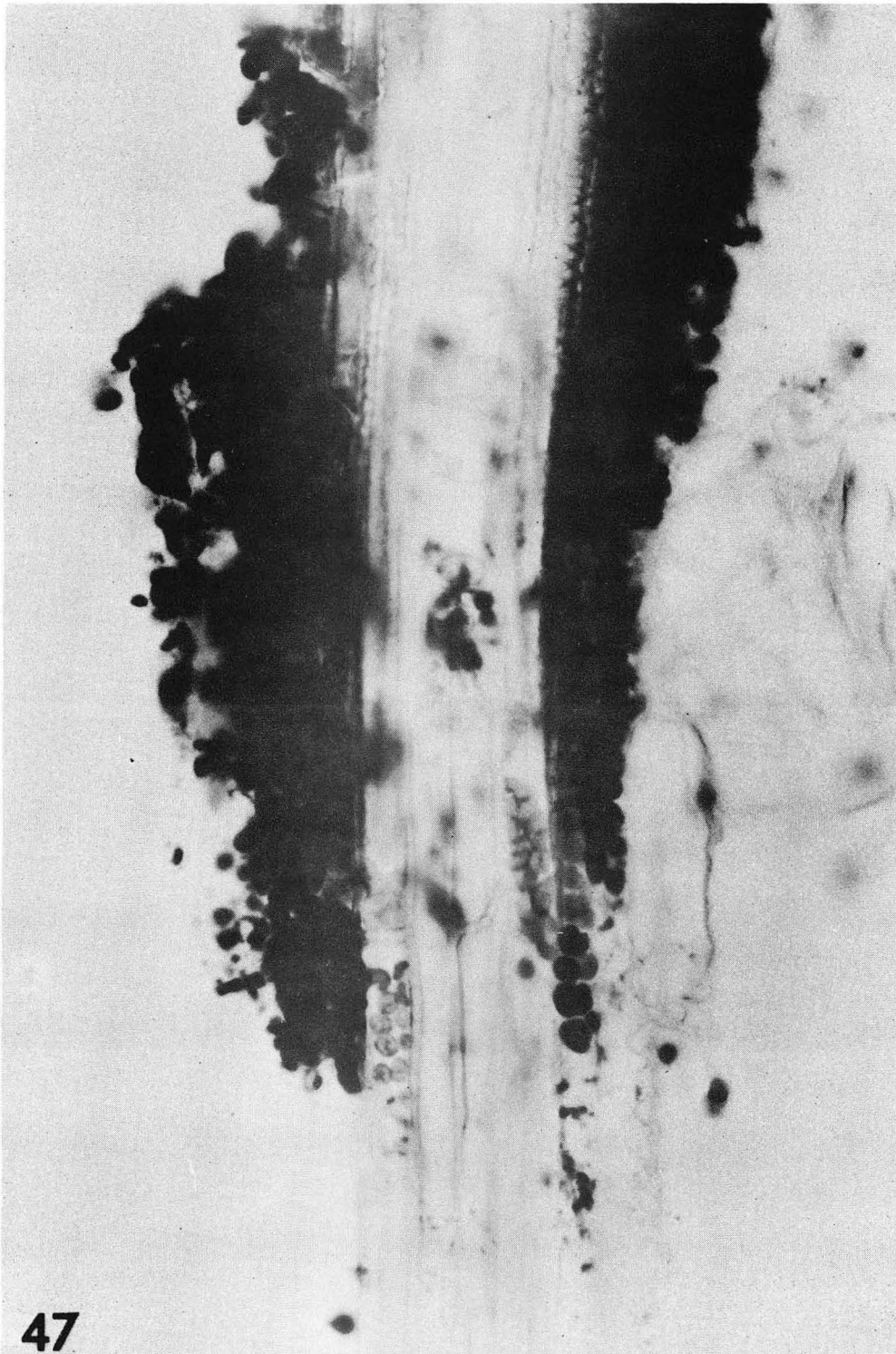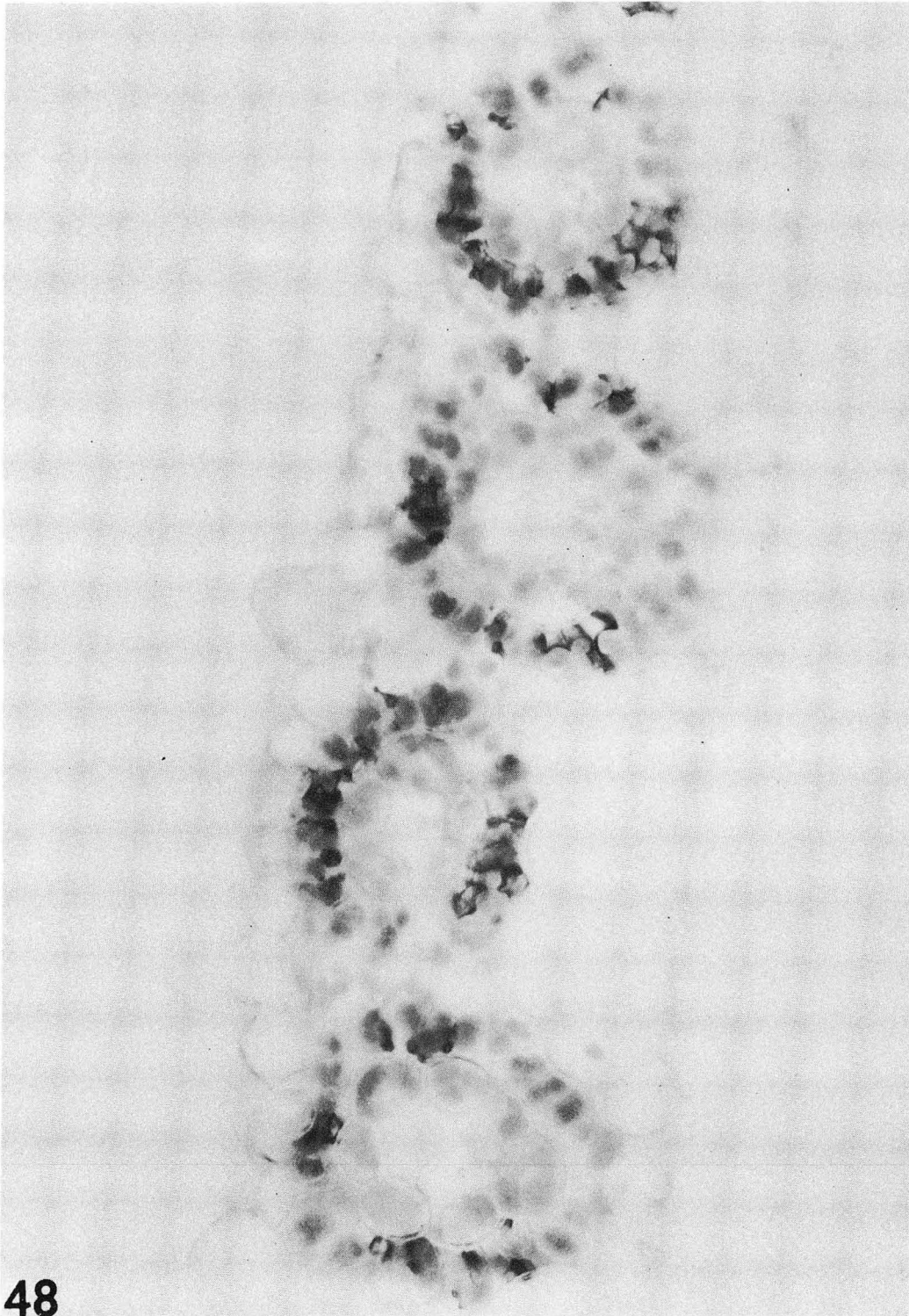
In a manner consistent with the Tris data, there is a slightly lowered mesophyll to bundle sheath fluorescence intensity ratio in DCMU treated material. By blocking the flow of electrons between PS II and PS I, DCMU treatment should result in an increase of PS II fluorescence relative to PS I fluorescence. If, as hypothesized in Section III, the bundle sheath chloroplasts lack PS II, then the relative M/BS fluorescence intensity should have strongly increased in the DCMU-treated material, provided the light intensity was below the level of saturation. Similarly, the fluorescence ratio determined after Tris-hydroxylamine treatment should have been significantly higher than that for Tris-treated material. This expectation stems from the supposed restoration of variable fluorescence by hydroxylamine (cf. Section I. C2).

Although sub-experiment H-122 did result in a greatly increased ratio, sub-experiments H-131, H-133A, H-133D resulted in ratios approximately equivalent to those observable with Tris treatment.

E. <u>The Ratio of Mesophyll to Bundle Sheath Chloroplast Fluorescence Intensities at 680 Nanometers</u>

The procedure described in Section IV-D, to measure the total fluorescence intensity ratio, needs only slight modification for calculating the ratio at 680 nm. Once perfected, this modified procedure may be adapted to provide fluorescence spectra.

During sub-experiment 106-680, a 680 nm interference filter with a 10 nm half band width is inserted between the specimen and the film. The resulting decrease in transmitted fluorescence intensity necessitates a ten-fold increase in exposure time.

Figure 49 illustrates the linear portions of the "Characteristic Curves" corresponding to the mesophyll and bundle sheath chloroplasts on a series of photographs. The data from which these curves are obtained are presented in Appendices B and C. Figure 49 also includes the entire "Characteristic Curve" for a single bundle sheath chloroplast.

An analysis of Figure 49 results in a computed relative mesophyll to bundle sheath fluorescence intensity ratio at 680 nm of 7.05. The probability is 95% that the actual ratio falls in the range of 6.31 to 7.89.

Similar data, obtained as a by-product of experiments 126-127 and 134-135, result in the following statistics:

Sub-experiments	Chemical Treatment	M/BS Ratio
126M/127BS	untreated	4.19
127M/126BS	untreated	5.11
M of 134BS/134BS	TRIS	6.01
135M/BS of 135M	TRIS	5.89
M of 135BS/135BS	TRIS	5.02

This ratio differs when computed at 730 nm (cf. Section IV.F2).

These data support the earlier findings of a greatly diminished far-red (680 nm) fluorescence component in bundle sheath
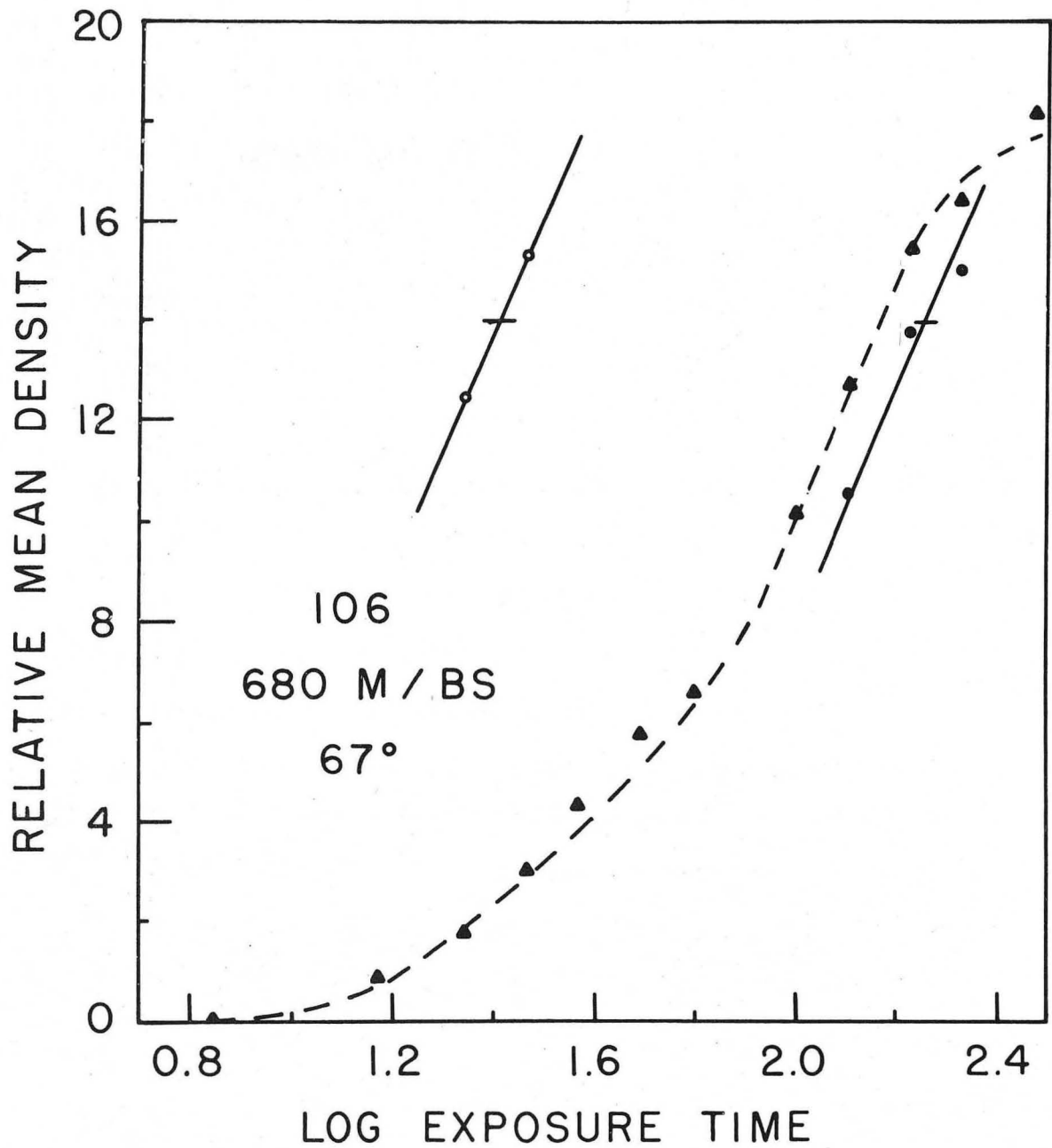
Fig. 49. Characteristic curves for <u>Dichanthium annulatum</u>
chloroplasts at 680 nm: open symbols, mesophyll; closed symbols,
bundle sheath: (▲) separate chloroplast used to plot a complete
characteristic curve.

XBL 719-5363

chloroplasts. However, since the relative mesophyll to bundle sheath total **fluorescence** ratio remains fairly constant, even under varying chemical treatment, it is appropriate to investigate other chloroplast parameters of a leaf actually used in one of the quantitative studies. Figures 50, 51, 52, and 53 show the ultrastructure of an adjacent untreated portion of the leaf used in experiment 134-135 Tris. Although some bundle sheath chloroplast profiles of <u>Dichanthium annulatum</u> lack lamellar appression (cf. Appendix A, Figure 3), the chloroplasts profiles studied in these quantitative experiments appear to have a slight amount of appression, similar in degree to that found in the bundle sheath chloroplasts of corn and <u>Sorghum</u> (Appendix A, Fig. 5 and 6). All three species, however, decidedly lack extensive grana formation in bundle sheath chloroplasts.

F. <u>Fluorescence Emission Spectra of Dichanthium annulatum</u>

The procedure used to obtain the relative mesophyll to bundle sheath fluorescence intensity at 680 nm (cf. Section IV may be modified to obtain a fluorescence emission spectrum. For this purpose, it is necessary to photograph a single specimen through a series of interference filters. The negatives photographed through each interference filter determine one "Characteristic Curve." In order to evaluate the fluorescence emission spectrum of the chloroplasts in a single leaf cross-section,

Fig. 50. Bundle sheath chloroplasts of _Dichanthium annulatum_ obtained from a portion of leaf adjacent to the one used in experiment 134-135T. X 14,700.

Fig. 51. Portion of a bundle sheath chloroplast obtained from the same source. X 48,300.

Fig. 52. Same as above. X 49,700.

Fig. 53. Same as above. X 62,700.

50

XBB 717-3315

51
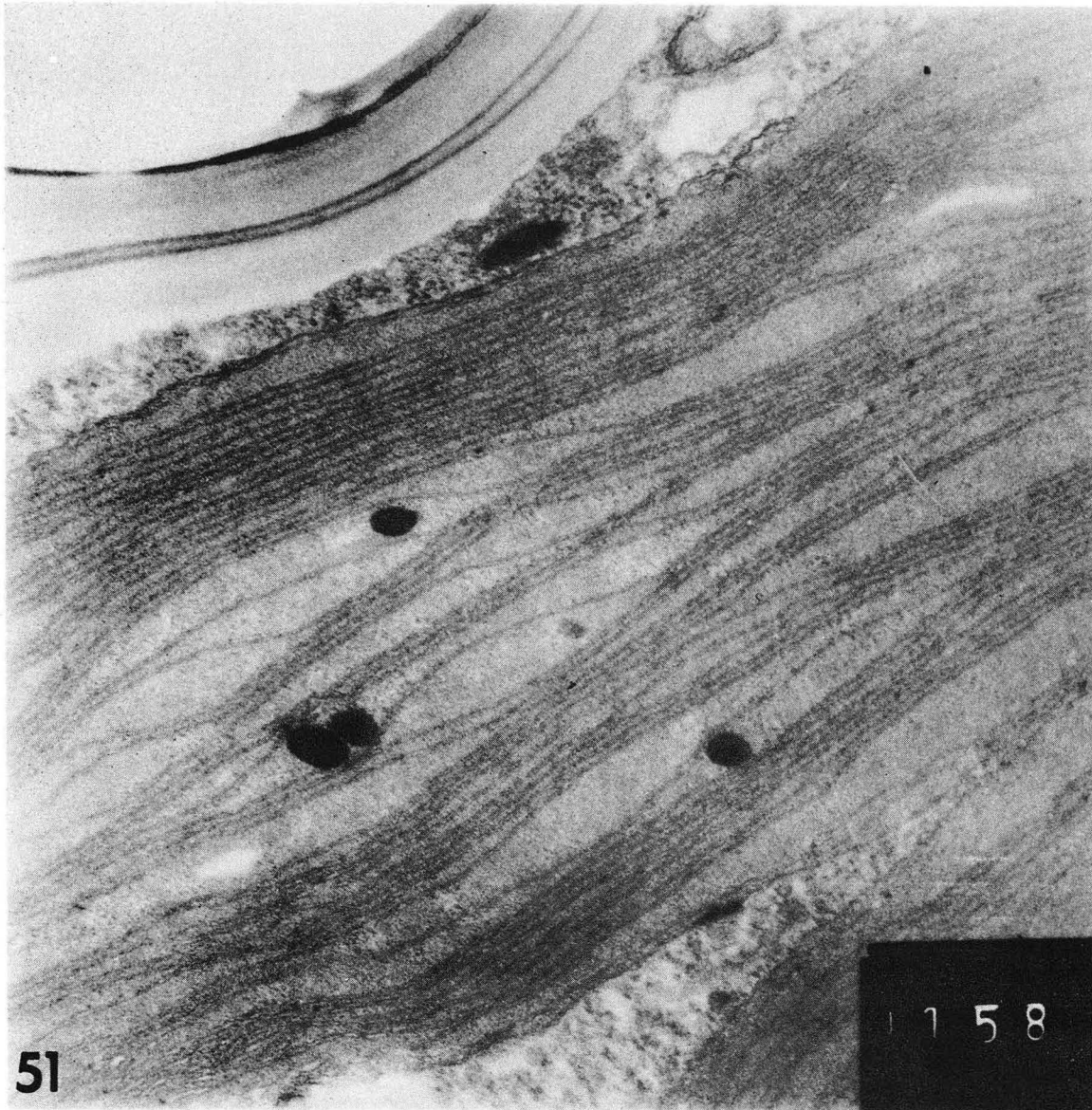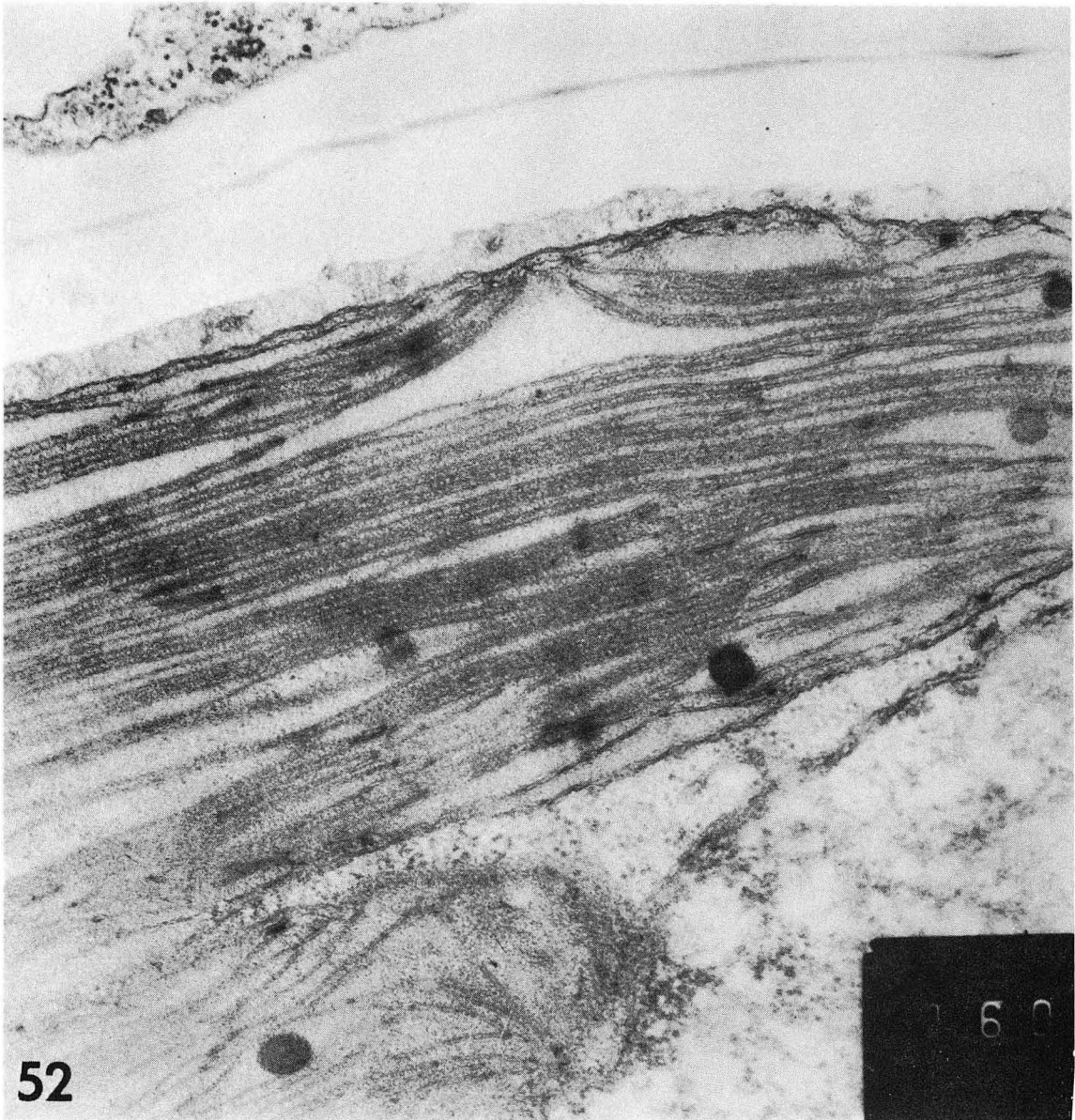
XBB 717-3317

52

XBB 717-3316

53

XBB 717-3314

ten filters, between 670 and 740 nm, are used. Figures 54, 55 and 56 show the densitometer tracings from three photographic negatives used in this type of analysis. With different interference filters, greatly different exposure times are necessary to obtain photographs of approximately equal density.

The data from ten related "Characteristic Curves," corresponding to the ten filters, are analyzed to determine the relative fluorescence emission spectra. Once again, the adjusted relative mean density ($\bar{D}$) is set close to the measured relative mean densities ($\bar{D}$). In this case it is necessary to interrelate ten separate "Characteristic Curves," which involve between 14 and 20 separate relative mean density ($\bar{D}$) data points. Once $\bar{D}_A$ is set, it is necessary to determine the exposure times (T_Q), necessary to obtain photographic negatives of an equal adjusted relative mean density ($\bar{D}_A$), when each photograph is taken through a different interference filter.

Photographic negatives of equal densities are obtained by equivalent exposure to light (cf. Section IV. A). In accordance with this restriction of equivalent exposure to light, the product of fluorescence intensity and time of exposure must remain constant (cf. Section IV. A). Consequently, the reciprocal of the exposure time is a direct measure of the fluorescence intensity. Therefore the reciprocal of the exposure times ($1/T_Q$), corresponding to a uniform photographic density ($\bar{D}_A$), when each photograph is taken through a different interference filter, can be used to
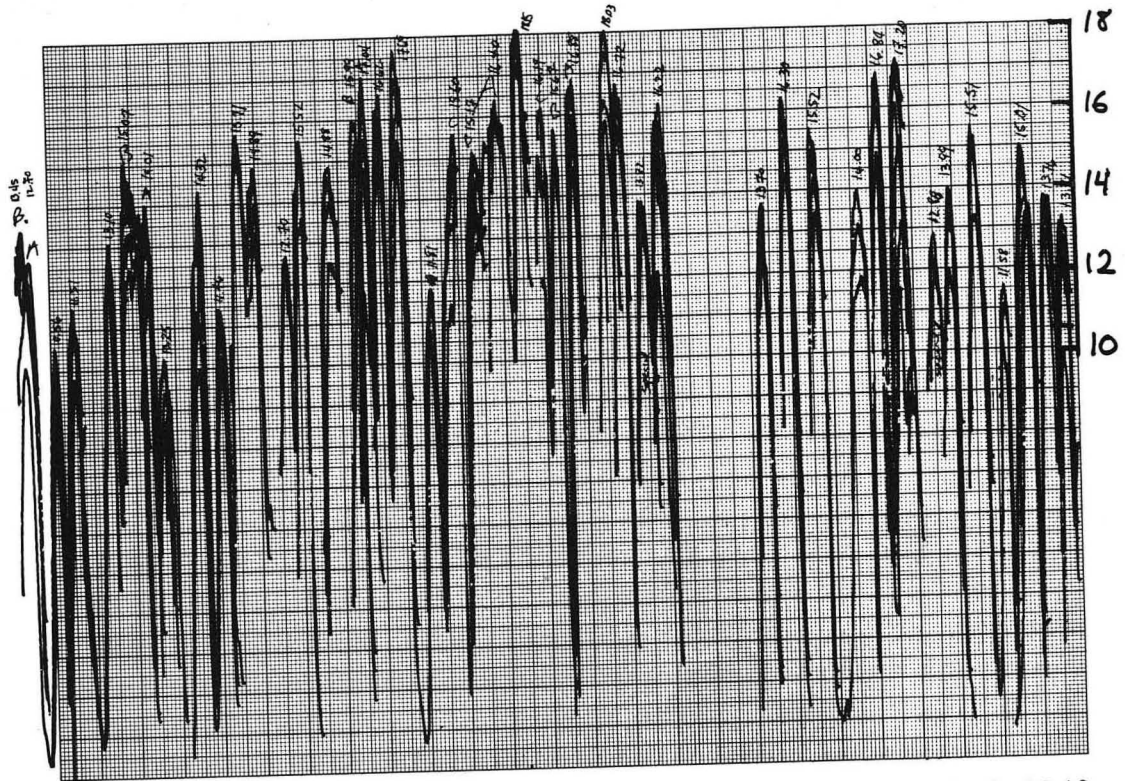
XBL 7310-1340

Fig. 54. Densitometer tracing of <u>Dichanthium annulatum</u>
bundle sheath chloroplasts (126BS-6) photographed through a
720 nm interference filter for 35 seconds.

XBL 7310-1338

Fig. 55. Densitometer tracing of a photograph of _Dichanthium_ _annulatum_ bundle sheath chloroplasts (126 BS - 4), photographed through a 730 nm interference filter for 36.1 seconds.

XBL 7310-1339

Fig. 56. Densitometer tracing of a photograph of <u>Dichanthium</u>
<u>annulatum</u> bundle sheath chloroplasts (126 BS - 2) photographed
through a 740 nm interference filter for 32 seconds.

determine the fluorescence intensity of that specimen at that wavelength. First, however, the calculated $1/T_Q$ must be corrected for the spectral characteristics of the filters and/or the film. $1/T_Q$ must be adjusted since the percentage transmission of the interference filters and the spectral response of the film both vary (cf. Section II. C).

It proves easiest to multiply T_Q by the necessary correction factor. Since fluorescence intensity is proportional to the reciprocal of T_Q, a correction factor which increases T_Q will effectively decrease the computed fluorescence intensity.

Table 18 shows the calculation of each of the thirteen correction constants. Since the raw data preferentially favor 740 nm, the other wavelengths need a correction constant smaller than 1.00 to increase their relative fluorescence accordingly. A correction constant less than 1.0, used to correct T_Q, results in a larger relative fluorescence intensity, as measured by $1/T_Q$.

Since each filter passes only two to ten per cent of the total fluorescence, exposure times must be increased between fifty and ten fold to adequately expose the film. The necessary exposure times vary from nine to twenty-five seconds for the mesophyll, and from 32 to 150 seconds for the bundle sheath. The photography for a mesophyll series takes approximately 45 minutes to complete, while the bundle sheath series requires approximately one hour. This is close to the amount of time

Table 18. Calculation of Time Correction Constant

Interference filter wavelength, nm	Film factor		Filter factor		Time correction constant
644	$\dfrac{11.24}{13.23}$	x	$\dfrac{0.22}{0.30}$	=	0.623
661	$\dfrac{10.61}{13.23}$	x	$\dfrac{0.29}{0.30}$	=	0.775
671	$\dfrac{10.90}{13.23}$	x	$\dfrac{0.28}{0.30}$	=	0.709
680	$\dfrac{11.03}{13.23}$	x	$\dfrac{0.21}{0.30}$	=	0.583
689	$\dfrac{11.89}{13.23}$	x	$\dfrac{0.29}{0.30}$	=	0.869
696	$\dfrac{12.65}{13.23}$	x	$\dfrac{0.28}{0.30}$	=	0.892
701	$\dfrac{12.52}{13.23}$	x	$\dfrac{0.22}{0.30}$	=	0.694
707	$\dfrac{12.90}{13.23}$	x	$\dfrac{0.28}{0.30}$	=	0.910
709	$\dfrac{12.90}{13.23}$	x	$\dfrac{0.12}{0.30}$	=	0.390
715	$\dfrac{13.20}{13.23}$	x	$\dfrac{0.24}{0.30}$	=	0.798
722	$\dfrac{12.99}{13.23}$	x	$\dfrac{0.26}{0.30}$	=	0.851
731	$\dfrac{12.91}{13.23}$	x	$\dfrac{0.23}{0.30}$	=	0.748
741	$\dfrac{13.23}{13.23}$	x	$\dfrac{0.30}{0.30}$	=	1

it takes for chloroplast fluorescence to irreversibly fade under the microscope. Fortunately, bundle sheath chloroplasts are more resistant to fading than mesophyll chloroplasts. In addition, chloroplasts at the periphery of the section tend to fade more readily. This fading is apparent by a visible loss of red fluorescence. Consequently, whenever the chloroplasts start to fade before the completion of a sub-experiment, that sub-experiment is discarded.

This fading problem necessitates limiting the number of separate photographs to an absolute minimum. Usually two rolls of film contain the data corresponding to four separate spectra. The data for each spectrum involve between thirteen and twenty photographic negatives, and ten "Characteristic Curves".

Approximately 20% of the "Characteristic Curves" corresponding to one experiment are determined by two or more data points. These "Characteristic Curves" are used to estimate the gamma (slope) of the remaining 80%. Therefore, of the forty "Characteristic Curves" involved in one experiment (ten for each of four spectra), eight are determined by two or more points, while the remaining thirty-two are determined by a single point and the computed gamma.

The relative fluorescence at 661 and 644 nm is determined by calculating the relative fluorescence intensities at 680, 661, and 644 nm, respectively. The 661 and 644 nm values are then expressed as a percentage of the 680 nm value.

Figure 57 shows the four "Characteristic Curves" of experiment 139. Two of these curves are used in determining the fluorescence intensity of mesophyll chloroplasts at 680 relative to 644 nm. An exposure of 12.59 seconds through the 680 nm filter develops the same $\bar{D}_A$ of 14.00 as an exposure of 1052.00 seconds through the 644 filter (cf. Appendix C). These estimated exposure times (T_Q) must be corrected for film and filter biases with the proper correction constant before the fluorescence intensity at 644 relative to 680 nm can be evaluated.

$$\frac{T_{Q(680)} \times CC_{680}}{T_{Q(644)} \times CC_{644}} = \frac{I_{644}}{I_{680}}$$

$$\frac{12.59 \times 0.583}{1052.00 \times 0.623} = 0.01$$

Therefore, if the relative fluorescence intensity at 680 nm is calculated as 8.00, then the relative fluorescence intensity at 644 nm can now be estimated as 0.08. Table 19 outlines the 661 and 644 values for all of the fluorescence spectra measured in this investigation. The raw data are included in Appendices B and C.

The bundle sheath fluorescence penetrating the 644 nm filter is barely capable of darkening the film. Since it is possible to measure a relative ratio as low as 0.01, as described above, the bundle sheath fluorescence at 644 nm is significantly less than 1% of the value at 680 nm. The assumption of a ratio as large as 0.01 would still result in a value of less than 0.025
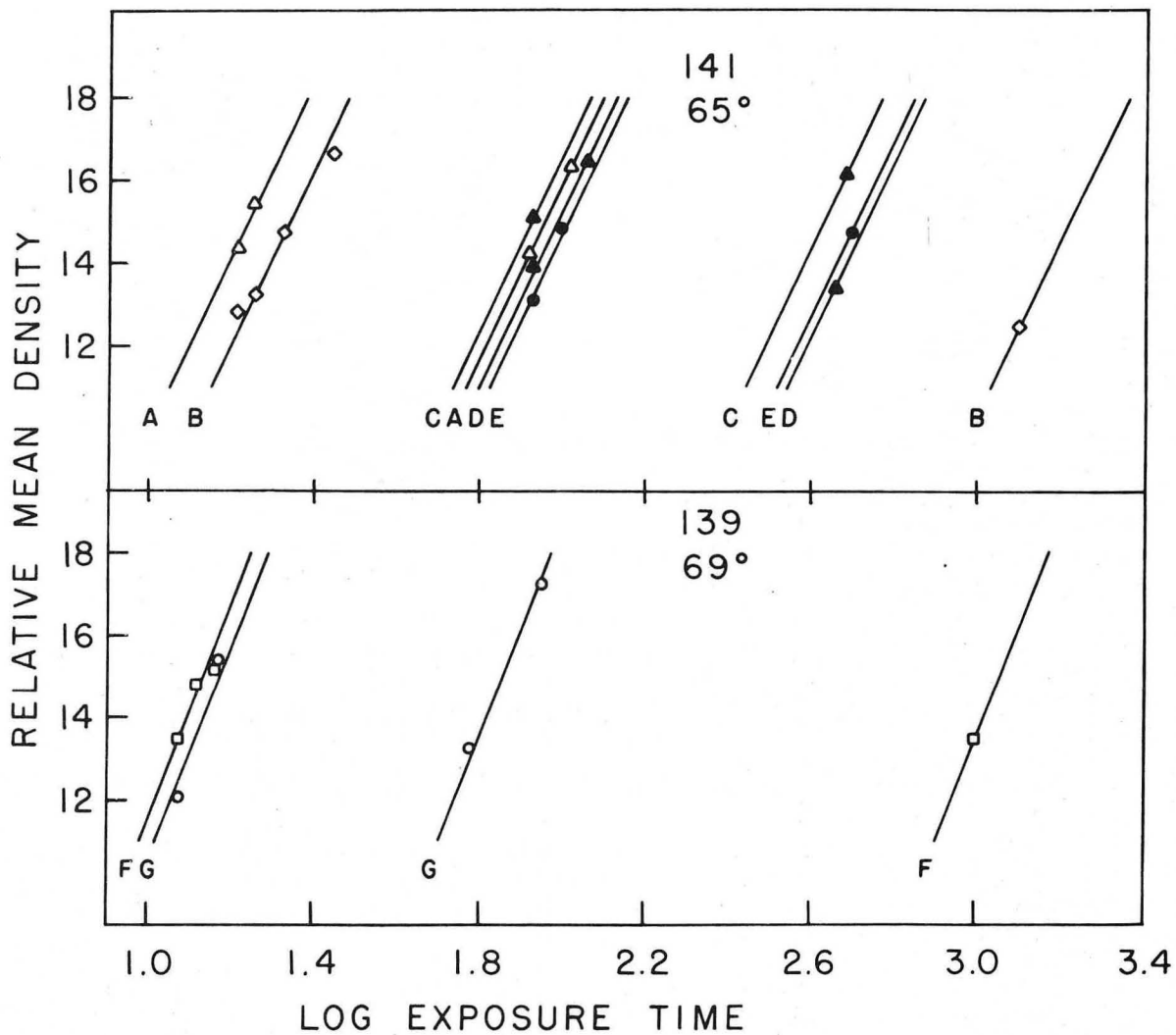
Fig. 57. Characteristic curves for experiments 139 and 141.
(A) 661/680, M-TRIS; (B) 644/680, M-TRIS; (C) 661/680, BS-TRIS;
(D) 661/680, BS-TRIS; (E) 661/680, BS-untreated; (F) 644/680,
M-untreated; (G) 661/680, M-untreated.

XBL 718-5349

Table 19. Relative Fluorescence Densities of <u>Dichanthium annulatum</u> Chloroplasts at 680, 661, and 644 nm.

	680	D'-661	661	680 MIN	F-661 MIN	661 MIN	680 MAX	F-661 MAX	661 MAX
					680-661				
126M	10.60	0.156	1.65	8.92	0.147	1.31	11.49	0.167	1.92
126M"	13.19	0.156	2.06						
127BS	2.53	0.152	0.38	2.31	0.128	0.30	2.74	0.179	0.44
127M	10.77	0.156	1.68	9.69	0.147	1.42	11.81	0.167	1.97
127M"	13.32	0.156	2.08						
126BS	2.06	0.152	0.31	1.86	0.128	0.24	2.25	0.179	0.40
134M-Tris	11.12	0.145	1.61	10.54	0.133	1.40	11.70	0.158	1.85
135BS-Tris	2 24	0.143	0.32	2.00	0.124	0.25	2.49	0.164	0.41
135M-Tris	10.48	0.145	1.52	9.89	0.133	1.32	11.00	0.158	1.74
134BS-Tris	1.74	0.143	0.25	1.55	0.124	0.19	1.96	0.164	0.32

	680	D'-644	644	680 MIN	D'-644 MIN	644 MIN	680 MAX	D'-644 MAX	644 MAX
					680-644				
126M	10.60	0.011	0.11	8.92	0.010	0.09	11.49	0.012	0.14
126M"	13.19	0.011	0.15						
127M	10.77	0.011	0.12	9.69	0.010	0.10	11.81	0.012	0.14
127M"	13.32	0.011	0.15						
134M-Tris	11.12	0.012	0.13	10.54	0.011	0.12	11.70	0.014	0.16
135M-Tris	10.48	0.012	0.13	9.89	0.011	0.11	11.00	0.014	0.15

relative fluorescence intensity units in comparison with the values between 1.50 and 3.00 calculated for the remainder of the spectrum. Therefore, although the absolute bundle sheath fluorescence intensity is not quite zero at 644 nm, within experimental error, the relative fluorescence is less than 0.03. This also indicates that the background fluorescence or baseline is nearly zero.

2. Spectra of Untreated Material

Experiment 126-127 measures the fluorescence emission spectra of untreated Dichanthium annulatum mesophyll and bundle sheath chloroplasts. Separate sub-experiments are used to determine two separate spectra for each type of chloroplast. Figures 54, 55, and 56 show the actual densitometer tracings made from photographs of bundle sheath chloroplasts recorded in sub-experiment 126 BS (Fig. 60).

The actual exposure times vary with the particular filter being used, and are estimated, in each case, in an attempt to achieve a photographic density between 9.0 and 18.5 relative density units. For example, in sub-experiment 126 BS, it is only necessary to expose the film for 42.90 seconds through the 680 nm filter to achieve a relative mean density ($\bar{D}$) of 16.08. In contrast, a 66.00 second exposure through the 701 nm filter is required to achieve a relative mean density ($\bar{D}$) of 15.73 (Fig. 58).
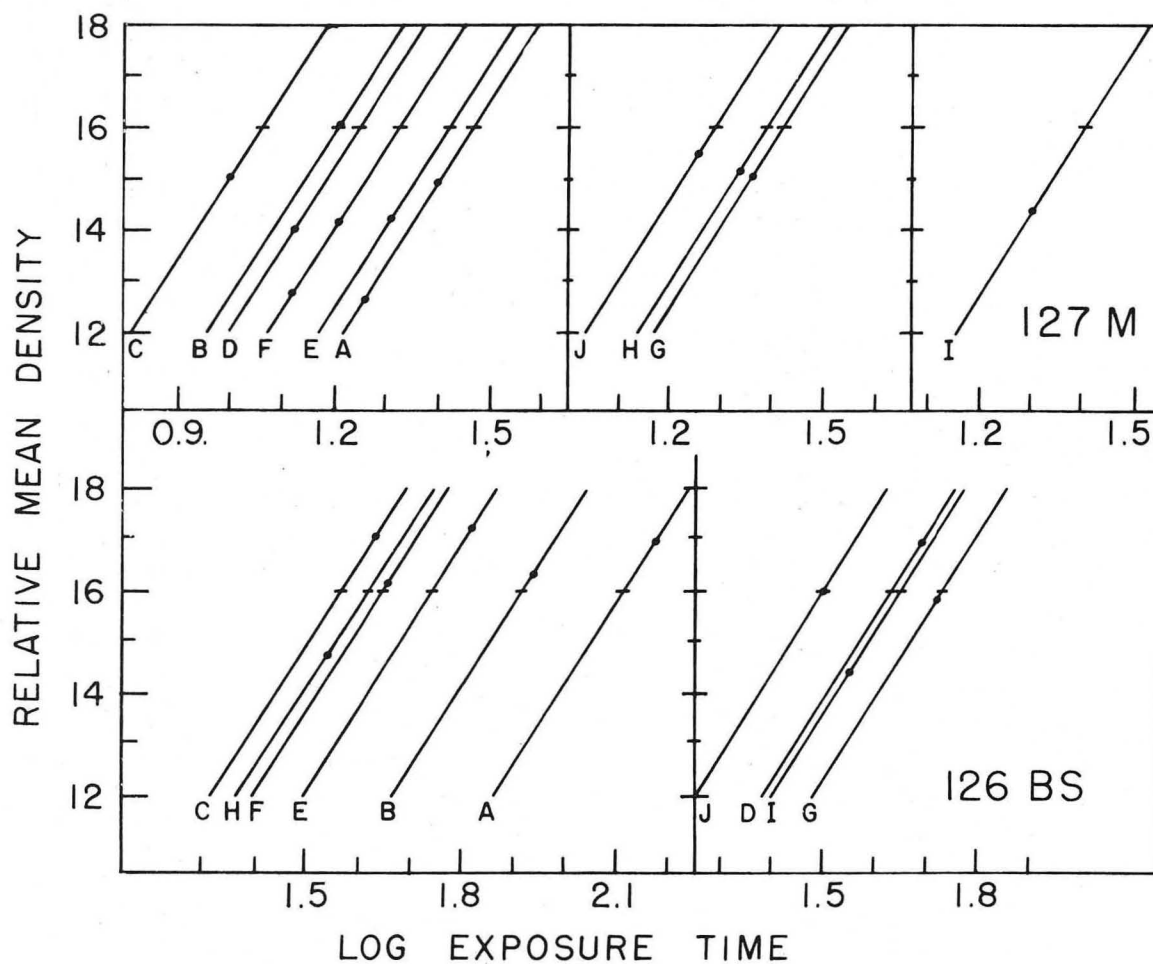
XBL717-5270

Fig. 58. Characteristic curves for experiments 126BS-127M.
Letters indicate wavelength maxima of the interference filters
used in each sub-experiment: A/671, B/680, C/689, D/696, E/701,
F/709, G/715, H/722, I/731, J/741. Cross lines indicate the
adjusted relative mean density.
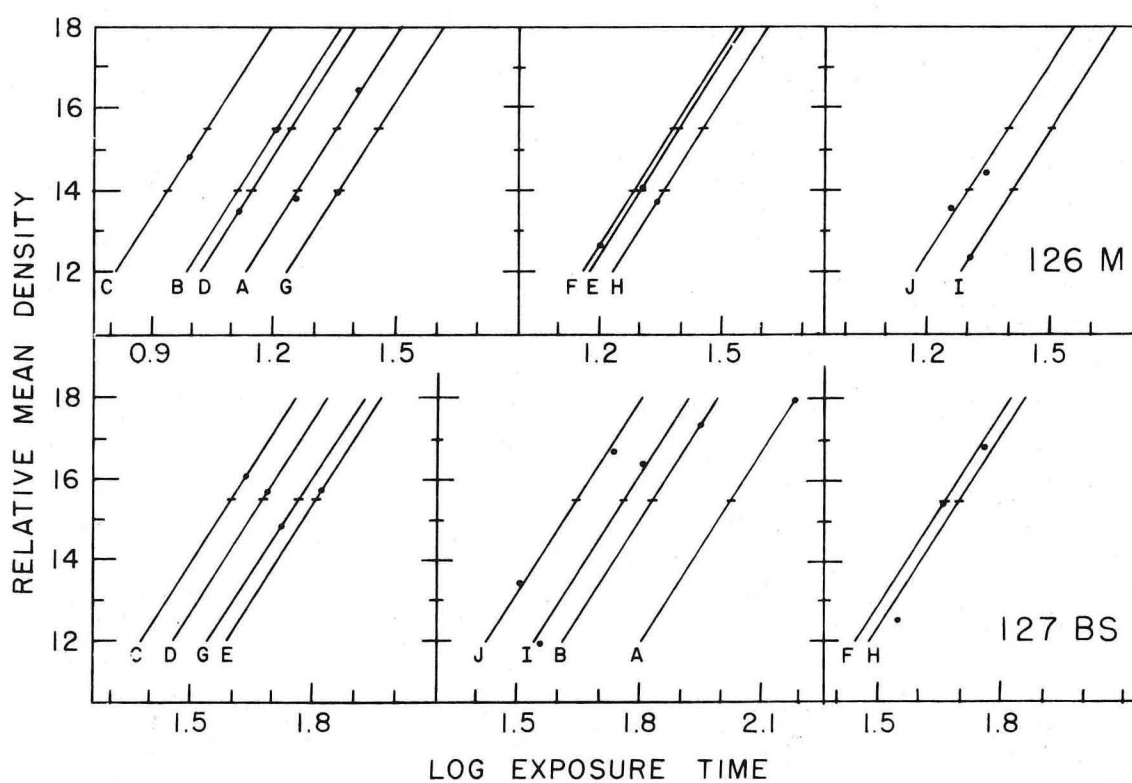
Fig. 59. Characteristic curves for experiments 126M-127BS.
A, B... (cf. Fig. 58).

XBL717-5271

Fig. 60. Infrared black and white photographs of the leaf

section used in sub-experiment 126 BS.

Fig. 60a. Control photograph, 1.1 seconds.

Fig. 60b. Interference filter (740 nm), 32 second

corrected exposure time.

Fig. 60c. Interference filter (680 nm), 150.8 second corrected

exposure time.

Fig. 60d. Interference filter (689 nm), 4.95 second corrected

exposure time.
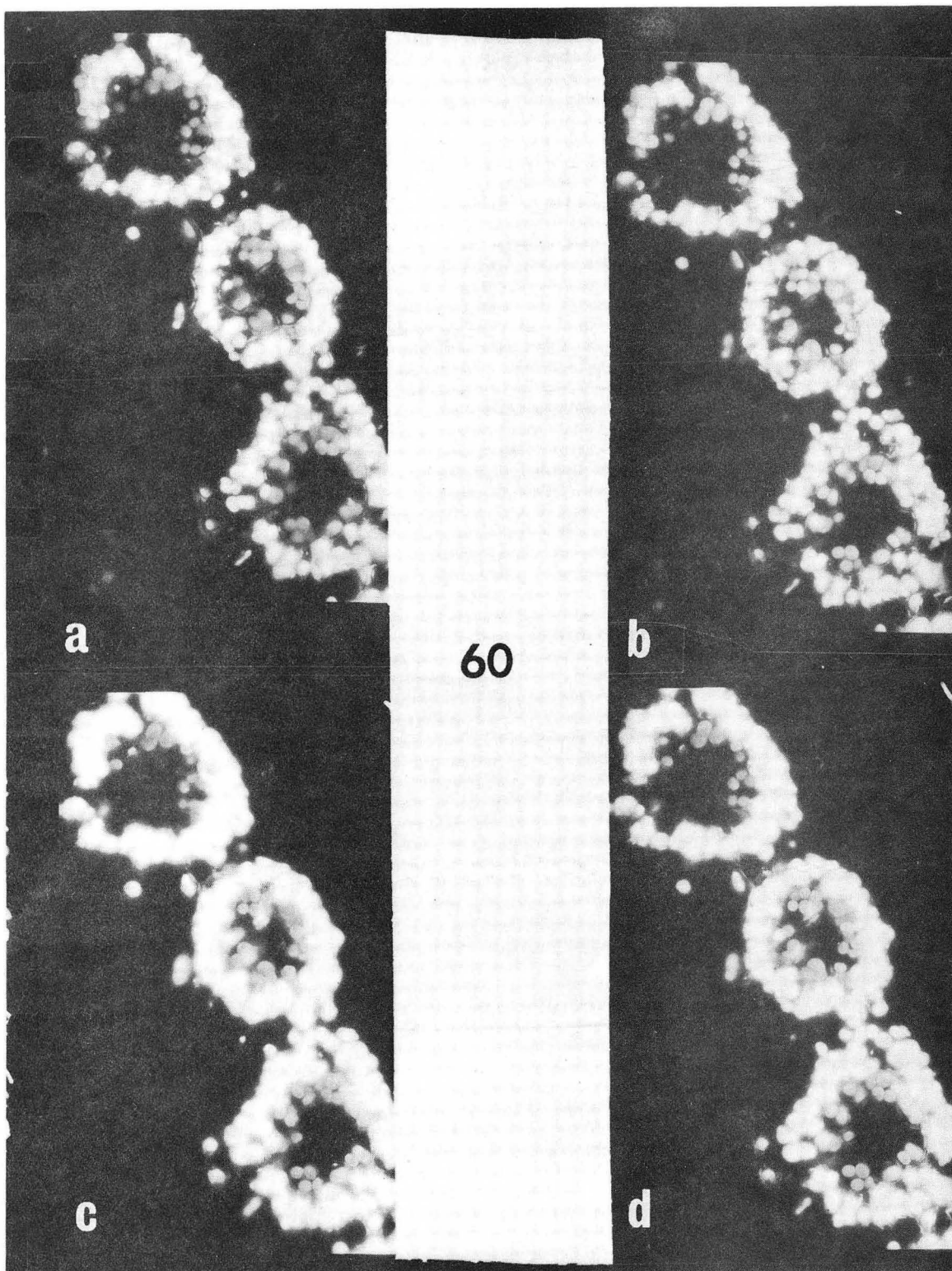
XBB 7310-6160

In order to interrelate all of the data for a given sub-experiment, it is necessary to examine the "Characteristic Curves" for each of the ten filters. Since experiment 126-127 includes four (sub-experiment) spectra, it also involves a set of forty "Characteristic Curves" (Fig. 58 and 59).

The next step in converting the raw data of sub-experiment 126 BS into a relative fluorescence spectrum consists of setting the value of $\bar{D}_A$ at 16.00. Each "Characteristic Curve" then determines Q, the antilog of which is the adjusted exposure time (T_Q) corresponding to this value of $\bar{D}_A$. The leaf photographed in sub-experiment 126 BS requires an adjusted time (T_Q) of 131.20 seconds through the 671 nm filter, 83.37 seconds through the 680 nm filter,... and 31.99 seconds through the 740 nm filter, to develop a $\bar{D}_A$ = 16.00 (cf. Appendix C). These values for T_Q must then be corrected for film and filter spectral characteristics before the reciprocals can be used as a measure of fluorescence intensity.

In summary, the procedure for obtaining a fluorescence spectrum with the MOFF technique is as follows:

1) Photograph a single leaf section through a series of interference filters.

2) Compute the relative mean density $(\bar{D})$ of each photographic negative for the appropriate type of chloroplast.

3) Draw the ten "Characteristic Curves" corresponding to the ten series of photographs obtained with the ten interference filters.

4) Select an adjusted mean relative density ($\bar{D}_A$) close to the observed relative mean densities ($\bar{D}$).

5) Determine each Q: The logarithm of the exposure time corresponding to a density of $\bar{D}_A$ on the "Characteristic Curves".

6) Determine each T_Q: the antilogarithm of Q, which corresponds to the exposure times required to develop the selected $\bar{D}_A$

7) Correct T_Q for film and filter spectral sensitivities by applying the appropriate correction factors.

8) Determine each R", the reciprocal of the corrected T_Q values. R" is proportional to relative fluorescence intensity.

9) Plot R" against the peak transmission wavelength of each filter.

10) Repeat steps 5-9 for $\bar{D}_A \pm L$ in order to compute the error bars.

11) Use Table 19 to determine the fluorescence intensity at 644 and 660 nm relative to 680 nm, and include these points on the graph.

This procedure is used to obtain the fluorescence spectra shown in Figures 61 and 62.

The spectra contained in any single figure are corrected with respect to each other; however, no specific relationship is maintained from one figure to the next. The magnitude of
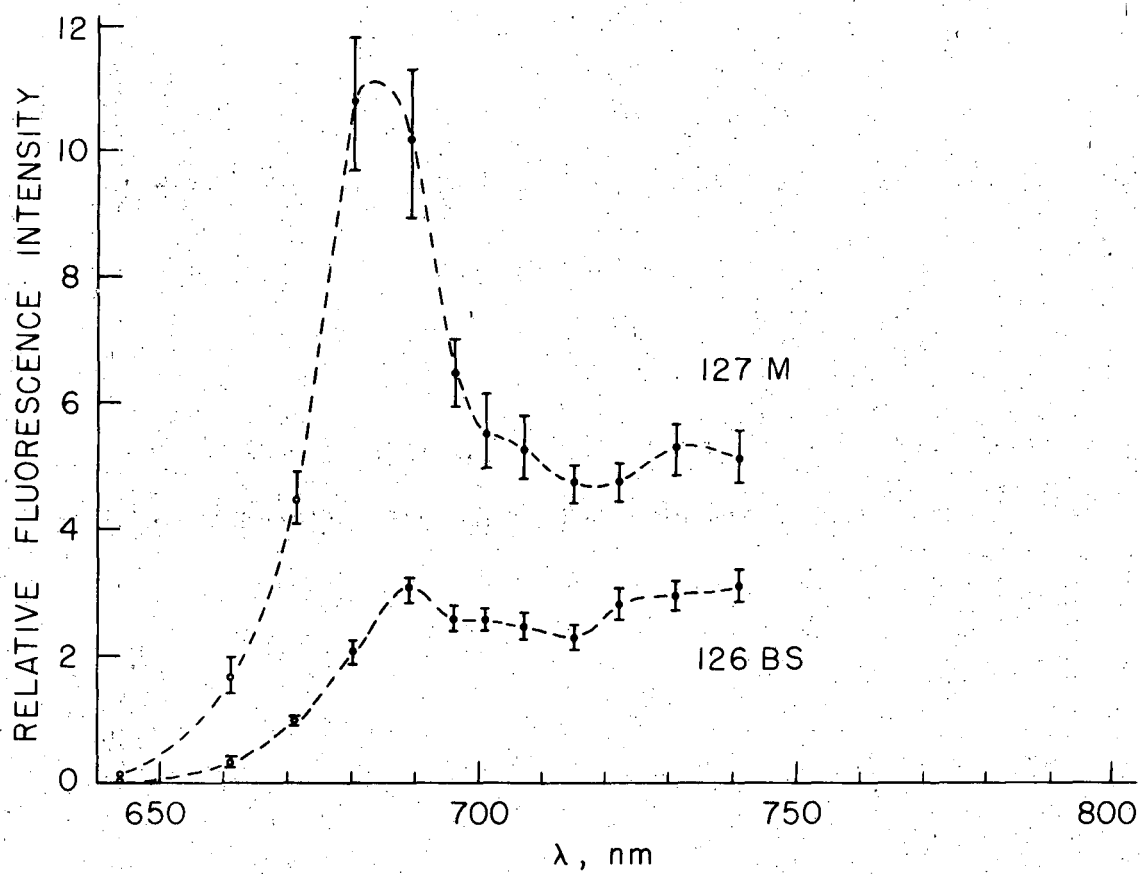
Fig. 61. Relative fluorescence emission spectra of untreated, in situ, Dichanthium annulatum chloroplasts.
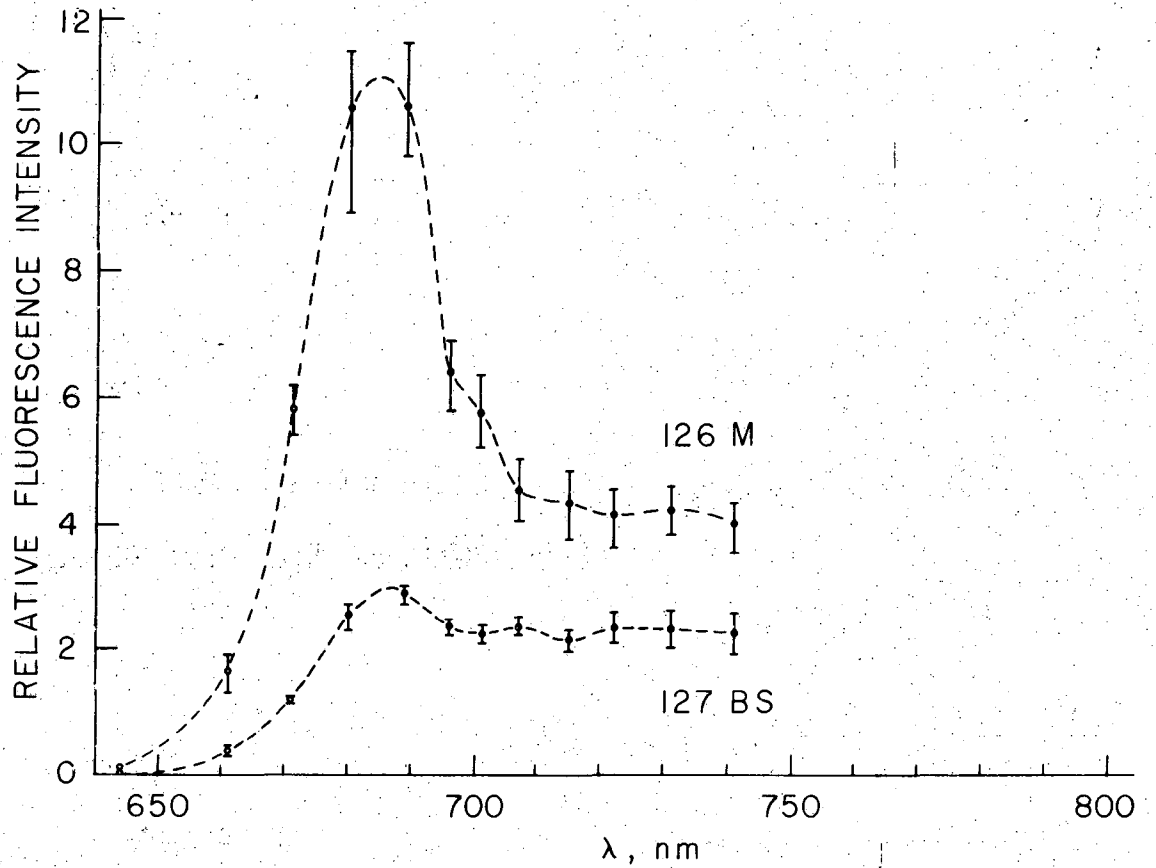
Fig. 62. Relative fluorescence emission spectra of untreated, in situ, Dichanthium annulatum chloroplasts.

XBL 718-5350

the fluorescence is a function of the chosen $\bar{D}_A$. The $\bar{D}_A$ of the
sub-experiments shown in a single figure are adjusted to each
other as a means of adjusting the entire spectrum. The $\bar{D}_A$ data
of different experiments are difficult to correlate because the
incident intensity cannot be precisely controlled.

The standard error bars indicate a probability of 95%
that the relative mean fluorescence of the chloroplasts at the
designated wavelength will be contained in the range determined
by the error bars.

3. Spectra of Tris-treated Material

The spectra of Tris-treated material can be determined by
the identical procedure used to obtain spectra in Figures 61
and 62. Figures 63 and 64 depict the characteristic curves
of the photographic raw data. Figures 65 and 66 illustrate the
calculated spectra. Once again, the spectra of a given figure
are corrected with respect to each other, although no specific
relationship exists between spectra of different figures. The
raw data are contained in Appendices B and C.

4. Discussion

The fluorescence spectra of untreated Dichanthium
annulatum chloroplasts reaffirm that the total fluorescence
intensity from bundle sheath chloroplasts is significantly
less than that from mesophyll chloroplasts. This relative
decrease is especially marked at wavelengths below 700 nm.
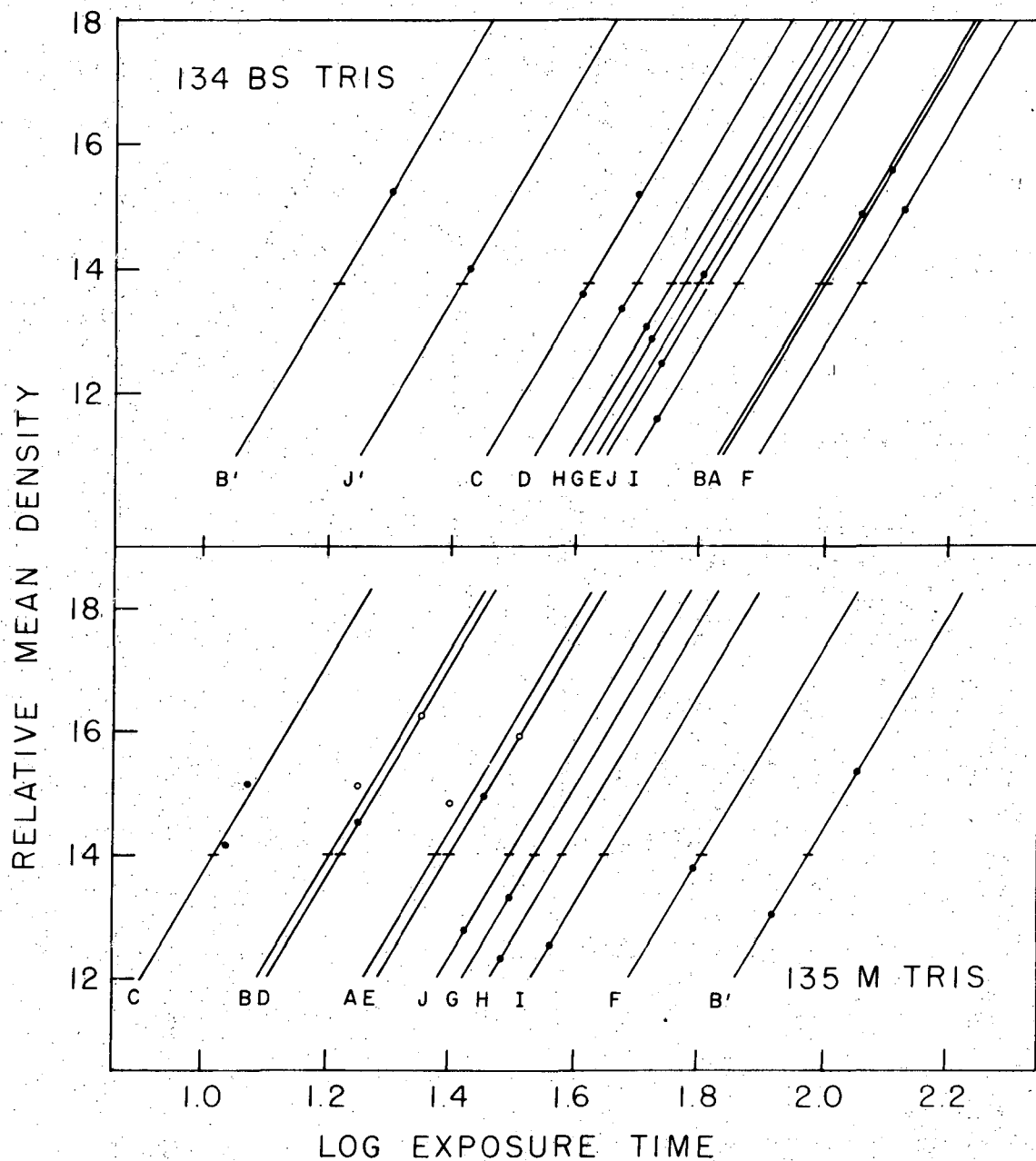
Fig. 63. Characteristic curves for experiments 134 BS Tris and
135 M Tris. B'/680 mesophyll, J'/741 mesophyll, A, B... (cf. Fig. 58).
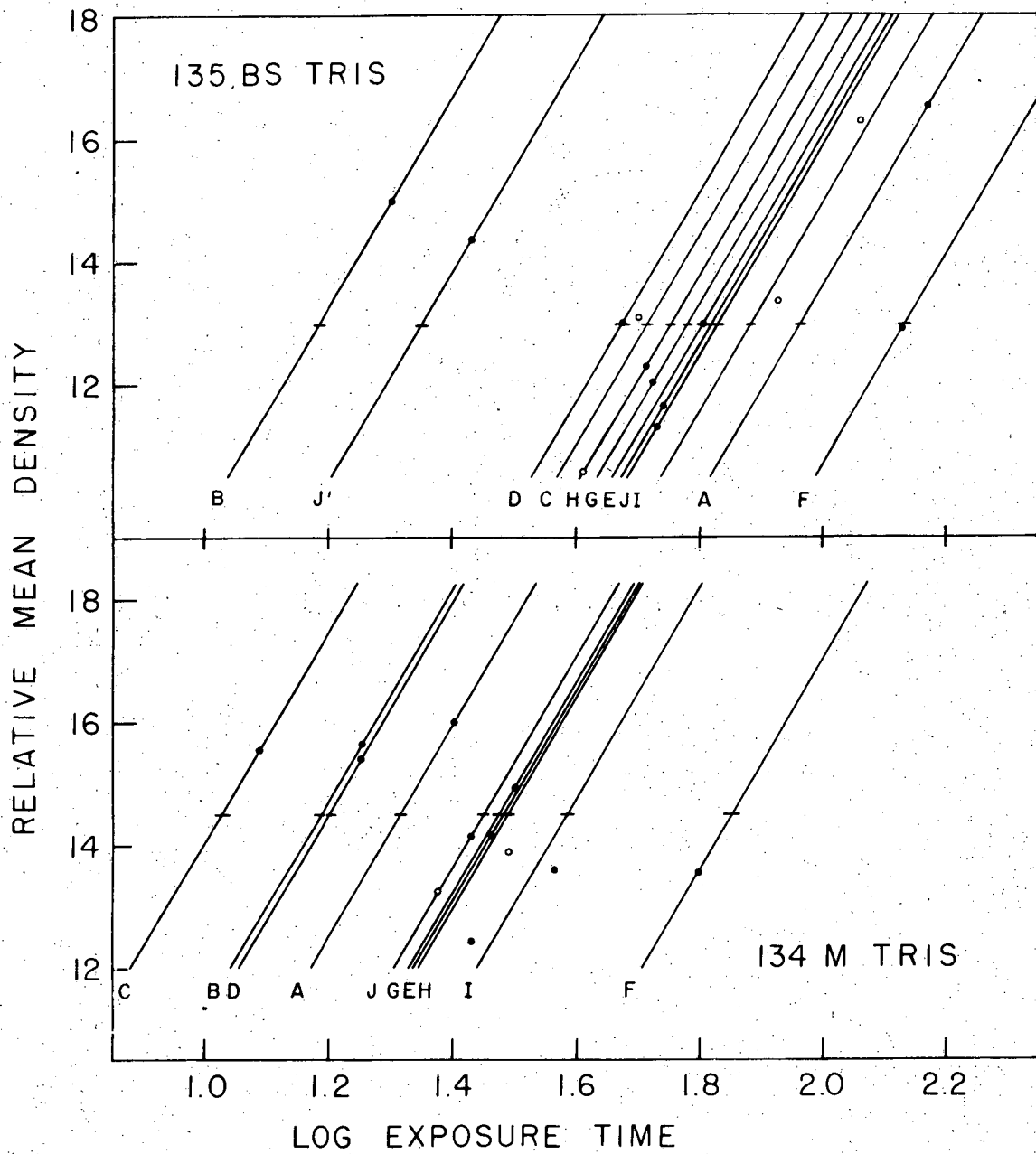
XBL 718-5334

Fig. 64. Characteristic curves for experiments 134 M Tris and
135 BS Tris. J'/741 mesophyll, A, B... (cf. Fig. 58).
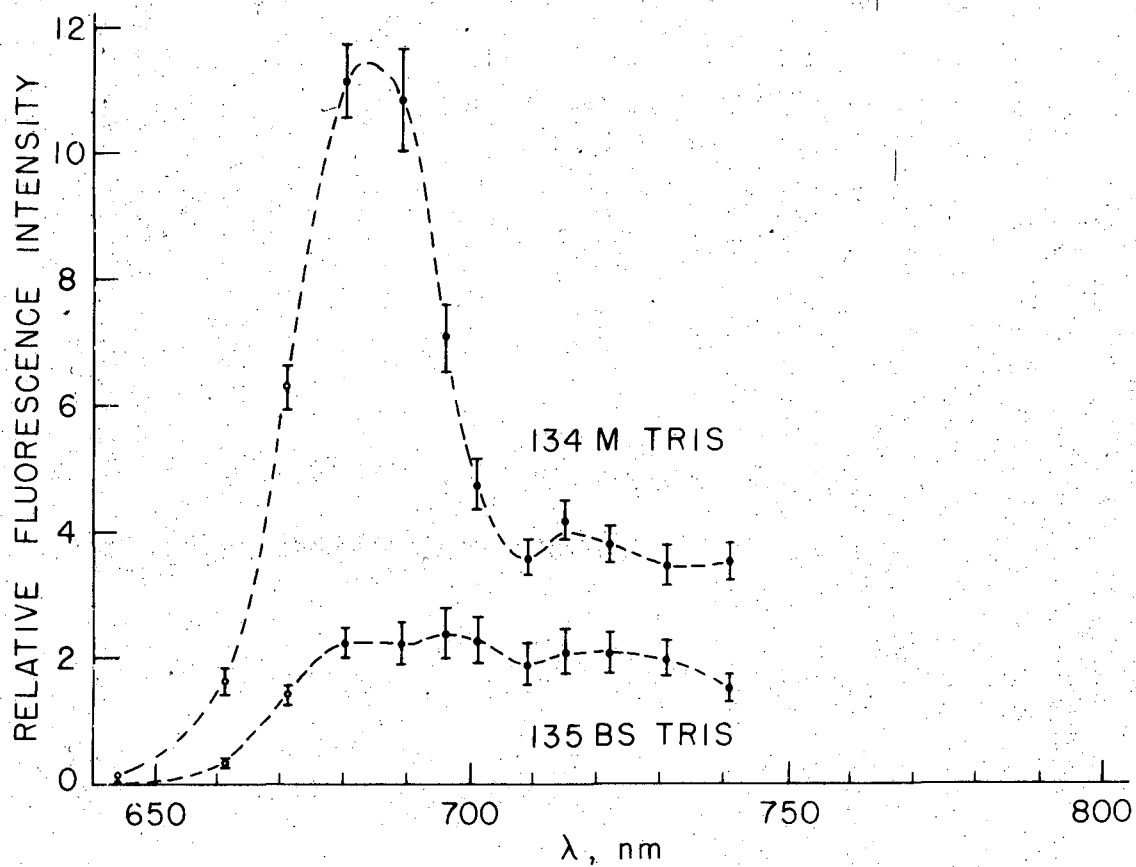
XBL 718-5333

Fig. 65. Relative fluorescence emission spectra of Tris-treated, in situ, _Dichanthium annulatum_ chloroplasts.
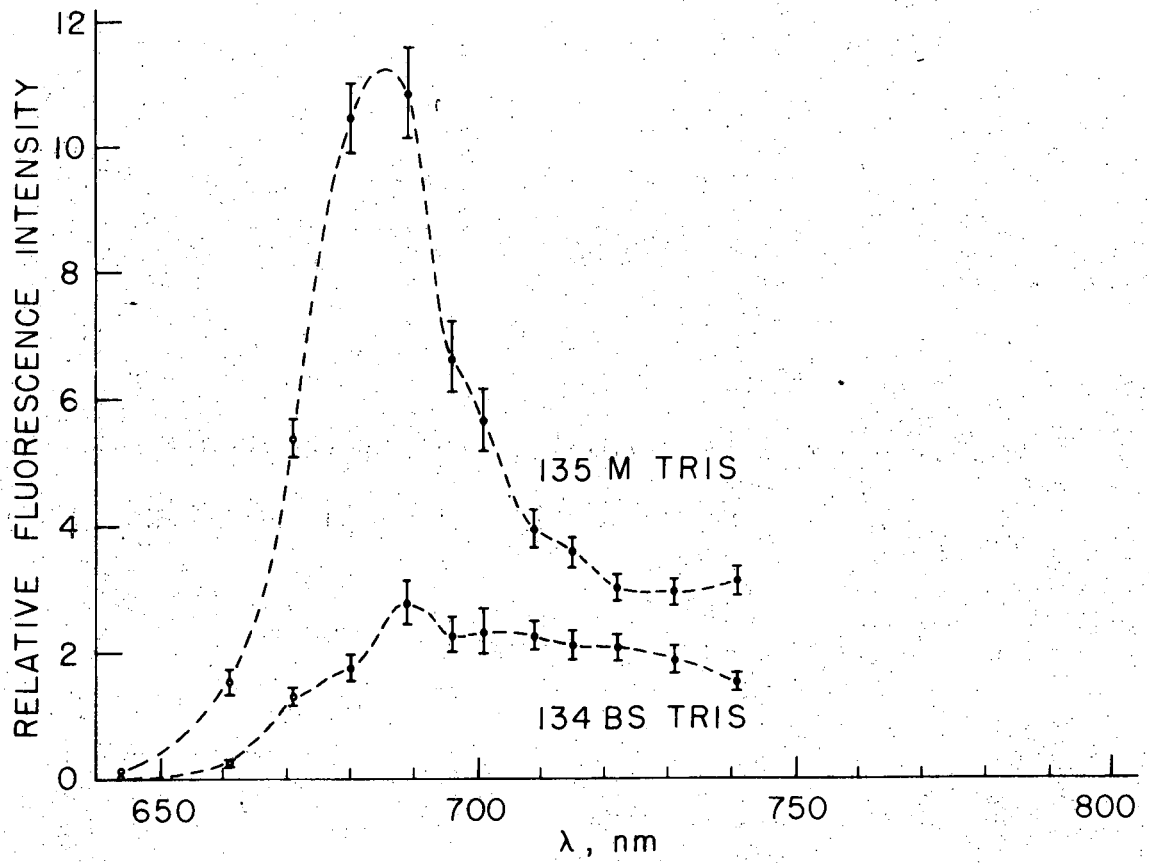
Fig. 66. Relative fluorescence emission spectra of Tris-treated, in situ, Dichanthium annulatum chloroplasts.

This is also consistent with the infrared color data (cf. III. C8 and V. B1).

Perhaps most striking is the similarity in shape of the spectra of untreated and Tris-treated material (cf. Fig. 61, 62, 65, and 66). This would seem to indicate an equally great effect of Tris on the infrared and far-red components of fluorescence. An integrated discussion of the data is conducted in Section V.

G. Quantitative Analysis of Fluorescence Spectra

It is possible to estimate the relative area under a curve by weighing a piece of paper cut to the precise shape of the curve. For comparative purposes, it is necessary to use a single uniform sheet of paper to trace all curves under direct comparison. The weighing method is used to estimate the relative areas under different portions of the fluorescence emission spectra measured in this study. Table 20 of Section V summarizes these data.

Each of the upper four pairs of data in Table 20 compares spectra obtained in connection with one experiment. It is impossible to compare accurately the data between two separate experiments because the condenser setting and the film development might vary. However, it is possible to perform a rough comparison by assuming that these differences are minimal. Spectrum 127M can be normalized to spectrum 134M Tris by choosing an identical $\bar{D}_A$ of 14.00 (127M"). Spectrum 126M can be normalized to spectrum 135M Tris by choosing an identical

$\bar{D}_A$ of 14.00 (126M"). Spectrum 126 BS can be normalized to 135 BS Tris by assuming an identical $\bar{D}_A$ of 13.00 (126BS"). Spectrum 127 BS can be normalized to spectrum 134BS Tris by choosing an identical $\bar{D}_A$ of 13.75. Figures 67-69 are obtained in this manner.

H. Experimental Error

Microscope analysis of C_4 plants necessitates thin sectioning which pierces the walls of most mesophyll and bundle sheath cells. Therefore, although specimen preservation is one of the major advantages of the MOFF technique, the chloroplasts are still exposed to chemical damage. Buffers are chosen to minimize this damage. The remaining cells walls protect the chloroplasts from mechanical injury.

In spite of the broken cell walls, tetrazolium dyes penetrate the monocot bundle sheath cells slowly (cf. Section I. D). The suberized layer of the bundle sheath cell walls probably constitutes this barrier. This suberized layer might also present a barrier, either partial or complete, to Tris, DCMU, or Hydroxylamine. Tris penetrates in sufficient quantities to alter chloroplast fluorescence (cf. Section IV. D2), but its concentration and effectiveness might be diminished.

The microscope condenser concentrates a strong light source on the specimen, thereby increasing the danger of pigment photobleaching. Tris increases the susceptibility of chloroplasts to photobleaching (290). Although all of the photobleached
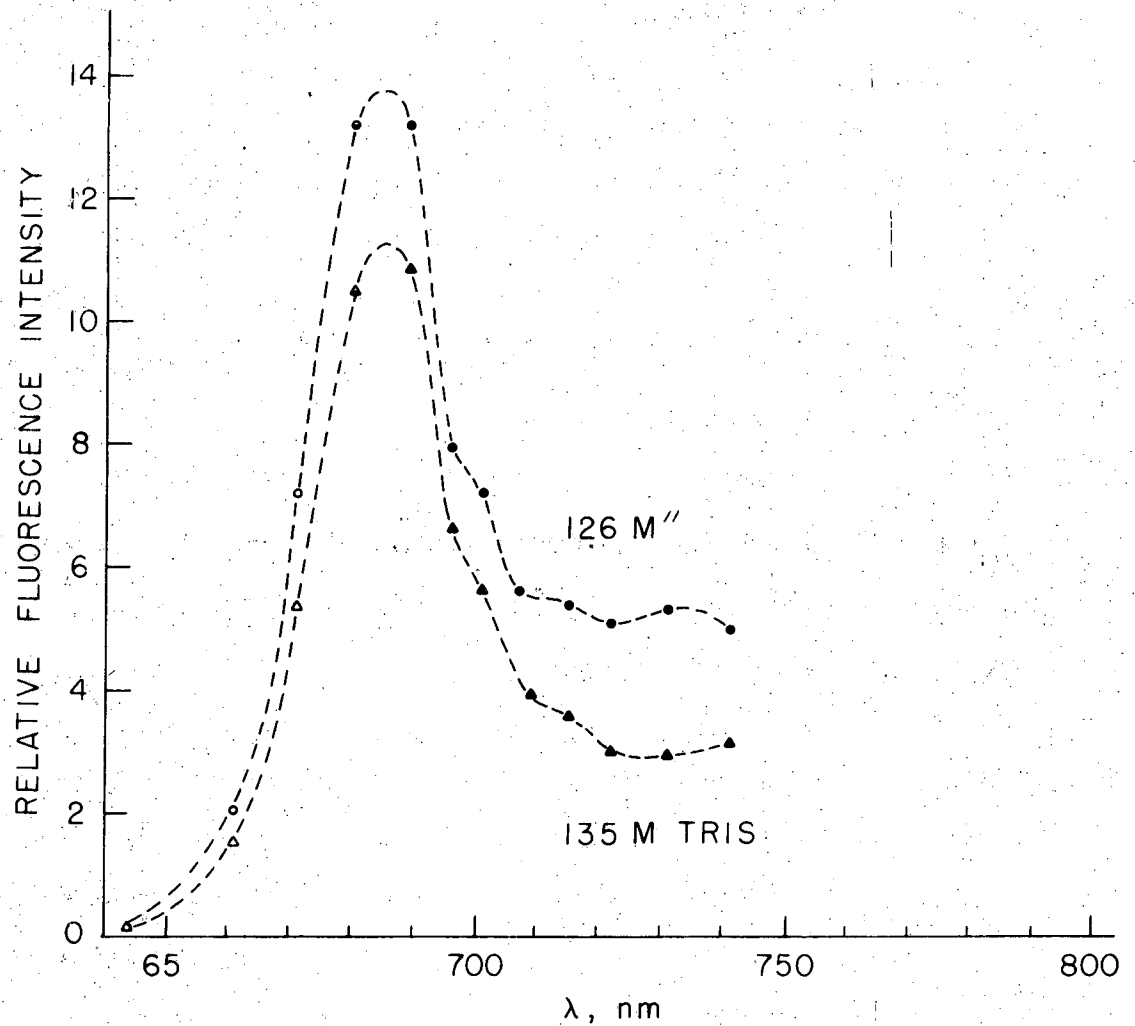
718-5354

Fig. 67. Relative fluorescence emission spectra of Tris and untreated _Dichanthium_ _annulatum_ mesophyll chloroplasts normalized by choosing an equivalent adjusted mean relative density; (▲) Tris, (o) untreated.
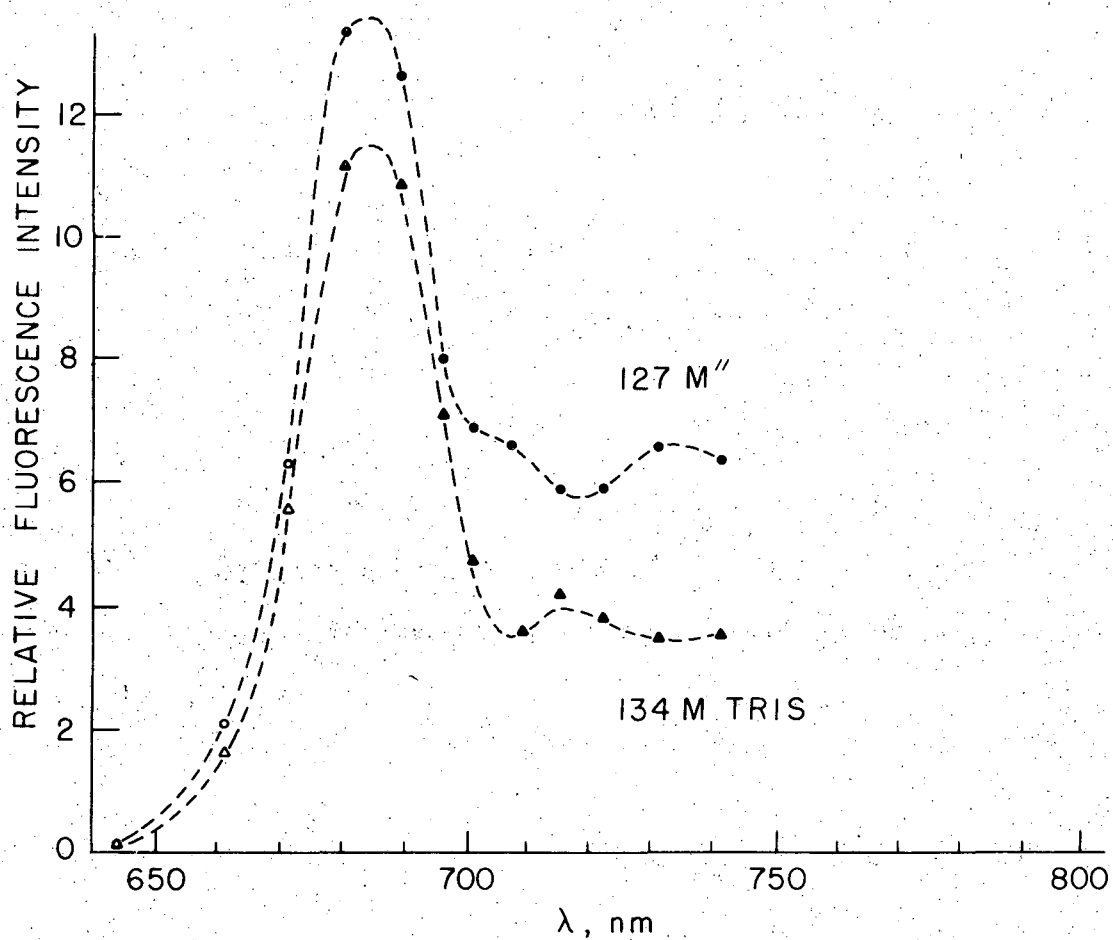
Fig. 68. Relative fluorescence emission specta of Tris and

untreated Dichanthium annulatum mesophyll chloroplasts normal-

ized by choosing an equivalent adjusted mean relative density;
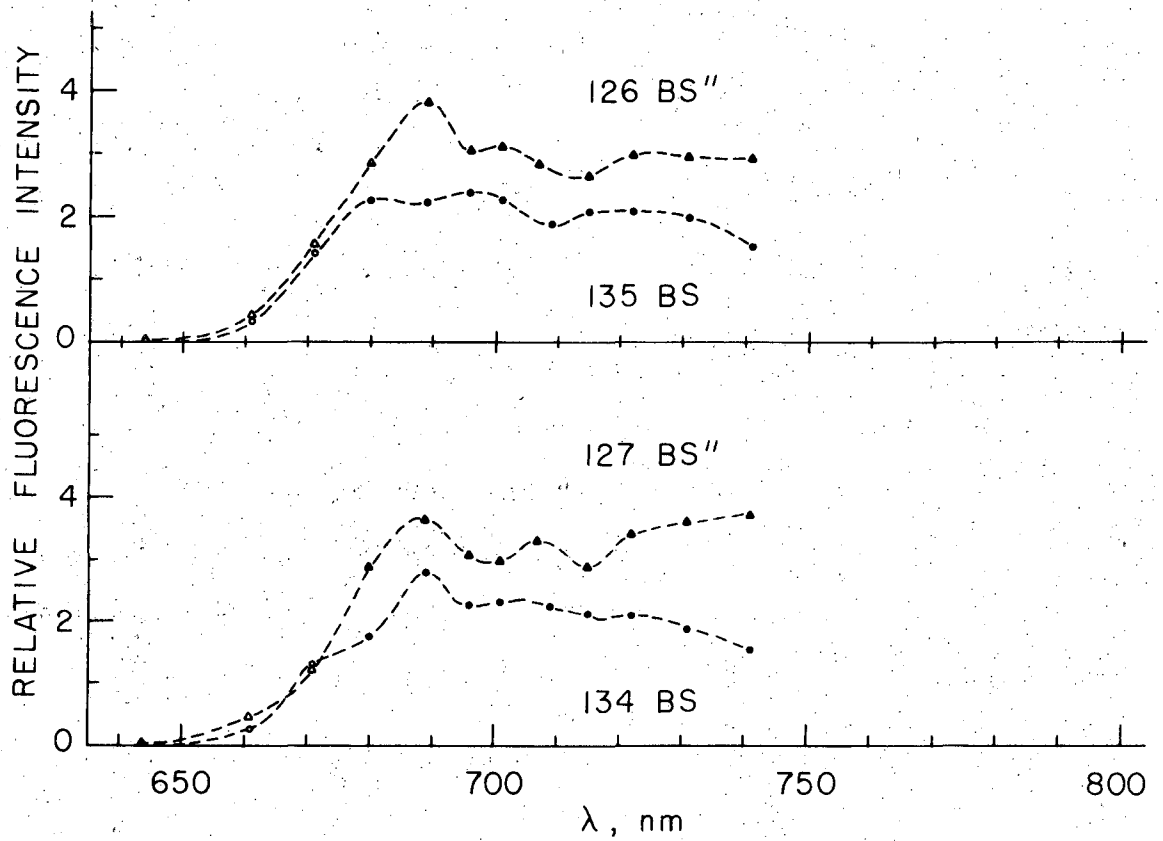
(▲) Tris, (o) untreated.

Fig. 69. Relative fluorescence emission spectra of Tris and untreated <u>Dichanthium</u> <u>annulatum</u> bundle sheath chloroplasts normalized by choosing an equivalent adjusted relative mean density; (▲) untreated, (o) Tris.

sections observed are discarded, it is possible that data involving partial bleaching, imperceptible to the eye, result in distorted spectra.

The use of the microscope necessitates the investigation of fluorescence at room temperature. Most published studies are monitored at low temperatures because of the increased available resolution (cf. Section I. C1). Consequently, it becomes difficult to compare data from different sources.

Any fluorescence measurements involving intact chloroplasts are potentially susceptible to error through self-absorption (cf. Section I. C1). Bundle sheath chloroplasts are larger than spinach chloroplasts and therefore might show greater self-absorption. If specimen integrity is critical for bundle sheath investigations, then this is one source of error that must be shared by all C_4 investigators.

There are many potential technical problems associated with the MOFF technique. They include: uneven film emulsion; incorrectly timed manual exposures; non-uniform development within a dual-capacity plastic developing tank; relative lack of spectral resolution by interference filters; non-uniform alignment of the microdensitometer; incomplete density scans due to the small beam size relative to the chloroplast image; and the presence of hidden fluorescing material beneath the chloroplasts being studied. It is possible to minimize these errors with large sample sizes and careful work. The uniformity of the four sets

of fluorescence spectra minimizes the possibility of significant random error in these experiments.

It is unusual that the MOFF technique consistently detects a difference between mesophyll and bundle sheath chloroplast fluorescence, at room temperature, which other techniques require low temperatures to detect (191, 192, 113, 286). There is a possibility of undetected systematic error. The room temperature data of Bazzaz and Govindjee (29) are similar to that obtained in this thesis at room temperature. Poor specimen integrity possibly accounts for the inability of other studies to detect differences in mesophyll and bundle sheath fluorescence at room temperature. There is also reasonable correlation between Dichanthium room temperature data, and other C_4 low temperature studies, although the difference in recording temperatures makes direct comparison difficult (29, 113, 191, 192, 286).

Mayne et al. detect no unusual room temperature fluorescence patterns in their pure bundle sheath and mesophyll chloroplast fragment preparations (191). Unfortunately, they did not, or could not, investigate the fluorescence of their isolated intact cells. These cells are probably too thick to be studied. The release of intact chloroplasts from isolated thick-walled bundle sheath cells would be difficult, however, only a small yield would be necessary.

Anderson et al. (5) have recently succeeded in isolating bundle sheath chloroplasts, but they have not yet re-examined bundle sheath fluorescence.

V. Discussion

A. <u>Summary of Experimental Results</u>

Before discussing the significance of these data, it would be valuable to recapitulate the key observations:

1) Infrared color and infrared black and white film data consistently indicate that the fluorescence properties of agranal bundle sheath chloroplasts are strikingly different from those of the mesophyll and other chloroplasts.

2) Infrared color film data indicate:

a) The ratio of fluorescence emission above 700 nm/ below 700 nm is greater in bundle sheath than in mesophyll chloroplasts.

b) The fluorescence yield is lower in bundle sheath than in mesophyll chloroplasts.

3) The black and white infrared film data confirm and extend the infrared color film data in the following ways:

a) The fluorescence emission spectra of mesophyll and bundle sheath chloroplasts of <u>Dichanthium annulatum</u> confirm the higher ratio of fluorescence above 700 nm/below 700 nm in bundle sheath relative to mesophyll chloroplasts. This ratio is approximately 2:1.

b) The fluorescence yield of bundle sheath chloro-
plasts is approximately half that of mesophyll
chloroplasts.

3. The altered fluorescence yields and spectra of C_4
chloroplasts can be positively correlated with the
degree of lamellar appression.

4. Dichanthium annulatum bundle sheath chloroplasts have
a variable component of fluorescence equal to that of
mesophyll chloroplasts.

5. The variable component of fluorescence in the mesophyll
and bundle sheath chloroplasts of Dichanthium annulatum
has a strong infrared component, in addition to the
expected far-red component.

Both the fluorescence yield and the shape of the fluorescence
spectrum of chloroplasts are affected by the buffers used, and by
the types and amounts of inorganic ions present. It is necessary
to minimize the physical and chemical specimen damage during
specimen preparation. C_4 chloroplasts seem unusually sensitive
to these factors when their outer membranes are damaged. Therefore,
whenever possible, class I chloroplasts should be used in these
studies. Unfortunately, the use of intact chloroplasts in fluores-
cence studies increases the probable contribution of self-absorp-
tion artifacts.

B. Internal Consistency of Data

Table 20 includes data comparing the relative areas under the fluorescence emission curves, above and below 700 nm, for each of the pairs of spectra shown in Figures 61, 62, and 65-69 of Section IV. These data correlate well with the spectral analysis of infrared color film as presented in Section III.

The color response of infrared film varies with the relative proportion of far-red and infrared light striking the film. An infrared/far-red ratio of 0.5 should cause a yellow color to develop on the film, while a ratio of 1.0 should result in a gold color. Untreated fluorescing mesophyll chloroplasts turn infrared color film either yellow or gold. According to Table 20, their infrared/far-red ratio is approximately 1.1

Infrared photographs of untreated fluorescing bundle sheath chloroplasts have a range of color from orange to red. Their infrared/far-red ratio varies between 2.1 and 2.9. A ratio of 2.0 causes an orange color to develop on the film while a 4.0 ratio results in a red-orange. A true red color usually does not develop until the ratio is greater than 4.0.

Tris treatment alters the color of fluorescing bundle sheath chloroplast photographs to either yellow-orange or gold. Similarly, Tris treatment lowers their ratio to approximately 1.7. Infrared photographs of fluorescing Tris-treated mesophyll chloroplasts are always yellow. Tris treatment lowers their ratio to 0.8.

Table 20. Relative Fluorescence Estimated by the Area Beneath
the Spectral Curves

spectra	640-740*	700-800*	640-700	$\dfrac{700\text{-}800*}{640\text{-}700}$	$\dfrac{M/BS}{640\text{-}740}$
126M	0.65	0.59	0.59	1.0	
127BS	0.23	0.33	0.16	2.1	2.8
127M	0.89	0.69	0.53	1.3	
126BS	0.33	0.41	0.14	2.9	2.7
135M Tris	0.82	0.45	0.54	0.8	
134BS Tris	0.28	0.23	0.13	1.8	2.9
134M Tris	0.88	0.48	0.58	0.8	
135BS Tris	0.28	0.22	0.14	1.6	3.1

					$\dfrac{M\ Tris}{M\ Plain}$
134M Tris	0.61				
127M Tris	0.86				0.7
135M Tris	0.60				
126M Tris	0.82				0.7

					$\dfrac{BS\ Tris}{BS\ Plain}$
135BS Tris	0.35				
126BS" Tris	0.50				0.7
134BS Tris	0.34				
127BS" Tris	0.52				0.7

*For the purposes of these calculations, it is assumed that the relative fluorescence intensity is approximately zero at 800 nm (cf. Fig. 61, 62, 65-69).

The average M/BS fluorescence ratio computed for untreated
Dichanthium annulatum chloroplasts in Section IV. is 2.2. Tris
treatment causes the ratio to be slightly higher (2.4). The
ratio computed by the weighing method, and summarized in Table 20,
is 2.8 for untreated tissue, and 3.0 for Tris-treated tissue. These
ratios, obtained by the weighing method, do not include wavelengths
longer than 740 nm, and consequently are slightly high. There-
fore the various sets of infrared black and white film data are
also internally consistent.

The spectra obtained for different experiments with the MOFF
analysis of fluorescence are almost identical. The further simi-
larity between the spectra of untreated and Tris-treated *Dichanthium
annulatum* is also striking.

C. Relationship to Other Studies
1. The Effect of Tris Treatment on the Fluorescence Yield

Tris treatment results in a lowered fluorescence yield. Park
et al. determined that the variable fluorescence accounts for
approximately half of the total fluorescence at the light intensities
used, and that this variable component is lost upon Tris treatment
(231). The normalized *Dichanthium annulatum* spectra in Figures
67-69, and summarized in Table 20, appear to retain between 60-
70% of their total fluorescence after Tris treatment with high
excitation intensity.

An examination of Figures 67-69 reveals the effect Tris treatment can have on the long wavelength components of chloroplast fluorescence in addition to its normally acknowledged effect on the shorter wavelength components. The bundle sheath spectra show approximately uniform decrease over the measured range 670 to 740 nm after Tris treatment. The mesophyll spectra show as great a decrease at 730 nm after Tris treatment as they do at 680 nm. Consequently, the effect of Tris at wavelengths between 700 and 740 nm is equal to or greater than its effect at wavelengths below 700 nm.

2. Low Temperature Fluorescence Properties of C_4 Plants

Table 3 and Figure 7 of Section I summarize the data from Mayne & Black (191). The Hill reaction activity includes both oxygen evolution and NADP photoreduction from water. The 77^OK fluorescence emission spectra, the F730/F685 ratio, and the variable fluorescence data are of particular relevance to the Dichanthium fluorescence data presented in this study. The room temperature spectra obtained by Mayne and Black are identical for both mesophyll and bundle sheath chloroplasts. At 77^OK, the spectra of both mesophyll and bundle sheath chloroplasts peak at F685, implying the presence of PS II in all plastids (191). All of Mayne and Black's data indicate the presence of PS II in bundle sheath chloroplasts although their assay for variable fluorescence differs from most studies on variable fluorescence in that it

does not involve Tris treatment. Mayne and Black detect a
M/BS variable fluorescence ratio of 2:1, in contrast to the
Dichanthium ratio of 1:1. Their fluorescence spectra resemble
the ones measured in the Woo et al. study (286) except that
Mayne and Black record a higher relative F685 for both mesophyll
and bundle sheath spectra.

3. Room Temperature Fluorescence Properties of C_4 Plants

Bazzaz and Govindjee examine the room temperature fluorescence
spectra of Zea mays bundle sheath and mesophyll chloroplasts (29).
Their Zea mays data agree qualitatively with the Dichanthium
data presented in this study in that there is a predominance of
long wavelength fluorescence in the bundle sheath relative to the
mesophyll chloroplasts. Quantitatively, in Dichanthium, the
relative M/BS fluorescence yield is 2.0. In corn it is 1.2-1.5.
After normalizing fluorescence spectra at 680 nm, the long wave-
length fluorescence component of Dichanthium is 3.5-5.5 fold
higher in the bundle sheath relative to the mesophyll. This
ratio is only 1.5 in corn.

These quantitative discrepancies could result from a struc-
tural difference between nearly agranal Dichanthium annulatum
bundle sheath chloroplast profiles and those of Zea mays which
show more thylakoid overlap. Since it is very difficult to
obtain a bundle sheath chloroplast preparation as pure as 70%,
mesophyll contamination of the corn bundle sheath preparation is

probably significant enough to diminish the detectable difference between the two fractions. Error in the _Dichanthium_ data could also contribute to the difference (cf. Section IV. H).

4. _Variable and Constant Fluorescence_

According to Govindjee et al., the spectra of variable and constant fluorescence, although distinctive, are remarkably similar (118). Variable fluorescence is only 1.2 fold greater than background fluorescence at 685 nm, and only 90% of the background fluorescence at 720 nm when the spectra are normalized at 700 nm. According to Clayton (76,77), the variable component of fluorescence is related to PS II, while constant fluorescence supposedly does not reflect changes in photochemistry. This view is supported by the constancy of background fluorescence in spite of varying conditions. For example, Clayton showed that the intensity of saturating light does affect the variable fluorescence, but does not affect the background component.

The similarity in the variable and constant fluorescence spectra is significant. If the total fluorescence emission spectra resemble the variable fluorescence emission spectra, then they must both resemble the constant fluorescence spectra. This pattern also occurs in both the mesophyll and bundle sheath chloroplasts of _Dichanthium_ _annulatum_. In addition, the relative M/BS fluorescence does not change after the elimination of variable fluorescence by Tris treatment. This

implies identical proportions of PS II in mesophyll and bundle sheath chloroplasts of Dichanthium annulatum.

Mohanty et al. investigate F730/F685 of untreated and Tris-washed chloroplasts (196). This ratio remains constant for both samples. This is consistent with the observed similarity between the variable and total fluorescence emission spectra of Dichanthium annulatum. Since they describe PS II as short wavelength and PS I as long wavelength, when reporting that the F730/F685 ratio does not change after Tris treatment, they seem to indirectly imply that Tris treatment equally effects Photosystems I and II.

5. Function of Chloroplast Lamellae

According to the work of Sane et al., stroma lamellae contain only PS I, and have only negligible variable fluorescence (241). These stroma lamellae should be weakly fluorescent, yet Lintilhac and Park (181) observed uniform fluorescence in all chloroplast lamellae (230). Spinach stroma lamellae might be functionally different from C_4 chloroplast lamellae.

The ontogeny of grana is often correlated with the functional development of PS II (48, 245). The grana of C_3 plastids might originate as folded stroma lamellae. Then the ontogeny of agranal sugar cane bundle sheath chloroplasts presents the reverse situation in that grana form which are subsequently lost (174). Park suggests that agranal bundle sheath chloro-

plast lamellae are partly unfolded grana (221). Since, according to this thesis, PS II activity is not lost in the nearly agranal bundle sheath plastids of <u>Dichanthium</u> <u>annulatum</u>, either the functional relationship between grana and stroma lamellae discovered by Sane et al. is restricted in its occurrence, or else C_4 plants are one of the few exceptions to the rule.

According to Lyttleton's experiment on <u>Amaranthus</u> <u>palmeri</u>, under conditions of high light intensity, grana do not form in the bundle sheath (189). Small grana develop under low light intensity conditions. If lamellar structure and function are correlated in C_4 plants, then the environment is capable of adjusting the photosynthetic apparatus in some C_4 plants. Therefore the C_4 lamellar system and spinach stroma lamellae are only homologous.

VI. Conclusions

C_4 plants have diverged on a slightly different evolutionary path from C_3 plants with regard to carbon fixation. It is possible that there are some additional differences in the light reactions; however, this appears unlikely because of the detection of PS II in agranal bundle sheath chloroplasts. The C_4 syndrome occurs in several different plant groups, and is an example of convergent evolution. It is possible that the light reaction apparatus has not evolved in such a uniform manner. The C_4 phenomenon might be an "evolutionary red herring" in the study of photosynthesis in that the supposedly different carbon fixation cycle appears to be a preliminary set of three reactions before the participation of the ubiquitous Calvin cycle (cf. I. E4); similarly, although the fluorescence properties of some bundle sheath chloroplasts differ from those of mesophyll and C_3 plastids, all non-mutant C_3 and C_4 chloroplasts appear to contain both photosystems (cf. I. E6).

The lower yield, and higher proportion of infrared fluorescence in bundle sheath relative to mesophyll chloroplasts, appears to be positively correlated with the degree of lamellar appression. Sane et al. (241) detect only PS I in unappressed spinach lamellae, yet nearly agranal Dichanthium annulatum bundle sheath chloroplasts appear to contain both PS I and PS II. This discrepancy might be explained if lamellar appression is needed for the development, but not the maintenance, of PS II. Immature sugar

cane bundle sheath chloroplasts contain small grana which are lost during subsequent maturation (174). Izawa and Good measure normal Hill reaction activity in chloroplasts with unfolded grana membranes (146). Therefore, unappressed bundle sheath chloroplast lamellae appear to be qualitatively different from both grana and stroma lamellae. Stroma lamellae probably represent a much simpler system than the complex bundle sheath lamellae.

In this study, the variable fluorescence component of bundle sheath chloroplast fluorescence is interpreted as evidence for a functional PS II in these chloroplasts. It appears that in Dichanthium annulatum, variable fluorescence has a larger long wavelength component than previously expected, and that the total and variable fluorescence emission spectra contain many similarities.

The presence of PS I in C_4 plants is agreed upon by all workers. Normally a high F735/F685 is associated with enriched PS I. In conclusion from the thesis data, and contrary to current doctrine, the F735/F685 ratio is not always correlated with the ratio between total and variable fluorescence. The relationship between the chl a/chl b ratio, photosystems I and II, fluorescence emission spectra, and variable emission spectra needs to be re-examined.

Photomicroscopy has proven to be a valuable technique for studying fluorescence. High optical resolution studies of chloroplast fluorescence can be performed in situ. The unique

spectral sensitivity of infrared color film renders it capable
of distinguishing between far-red and infrared chloroplast
fluorescence. These photographs can therefore be used as a
detector for chloroplasts with enriched infrared fluorescence
patterns.

High speed black and white infrared film is suitable for
quantitative studies of chloroplast fluorescence. The results
are reproducible and internally consistent. The room temperature
fluorescence studies agree qualitatively with the 77°K fluores-
cence studies performed in other laboratories.

It would also be informative to study the freeze fracture
patterns of agranal bundle sheath chloroplasts in an effort to
correlate the internal lamellar structure with function. In
spinach stroma lamellae, only PS I and small particles are found
(24). The presence of large particles in unappressed bundle
sheath lamellae would indicate a possible difference in function.
The absence of large particles would indicate that a correlation
exists between particle size and lamellar appression.

It would be preferable to extend these freeze fracture investi-
gations to other unappressed lamellae. Chloroplast mutants and
low salt dissociated grana would make excellent subjects. The
granal chloroplasts of romaine lettuce would also yield informa-
tive freeze fracture patterns and infrared fluorescence photomicro-
graphs because of their high chl a/chl b ratio.

APPENDIX A

Electron Micrographs of C_4

Grass Leaves

Table A1. Part I. Figure Legends for the Electron Micrographs of C_4 Plants (W. M. Laetsch)*

Figure	Plant	Plastid	Group	Magnification	Source
A1	Sugar cane	BS	IA	51,400	C
A2	Sugar cane	BS	IA	24,500	C
A3	Dichanthium annulatum	BS	IA	17,530	G
A4	Dichanthium annulatum	M	IA	24,530	G
A5	Corn	BS	IB		
A6	Sorghum	BS	IB		C
A7	Digitaria sanguinalis	BS	IC	12,800	G
A8	Digitaria sanguinalis	BS	IC	5,200	G
A9	Digitaria sanguinalis flowering	BS	IC	7,000	C
A10	Digitaria sanguinalis flowering	BS	IC	19,000	C
A11	Echinochloa colonum	BS	ID	25,980	G
A12	Cenchrus sativa	BS & M	ID	18,900	G
A13	Cenchrus sativa	BS & M	ID	14,490	G
A14	Cenchrus sativa	BS	ID	57,700	G
A15	Euphorbia serphyllifolia	BS	ID	18,620	C

Table A1. Part II.

Figure	Plant	Plastid	Group	Magnification	Source
A16	Euphorbia maculata	BS	ID	18,000	C
A17	Spartina foliosa	BS	IIA	18,390	F
A18	Spartina foliosa	M	IIA	23,300	F
A19	Cynodon dactylon	BS			F
A20	Amaranthus edulis	BS	IIA	44,500	C
A21	Mollugo verticillata	BS	IIA	22,950	C
A22	Froelichia gracilis	BS	IIB	24,330	C
A23	Atriplex lentiformis	BS	IIB	18,640	C
A24	Atriplex lentiformis	M	IIB	29,850	C
A25	Cotyledon of Amaranthus edulis	BS	IIB	38,100	C
A26	Cotyledon of Amaranthus edulis	BS	IIB	23,050	C
A27	Mollugo cerviana	BS	IIB	10,570	C
A28	Mollugo cerviana	M	IIB	21.750	C
A29	Portulaca oleracea	BS	IIB	63,300	G
A30	Portulaca oleracea	M	IIB	23,880	G

Table A1. Part III

Plate A5 courtesy of Dr. Weier.

Plate A6 after Bisalputra et al. (35).

Plate A19 after Black et al. (42).

*All others courtesy of Dr. Laetsch.

(C) growth chamber, (G) greenhouse, (F) field grown
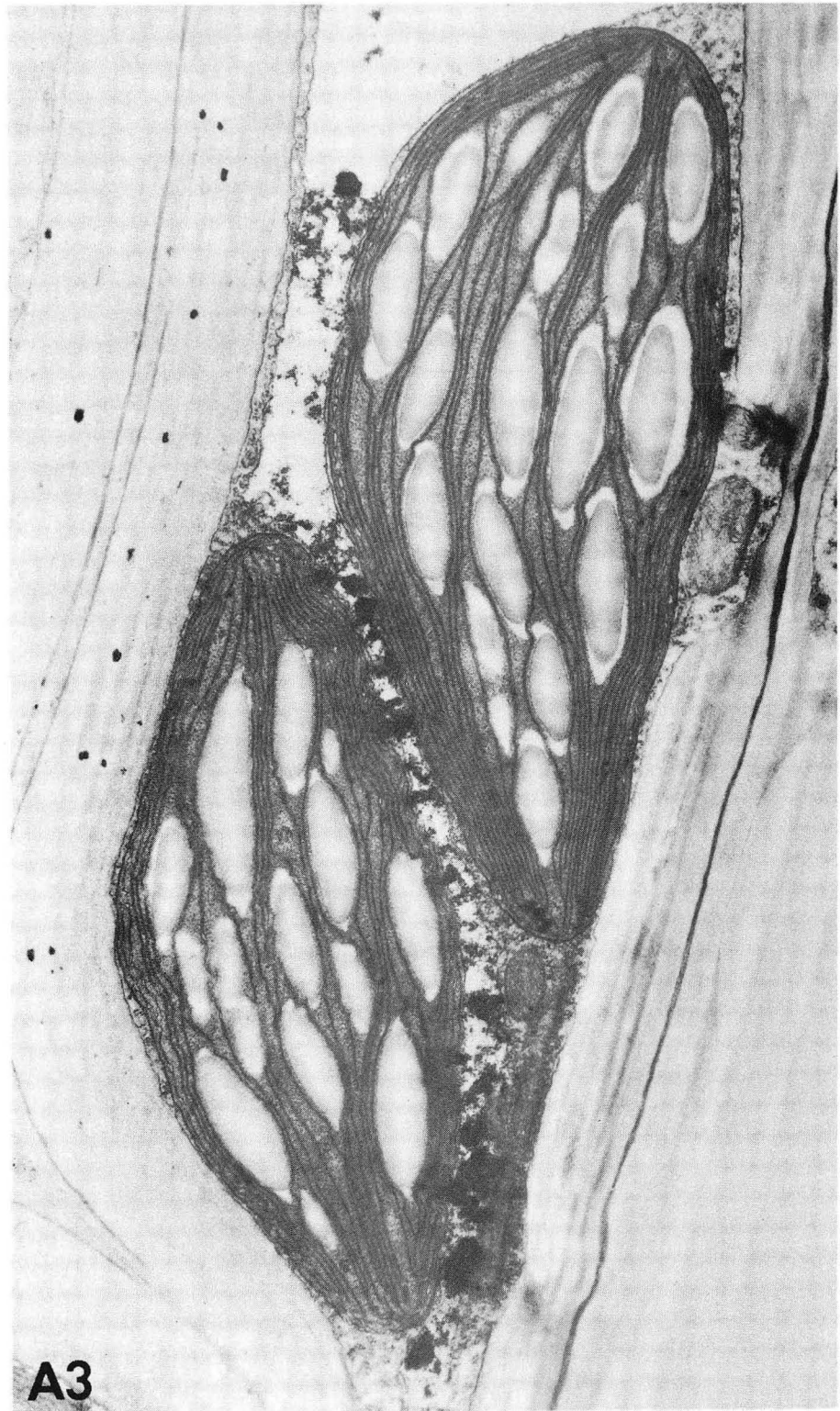
A1

XBB 717-3072

A2

A3

A7

XBB 718-3568

A8

A9

XBB 718-3565

A10
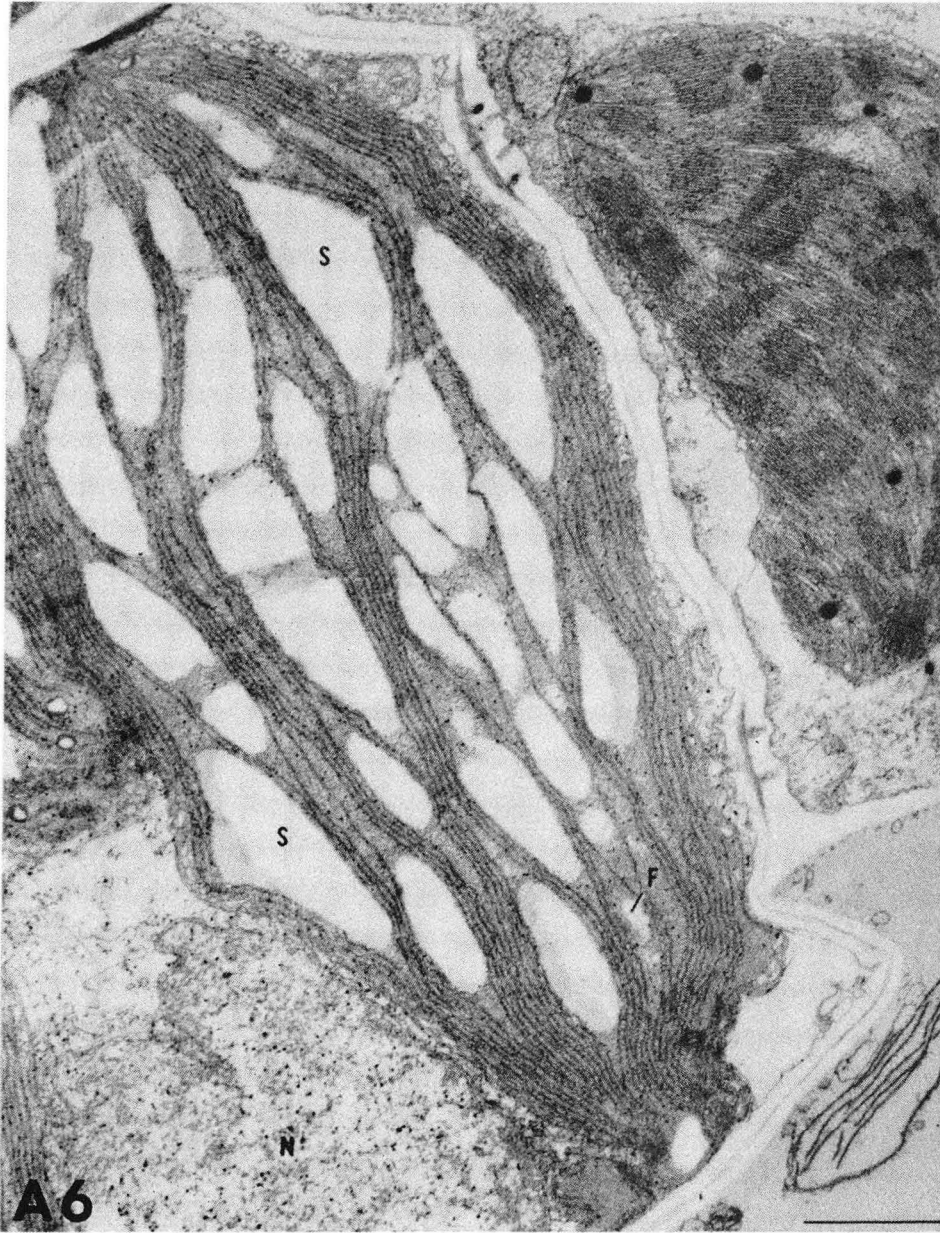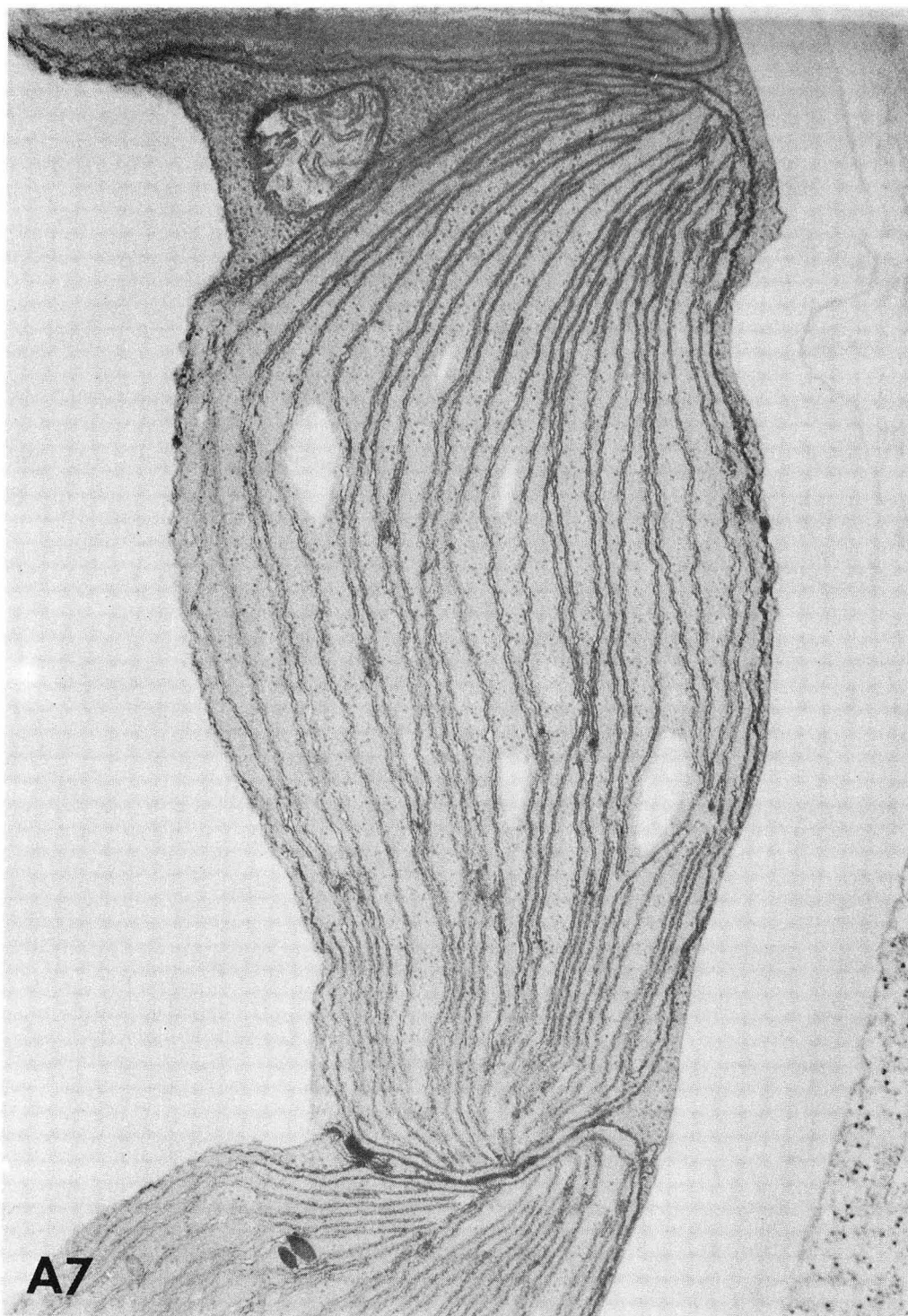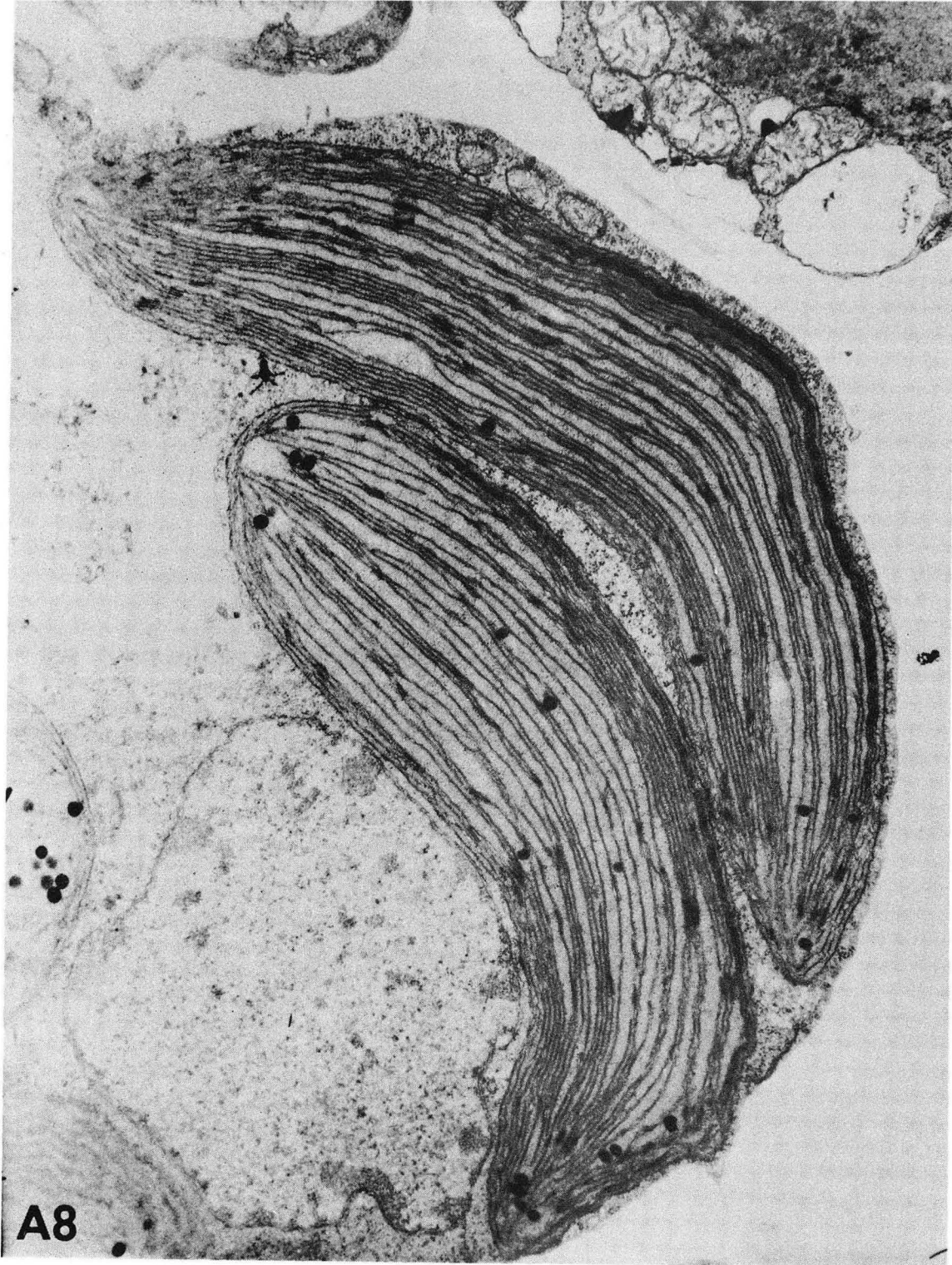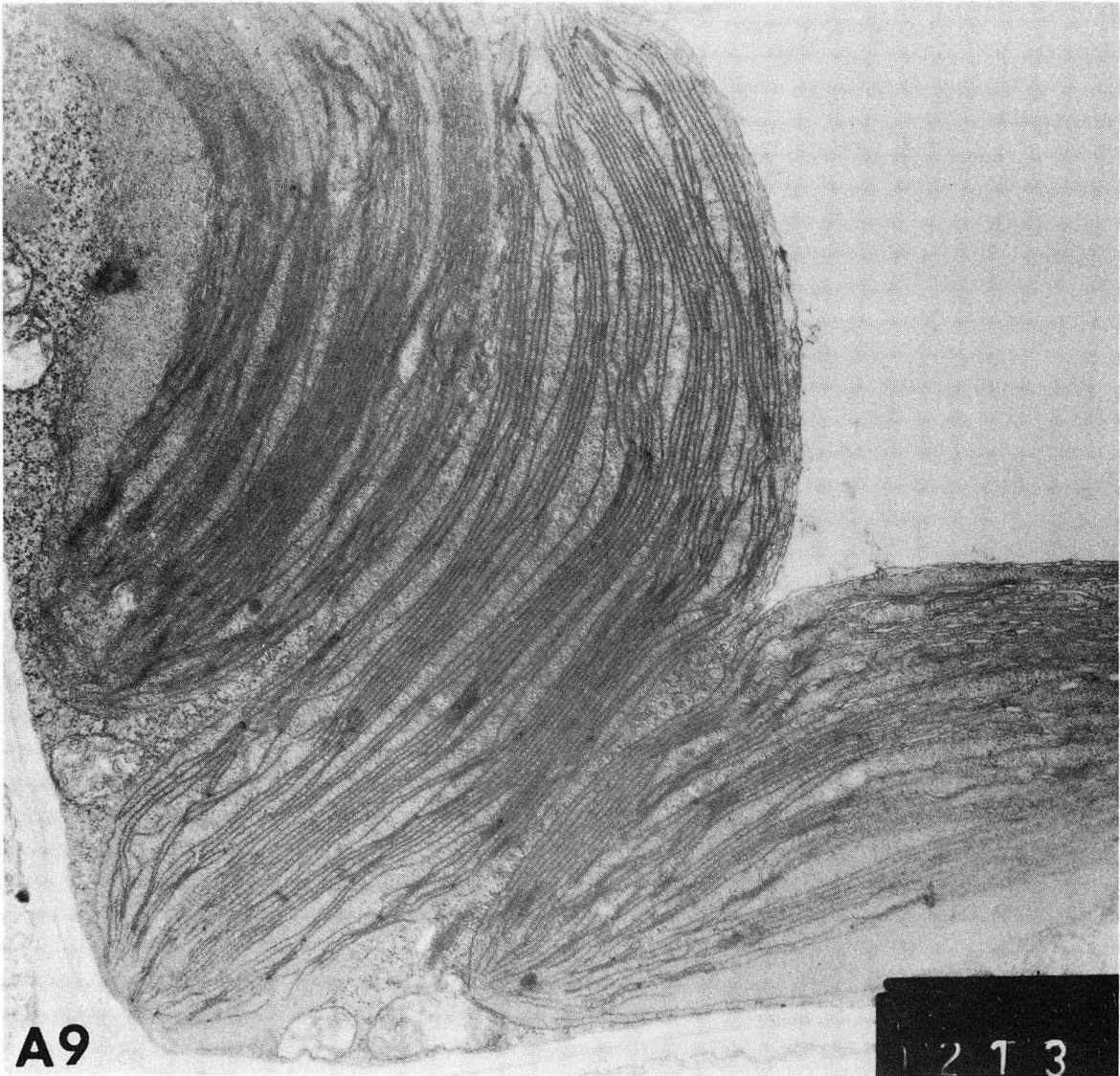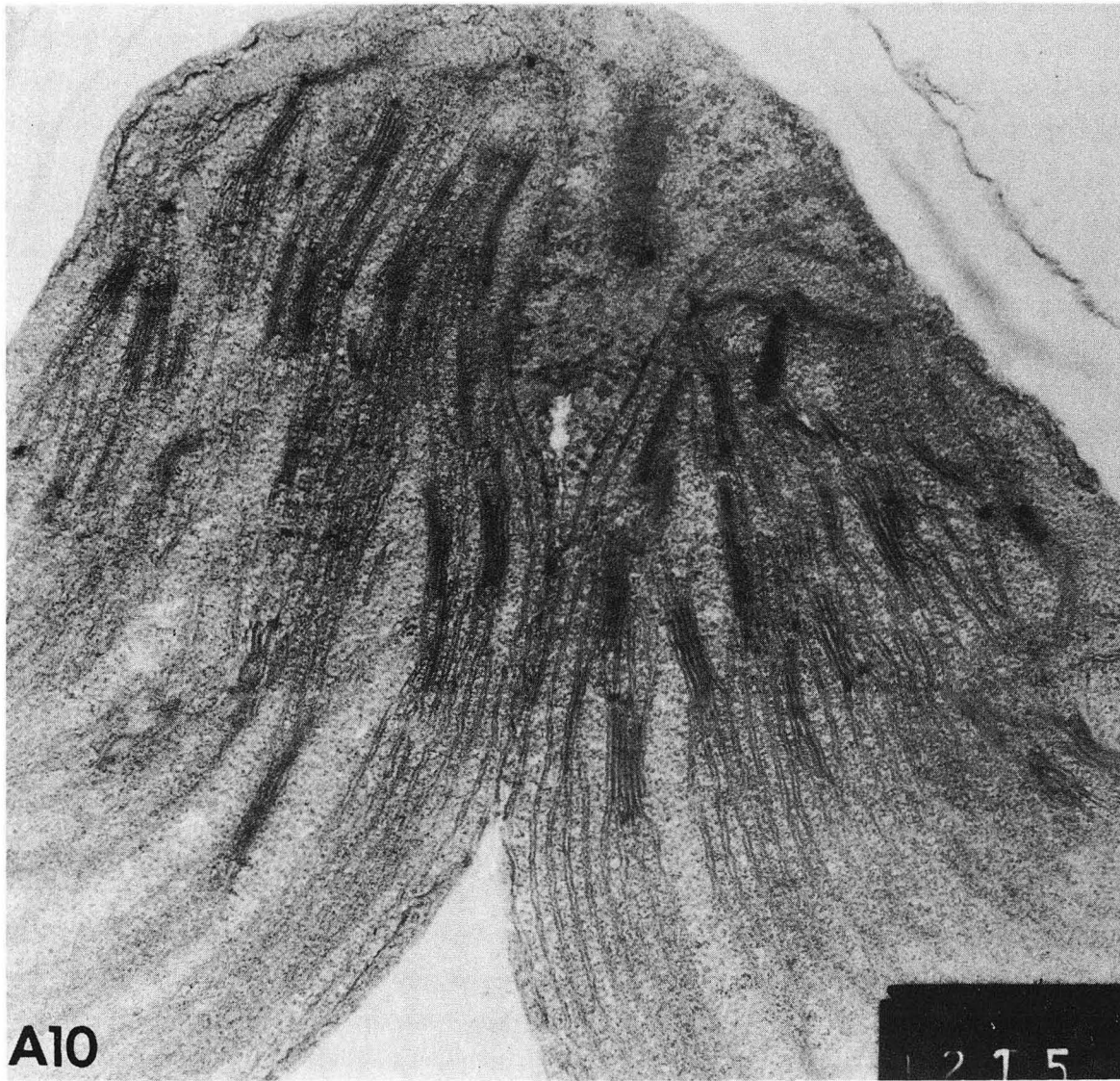
XBB 718-3566

A11
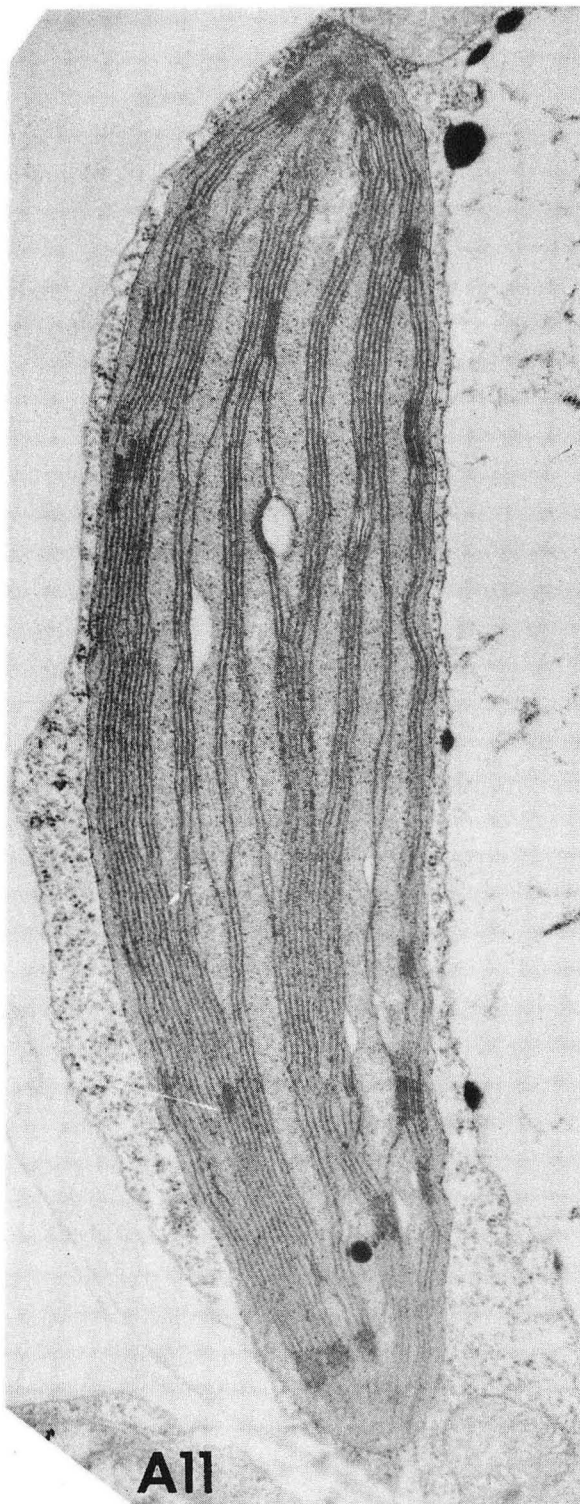
XBB 717-3062

A12

XBB 717-3264

A13

XBB 717-3266

A15

XBB 717-3144

A16
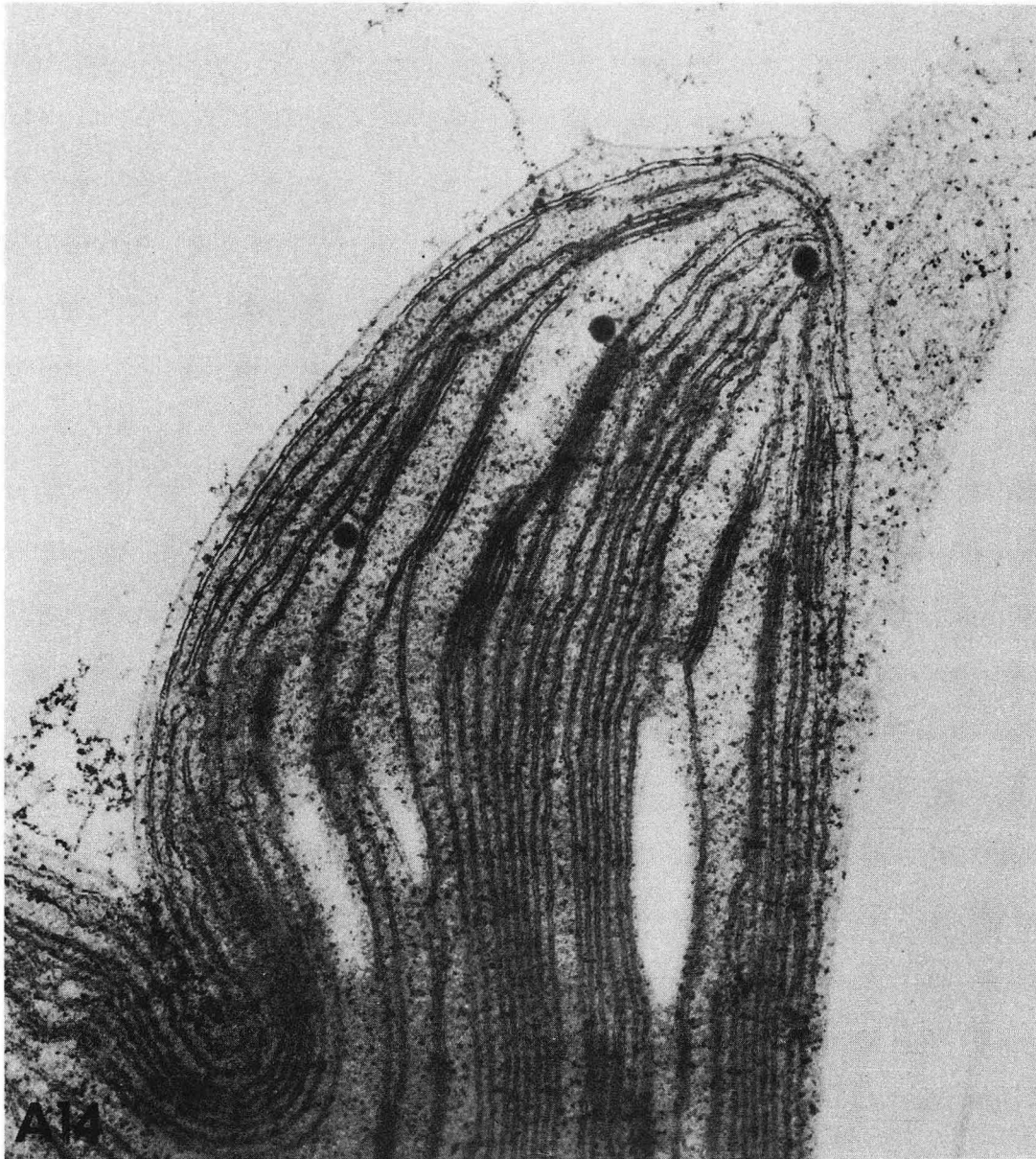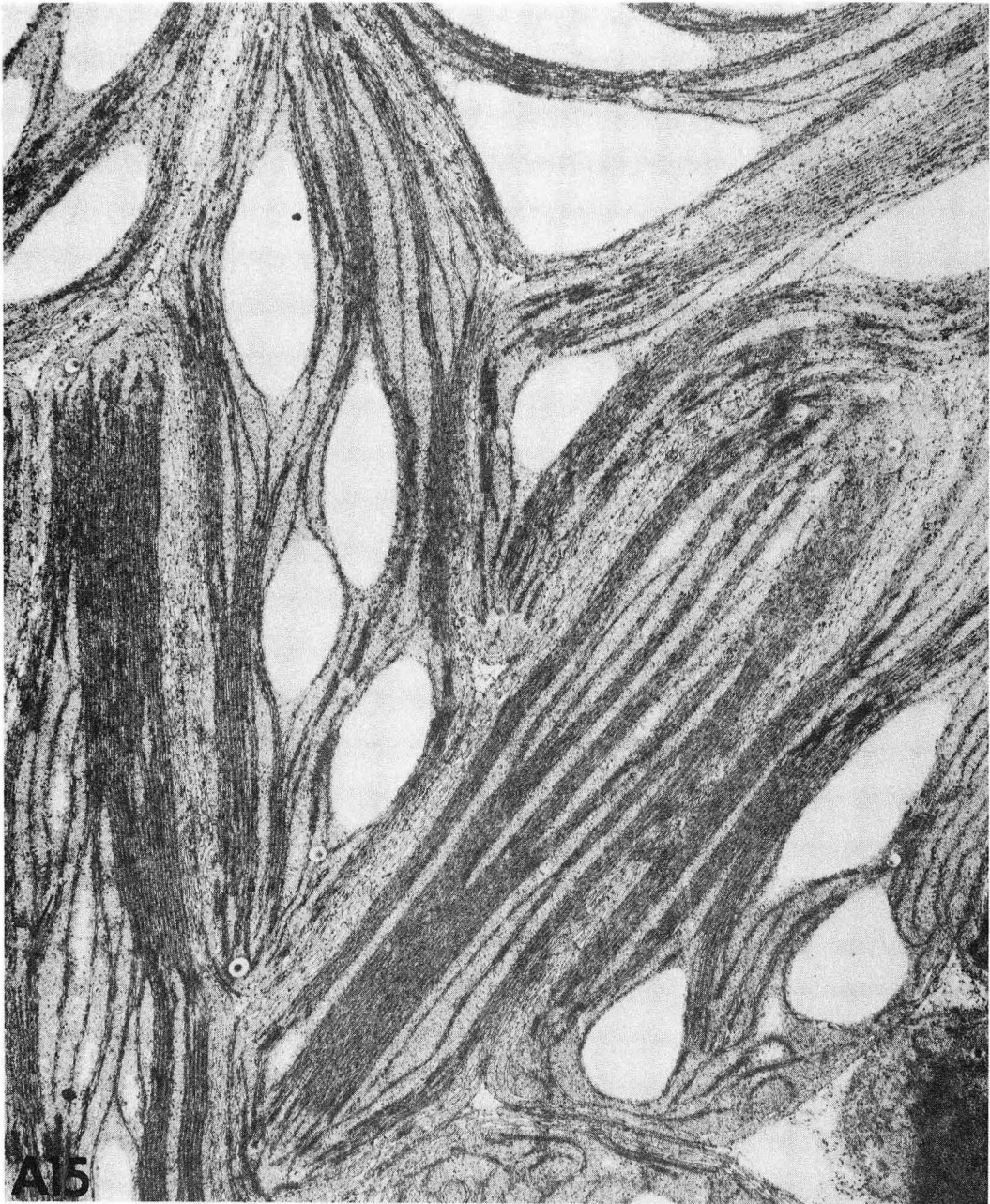
XBB 717-3146

A17

XBB 717-3143
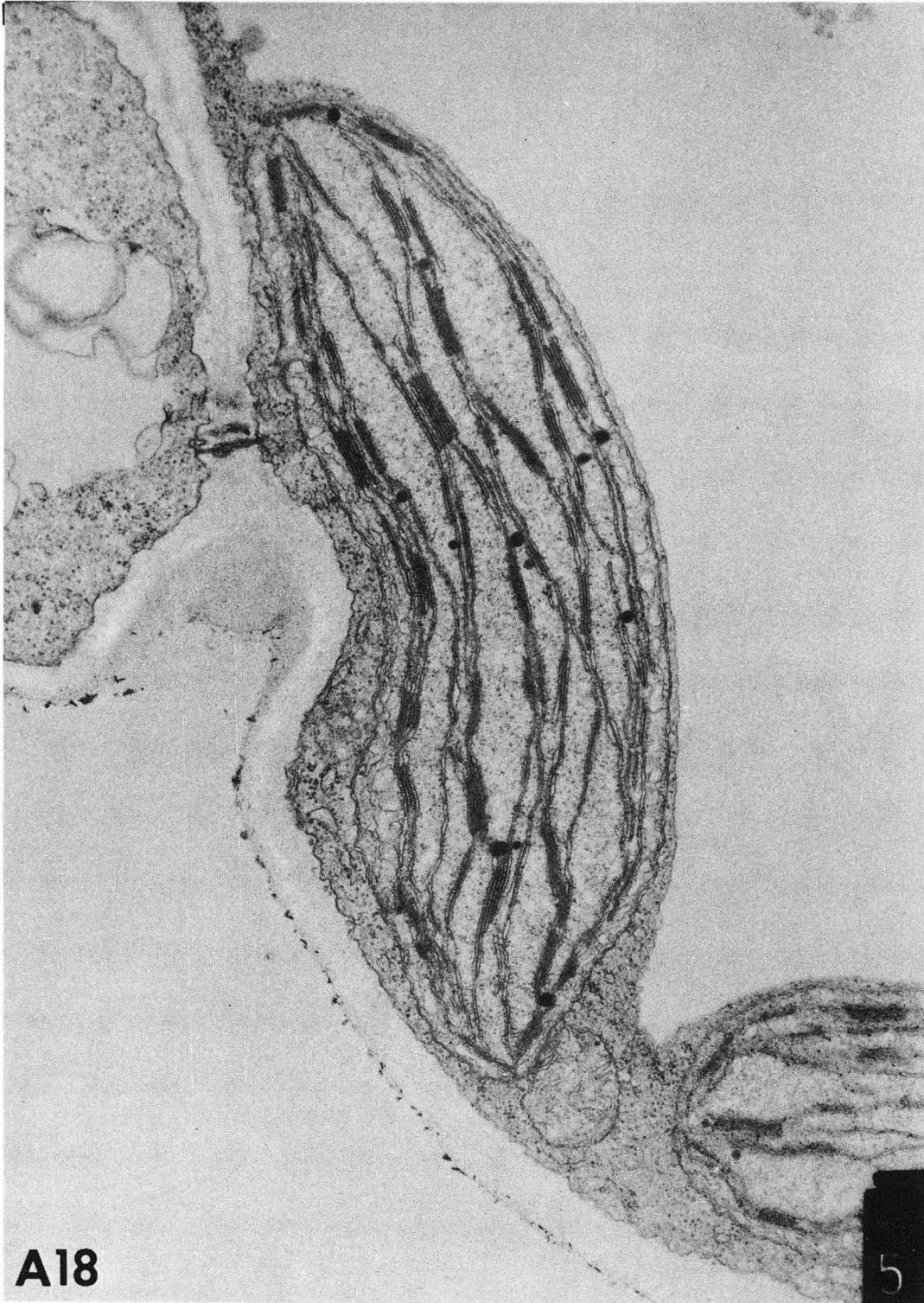
A18

5

XBB 718-3564

XBB 7310-6157
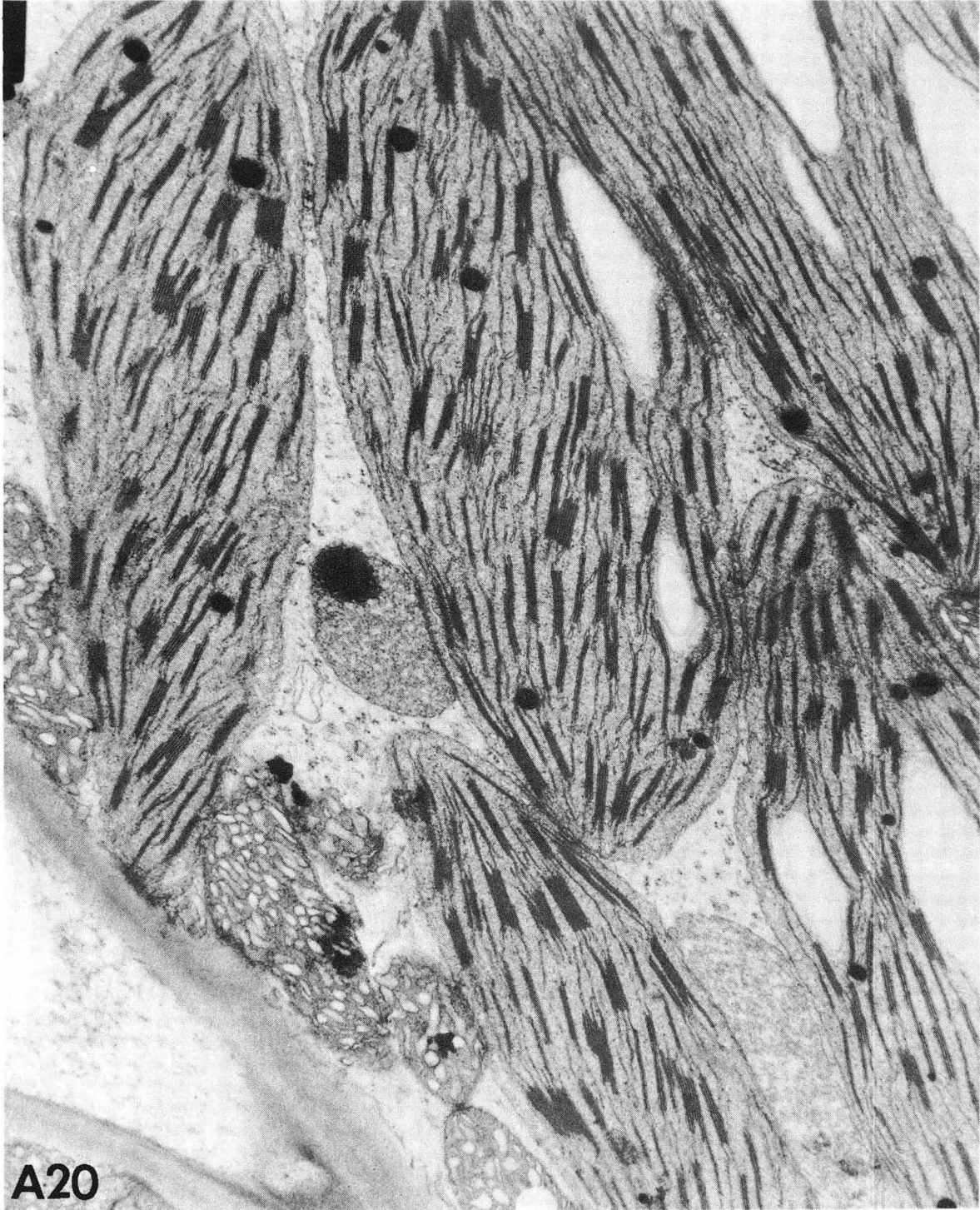
A20

XBB 717-3066

A21

A22

A25

A26

XBB 717-3063

A27
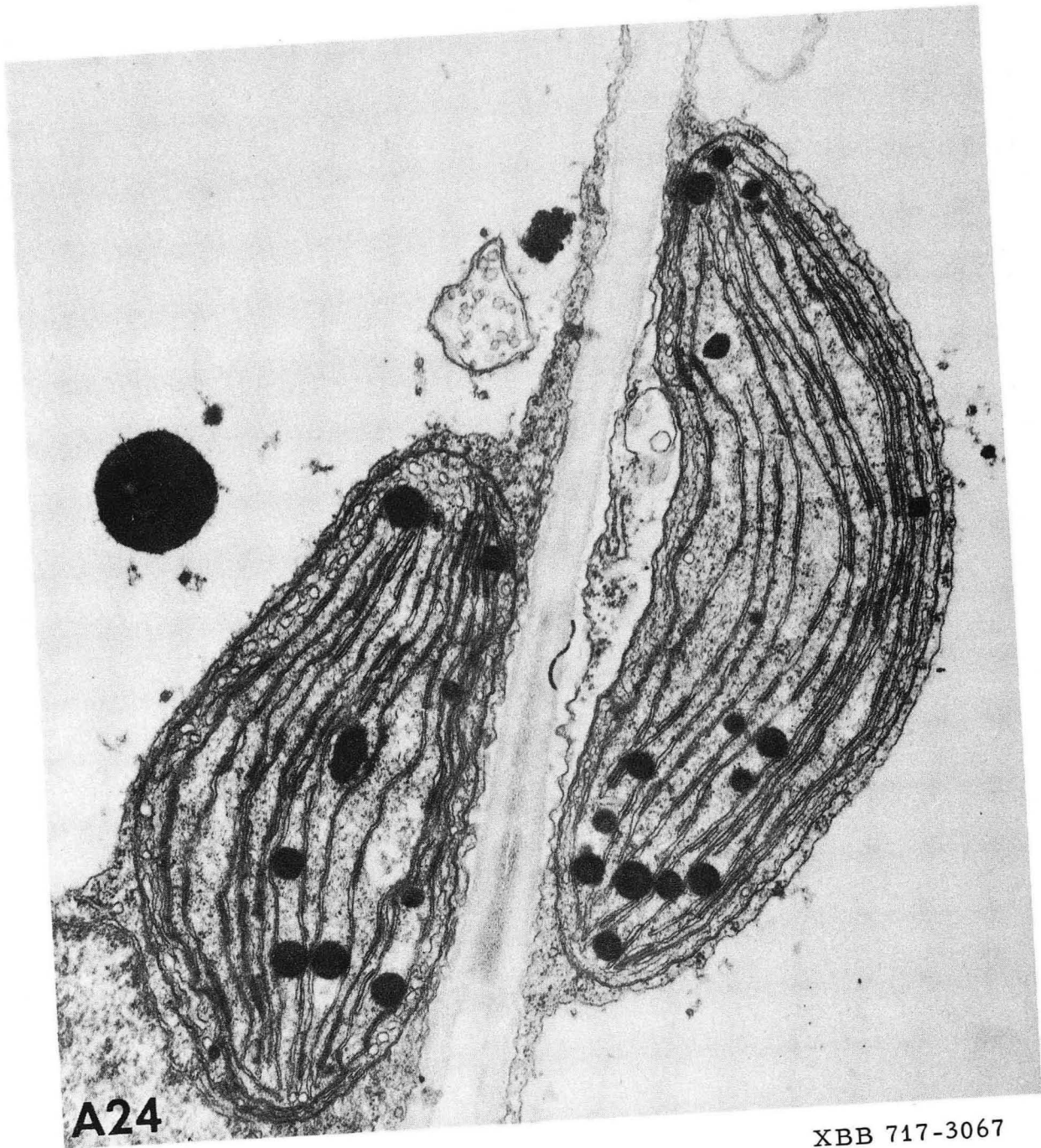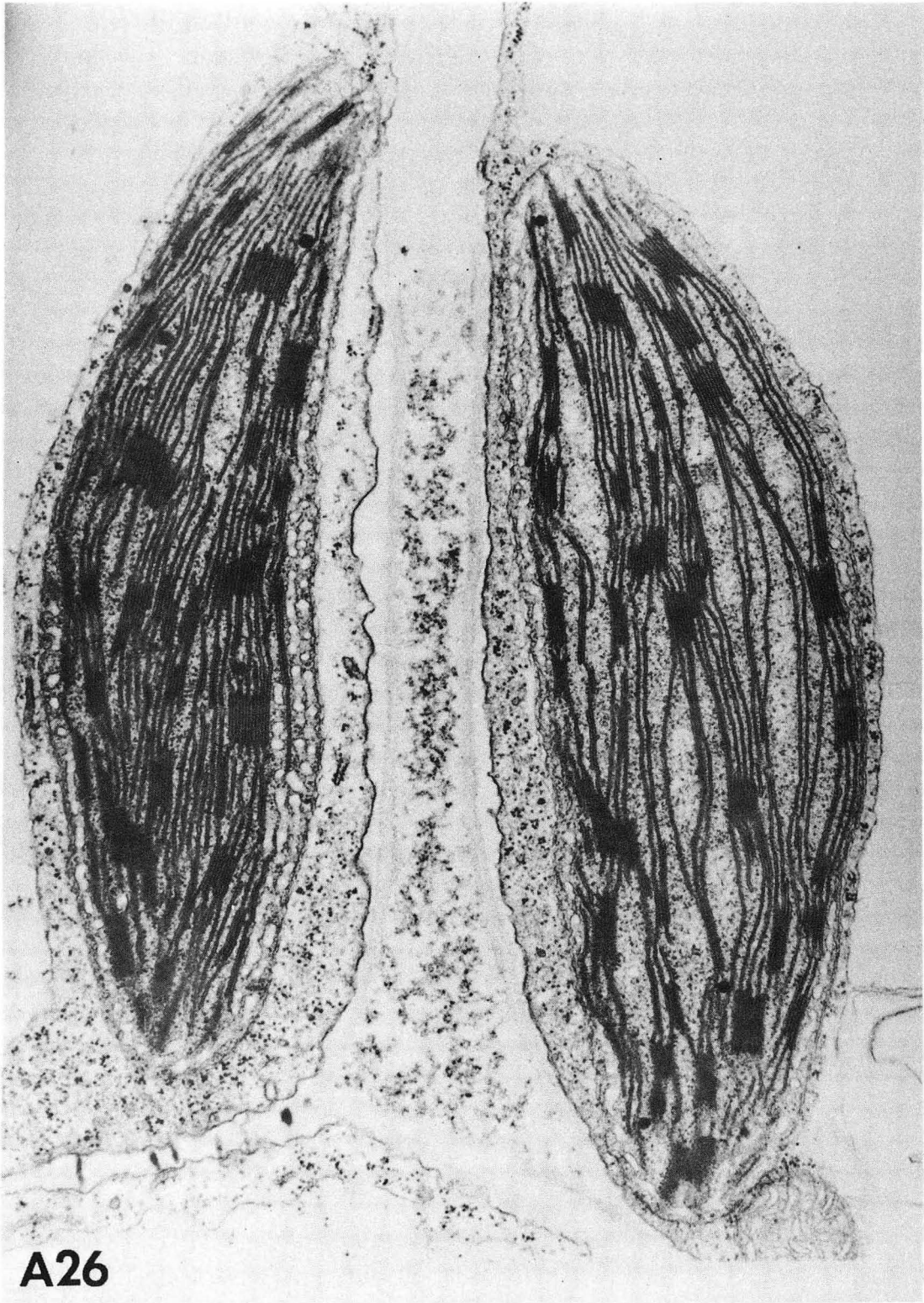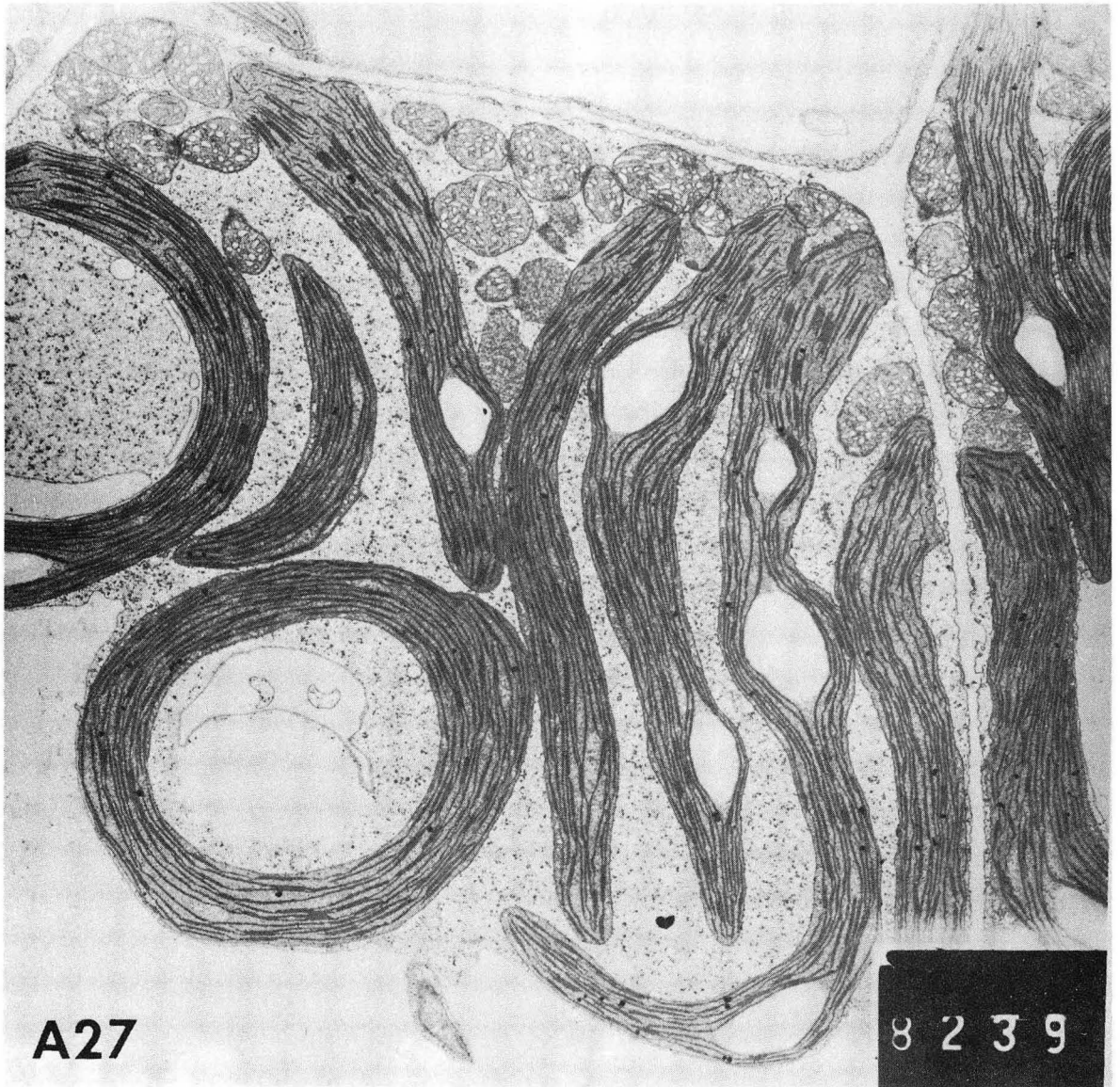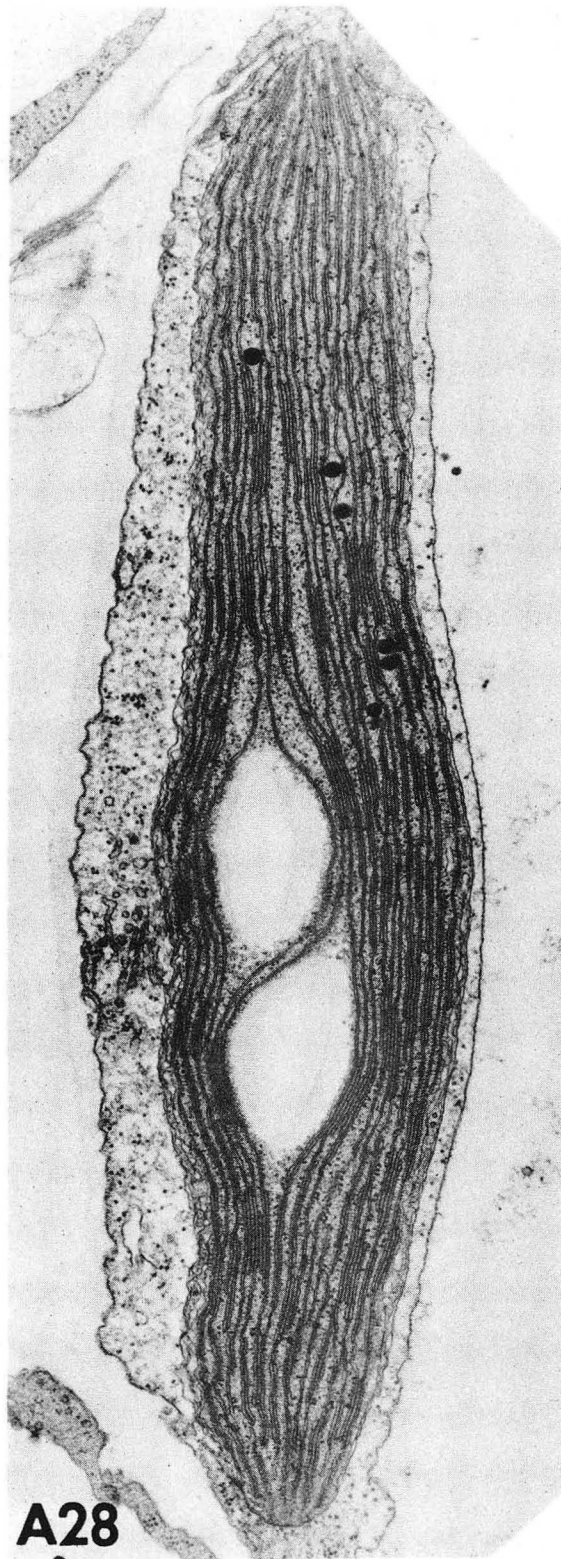
XBB 717-3271

A29

XBB 717-3265

A30
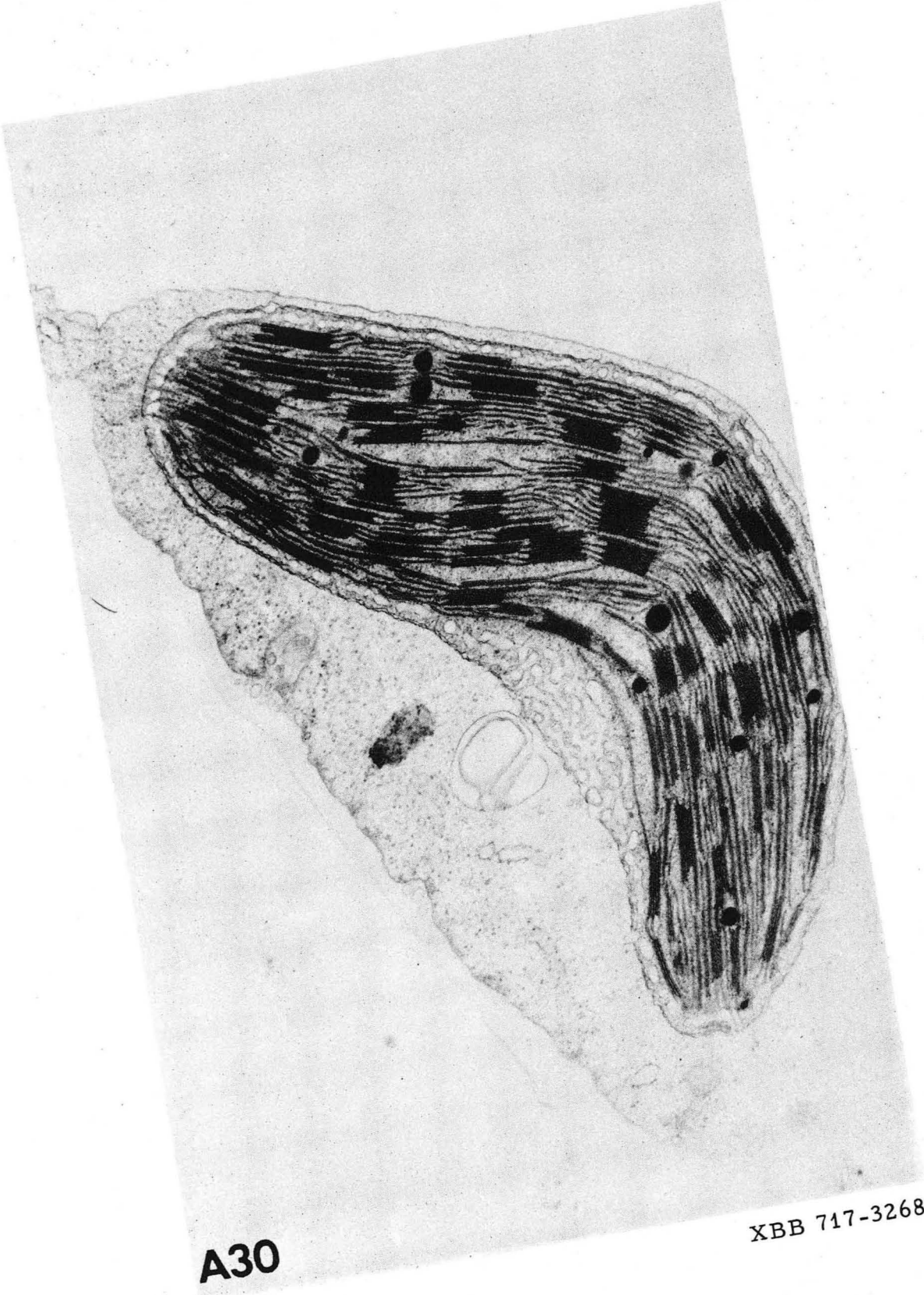
APPENDIX B

Infrared Black and White

Photographs of Experimental

Leaf Cross Sections

Table B1. Part I. Figure Legends for the Photographs of Experi-
mental Leaf Sections

Figure	Experimental Treatment	Plastid Type	Film Frame	Exposure Time (sec)	Corrected Exposure Time
B1-a	680 nm	M	126-21	16	27.44
B1-b		M	126-18	1.1	1.89
B1-c	689 nm	M	126-23	9.9	11.39
B1-d	741 nm	M	126-34	22	22
B2-a	680 nm	M	127-11	16.05	27.53
B2-b		M	127-07	1.1	1.89
B2-c	689 nm	M	127-13	9.9	11.39
B2-d	741 nm	M	127-22	18.1	18.1
B3-a	680 nm	BS	127-40	88.1	151.12
B3-b	701 nm	BS	127-36	66	95.1
B3-c	689 nm	BS	127-39	42.9	49.36
B3-d	741 nm	BS	127-25	54	54
B4-c	680 nm Tris	M	134-22	18.05	30.95
B4-a	701 nm Tris	M	134-28	29.19	42.03
B4-d	689 nm Tris	M	134-24	12.30	14.15
B4-b	741 nm Tris	M	134-35	27.04	27.04
B5-c	680 nm Tris	M	134T-14	20.15	34.56
B5-a	680 nm Tris	BS	134T-16	115.05	197.31
B5-d	701 nm Tris	BS	134T-10	64	92.21
B5-b	741 nm Tris	BS	134T-05	55	55

Table B1. Part II

Figure	Experimental Treatment	Plastid Type	Film Frame	Exposure Time	Corrected Exposure Time
B6-c	680 nm Tris	M	135-22	18.1	31.04
B6-a	680 nm Tris	BS	135-39	115.02	197.25
B6-d	701 nm Tris	M	135-30	28.98	41.75
B6-b	741 nm	M	135-37	27.08	27.08
B7-c	680 nm Tris	BS	135-15	85.04	145.84
B7-a	680 nm Tris	-M	135-14	20.07	34.42
B7-d	701 nm Tris	BS	135-10	64.10	92.30
B7-b	741 nm	BS	135-05	55.15	55.15
B8-c	680 nm	M	139-1	12	20.59
B8-a	661 nm	M	139-6	60	77.41
B8-d	661 nm Tris	BS	141-3	450.01	580.51
B8-b	680 nm Tris	BS	141-1	85.19	146.10
B9-c	680 nm	M	139-23	12.01	20.59
B9-a	645 nm	M	139-31	1000	1605
B9-d	680 nm Tris	M	141-19	16.54	28.36
B9-b	645 nm Tris	M	141-23	1250	2006.25
B10-c	Untreated	M	120D-19	0.55	
B10-a	Untreated	M	117B-17	0.55	
B10-d	Untreated	BS	117D-22	1.95	
B10-b	Untreated	BS	119B-19	1.6	

Table B1. Part III.

Figure	Experimental Treatment	Plastid Type	Film Frame	Exposure Time	Corrected Exposure Time
B11-c	Untreated	M	131E-31	1.1	
B11-a	Untreated	M	131D-27	1.1	
B11-d	Untreated	BS	131E-32	2.3	
B11-b	Untreated	BS	131D-28	2.3	
B12-c	Tris	M	131G-39	1.1	
B12-a	Tris	M	131F-35	1.1	
B12-d	Tris	BS	131G-40	2.6	
B12-b	Tris	BS	131F-36	2.3	
B13-c	HA*	M	133C-36	1.1	
B13-a	HA	BS	133C-39	2.8	
B13-d	HA	M	122HA-2	0.55	
B13-b	HA	BS	122HA-4	2.1	
B14-c	DCMU	M	132C-10	1.1	
B14-a	DCMU	BS	132C-11	2.35	
B14-d	DCMU	M	132D-13	1.1	
B14-b	DCMU	BS	132D-14	2.4	
B15-a	Tris	M	130-38	1.1	
B15-b	Tris	M	130-39	1.9	
B15-c	Tris	BS	130-40	3.1	
B15-d	Tris	BS	130-41	2.82	

*hydroxylamine
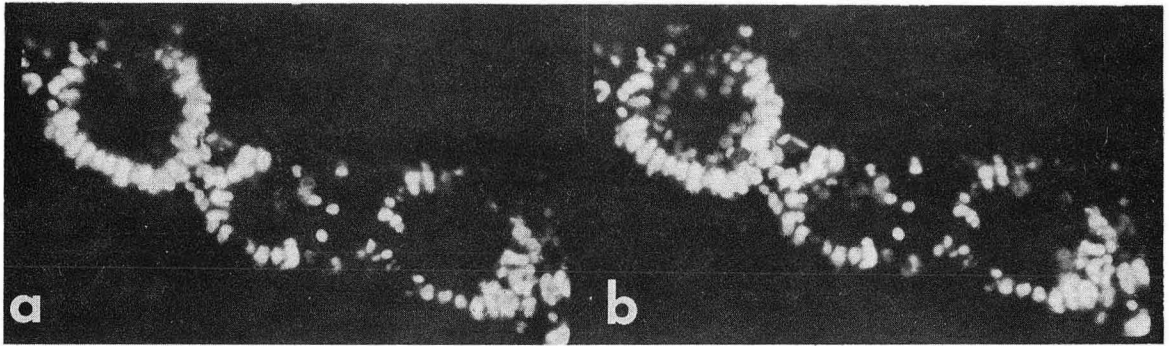
B1
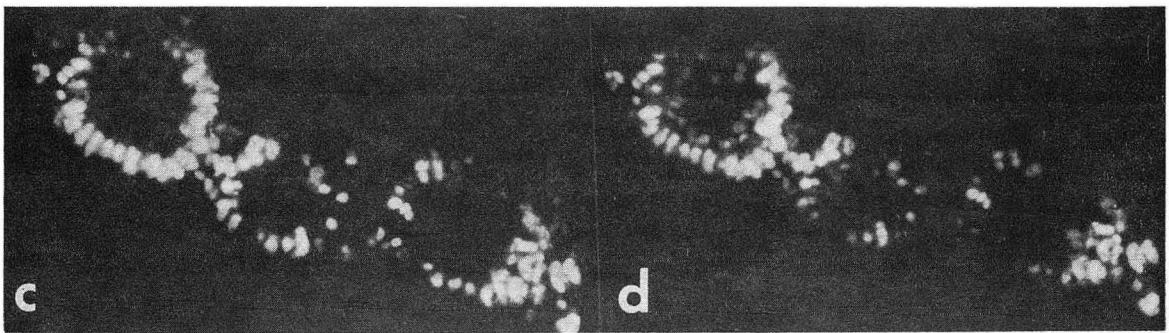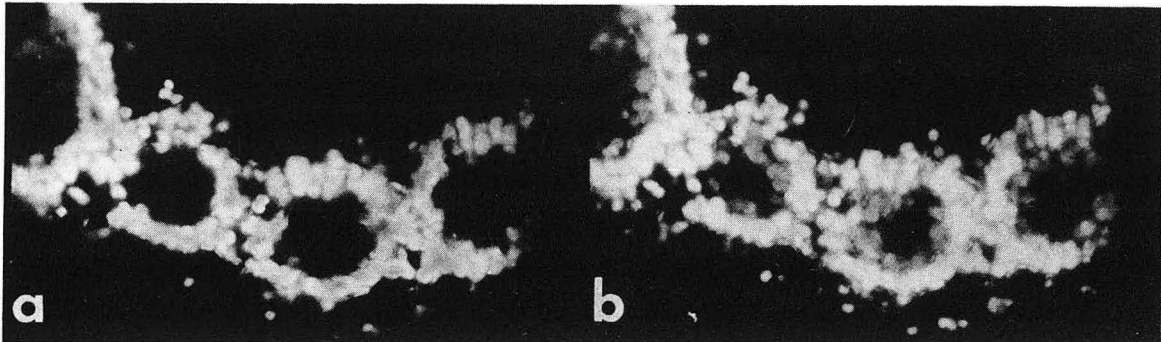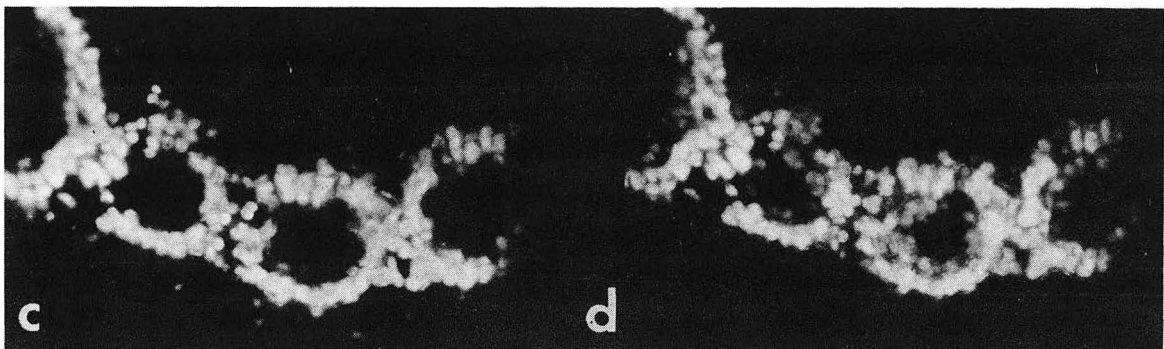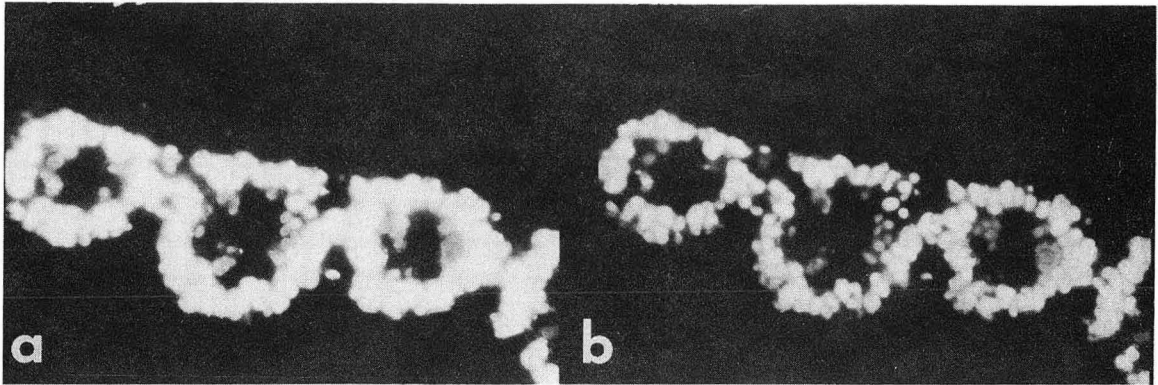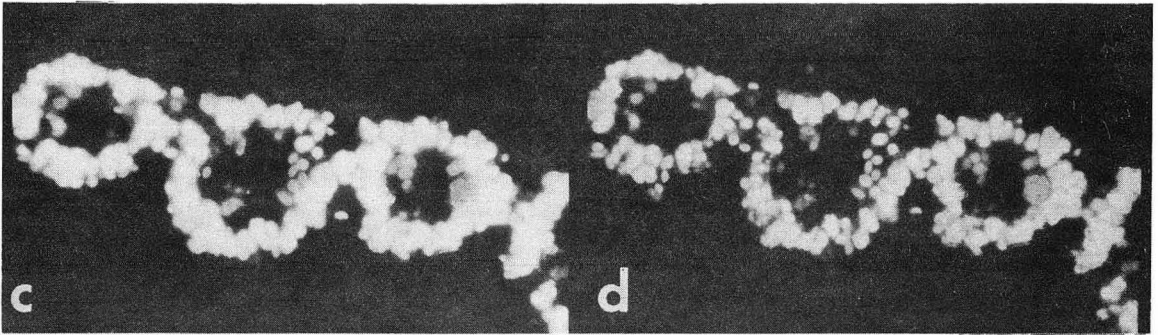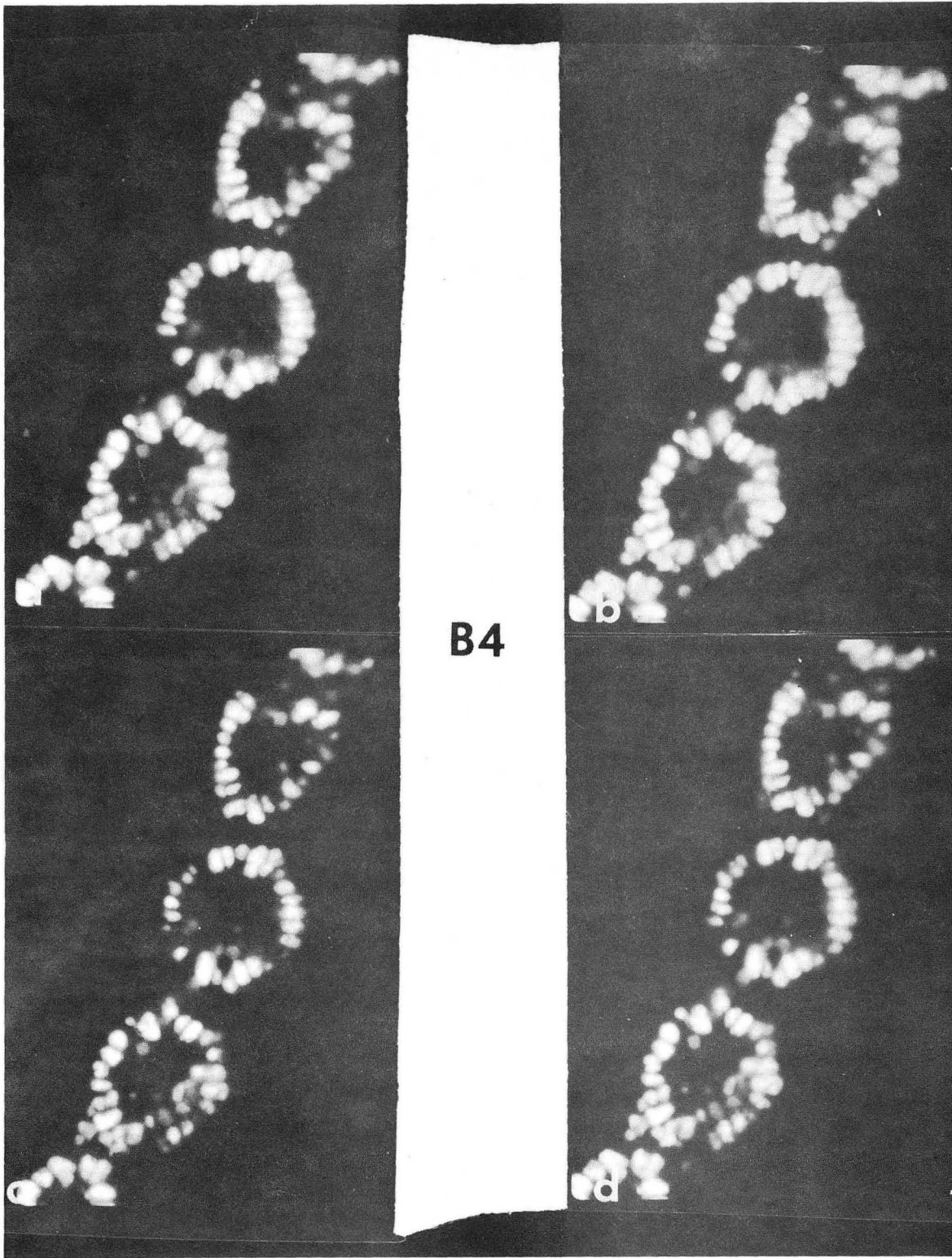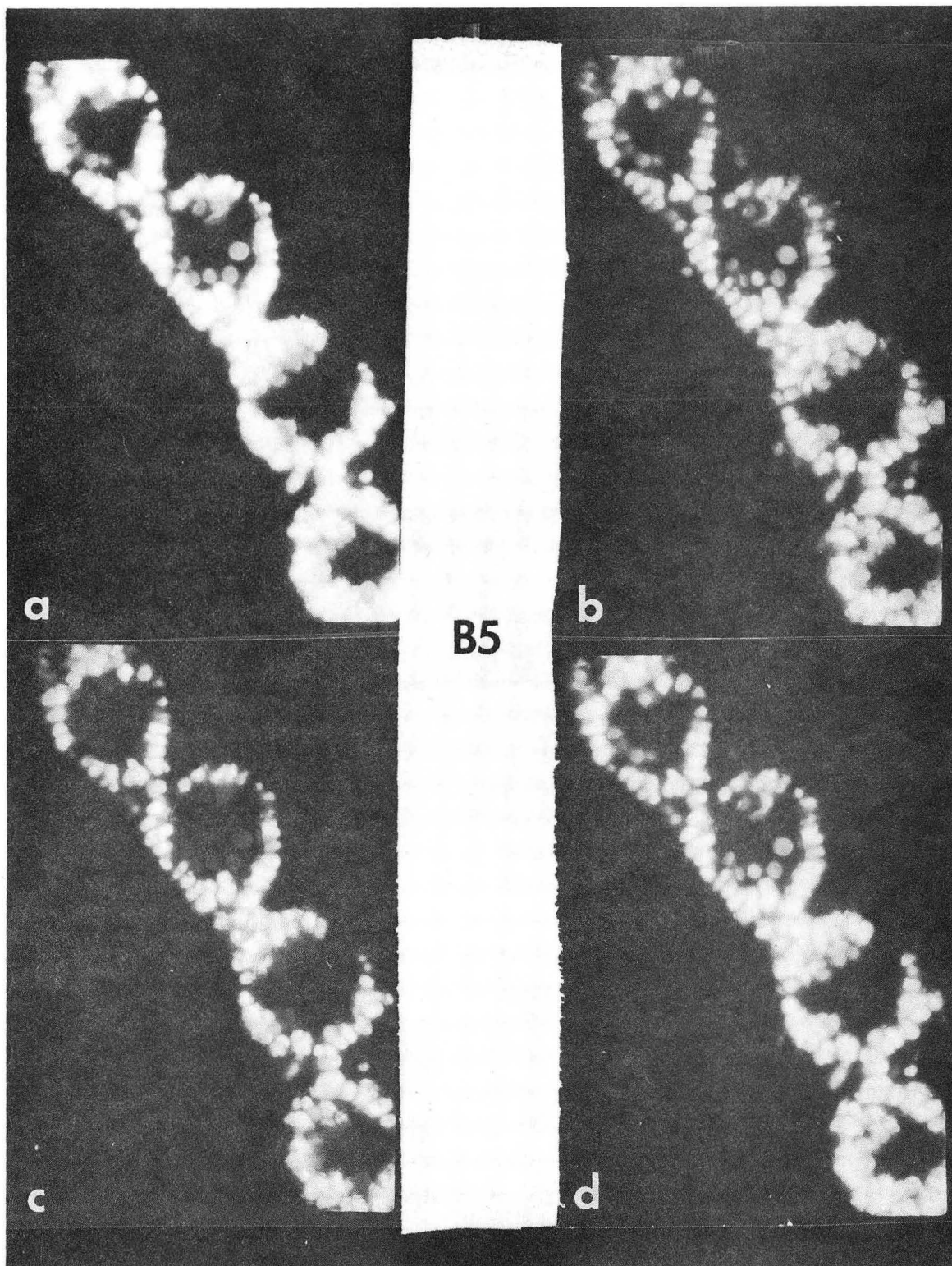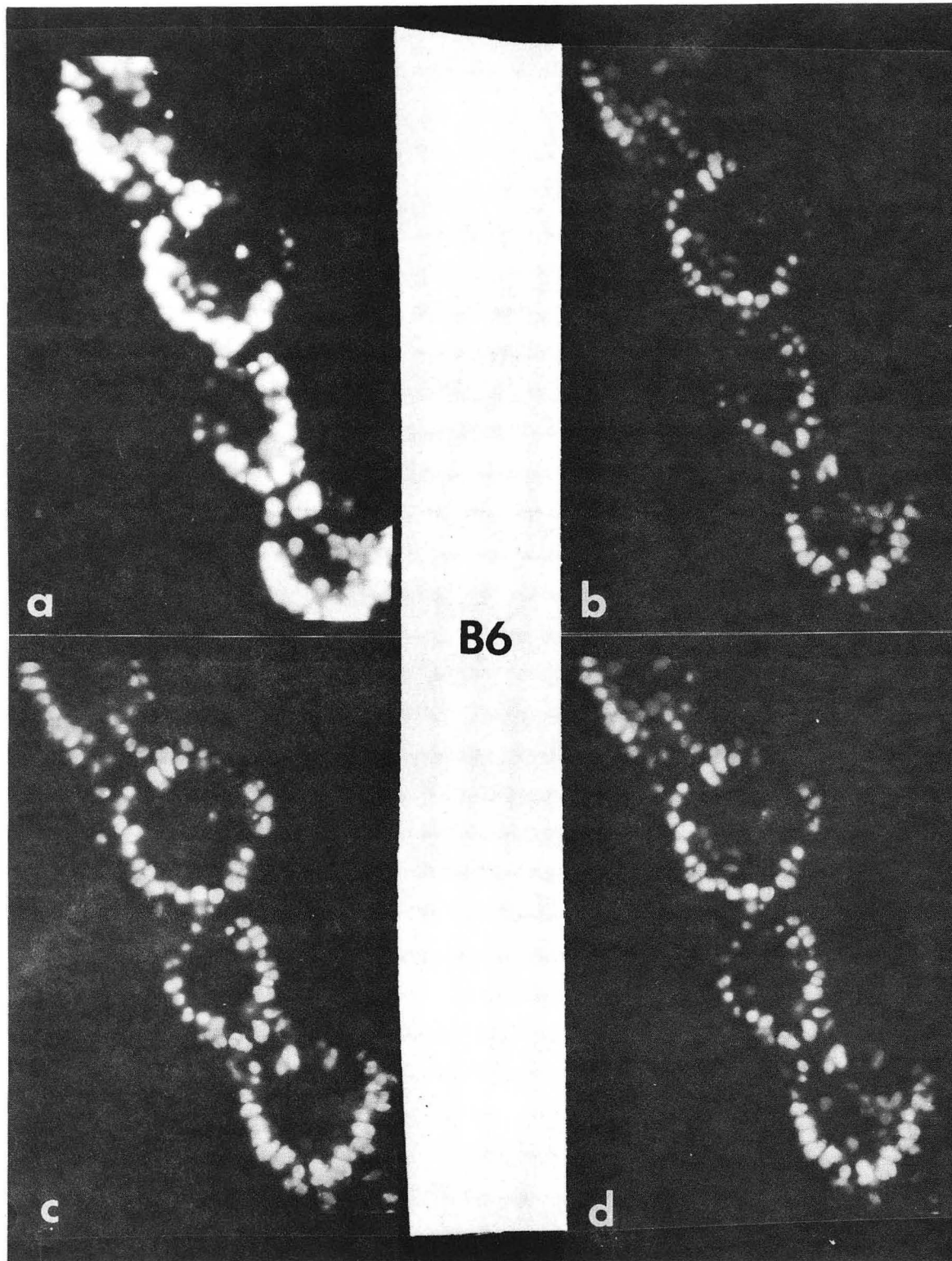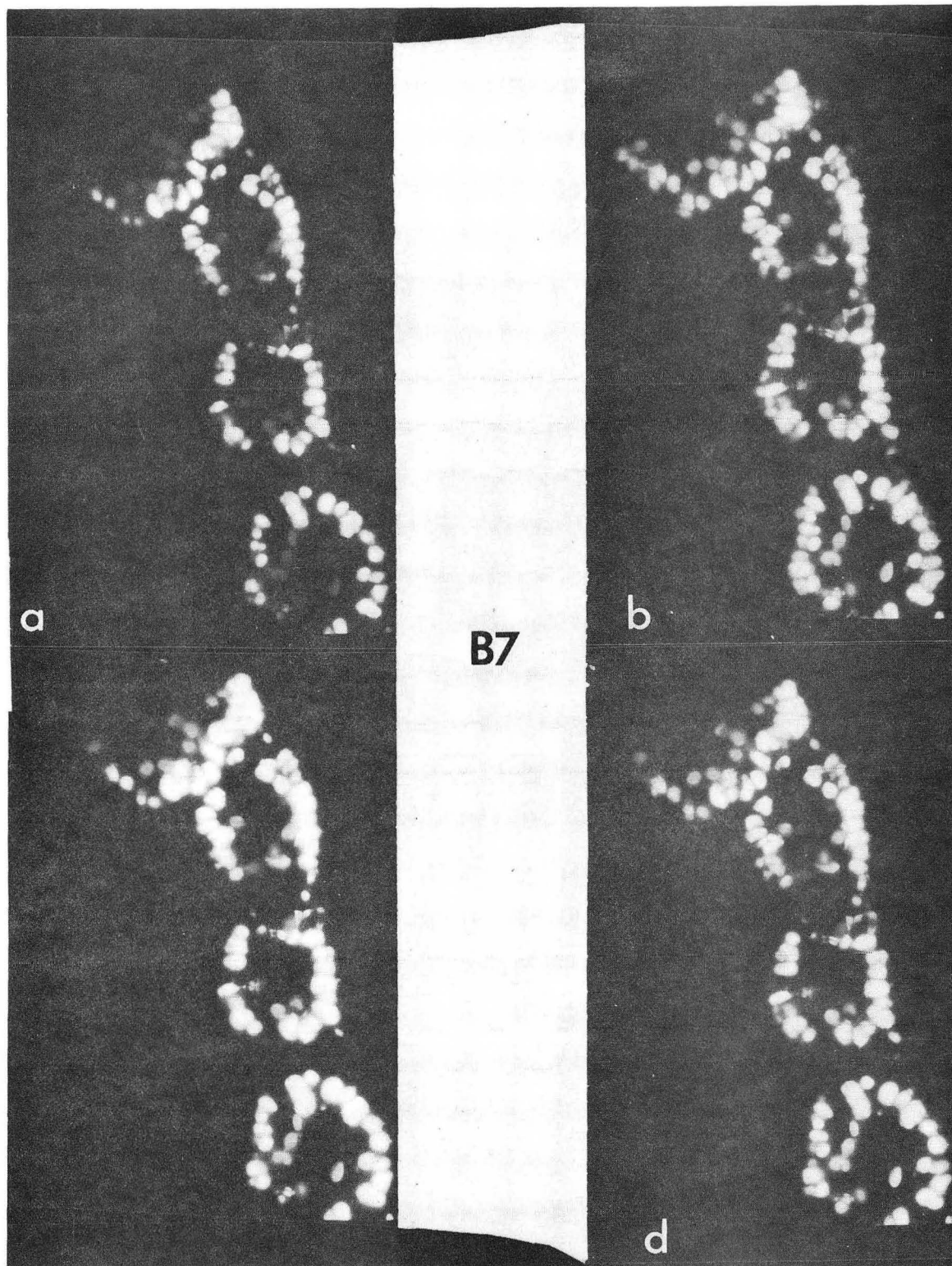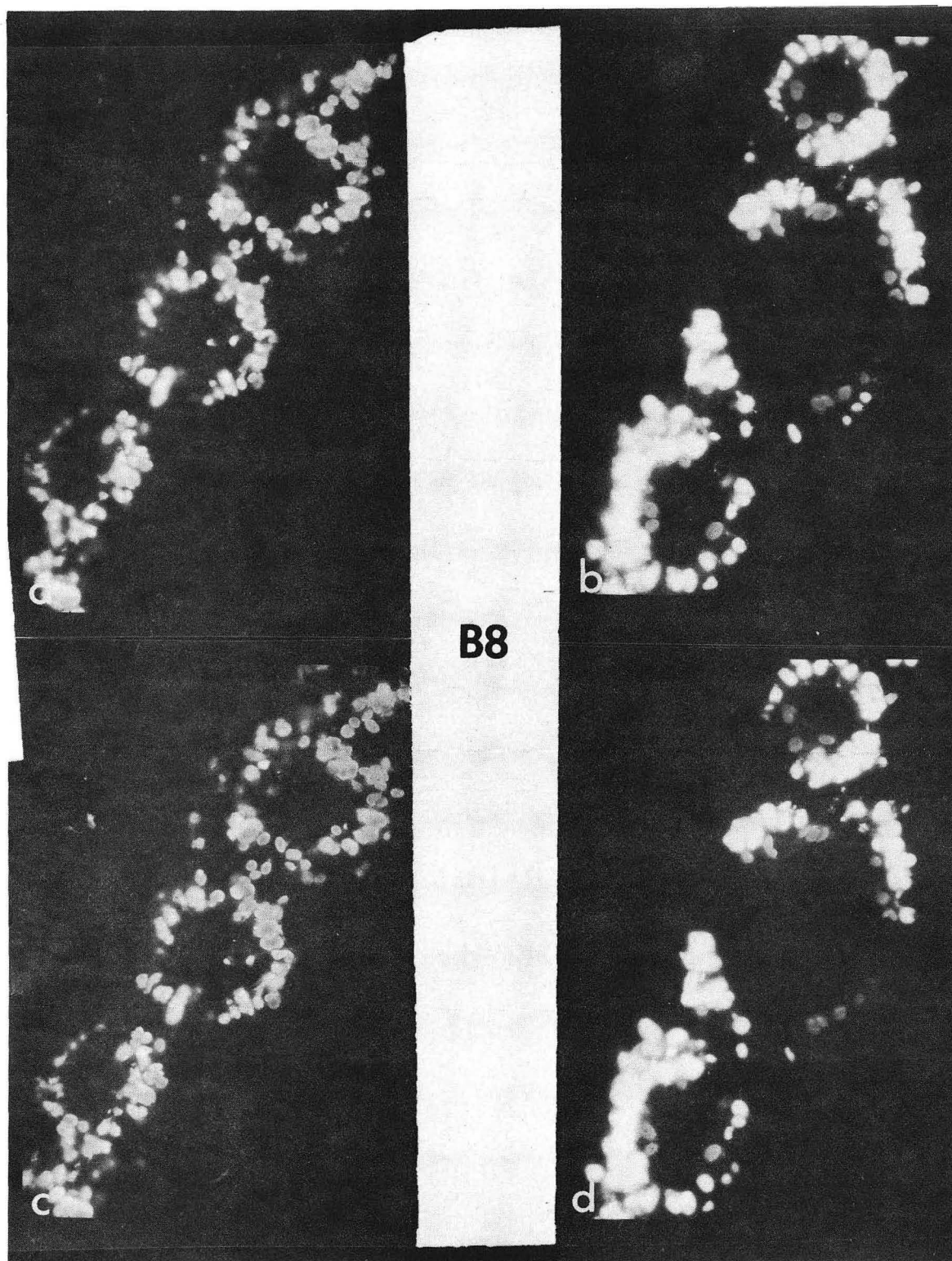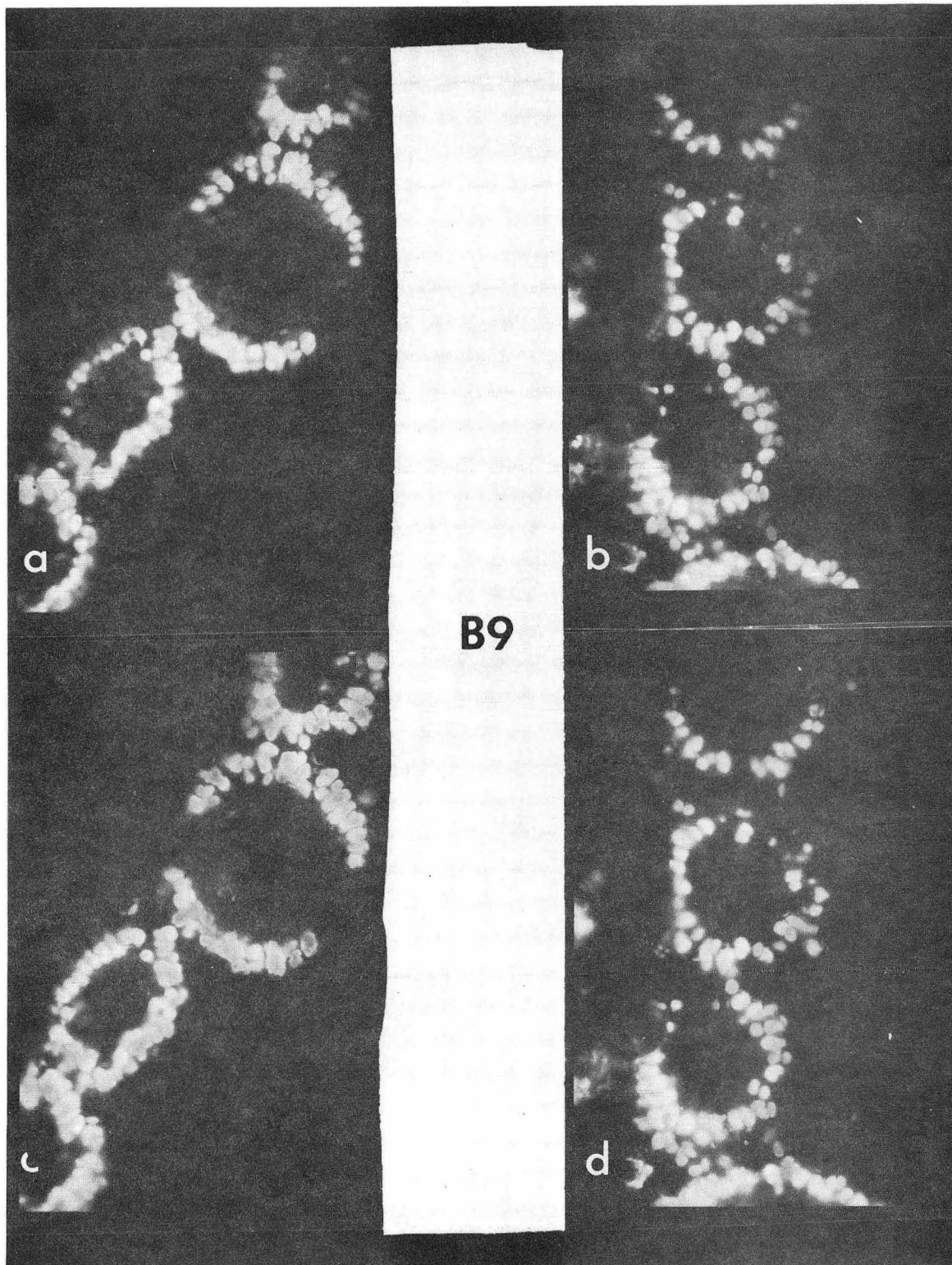
B2

B3

B4

B5

B7

XBB 7310-6153

B8

B11

XBB 7310-6149

B12

XBB 7310-6148

B14

B15
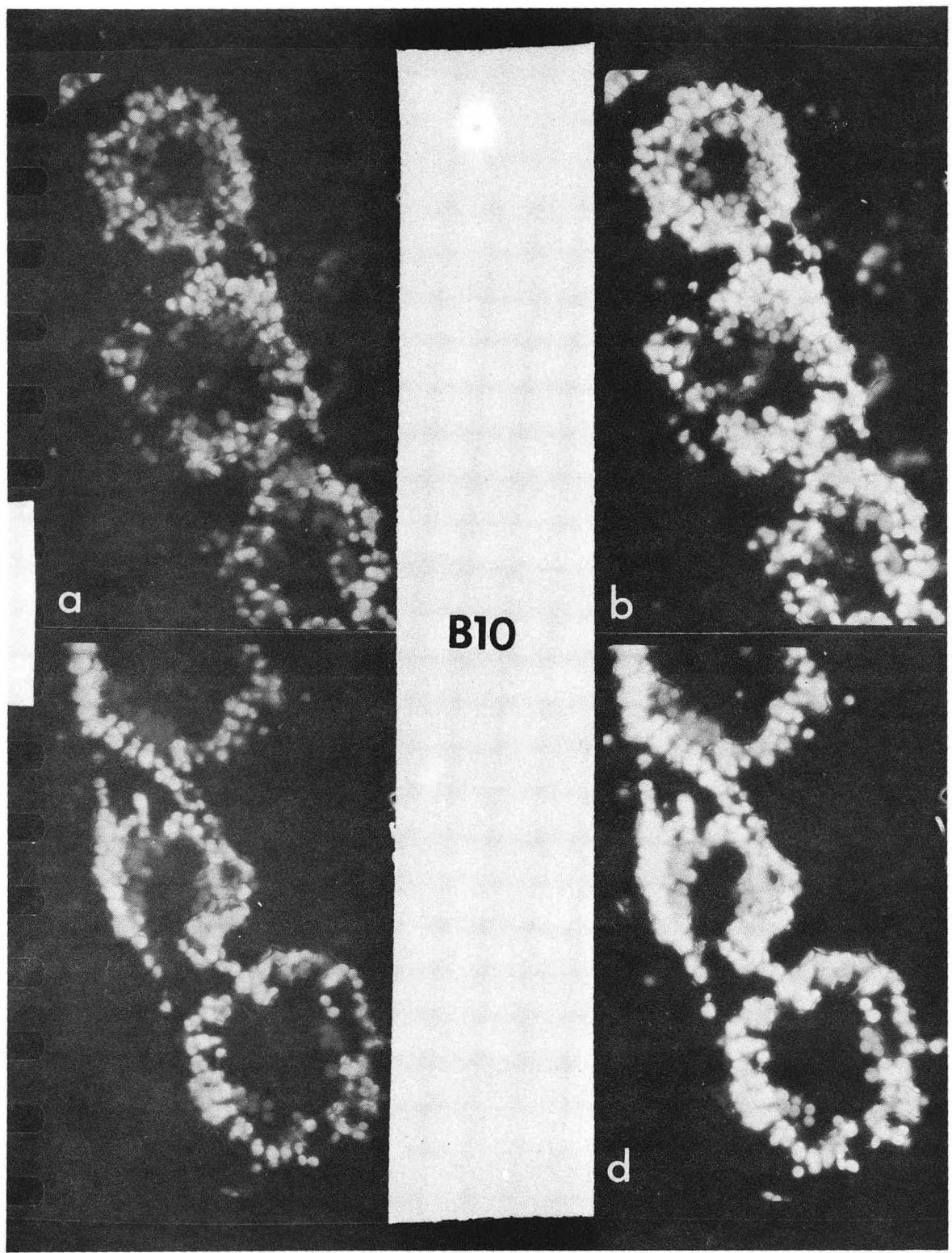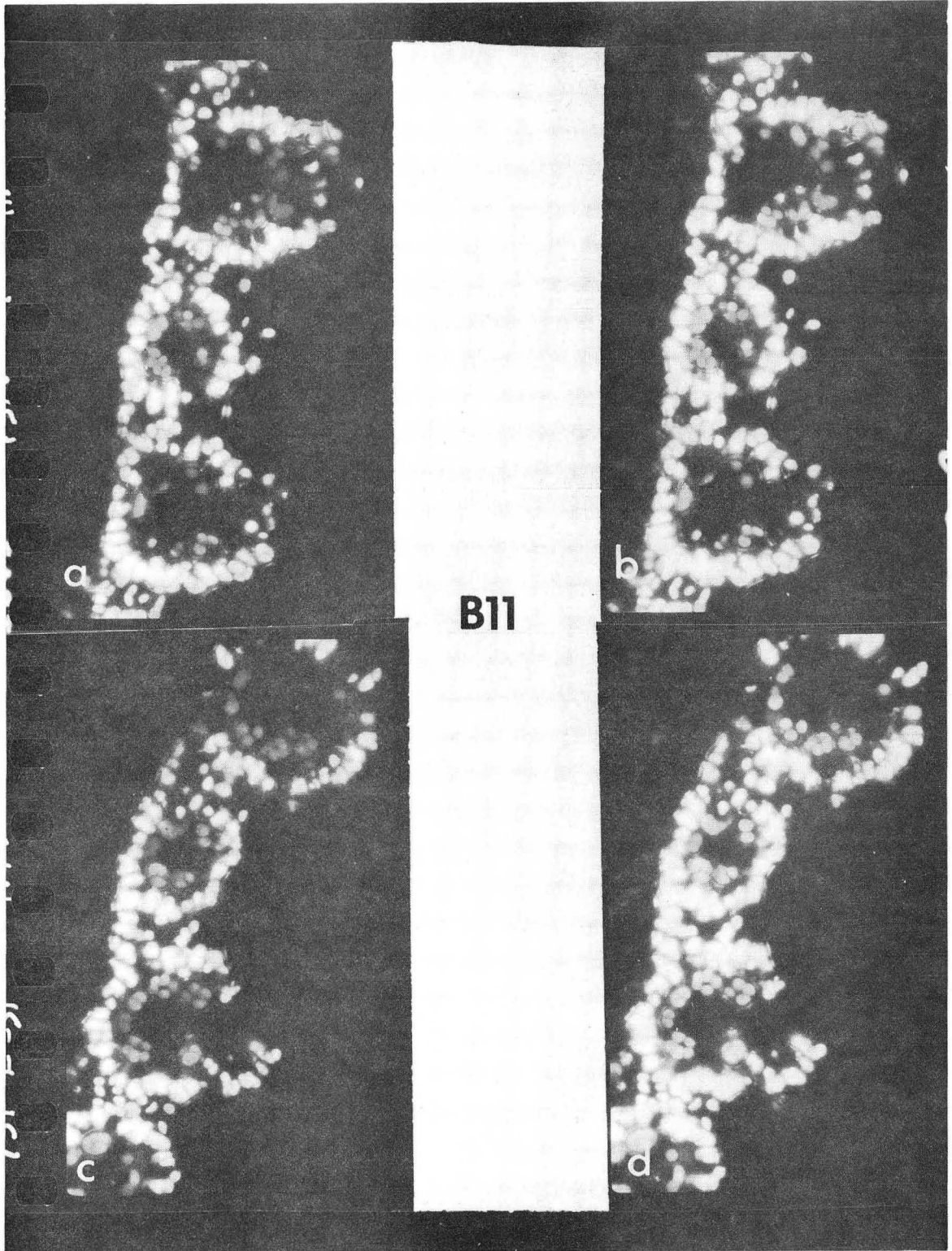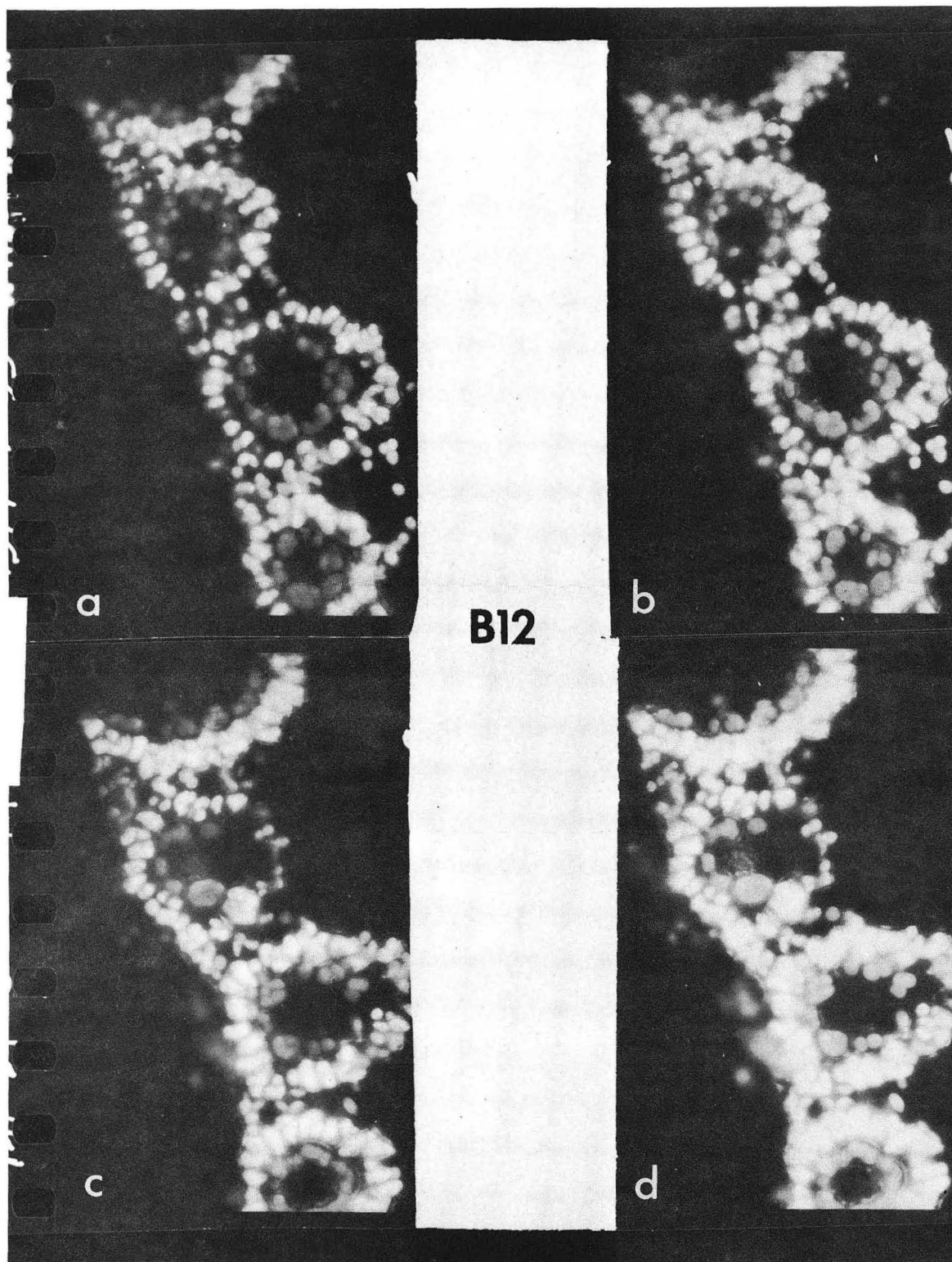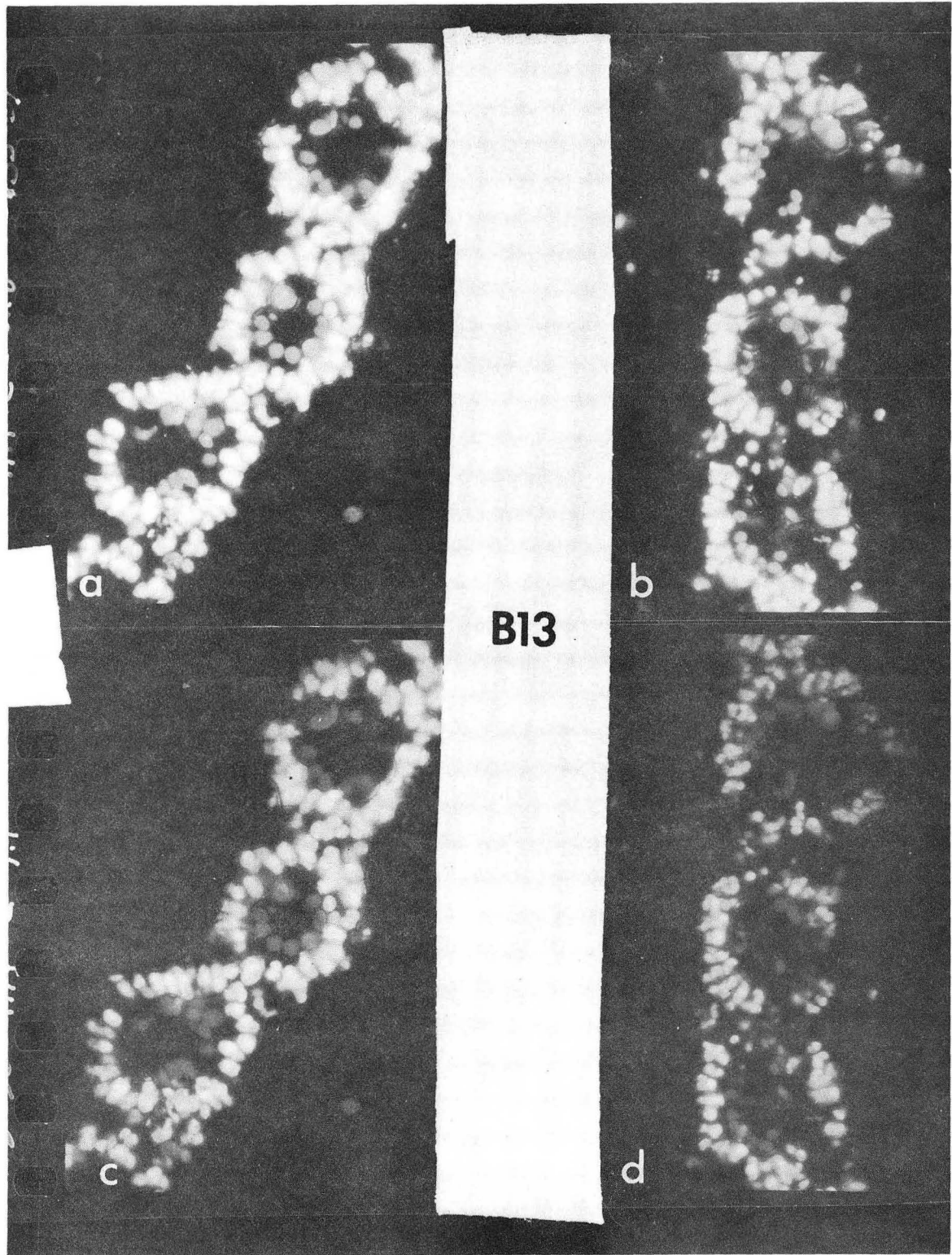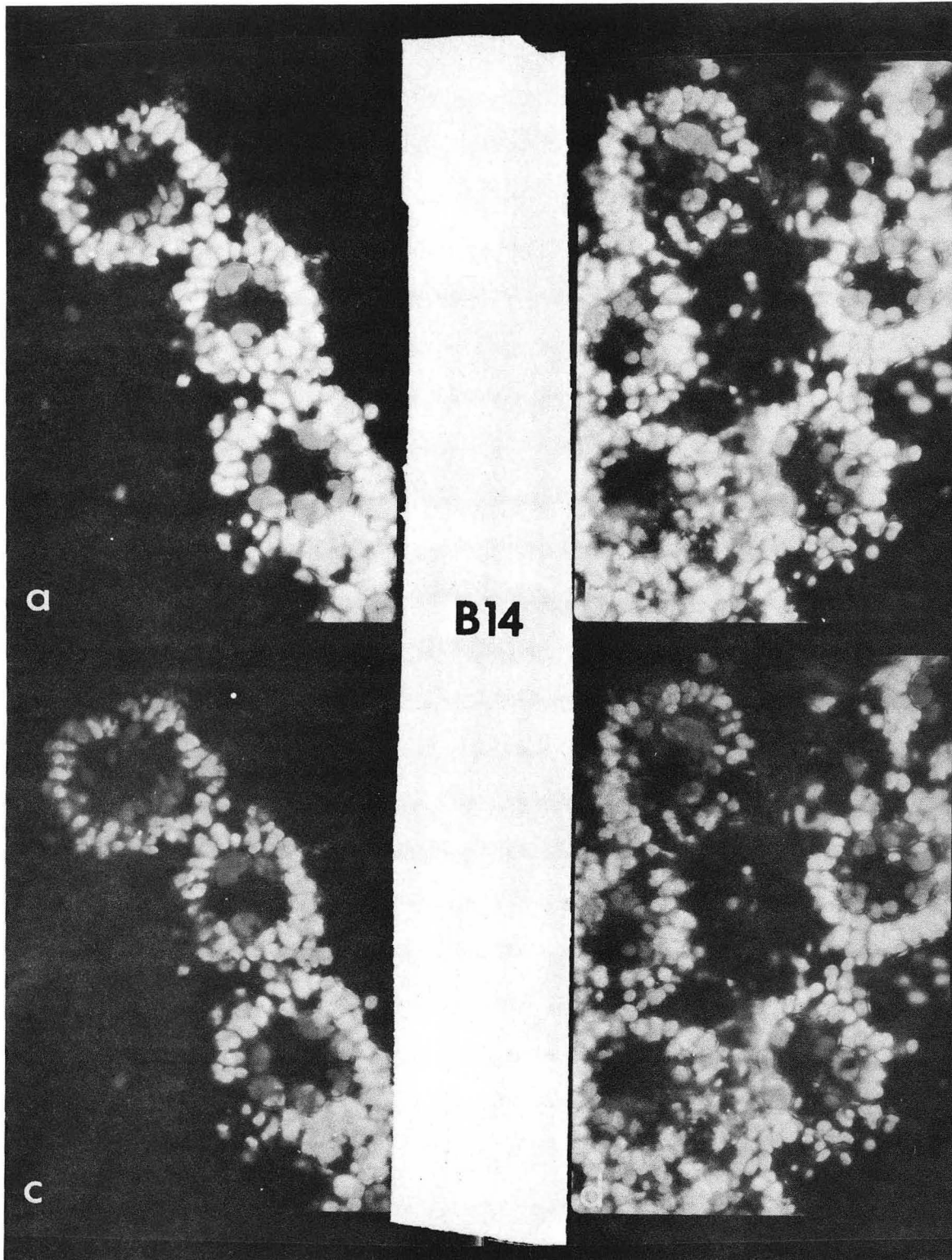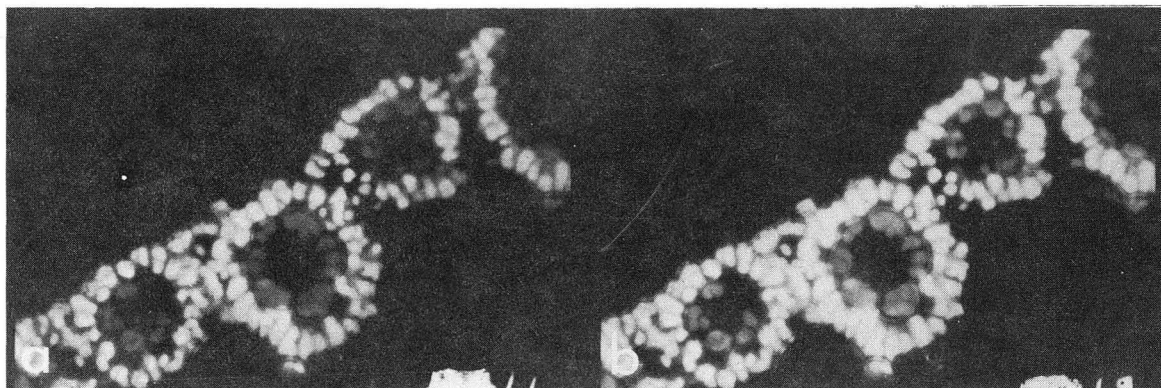
APPENDIX C

Data Tables

ABBREVIATIONS

(T_e)	exposure time
$(\bar{D})$	relative mean density
(σ)	standard deviation
(N)	sample number
$(t_{.05_{n-1}})$	the .05 confidence limit of the t distribution for (n-1) degrees of freedom.
(E)	standard error of the mean
(L)	magnitude of error as defined in the text
$(\bar{D}_A)$	adjusted relative mean density
(Q)	log of exposure time corresponding to $\bar{D}_A$
(T_Q)	antilog of Q, the exposure time corresponding to $\bar{D}_A$
(F)	Relative fluorescence of M/BS
$(\bar{L})$	average error
$(\bar{D}_A \pm L)$	0.05 confidence limits of $\bar{D}_A$
$(T_Q^+ \text{ and } T_Q^-)$	0.05 confidence limits of T_Q
$(F_{MAX} \text{ and } F_{MIN})$	Maximum and minimum F

Table C1. Data for the "Characteristic Curve"

of a Single Chloroplast

Specimen	T_e	Log T_e	D
BS/680-13	7.05	0.8482	0.00
BS/680-14	14.80	1.1703	0.88
BS/680-15	21.90	1.3404	1.78
BS/680-16	29.35	1.4676	3.01
BS/680-17	37.15	1.5700	4.33
BS/680-18	49.00	1.6902	5.78
BS/680-19	63.00	1.7993	6.60
BS/680-20	100.15	2.0006	10.13
BS/680-21	128.45	2.1088	12.71
BS/680-23	169.50	2.2292	15.42
BS/680-24	213.50	2.3294	16.42
BS/680-25	300.00	2.4771	18.13

Experiment 106-680

Specimen	T_e	Log T_e	$\bar{D}$	σ	N	$t^{(.05)}_{(N-1)}$	E	L	$\bar{D}_A$	Q	T_Q	F
M/680-15	21.90	1.3404	12.47	1.41	39	2.025	0.225	0.456				
M/680-16	29.35	1.4676	15.30	1.56	38	2.027	0.250	0.507	14.0	1.409	25.65	
M/680-21	128.45	2.1088	10.51	1.39	19	2.101	0.317	0.666	14.0	2.257	180.73	7.05
BS/680-23	169.50	2.2292	13.74	1.21	18	2.110	0.284	0.599				
BS/680-24	213.50	2.3294	15.00	1.18	18	2.110	0.277	0.584				

Specimen	$\bar{L}$	$\bar{D}_A+\bar{L}$	Q_+	T_{Q+}	$\bar{D}_A-\bar{L}$	Q_-	T_{Q-}	F_{MAX}	F_{MIN}
M/680	0.482	14.48	1.429	26.85	13.52	1.389	24.49	$\frac{193.20}{24.49}=7.89$	
BS/680	0.616	14.62	2.286	193.20	13.38	2.229	169.40		$\frac{169.40}{26.85}=6.31$

Table C2. Data for Experiment 106-680.

Table C3. Data for Experiments 121 and 122.

Specimen	T_e	Log T_e	$\bar{D}$	σ	N	$t_{(\overset{.05}{N-1})}$	E	L	$\bar{D}_A$	Q	T_Q	F
					Sub-experiment P-122							
N/P-122	1.10	0.0414	14.15	1.49	28	2.052	0.282	0.58	14.25	0.050	1.122	
BS/P-122	2.00	0.3010	11.47	1.84	16	2.131	0.461	0.98	14.25	+0.431	2.697	2.40
BS/P-122	3.30	0.5185	16.45	1.75	15	2.145	0.453	0.97				
					Sub-experiment T-121							
N/T-121	0.55	-0.2596	11.44	1.26	26	2.060	0.246	0.51				
N/T-121	1.10	0.0414	15.35	1.42	30	2.045	0.258	0.53	14.75	0.002	1.000	
BS/T-121	2.30	0.3617	14.97	1.59	26	2.060	0.312	0.64	14.75	0.343	2.203	2.20
					Sub-experiment H-122							
N/H-122	0.55	-0.2596	12.02	1.19	27	2.056	0.230	0.47				
N/H-122	1.10	0.0414	16.44	1.34	28	2.052	0.252	0.52	14.25	-0.107	0.781	
BS/H-122	2.10	0.3222	12.96	0.76	18	2.110	0.178	0.38	14.25	+0.431	2.697	3.45
BS/H-122	3.20	0.5051	15.11	0.68	17	2.120	0.165	0.35				
BS/H-122	4.10	0.6128	16.45	0.53	16	2.131	0.132	0.28				

Table C4, Part 1. Data for Experiment 126-127.

Filter	T_e	$\log T_e$	$\bar{D}$	σ	N	$t^{.05}_{(N-1)}$	E	L
				126 M				
671	18.10	1.2577	13.80	0.87	18	2.110	0.204	0.43
671	25.50	1.4065	16.45	0.91	21	2.086	0.198	0.41
680	16.00	1.2041	15.44	1.58	32	2.040	0.278	0.57
689	9.90	0.9956	14.88	1.82	35	2.030	0.306	0.62
696	13.10	1.1173	13.49	1.75	35	2.030	0.294	0.60
701	20.15	1.3043	14.08	1.99	36	2.030	0.330	0.67
707	16.10	1.2068	12.61	2.16	32	2.040	0.380	0.78
715	23.00	1.3617	13.96	2.37	32	2.040	0.417	0.85
722	21.90	1.3404	13.72	2.07	35	2.030	0.349	0.71
731	20.00	1.3010	12.31	1.87	31	2.042	0.334	0.68
741	18.10	1.2577	13.58	2.09	30	2.045	0.382	0.78
741	22.00	1.3424	14.47	1.99	28	2.052	0.374	0.77
				127 M				
671	18.10	1.2577	12.65	1.32	23	2.074	0.273	0.57
671	24.95	1.3971	14.90	1.42	21	2.086	0.309	0.64
680	16.05	1.2054	16.07	1.46	20	2.093	0.325	0.68
689	9.90	0.9956	15.06	1.61	19	2.101	0.370	0.78
696	13.00	1.1139	14.01	1.28	23	2.074	0.266	0.55
701	20.27	1.3069	14.24	1.78	26	2.060	0.347	0.71
707	13.10	1.1173	12.79	1.88	22	2.080	0.401	0.83
707	16.00	1.2041	14.20	1.62	29	2.048	0.300	0.61
715	23.00	1.3617	15.04	1.33	25	2.064	0.264	0.54
715	23.00	1.3617	15.02	1.13	26	2.060	0.221	0.46
722	21.95	1.3414	15.16	1.18	25	2.064	0.234	0.48
731	20.00	1.3010	14.40	1.31	26	2.060	0.256	0.53
741	18.10	1.2577	15.49	1.36	27	2.056	0.260	0.53

Table C4, Part 2. Data for Experiment 126-127.

Filter	$\bar{D}$	Q	T_Q	R	$\bar{D}_A$	Q"	T_Q"	R"
				I26 M				
671	15.50	1.350	22.39	5.81	14.00	1.258	18.11	7.18
680		1.209	16.18	10.60		1.114	13.00	13.19
689		1.035	10.84	10.62		0.941	8.73	13.18
696		1.244	17.54	6.39		1.15	14.13	7.93
701		1.398	25.01	5.76		1.301	20.00	7.20
707		1.385	24.27	4.53		1.291	19.54	5.62
715		1.460	28.83	4.35		1.367	23.28	5.38
722		1.452	28.31	4.15		1.360	22.91	5.13
731		1.500	31.62	4.23		1.409	25.17	5.31
741		1.398	25.01	4.00		1.302	20.05	4.99
				127 M				
671	16.00	1.462	28.97	4.49	14.50	1.370	23.44	5.55
680		1.202	15.92	10.77		1.110	12.88	13.32
689		1.054	11.32	10.17		0.961	9.14	12.59
696		1.238	17.30	6.48		1.147	14.03	7.99
701		1.418	26.18	5.50		1.322	20.99	6.86
707		1.319	20.84	5.27		1.223	16.71	6.58
715		1.421	26.36	4.75		1.329	21.33	5.87
722		1.393	24.71	4.76		1.300	19.95	5.89
731		1.402	25.23	5.30		1.310	20.42	6.55
741		1.290	19.50	5.13		1.198	15.77	6.34

Table C4, Part 3. Data for Experiment 126-127

Filter	$\bar{D}_A{+}L$	Q_+	T_{Q+}	R_+	$\bar{D}_A{-}L$	Q_-	T_{Q-}	R_-
				126 M				
671	15.91	1.380	23.98	5.42	15.09	1.322	20.99	6.20
680	16.07	1.284	19.23	8.92	14.93	1.174	14.93	11.49
689	16.12	1.069	11.72	9.81	14.88	0.996	9.90	11.62
696	16.10	1.286	19.32	5.80	14.90	1.209	16.18	6.93
701	16.17	1.441	27.67	5.22	14.83	1.355	22.64	6.36
707	16.28	1.432	27.04	4.06	14.72	1.338	21.77	5.05
715	16.35	1.523	33.35	3.76	14.65	1.410	25.71	4.87
722	16.21	1.501	32.36	3.63	14.79	1.411	25.77	4.56
731	16.18	1.543	34.91	3.83	14.82	1.461	28.91	4.62
741	16.27	1.448	28.05	3.57	14.73	1.350	22.91	4.36
				127 M				
671	16.64	1.502	31.76	4.09	15.36	1.422	26.43	4.92
680	16.68	1.248	17.70	9.69	15.32	1.162	14.52	11.81
689	16.78	1.101	12.88	8.93	15.22	1.008	10.19	11.29
696	16.55	1.277	18.92	5.93	15.45	1.206	16.07	6.98
701	16.75	1.463	29.04	4.96	15.29	1.370	23.45	6.14
707	16.61	1.356	22.70	4.80	15.39	1.279	19.01	5.78
715	16.46	1.451	28.25	4.44	15.54	1.398	25.01	5.01
722	16.48	1.422	26.42	4.45	15.52	1.367	23.28	5.05
731	16.53	1.439	27.47	4.87	15.47	1.372	23.55	5.68
741	16.53	1.323	21.04	4.75	15.47	1.255	17.98	5.56

Table C5. Part 1. Data for Experiment 126-127.

Filter	T_e	log T_e	$\bar{D}$	σ	N	$t^{(.05)}_{(N-1)}$	E	L
				126 BS				
671	150.15	2.1765	16.96	1.49	32	2.042	0.262	0.53
680	87.95	1.9442	16.32	1.72	26	2.060	0.337	0.69
689	43.05	1.6340	17.05	1.64	42	2.020	0.250	0.51
696	49.10	1.6911	16.92	1.62	40	2.020	0.254	0.51
701	66.00	1.8195	17.21	1.46	44	2.020	0.219	0.44
707	44.90	1.6522	16.14	1.72	41	2.021	0.268	0.54
715	53.00	1.7243	15.82	1.95	41	2.021	0.303	0.61
722	35.00	1.5441	14.72	2.02	44	2.020	0.303	0.61
731	36.10	1.5575	14.42	1.93	44	2.020	0.289	0.58
741	32.00	1.5051	16.00	1.92	42	2.020	0.294	0.59
				127 BS				
671	150.00	2.1761	17.963	0.867	20	2.093	0.192	0.40
680	88.10	1.9450	17.361	1.197	17	2.120	0.289	0.61
689	42.90	1.6325	16.08	1.04	21	2.086	0.225	0.47
696	48.90	1.6893	15.70	0.71	19	2.101	0.161	0.34
701	66.00	1.8195	15.73	0.89	20	2.093	0.197	0.41
707	45.00	1.6532	15.37	1.13	19	2.101	0.258	0.41
715	53.00	1.7243	14.82	1.26	20	2.093	0.281	0.59
722	35.10	1.5453	12.53	1.42	20	2.093	0.316	0.66
722	57.10	1.7566	16.80	1.53	17	2.120	0.371	0.79
731	36.00	1.5563	11.94	1.59	19	2.101	0.364	0.76
731	64.10	1.8069	16.40	1.97	19	2.101	0.452	0.95
741	32.00	1.5051	13.46	1.90	20	2.093	0.337	0.71
741	54.00	1.7324	16.69	1.48	19	2.101	0.424	0.89

Table C5. Part 2. Data for Experiment 126-127.

Filter	$\bar{D}_A$	Q	T_Q	R
		126 BS		
671	16.00	2.118	131.20	0.99
680		1.921	83.37	2.06
689		1.571	37.24	3.09
696		1.635	43.15	2.60
701		1.746	55.71	2.59
707		1.649	44.56	2.47
715		1.737	54.57	2.30
722		1.620	41.69	2.82
731		1.655	45.18	2.96
741		1.505	31.99	3.12
		127 BS		
671	15.50	2.028	106.65	1.21
680		1.831	67.76	2.53
689		1.599	39.72	2.90
696		1.6771	47.53	2.36
701		1.804	63.67	2.26
707		1.666	46.34	2.37
715		1.765	58.21	2.15
722		1.697	49.77	2.36
731		1.760	57.54	2.32
741		1.647	44.36	2.25

276

Table C5. Part 3. Data for Experiment 126-127.

Filter	$\bar{D}_A+L$	Q_+	T_{Q+}	R_+	$\bar{D}_{A-L}$	Q	T_{Q-}	R
				126 BS				
671	16.53	2.152	141.90	0.91	15.47	2.089	122.70	1.05
680	16.69	1.963	91.84	1.86	15.31	1.882	76.20	2.25
689	16.51	1.609	40.65	2.83	15.50	1.549	35.40	3.25
696	16.51	1.669	46.66	2.40	15.49	1.600	39.81	2.81
701	16.44	1.779	60.11	2.39	15.56	1.717	52.12	2.76
707	16.54	1.685	48.42	2.26	15.46	1.612	40.85	2.69
715	16.61	1.772	59.15	2.11	15.39	1.700	50.12	2.50
722	16.61	1.660	45.71	2.57	15.39	1.583	38.28	3.06
731	16.58	1.691	49.09	2.72	15.42	1.620	41.69	3.20
741	16.59	1.543	34.92	2.86	15.41	1.470	29.52	3.39
				127 BS				
671	15.90	2.052	112.75	1.15	15.10	2.010	102.34	1.27
680	16.11	1.871	74.30	2.31	14.89	1.797	62.66	2.74
689	15.97	1.625	42.17	2.72	15.03	1.577	37.75	3.04
696	15.84	1.699	50.00	2.24	15.16	1.653	44.98	2.49
701	15.91	1.832	67.91	2.12	15.09	1.780	60.24	2.39
707	15.91	1.690	48.98	2.24	15.09	1.633	42.95	2.55
715	16.09	1.800	63.10	1.98	14.91	1.729	53.58	2.33
722	16.29	1.742	55.21	2.12	14.71	1.651	44.77	2.62
731	16.45	1.818	65.76	2.03	14.55	1.703	50.47	2.64
741	16.39	1.707	50.93	1.96	14.61	1.581	38.11	2.62

Table C6. Data for Experiment 130-131.

Specimen	T_e	$\log T_e$	$\bar{D}$	σ	N	$t_{(.05)}$ $_{N-1}$	E	L	$\bar{D}_A$	Q	T_Q	F
M/P-131C	1.10	0.0414	14.01	1.67	33	2.0378	0.29	0.59	14.01	0.0414	1.100	
BS/P-131C	2.30	0.3617	12.91	1.45	39	2.0252	0.23	0.47	14.01	0.3860	2.432	2.21
BS/P-131C	2.80	0.4472	16.28	1.30	35	2.0336	0.22	0.45				
M/P-131D	1.10	0.0414	14.08	1.63	46	2.0158	0.24	0.48	14.08	0.0414	1.100	
BS/P-131D	2.30	0.3617	13.49	1.63	32	2.0399	0.29	0.59	14.08	0.3880	2.443	2.22
BS/P-131D	3.20	0.5051	16.15	1.63	30	2.0450	0.30	0.61				
M/P-131E	1.10	0.0414	14.85	1.15	48	2.0137	0.16	0.32	14.85	0.0414	1.100	
BS/P-131E	2.30	0.3617	15.00	1.51	42	2.0200	0.23	0.46	14.85	0.3520	2.432	2.21
BS/P-131E	2.97	0.4728	16.70	1.55	39	2.0252	0.25	0.51				
M/T-131F	1.10	0.0414	13.36	1.05	49	2.0126	0.15	0.30	13.36	0.0414	1.100	
BS/T-131F	2.30	0.3617	11.71	0.99	53	2.0084	0.13	0.26	13.36	0.4490	2.812	2.56
BS/T-131F	3.10	0.4914	14.10	1.23	43	2.0189	0.19	0.38				
M/T-131G	1.10	0.0414	13.22	1.48	44	2.0179	0.22	0.44	13.22	0.0414	1.100	
BS/T-131G	2.60	0.4150	13.33	1.26	35	2.0336	0.21	0.43	13.22	0.4310	2.697	2.45
BS/T-131G	3.20	0.5051	14.02	1.44	36	2.0315	0.24	0.49				
M/T-130	0.95	-0.0223	12.40	1.29	33	2.0378	0.22	0.45	—			
M/T-130	1.61	0.2068	16.07	1.37	40	2.0231	0.21	0.42	14.00	0.0790	1.199	
BS/T-130	2.18	0.3385	11.95	1.67	30	2.0450	0.30	0.61	14.00	0.4620	2.897	2.42
BS/T-130	2.38	0.3766	12.89	1.71	35	2.0336	0.29	0.59				
BS/T-130	2.82	0.4502	13.67	1.39	38	2.0273	0.22	0.45				
M/T-130T	1.10	0.0414	14.49	1.02	36	2.0315	0.17	0.35	14.49	0.0414	1.100	
BS/T-130T	1.90	0.2788	12.31	1.05	39	2.0252	0.17	0.34	14.49	0.3720	2.355	2.14
BS/T-130T	2.82	0.4502	16.95	1.04	46	2.0158	0.15	0.30				
BS/T-130T	3.10	0.4928	16.48	1.03	45	2.0168	0.15	0.30				
M/H-131	1.10	0.0414	12.79	1.26	31	2.0420	0.23	0.47				
M/H-131	1.38	0.1399	15.85	1.12	35	2.0336	0.19	0.39	14.00	0.0820	1.208	
BS/H-131	2.10	0.3222	10.18	1.34	27	2.0560	0.26	0.53	14.00	0.4020	2.523	2.09
BS/H-131	2.40	0.3802	13.36	1.51	28	2.0520	0.28	0.57				
BS/H-131	3.12	0.4942	16.93	1.28	28	2.0520	0.24	0.49				

Table C7. Data for Experiment 130-131.

Experiment	Γ	$\bar{D}_A+\Gamma$	Q_+	T_{Q+}	$\bar{D}_A-\Gamma$	Q_-	T_{Q-}	F_{MAX}	F_{MIN}
N/P-131C	0.59	14.60	0.060	1.15	13.42	0.026	1.06	$\frac{2.50}{1.06}=2.36$	$\frac{2.35}{1.15}=2.04$
BS/P-131C	0.46	14.47	0.398	2.50	13.55	0.371	2.35		
N/P-131D	0.48	14.56	0.065	1.16	13.60	0.022	1.05	$\frac{2.59}{1.05}=2.47$	$\frac{2.31}{1.16}=1.99$
BS/P-131D	0.60	14.68	0.414	2.59	13.48	0.363	2.31		
N/P-131E	0.32	15.17	0.064	1.16	14.53	0.022	1.05	$\frac{2.42}{1.05}=2.30$	$\frac{2.10}{1.16}=1.81$
BS/P-131E	0.49	15.34	0.384	2.42	14.36	0.323	2.10		
N/T-131F	0.30	13.66	0.058	1.14	13.06	0.029	1.07	$\frac{2.90}{1.07}=2.71$	$\frac{2.74}{1.14}=2.40$
BS/T-131F	0.32	13.68	0.462	2.90	13.04	0.437	2.74		
N/T-131G	0.44	13.66	0.062	1.15	12.78	0.023	1.05	$\frac{2.83}{1.05}=2.70$	$\frac{2.58}{1.15}=2.24$
BS/T-131G	0.46	13.68	0.451	2.83	12.76	0.411	2.58		
N/T-130	0.44	14.44	0.162	1.45	13.56	0.052	1.13	$\frac{3.15}{1.13}=2.79$	$\frac{2.69}{1.45}=1.86$
BS/T-130	0.55	14.55	0.498	3.15	13.45	0.429	2.69		
N/T-130T	0.35	14.84	0.060	1.15	14.14	0.027	1.06	$\frac{2.44}{1.06}=2.30$	$\frac{2.29}{1.15}=1.99$
BS/T-130T	0.32	14.81	0.388	2.44	14.17	0.359	2.29		
N/H-131	0.43	14.43	0.095	1.25	13.57	0.069	1.17	$\frac{2.63}{1.17}=2.25$	$\frac{2.43}{1.25}=1.94$
BS/H-131	0.53	14.53	0.420	2.63	13.47	0.386	2.43		

Table C8. Data for Experiment 132-133.

Specimen	T_e	Log T_e	$\bar{D}$	σ	N	$t_{(.05, N-1)}$	E	L	$\bar{D}_A$	Q	T_Q	F
M/D-132A	1.10	0.0414	14.02	1.39	43	2.019	0.211	0.43	14.25	0.053	1.131	2.11
BS/P-132A	2.28	0.3579	14.19	1.21	23	2.074	0.251	0.52	14.25	0.378	2.387	
BS/D-132A	3.10	0.4914	16.21	1.14	23	2.074	0.237	0.49				
M/D-132B	1.10	0.0414	13.08	1.27	47	2.015	0.185	0.37	13.25	0.050	1.122	1.97
BS/D-132B	2.30	0.3617	13.53	1.20	37	2.029	0.197	0.40	13.25	0.345	2.213	
BS/D-132B	2.88	0.4594	15.51	1.13	37	2.029	0.185	0.38				
M/D-132C	1.10	0.0414	11.47	0.98	38	2.027	0.159	0.32	12.00	0.068	1.169	1.91
BS/D-132C	2.35	0.3711	12.41	1.14	34	2.036	0.196	0.40	12.00	0.349	2.233	
M/D-132D	1.10	0.0414	12.05	1.18	40	2.023	0.186	0.38	12.25	0.052	1.127	2.07
BS/D-132D	2.40	0.3802	12.40	0.88	17	2.120	0.214	0.45	12.25	0.369	2.338	
BS/D-132D	2.80	0.4472	13.83	0.98	17	2.120	0.237	0.50				
M/D-132DD	1.10	0.0414	12.81	1.27	24	2.036	0.218	0.44	13.75	0.090	1.230	1.88
BS/D-132DD	2.40	0.3802	13.63	1.44	24	2.069	0.294	0.61	13.75	0.365	2.317	
BS/D-132DD	2.80	0.4472	15.81	1.10	24	2.069	0.225	0.47				
M/D-132E	1.10	0.0414	10.82	0.82	33	2.038	0.142	0.29	11.00	0.051	1.125	2.05
BS/D-132E	2.39	0.3784	11.28	0.85	31	2.042	0.152	0.31	11.00	0.363	2.307	
M/H-133A	1.10	0.0414	14.03	1.19	27	2.056	0.230	0.47	13.75	0.075	1.188	
M/H-133A	1.58	0.1987	15.25	1.18	27	2.056	0.227	0.47				2.09
BS/H-133A	2.10	0.3222	12.57	1.03	23	2.074	0.214	0.44	13.75	0.395	2.483	
BS/H-133A	2.41	0.3820	13.31	1.30	23	2.074	0.272	0.56				
M/H-133C	1.10	0.0414	11.89	1.22	35	2.034	0.207	0.42	12.50	0.101	1.262	
M/H-133C	1.47	0.1673	13.26	1.14	35	2.034	0.192	0.39				2.37
BS/H-133C	2.80	0.4472	11.95	1.24	29	2.048	0.230	0.47	12.50	0.475	2.981	
M/H-133D	1.10	0.0414	11.75	0.94	47	2.015	0.137	0.28	11.00	0.003	1.000	
BS/H-133D	2.39	0.3784	10.02	0.71	25	2.064	0.142	0.29	11.00	0.429	2.683	2.69
M/T-132	1.10	0.0414	14.07	1.28	39	2.025	0.205	0.42	13.75	0.025	1.059	
BS/T-132	2.20	0.3424	12.38	1.71	23	2.074	0.357	0.74	13.75	0.426	2.666	2.52
BS/T-132	2.60	0.4150	13.59	1.81	23	2.074	0.378	0.78				
BS/T-132	2.90	0.4624	14.06	1.57	23	2.074	0.328	0.68				

Table C9. Data for Experiment 132-133.

Specimen	$\bar{L}$	$\bar{\delta}_A + \bar{L}$	Q_+	T_{Q+}	$\bar{\delta}_A - \bar{L}$	Q_-	T_{Q-}	F_{MAX}	F_{MIN}
				Sub-experiment D-132A					
M/D-132A	0.43	14.68	0.076	1.191	13.82	0.032	1.076	$\frac{2.535}{1.076} = 2.36$	$\frac{2.249}{1.191} = 1.89$
BS/D-132A	0.51	14.76	0.404	2.535	13.74	0.352	2.249		
				Sub-experiment D-132B					
M/D-132B	0.37	13.62	0.069	1.172	12.88	0.031	1.074	$\frac{2.338}{1.074} = 2.18$	$\frac{2.109}{1.172} = 1.80$
BS/D-132B	0.39	13.64	0.369	2.338	12.86	0.324	2.109		
				Sub-experiment D-132C					
M/D-132C	0.32	12.32	0.084	1.213	11.68	0.051	1.125	$\frac{2.345}{1.125} = 2.08$	$\frac{2.128}{1.213} = 1.75$
BS/D-132C	0.40	12.40	0.370	2.345	11.60	0.328	2.128		
				Sub-experiment D-132D					
M/D-132D	0.38	12.63	0.073	1.183	11.87	0.033	1.079	$\frac{2.478}{1.079} = 2.30$	$\frac{2.203}{1.183} = 1.86$
BS/D-132D	0.48	12.73	0.394	2.478	11.77	0.343	2.203		
				Sub-experiment D-132DD					
M/D-132DD	0.44	14.19	0.113	1.297	13.31	0.068	1.169	$\frac{2.472}{1.169} = 2.11$	$\frac{2.177}{1.297} = 1.68$
BS/D-132DD	0.54	14.29	0.393	2.472	13.21	0.338	2.177		
				Sub-experiment D-132E					
M/D-132E	0.29	11.29	0.066	1.164	10.71	0.036	1.086	$\frac{2.387}{1.086} = 2.20$	$\frac{2.223}{1.164} = 1.91$
BS/D-132E	0.31	11.31	0.378	2.387	10.69	0.347	2.223		
				Sub-experiment H-133A					
M/H-133A	0.47	14.22	0.099	1.256	13.28	0.051	1.125	$\frac{2.630}{1.125} = 2.34$	$\frac{2.338}{1.256} = 1.86$
BS/H-133A	0.50	14.25	0.420	2.630	13.25	0.369	2.338		
				Sub-experiment H-133C					
M/H-133C	0.41	12.91	0.133	1.358	12.10	0.081	1.205	$\frac{3.162}{1.205} = 2.62$	$\frac{2.831}{1.358} = 2.08$
BS/H-133C	0.47	12.97	0.500	3.162	12.03	0.452	2.831		
				Sub-experiment H-133D					
M/H-133D	0.28	11.28	0.017	1.040	10.72	-0.012	0.973	$\frac{2.773}{0.973} = 2.85$	$\frac{2.594}{1.040} = 2.49$
BS/H-133D	0.29	11.29	0.443	2.773	10.71	0.414	2.594		
				Sub-experiment T-132					
M/T-132	0.42	14.17	0.048	1.117	13.33	0.004	1.000	$\frac{2.931}{1.000} = 2.93$	$\frac{2.443}{1.117} = 2.19$
BS/T-132	0.73	14.48	0.467	2.931	13.02	0.388	2.443		

Table C10, Part 1. Data for Experiment 134-135.

Filter	T_e	$\log T_e$	$\bar{D}$	σ	N	$t^{(.05)}_{N-1}$	E	L
			135BS-Tris					
671	148.10	2.1706	16.53	1.71	18	2.110	0.403	0.85
680M	20.07	1.3025	15.02	1.38	36	2.031	0.230	0.47
680	85.04	1.9296	13.38	1.48	18	2.110	0.350	0.74
680	115.03	2.0608	16.32	1.76	18	2.110	0.415	0.88
689	40.75	1.6101	10.62	2.11	18	2.110	0.521	1.10
689	50.45	1.7028	13.13	2.29	18	2.110	0.539	1.14
695	47.44	1.6762	13.01	2.55	18	2.110	0.600	1.23
701	64.10	1.8069	13.00	2.37	18	2.110	0.558	1.18
709	134.81	2.1297	12.92	2.49	18	2.110	0.586	1.24
715	53.01	1.7244	12.04	2.49	18	2.110	0.588	1.24
722	51.93	1.7155	12.32	2.32	18	2.110	0.550	1.16
731	54.02	1.7326	11.32	2.11	18	2.110	0.496	1.05
741M	27.02	1.4317	14.37	1.47	37	2.029	0.241	0.49
741	55.15	1.7416	11.65	2.17	18	2.110	0.512	1.08

Table C10, Part 2. Data for Experiment 134-135.

Filter	T_e	$\log T_e$	$\bar{D}$	σ	N	$t^{(.05)}_{N-1}$	E	L
				134M-Tris				
671	25.45	1.4057	16.00	1.30	39	2.025	0.209	0.42
680	18.05	1.2565	15.64	1.16	38	2.027	0.187	0.38
689	12.30	1.0899	15.55	1.62	35	2.033	0.273	0.56
696	17.99	1.2551	15.41	1.59	34	2.035	0.272	0.55
701	29.19	1.4652	14.17	1.78	34	2.035	0.304	0.62
709	62.99	1.7993	13.55	1.48	30	2.045	0.270	0.55
715	31.90	1.5038	14.94	1.43	29	2.048	0.266	0.54
722	24.02	1.3806	13.23	1.44	27	2.056	0.278	0.57
722	31.10	1.4928	13.90	1.41	28	2.052	0.266	0.55
731	27.04	1.4320	12.44	1.66	29	2.048	0.308	0.63
731	36.97	1.5678	13.60	1.85	30	2.045	0.338	0.69
741	27.07	1.4325	14.14	1.69	30	2.045	0.308	0.63

Table C10. Part 3. Data for Experiment 134-135.

Filter	$\bar{D}_A$	Q	T_Q	R	$\bar{D}_{A+L}$	Q_+	T_{Q+}	R_+	$\bar{D}_{A-L}$	Q_-	T_{Q-}	R_-
						135BS-Tris						
671	13.00	1.966	92.46	1.41	13.85	2.015	103.52	1.25	12.15	1.917	82.60	1.57
680M	13.00	1.162	15.21	11.28	13.47	1.212	16.27	10.54	12.53	1.158	14.39	11.92
680	13.00	1.885	76.73	2.24	13.81	1.933	85.70	2.00	12.19	1.838	68.87	2.49
689	13.00	1.717	52.12	2.21	14.12	1.782	60.53	1.90	11.88	1.651	44.77	2.57
696	13.00	1.675	47.31	2.37	14.23	1.748	55.98	2.00	11.77	1.604	40.18	2.79
701	13.00	1.807	64.11	2.25	14.18	1.877	75.33	1.91	11.82	1.737	54.57	2.64
709	13.00	2.135	136.50	1.88	14.24	2.207	161.10	1.59	11.76	2.063	115.60	2.22
715	13.00	1.781	60.40	2.07	14.24	1.854	71.45	1.75	11.76	1.709	51.17	2.45
722	13.00	1.755	56.89	2.06	14.16	1.823	66.53	1.76	11.84	1.688	48.76	2.41
731	13.00	1.831	67.76	1.97	14.05	1.892	77.99	1.71	11.95	1.769	58.76	2.28
741M	13.00	1.351	22.44	4.46	13.49	1.380	23.99	4.16	12.51	1.322	20.99	4.76
741	13.00	1.821	66.21	1.51	14.08	1.884	76.56	1.30	11.92	1.758	57.28	1.75
						134M-Tris						
671	14.50	1.316	20.70	6.28	14.92	1.342	21.98	5.91	14.08	1.293	19.63	6.62
680	14.50	1.188	15.42	11.12	14.88	1.211	16.26	10.54	14.12	1.166	14.65	11.70
689	14.50	1.026	10.62	10.83	15.06	1.060	11.48	10.02	13.94	0.995	9.88	11.64
696	14.50	1.201	15.85	7.07	15.05	1.235	17.18	6.52	13.95	1.169	14.76	7.59
701	14.50	1.484	30.48	4.72	15.12	1.520	33.12	4.35	13.88	1.447	27.99	5.14
709	14.50	1.854	71.45	3.58	15.05	1.886	76.92	3.33	13.95	1.822	66.38	3.86
715	14.50	1.477	29.99	4.17	15.04	1.508	32.21	3.89	13.96	1.445	27.87	4.49
722	14.50	1.490	30.90	3.80	15.06	1.523	33.35	3.52	13.94	1.458	28.70	4.09
731	14.50	1.586	38.54	3.46	15.16	1.624	42.08	3.17	13.84	1.549	35.40	3.77
741	14.50	1.452	28.31	3.53	15.13	1.489	30.83	3.24	13.87	1.415	26.00	3.84

Table C11, Part 1. Data for Experiment 134-135.

Filter	T_e	$\log T_e$	$\bar{D}$	σ	N	$t^{(\cdot 05)}_{N-1}$	E	L
				134BS-Tris				
671	128.5	2.1089	15.61	1.88	21	2.086	0.410	0.86
680M	20.15	1.3043	15.27	1.27	35	2.033	0.210	0.43
680	115.05	2.0609	14.89	1.90	21	2.086	0.416	0.87
689	50.53	1.7036	15.21	1.78	21	2.086	0.387	0.81
689	40.90	1.6117	13.62	2.26	21	2.086	0.494	1.03
696	47.46	1.6763	13.38	1.92	21	2.086	0.419	0.87
701	64.00	1.8062	13.90	2.07	21	2.086	0.451	1.13
709	134.78	2.1296	14.97	1.62	21	2.086	0.353	0.74
715	53.02	1.7245	12.90	1.76	21	2.086	0.385	0.80
722	52.04	1.7163	13.06	1.70	21	2.086	0.370	0.77
722	52.04	1.7163	13.10	1.72	21	2.086	0.376	0.78
731	54.09	1.7331	11.54	1.85	21	2.086	0.403	0.84
731	54.09	1.7331	11.62	1.85	21	2.086	0.403	0.84
741	55.0	1.7404	12.48	1.68	21	2.086	0.367	0.77

Table C11, Part 2. Data for Experiment 134-135.

Filter	T_e	log T_e	$\bar{D}$	σ	N	$t_{(.05)}^{N-1}$	E	L
				135-M-Tris				
671	25.46	1.4058	14.79	1.18	35	2.033	0.198	0.40
671	33.20	1.5211	15.92	1.25	35	2.033	0.212	0.43
680	18.10	1.2577	15.07	1.00	36	2.031	0.167	0.34
680	22.94	1.3606	16.19	1.05	31	2.042	0.189	0.39
680BS	85.12	1.9300	13.01	1.55	22	2.080	0.330	0.69
680BS	115.02	2.0608	15.34	1.65	23	2.074	0.344	0.71
689	11.10	1.0453	13.90	1.30	29	2.048	0.241	0.49
689	11.10	1.0453	14.11	1.23	28	2.052	0.232	0.48
689	12.10	1.0828	15.10	1.45	30	2.045	0.264	0.54
696	18.10	1.2577	14.51	1.63	32	2.040	0.287	0.59
701	28.98	1.4621	14.92	1.68	30	2.045	0.307	0.63
709	63.20	1.8007	13.77	1.42	27	2.056	0.270	0.56
715	31.80	1.5024	13.28	1.30	31	2.042	0.233	0.48
722	30.97	1.4910	12.29	1.41	30	2.045	0.258	0.53
731	37.15	1.5700	12.52	1.34	27	2.056	0.258	0.53
741	27.08	1.4327	12.76	1.32	27	2.056	0.255	0.52

Table C11, Part 3. Data for Experiment 134-135

Filter	$\bar{D}_A$	Q	T_Q	R	$\bar{D}_{A+L}$	Q_+	T_{Q+}	R_+	$\bar{D}_{A-L}$	Q_-	T_{Q-}	R_-
						134BS-Tris						
671	13.75	2.001	100.00	1.30	14.61	2.051	112.48	1.16	12.89	1.950	89.13	1.46
680M	13.75	1.216	16.44	10.43	14.18	1.242	17.46	9.82	13.32	1.191	15.53	11.04
680	13.75	1.993	98.40	1.74	14.62	2.043	110.40	1.55	12.88	1.943	87.70	1.96
689	13.75	1.618	41.50	2.77	14.67	1.672	46.99	2.45	12.83	1.565	36.74	3.13
696	13.75	1.696	49.66	2.26	14.62	1.748	55.98	2.00	12.88	1.647	44.36	2.53
701	13.75	1.796	62.51	2.31	14.88	1.863	72.95	1.98	12.62	1.731	53.83	2.68
709	13.75	2.058	114.30	2.24	14.49	2.101	125.90	2.04	13.01	2.015	103.50	2.48
715	13.75	1.775	59.57	2.10	14.55	1.820	66.07	1.90	12.95	1.727	53.34	2.35
722	13.75	1.755	56.89	2.07	14.52	1.800	63.10	1.86	12.98	1.710	51.28	2.29
731	13.75	1.857	71.95	1.86	14.59	1.907	80.71	1.66	12.91	1.803	63.53	2.10
741M	13.75	1.415	26.00	3.85	14.24	1.443	27.73	3.61	13.26	1.386	24.32	4.12
741	13.75	1.813	65.01	1.54	14.52	1.860	72.45	1.38	12.98	1.769	58.75	1.70
						135M-Tris						
671	14.00	1.384	24.21	5.37	14.41	1.408	25.59	5.08	13.59	1.359	22.86	5.89
680	14.00	1.214	16.37	10.48	14.36	1.239	17.34	9.89	13.64	1.193	15.60	11.10
680BS	14.00	1.984	96.39	1.78	14.70	2.025	105.90	1.62	13.30	1.943	87.70	1.96
689	14.00	1.026	10.62	10.84	14.50	1.055	11.35	10.14	13.50	0.998	9.36	11.55
696	14.00	1.229	16.94	6.61	14.59	1.263	18.32	6.12	13.41	1.194	15.63	7.17
701	14.00	1.407	25.53	5.64	14.63	1.444	27.80	5.18	13.37	1.370	23.45	6.14
709	14.00	1.815	65.32	3.93	14.56	1.847	70.30	3.65	13.44	1.781	60.00	4.25
715	14.00	1.544	35.00	3.58	14.48	1.573	37.41	3.35	13.52	1.517	32.88	3.81
722	14.00	1.590	38.91	3.02	14.53	1.622	41.88	2.81	13.47	1.560	36.31	3.24
731	14.00	1.656	45.29	2.95	14.53	1.687	48.64	2.75	13.47	1.626	42.27	3.16
741	14.00	1.504	31.92	3.13	14.52	1.535	34.28	2.92	13.48	1.474	29.78	3.36

Table C12. Data for 139-141.

Filter	T_e	$\log T_e$	$\bar{D}$	σ	N	$t_{(\substack{.05 \\ N-1})}$	E	L	$\bar{D}_A$	Q	T_Q	F'
						Experiment 139						
M/P-680	12.00	1.0792	12.05	1.57	44	2.0179	0.236	0.48	14.00			
M/P-680	14.90	1.1732	15.41	1.43	44	2.0179	0.216	0.44	14.00	1.136	13.68	
M/P-661	60.00	1.7782	13.24	1.13	44	2.0179	0.170	0.34	14.00	1.820	66.08	0.156
M/P-661	90.01	1.9542	17.26	1.10	44	2.0179	0.166	0.34	14.00			
M/P-680	12.01	1.0795	13.46	1.33	42	2.0200	0.205	0.41	14.00			
M/P-680	13.22	1.1212	14.80	1.18	42	2.0200	0.182	0.37	14.00			
M/P-680	14.60	1.1644	15.19	1.46	42	2.0200	0.224	0.45	14.00	1.100	12.59	
M/P-644	1000.05	3.0000	13.50	1.57	42	2.0200	0.242	0.49	14.00	3.022	1052.00	0.011
						Experiment 141						
M/T-680	16.54	1.2186	12.80	1.47	36	2.0315	0.245	0.50				
M/T-680	18.17	1.2593	13.27	1.49	36	2.0315	0.248	0.50				
M/T-680	21.23	1.3269	14.76	1.45	36	2.0315	0.242	0.49				
M/T-680	27.88	1.4453	16.67	1.34	36	2.0315	0.224	0.45	12.50	1.221	16.63	
M/T-644	1250.08	3.0969	12.47	1.40	36	2.0315	0.232	0.47	12.50	3.101	1261.75	0.012
BS/P-680	85.04	1.9296	13.18	2.06	32	2.0399	0.364	0.74				
BS/P-680	99.55	1.9980	14.83	2.17	32	2.0399	0.383	0.78	14.50	1.988	97.26	
BS/P-661	500.15	2.6992	14.80	2.24	32	2.0399	0.395	0.81	14.50	2.683	482.00	0.152
BS/T-680	84.96	1.9292	15.12	1.41	25	2.0640	0.282	0.58	15.50	1.949	88.93	
BS/T-661	480.10	2.6813	16.18	1.46	25	2.0640	0.292	0.60	15.50	2.651	447.70	0.149
M/T-680	16.50	1.2175	14.43	1.29	41	2.0210	0.202	0.41				
M/T-680	18.09	1.2574	15.41	1.27	41	2.0210	0.197	0.40	14.50	1.217	16.48	
M/T-661	83.00	1.9191	14.21	1.28	41	2.0210	0.199	0.40				0.145
M/T-661	104.98	2.0211	16.36	1.27	41	2.0210	0.197	0.40	14.50	1.932	85.50	
BS/T-680	85.19	1.9304	13.92	1.38	20	2.0930	0.309	0.65				
BS/T-680	115.01	2.0607	16.48	1.35	20	2.0930	0.302	0.63	13.50	1.918	82.80	
BS/T-661	450.01	2.6532	13.42	1.60	20	2.0930	0.358	0.75	13.50	2.660	457.10	0.136

Table C13. Data for Experiment 139-141.

Experiment	$\bar{L}$	$\bar{D}_A + \bar{L}$	Q_+	T_{Q+}	$\bar{D}_A - \bar{L}$	Q_-	T_{Q-}	F'_{MAX}	F'_{MIN}
				Experiment 139					
M/P-680	0.46	14.46	1.153	14.22	13.54	1.120	13.18	0.167	0.147
M/P-661	0.34	14.34	1.833	68.08	13.66	1.806	63.98		
M/P-680	0.41	14.41	1.126	13.37	13.59	1.084	12.14	0.012	0.010
M/P-644	0.49	14.49	3.041	1099.00	13.51	3.002	1004.80		
				Experiment 141					
M/T-680	0.49	12.99	1.245	17.58	12.01	1.199	15.83	0.014	0.011
M/T-644	0.47	12.97	3.122	1324.33	12.03	3.080	1202.33		
BS/P-680	0.76	15.26	2.024	105.68	13.74	1.952	89.55	0.179	0.128
BS/P-661	0.81	15.31	2.722	527.30	13.69	2.648	444.60		
BS/T-680	0.58	16.08	1.975	94.40	14.92	1.921	83.38	0.169	0.131
BS/T-661	0.60	16.10	2.679	477.60	14.90	2.623	419.80		
M/T-680	0.41	14.91	1.236	17.22	14.09	1.198	15.78	0.158	0.133
M/T-661	0.40	14.90	1.952	89.55	14.10	1.914	82.04		
BS/T-680	0.64	14.14	1.947	88.53	12.86	1.886	76.92	0.158	0.117
BS/T-661	0.75	14.25	2.695	495.50	12.75	2.625	421.70		

Table C14. Data for Experiment 139-141.

Filter	$\dfrac{R_{126BS}}{R_{127M}}$	$\dfrac{R_{127BS}}{R_{126M}}$	$\dfrac{R_{BS}}{P_M}$	R'' 127 M	R'' 127 BS	R 134 BS	R'' 126 M	R'' 126 BS	R 135 BS
661	$\frac{0.31}{1.68}$ = 0.185	$\frac{0.38}{1.65}$ = 0.230	0.207	2.08	0.43	0.25	2.06	0.43	0.32
671	$\frac{0.99}{4.49}$ = 0.220	$\frac{1.21}{5.81}$ = 0.208	0.214	5.55	1.19	1.30	7.18	1.54	1.41
680	$\frac{2.06}{10.77}$ = 0.191	$\frac{2.53}{10.60}$ = 0.239	0.215	13.32	2.86	1.74	13.19	2.84	2.24
689	$\frac{3.09}{10.17}$ = 0.304	$\frac{2.90}{10.62}$ = 0.273	0.289	12.59	3.64	2.77	13.18	3.81	2.21
696	$\frac{2.60}{6.48}$ = 0.401	$\frac{2.36}{6.39}$ = 0.369	0.385	7.99	3.08	2.26	7.93	3.05	2.37
701	$\frac{2.59}{5.50}$ = 0.470	$\frac{2.26}{5.76}$ = 0.392	0.431	6.86	2.95	2.31	7.20	3.10	2.25
707	$\frac{2.47}{5.27}$ = 0.469	$\frac{2.37}{4.53}$ = 0.523	0.501	6.58	3.30		5.62	2.82	
709						2.24			1.88
715	$\frac{2.30}{4.75}$ = 0.484	$\frac{2.15}{4.35}$ = 0.494	0.489	5.87	2.87	2.10	5.38	2.63	2.07
722	$\frac{2.82}{4.76}$ = 0.592	$\frac{2.36}{4.15}$ = 0.569	0.581	5.89	3.42	2.07	5.13	2.98	2.06
731	$\frac{2.96}{5.30}$ = 0.558	$\frac{2.32}{4.23}$ = 0.548	0.553	6.55	3.62	1.86	5.31	2.94	1.97
741	$\frac{3.12}{5.13}$ = 0.608	$\frac{2.25}{4.00}$ = 0.563	0.586	6.34	3.72	1.54	4.99	2.92	1.51

REFERENCES

1. Allen, C. F., Good, P., Trosper, T., and Park, R. B., Chlorophyll, Glycerolipid and Protein Ratios in Spinach Chloroplast Grana and Stroma Lamellae, Biochem. Biophys. Res. Commun. 48: 907-913 (1972).

2. Andersen, K. S., Bain, J. M., Bishop, D. G. and Smillie, R. M., Photosystem II Activity in Agranal Bundle Sheath Chloroplasts from Zea mays Plant Physiol. 49: 461-466 (1972).

3. Anderson, J. M., Studies with Mesophyll and Bundle Sheath Chloroplasts of C_4-Plants in Chloroplast Fragments: A Discussion of the Biophysical and Biochemical Properties, Gottingen, 1972 (University of Gottingen, Gottingen, 1972), p. 60-67.

4. Anderson, J. M. and Boardman, N. K., Fractionation of the Photochemical Systems of Photosynthesis 1 - Chlorophyll Contents and Photochemical Activities of Particles Isolated from Spinach Chloroplasts, Biochim. Biophys. Acta 112: 403-421 (1966).

5. Anderson, J. M., Boardman, N. K. and Spencer, D., Phosphorylation by Intact Bundle Sheath Chloroplasts from Maize, Biochim. Biophys. Acta 245: 253-258 (1971).

6. Anderson, J. M., Woo, K. C. and Boardman, N. K., Photochemical Systems in Mesophyll and Bundle Sheath Chloroplasts of C_4 Plants, Biochim. Biophys. Acta 245: 398-408 (1971).

7. Anderson, J. M., Woo, K. C. and Boardman, N. K., Photochemical Properties of Mesophyll and Bundle Sheath Chloroplasts from C_4

Plants, in *Photosynthesis and Photorespiration*, edited by Hatch (John Wiley and Sons, Inc., New York, 1971), 353-360.

8. Andrews, T. J. and Hatch, M. D., Properties and Mechanism of Action of Pyruvate Phosphate Dikinase from Leaves, Biochem. J. 114: 117-125 (1969).

9. Andrews, T. J. and Hatch, M. D., Activity and Properties of Ribulose Diphosphate Carboxylase from Plants with the C_4-Dicarboxylic Acid Pathway of Photosynthesis, Phytochemistry 10: 5-9 (1971).

10. Andrews, T. J., Johnson, H. S., Slack, C. R. and Hatch, M. D., Malic Enzyme and Aminotransferases in Relation to 3-Phospho-glycerate Formation in Plants with the C_4-Dicarboxylic Acid Pathway of Photosynthesis, Phytochemistry 10: 2005-2013 (1971).

11. Arnon, D. I., Tsujimoto, H. Y. and McSwain, B. D., Quenching of Chloroplast Fluorescence by Photosynthetic Phosphorylation and Electron Transfer, Proc. Nat. Acad. Sci. U.S.A. 54: 927-934 (1965).

12. Arnzten, C. G., Dilley, R. A. and Crane, F. L., A Comparison of Chloroplast Membrane Surfaces Visualized by Freeze-etch and Negative-staining Techniques, and Ultrastructural Characteri-zation of Membrane Fractions Obtained from Digitonin-treated Spinach Chloroplasts, J. Cell Biol. 43: 16-31 (1969).

13. Arntzen, C. J., Dilley, R. A., Peters, G. A. and Shaw, E. R., Photochemical Activity and Structural Studies of Photosystems Derived from Chloroplast Grana and Stroma Lamellae, Biochim. Biophys. Acta 256: 85-107 (1972).

14. Asada, K. and Takahashi, M., Effect of Potassium Chloride on Photosystem II of Spinach Chloroplasts, in Photosynthesis and Photorespiration, edited by Hatch (John Wiley and Sons, Inc., New York, 1971), 387-393.

15. Avadhani, P. N., Osmond, C. B. and Tan, K. K., Crassulacean Acid Metabolism and the C_4 Pathway of Photosynthesis in Succulent Plants, in Photosynthesis and Photorespiration, edited by Hatch (John Wiley and Sons, Inc., New York, 1971), 288-293.

16. Bailey, J. L., Downton, W. J. S. and Mäsilar, E., The Proteins of Photosystems I and II in Mesophyll and Bundle Sheath Chloroplasts of Sorghum bicolor, in Photosynthesis and Photorespiration, edited by Hatch (John Wiley and Sons, Inc., New York, 1971), 382-386.

17. _____, Optical Interference Filters, Baird-Atomic, Inc., Cambridge, Mass., Technical Data XK-2 and XK-7.

18. Baldry, C. W. (Tate and Lyle Institute, London, England), private communication, October, 1969.

19. Baldry, C. W., Bucke, C. and Coombs, J., Light/Phosphoenolpyruvate Dependent Carbon Dioxide Fixation by Isolated Sugar Cane Chloroplasts, Biochem. Biophys. Res. Commun. 37: 828-832 (1969).

20. Baldry, C. W., Bucke, C. and Coombs, J., Effects of Some Phenoloxidase Inhibitors on Chloroplasts and Carboxylating Enzymes of Sugar Cane and Spinach, Planta 94: 124-133 (1970).

21. Baldry, C. W., Bucke, C. and Coombs, J., Progressive Release of Carboxylating Enzymes during Mechanical Grinding of Sugar Cane Leaves, Planta 97: 310-319 (1971).

22. Baldry, C. W., Coombs, J. and Gross, D., Isolation and Separation of Chloroplasts from Sugar Cane, Z. Pflanzenphysiol. 60: 78-81 (1968).

23. Baldry, C. W., Bucke, C. and Gross, D., Phenols, Phenoloxidase, and Photosynthetic Activity of Chloroplasts Isolated from Sugar Cane and Spinach, Planta 94: 107-123 (1970).

24. Baldry, C. W., Walker, D. A. and Bucke, C., Calvin-Cycle Intermediates in Relation to Induction Phenomena in Photosynthetic Carbon Dioxide Fixation by Isolated Chloroplasts, Biochem. J. 101: 642-646 (1966).

25. Barber, J. and Kraan, G. P. B., Salt-Induced Light Emission from Chloroplasts, Biochim. Biophys. Acta 197: 49:59 (1970).

26. Bassham, J. A., An Introduction to Photosynthesis, UCRL-19425, Nov. 1969.

27. Bassham, J. A., The Control of Photosynthetic Carbon Metabolism, Science 172: 526-534 (1971).

28. Bassham, J. A., Photosynthetic Carbon Metabolism, Proc. Nat. Acad. Sci. U.S.A. 68: 2877-2882 (1971).

29. Bazzaz, M. and Govindjee (University of Illinois, Urbana, Ill.), Personal communication, June, 1971.

30. Bender, M. M., Variations in the $^{13}C/^{12}C$ Ratios of Plants in Relation to the Pathway of Photosynthetic Carbon Dioxide Fixation, Phytochemistry 10: 1239-1244 (1971).

31. Benedict, C. R. and Kohel, R. J., Photosynthetic Rate of a Virescent Cotton Mutant Lacking Chloroplast Grana, Plant Physiol. 45: 519-521 (1970).

32. Ben-Hayyim, G. and Avron, M., Light Distribution and Electron
     Donation in the Z Scheme, Photochem. Photobiol. 14: 389-396
     (1971).

33. Berry, J. A., The B-Carboxylation Pathway of Photosynthesis
     (Ph.D. Thesis) 1970.

34. Berry, J. A., Downton, W. J. S. and Tregunna, E. B., The Photo-
     synthetic Carbon Metabolism of Zea mays and Gomphrena globosa:
     the Location of the CO_2 Fixation and the Carboxyl Transfer
     Reactions, Can. J. Bot. 48: 777-786 (1970).

35. Bisalputra, T., Downton, W. J. S. and Tregunna, E. B., The Dis-
     tribution and Ultra Structure of Chloroplasts in Leaves Differ-
     ing in Photosynthetic Carbon Metabolism, Can. J. Bot. 47: 15-21
     (1969).

36. Bishop, N. I., Photosynthesis: The Electron Transport System of
     Green Plants, Ann. Rev. Biochem. 40: 197-226 (1971).

37. Bishop, D. G., Andersen, K. S. and Smillie, R. M., Incomplete
     Membrane-Bound Photosynthetic Electron Transfer Pathway in
     Agranal Chloroplasts, Biochem. Biophys. Res. Commun. 42: 74-81
     (1971).

38. Bishop, D. G., Andersen, D. S. and Smillie, R. M., Lamellae
     Structure and Composition in Relation to Photochemical Activity,
     in Photosynthesis and Photorespiration, edited by Hatch (John
     Wiley and Sons, Inc., New York, 1971), 372-381.

39. Bishop, D. G., Andersen, K. S. and Smillie, R. M., Photoreduc-
     tion and Oxidation of Cytochrome f in Bundle Sheath Cells of
     Maize, Plant Physiol. 49: 467-470 (1972).

40. Bjorkman, O. and Bauhl, E., Carboxydismutase Activity in Plants with and without B-Carboxylation Photosynthesis, Planta 88: 197-203 (1969).

41. Black, C. C. and Mayne, B. C., P 700 Activity and Chlorophyll Content of Plants with Different Photosynthetic Carbon Dioxide Fixation Cycles, Plant Physiol. 45: 738-741 (1970).

42. Black, C. C. and Mollenhauer, H. H., Structure and Distribution of Chloroplasts and Other Organelles in Leaves with Various Rates of Photosynthesis, Plant Physiol. 47: 15-23 (1971).

43. Boardman, N. K., Physical Separation of the Photosynthetic Photochemical Systems, Proc. Nat. Acad. Sci. USA 56: 586-593 (1966).

44. Boardman, N. K., The Photochemical Systems of Photosynthesis, Adv. in Enzymol. 30: 1-79 (1968).

45. Boardman, N. K., The Photochemical Systems of Photosynthesis, Aust. J. Sci. 32: 36-45 (1969).

46. Boardman, N. K., Physical Separation of the Photosynthetic Photochemical Systems, Annu. Rev. Plant Physiol. 21: 115-140 (1970).

47. Boardman, N. K., The Photochemical Systems in C_3 and C_4 Plants, in Photosynthesis and Photorespiration, edited by Hatch (John Wiley and Sons, Inc., New York, 1971), 309-322.

48. Boardman, N. K., Anderson, J. M., Kahn, A., Thorne, S. W., and Treffry, T. E., Formation of Photosynthetic Membranes during Chloroplast Development, in Autonomy and Biogenesis of Mitochondria and Chloroplasts, (North-Holland, 1970).

49. Boardman, N. K. and Highkin, H. R., Studies on a Barley Mutant Lacking Chlorophyll b, 1. Photochemical Activity of Isolated Chloroplasts, Biochim. Biophys. Acta 126: 189-199 (1966).

50. Boardman, N. K. and Thorne, S. W., Studies on a Barley Mutant Lacking Chlorophyll b, II. Fluorescence Properties of Isolated Chloroplasts, Biochim. Biophys. Acta 153: 448-458 (1968).

51. Boardman, N. K. and Thorne, S. W., Fluorescence Properties of Fragments from Sonicated Spinach Chloroplasts, Biochim. Biophys. Acta 189: 294-297 (1969).

52. Boardman, N. K. and Thorne, S. W., Sensitive Fluorescence Method for the Determination of Chlorophyll a/Chlorophyll b Ratios, Biochim. Biophys. Acta 253: 222-231 (1971).

53. Boardman, N. K., Thorne, S. W. and Anderson, J. M., Fluorescence Properties of Particles Obtained by Digitonin Fragmentation of Spinach Chloroplasts, Proc. Nat. Acad. Sci. USA 56: 586-593 (1966).

54. Brangeon, J., Krivitzky, M. et Bourdu, R., Le Fractionnement des Deux Formes Chloroplastiques des Feuilles de Zea Mays, Photosynthetica 5: 384-388 (1971).

55. Branton, D. and Park, R., Subunits in Chloroplast Lamellae, J. Ultrastruct. Res. 19: 283-303 (1967).

56. Briantais, J. M. and Picaird, M., Immunological Evidences for a Localization of System 1 on the Outside Face and of System II on the Inside Face of the Chloroplast Lamellae, FEBS (Fed. Eur. Biochem. Soc.) Lett. 20: 100-104 (1972).

57. Briggs, L. J. and Shantz, H. L., The Water Requirement of Plants, 1. Investigations in Great Plains, 1910-1911, Bulletin 284, U.S. Dept. of Agriculture, October 16, 1913.

58. Bril, C., Van Der Horst, D. J., Poort, S. R. and Thomas, J. B., Fractionation of Spinach Chloroplasts with Sodium Deoxycholate, Biochim. Biophys. Acta 172: 345-348 (1969).

59. Brown, J. S., Fluorometric Evidence for the Participation of Chlorophyll a-695 in System 2 of Photosynthesis, Biochim. Biophys. Acta 143: 391-398 (1967).

60. Brown, J. S., Absorption and Fluorescence of Chlorophyll a in Particle Fractions from Different Plants, Biophys. J. 9: 1542-1552 (1969).

61. Brown, J. S., Forms of Chlorophyll In Vivo, Annu. Rev. Plant Physiol. 23: 73-86 (1972).

62. Brown, W. V., Leaf Anatomy in Grass Systematics, Bot. Gaz. 119: 170-178 (1958).

63. Bucke, C. and Long, S. P., Release of Carboxylating Enzymes from Maize and Sugar Cane Leaf Tissue during Progressive Grinding, Planta 99: 199-210 (1971).

64. Bulley, N. R. and Tregunna, E. B., Photosynthesis and Photorespiration Rates at the CO_2 Compensation Point, Can. J. Bot. 48: 1271-1276 (1970).

65. Burba, Ivan (Zeiss Microscope, San Francisco Bay Area repairman), private communication, 1970.

66. Burr, G. O. and Kong, L., Photosynthesis and Photorespiration in C_3 and C_4 Plants: Effects of Oxygen, Taiwan Sugar Experiment Station Research Report 7: February, 1972.

67. Butler, W. L., A Far-Red Absorbing Form of Chlorophyll, In Vivo, Arch. Biochem. Biophys. 93: 413-422 (1961).

68. Butler, W. L., Fluorescence, in The Chlorophylls, edited by Vernon, L. P. and Seely, G. R. (Academic Press, New York, 1966).

69. Calvin, M. and Benson, A. A., The Path of Carbon in Photosynthesis, Science 107: 476-480 (1948).

70. Chance, B., Mayer, D. and Legallais, V., A Dual-Wavelength Spectrophotometer and Fluorometer Using Interference Filters, Anal. Biochem. $\underline{42}$: 494-504 (1971).

71. Chang, F. H. and Troughton, J. H., Chlorophyll a/b Ratios in C_3 and C_4 Plants, Photosynthetica $\underline{6}$: 57-65 (1972).

72. Chen, T. M., Brown, R. H. and Black, C. C., Photosynthetic $^{14}CO_2$ Fixation Products and Activities of Enzymes Related to Photosynthesis in Bermudagrass and Other Plants, Plant Physiol. $\underline{47}$: 199-203 (1971).

73. Cho, F. and Govindjee, Low-Temperature (4-77°K) Spectroscopy of Chlorella; Temperature Dependence of Energy Transfer Efficiency, Biochim. Biophys. Acta $\underline{216}$: 139-150 (1970).

74. Chollet, R. and Ogren, W. L., Oxygen Inhibits Maize Bundle Sheath Photosynthesis, Biochem. Biophys. Res. Commun. $\underline{46}$: 2062-2066 (1972).

75. Clayton, R. K., Processes Involving Chlorophylls In Vivo, in The Chlorophylls, edited by L. P. Vernon and G. R. Seeley (Academic Press, New York, 1966), Chapter 19.

76. Clayton, R. K., An Analysis of the Relations between Fluorescence and Photochemistry during Photosynthesis, J. Theoret. Biol. $\underline{14}$: 173-186 (1967).

77. Clayton, R. K., Light and Living Matter, Vol. 1: The Physical Part (McGraw-Hill, Inc., New York, 1970).

78. Cooper, T. G., Filmer, D., Wishnick, M. and Lane, M. D., The Active Species of "CO_2" Utilized by Ribulose Diphosphate Carboxylase, J. Biol. Chem. $\underline{244}$: 1081-1083 (1969).

79. Cooper, T. G., Tchen, T. T., Wood, H. G. and Benedict, C. R., The Carboxylation of Phosphoenolpyruvate and Pyruvate, 1. The Active Species of "CO_2" Utilized by Phosphoenolpyruvate Carboxykinase, Carboxytransphosphorylase, and Pyruvate Carboxylase, J. Biol. Chem. 243: 3857-3863 (1968).

80.   , Corning Glass Filters, Corning Glass Works, Corning, New York, (1970), Bulletin CFG.

81. Criddle, R. S. and Park, L., Isolation and Properties of a Structural Protein from Chloroplasts, Biochem. Biophys. Res. Commun. 17: 74-79 (1964).

82. Das, M. and Govindjee, A Long-Wave Absorbing Form of Chlorophyll a Responsible for the "Red Drop" in Fluorescence at 298°K and the F723 Band at 77°K, Biochim. Biophys. Acta 143: 570-576 (1967).

83. Denius, H. R. and Homann, P. H., The Relation between Photosynthesis, Respiration, and Crassulacean Acid Metabolism in Leaf Slices of Aloe arborescens Mill, Plant Physiol. 49: 873-880 (1972).

84. Downton, W. J. S., Preferential C_4-Dicarboxylic Acid Synthesis, the Post-Illumination CO_2 Burst, Carboxyl Transfer Step and Grana Configurations in Plants with C_4-Photosynthesis, Can. J. Bot. 48: 1795-1800 (1970).

85. Downton, W. J. S., The Chloroplasts and Mitochondria of Bundle Sheath Cells in Relation to C_4 Photosynthesis, in Photosynthesis and Photorespiration, edited by Hatch (John Wiley and Sons, Inc., New York, 1971), 419-425.

86. Downton, W. J. S., Further Evidence for Two Modes of Carboxyl Transfer in Plants with C_4-Photosynthesis, Can. J. Bot. 49: 1439-1442 (1971).

87. Downton, W. J. S., Berry, J. A. and Tregunna, E. B., C_4-Photosynthesis: Non-Cyclic Flow and Grana Development in Bundle Sheath Chloroplasts, Z. Pflanzenphysiol. 63: 194-198 (1970).

88. Downton, W. J. S., Bisalputra, T. and Tregunna, E. B., The Distribution and Ultrastructure of Chloroplasts in Leaves Differing in Photosynthetic Carbon Metabolism, II. Atriplex rosea and Atriplex hastata, Can. J. Bot. 47: 915-919 (1969).

89. Downton, W. J. S. and Pyliotis, N. A., Loss of Photosystem II during Ontogeny of Sorghum Bundle Sheath Chloroplasts, Can. J. Bot. 49: 179-180 (1970).

90. Downton, W. J. S. and Tregunna, E. B., Carbon Dioxide Compensation: Its Relation to Photosynthetic Carboxylation Reactions, Systematics of the Gramineae, and Leaf Anatomy, Can. J. Bot. 46: 207 (1968).

91. Downton, W. J. S., Woo, K. C. and Osmond, C. B., Photosynthetic Processes in Two Types of Chloroplasts from Leaves of C_4-Plants, Proc. Aust. Biochem. Soc. 3: 87 (1970).

92. Drury, K. Susan, The Effect of Certain Environmental Factors on the Structure and Function of Isolated Spinach Chloroplasts (Ph.D. Thesis) University of California, Berkeley, 1968.

93. Duysens, L. N. M., Primary Photosynthetic Reactions in Relation to Transfer of Excitation Energy, Brookhaven Symposia in Biology 19: 71-80 (1966).

94. Duysens, L. N. M. and Sweers, H. E., Mechanisms of Two Photochemical Reactions in Algae as Studied by Means of Fluorescence, in Studies on Microalgae and Photosynthetic Bacteria, Special Issue of Plant Cell Physiology, Tokyo (University of Tokyo Press, 1963), 353-372.

95. Edwards, G. E. and Black, C. C., Isolation of Mesophyll Cells and Bundle Sheath Cells from Digitaria sanguinalis (L.) Scop. Leaves and a Scanning Microscope Study of the Internal Leaf Cell Morphology, Plant Physiol. 47: 149-156 (1971).

96. Edwards, G. E. and Black, C. C., Photosynthesis in Mesophyll Cells and Bundle Sheath Cells Isolated from Digitaria sanguinalis (L.) Scop. Leaves, in Photosynthesis and Photorespiration, edited by Hatch (John Wiley and Sons, Inc., New York, 1971), 153-168.

97. Edwards, G. E., Kanai, R. and Black, C. C., Phosphoenolpyruvate Carboxykinase in Leaves of Certain Plants which Fix CO_2 by the C_4-Dicarboxylic Acid Cycle of Photosynthesis, Biochem. Biophys. Res. Commun. 45: 278-285 (1971).

98. Edwards, G. E., Lee, S. S., Chen, T. M. and Black, C. C., Carboxylation Reactions and Photosynthesis of Carbon Compounds in Isolated Mesophyll and Bundle Sheath Cells of Digitaria sanguinalis (L.) Scop., Biochem. Biophys. Res. Commun. 39: 389-395 (1970).

99. Erixon, K. and Butler, W. L., Destruction of C-550 by Ultraviolet Radiation, Biochim. Biophys. Acta 253: 483-486 (1971).

100. Everson, R. G. and Slack, C. R., Distribution of Carbonic Anhydrase in Relation to the C_4 Pathway of Photosynthesis, Phytochemistry 7: 581-584 (1968).

101. Farineau, J., A Comparative Study of the Activities of Photosynthetic Carboxylation in a C_4 and a Calvin-Type Plant (The Sites of CO_2 Fixation in C_4 Plants), in Photosynthesis and Photorespiration, edited by Hatch (John Wiley and Sons, Inc., New York, 1971) 202-210.

102. Gaffron, H., Photosynthesis, in The Encyclopedia Britannica (Encyclopedia Britannica, Inc., Chicago, 1971), vol. 12, pp. 1002-1007.

103. Gibbs, M., Photophosphorylation and O_2 Evolution: Assessment, in Photosynthesis and Photorespiration, edited by Hatch (John Wiley and Sons, Inc., New York, 1971), 428-429.

104. Gibbs, M., Latzko, E., O'Neal, D., Hew, C., Photosynthetic Carbon Fixation by Isolated Maize Chloroplasts, Biochem. Bio-Phys. Res. Comm. 40: 1356-1361 (1970).

105. Goedheer, J. C., Fluorescence Bands and Chlorophyll a Forms, Biochim. Biophys. Acta 88: 304-317 (1964).

106. Goedheer, J. C., Fluorescence Action Spectra of Algae and Bean Leaves at Room and Liquid Nitrogen Temperatures, Biochem. Bio-Phys. Acta 102: 73-79 (1965).

107. Goldsworthy, A., Comparison of Kinetics of Photosynthetic Carbon Dioxide Fixation in Maize, Sugar Cane and Tobacco, and Its' Relation to Photorespiration, Nature 217: 62 (1968).

108. Goodchild, D. J., Chloroplast Sturcture: Assessment, in Photo-synthesis and Photorespiration, edited by Hatch (John Wiley and Sons, Inc., New York, 1971), 426-427.

109. Goodchild, D. J., The Relationship Between Grana and Stroma Lamellae and Photosystems 1 and 11 in Spinach Chloroplasts, in Photosynthesis and Photorespiration, edited by Hatch (John Wiley and Son, Inc., New York, 1971), 400-405.

110. Goodchild, D. J., and Park, R. B., Further Evidence for Stroma Lamellae as a Source of Photosystem 1 Fractions from Spinach Chloroplasts, Biochim. Biophys. Acta 226: 393-399 (1971).

111. Goodenough, V. W., Armstrong, J. J., and Levine, R.P., Photo-
synthetic Properties of ac-31, a Mutant Strain of Chlamydomo-
nas reinharde Devoid of Chloroplast Membrane Stacking, Plant
Physiol. 44: 1001-1012 (1969).

112. Govindjee, Transformation of Light Energy into Chemical Energy:
Photochemical Aspects of Photosynthesis, Crop Sci. 7: 551-560
(1967).

113. Govindjee, Discussions on Chlorophyll Fluorescence in vivo;
Techniques and Applications, in Chloroplast Fragments: Dis-
cussion of the Biophysical and Biochemical Properties, Gottin-
gen, 1972.

114. Govindjee and Mohanty, P., Chlorophyll a Fluorescence in the
Study of Photosynthesis, Fluorescence News 6: 1-3 (1971).

115. Govindjee, and Papageorgious, G., Chlorophyll Fluorescence
and Photosynthesis: Fluorescence Transients, in Photophysio-
logy, Volume VI, edited by Arthur C. Giese (Academic Press,
Inc., New York, 1971).

116. Govindjee, Papageorgious, G., and Rabinowitch, E., Chlorophyll
Fluorescence and Photosynthesis, in Fluorescence Theory,
Instrumentation and Practice, edited by G. Guilbault (Marcel
Dekker, Inc., New York, 1967), Chapter 12.

117. Govindjee, and Yang, L., Structure of the Red Fluorescence Band
in Chloroplasts, J. Gen. Physiol. 49: 763-780 (1966).

118. Govindjee, R., Govindjee, Lavorel, J., and Briantais, J. M.,
Fluorescence Characteristics of Lyophilized Maize Chloroplasts
Suspended in Buffer, Biochim. Biophys. Acta 205: 361-370 (1970).

119. Gracen, V. E., Hilliard, J. H., and West, H. H., Presence of

Peripheral Reticulum in Chloroplasts of Calvin Cycle Cells, J. Ultrastruct. Res., $\underline{38}$: 262-264 (1972).

120. Graham, D., Hatch, M.D., Slack, C. R., and Smillie, R. M., Light-Induced Formation of Enzymes of the C_4-Dicarboxylic Acid Pathway of Photosynthesis in Detached Leaves, Phytochemistry $\underline{9}$: 521-532 (1970).

121. Haberlandt, G. Physiological Plant Anatomy (Today and Tomorrow Book Agency, New Delhi, 1965).

122. Hall, D. O., Nomenclature for Isolated Chloroplasts, Nat. New Biology $\underline{235}$: 125-126 (1972).

123. Hall, D. O., Edge, H., and Kalina, M., The Site of Ferricyanide Photoreduction in the Lamellae of Isolated Spinach Chloroplasts: A Cytochemical Study. J. Cell. Sci. $\underline{9}$: 289-303 (1971).

124. Hammond, Steven (Photographer), Hammond and Associates, Berkeley, California, 1970.

125. Hart, A. L., and Tregunna, E. B., Some Aspects of Environmental Control of the Photosynthetic Apparatus in Gomphrena globosa, in Photosynthesis and Photorespiration, edited by Hatch (John Wiley and Sons, Inc., New York, 1971), 413-418.

126. Hatch, M. D., Mechanism and Function of the C_4 Pathway of Photosynthesis, in Photosynthesis and Photorespiration, edited by Hatch (John Wiley and Sons, Inc., New York, 1971), 139-152.

127. Hatch, M. D., The C_4-Pathway of Photosynthesis, Biochem. J. $\underline{125}$: 425-432 (1971).

128. Hatch, M. D. and Slack, C. R., Photosynthesis by Sugar Cane Leaves, A New Carboxylation Reaction and the Pathway of Sugar Formation, Biochem. J. $\underline{101}$: 103-111 (1966).

129. Hatch, M. D. and Slack, C. R., A New Enzyme for the Interconversion of Pyruvate and Phosphopyruvate and Its Role in the C_4 Dicarboxylic Acid Pathway of Photosynthesis, Biochem. J. <u>106</u>: 141-146 (1968).

130. Hatch, M. D. and Slack, C. R., NADP-Specific Malate Dehydrogenase and Glycerate Kinase in Leaves and Evidence For Their Location in Chloroplasts, Biochem. Biophys. Res. Commun. <u>34</u>: 589-594 (1969).

131. Hatch, M. D. and Slack, C. R., Studies on the Mechanism of Activation and Inactivation of Pyruvate, Phosphate Dikinase. Biochem. J. <u>112</u>: 549-558 (1969).

132. Hatch, M. D. and Slack, C. R., Photosynthetic CO_2-Fixation Pathways, Annu. Rev. Plant Physiol. <u>21</u>: 141-162 (1970).

133. Hatch, M. D., Slack, C. R., Bull, T. A., Light-Induced Changes in the Content of Some Enzymes of the C_4-Dicarboxylic Acid Pathway of Photosynthesis and Its Effect on Other Characteristics of Photosynthesis, Phytochemistry <u>43</u>: 697-706 (1969).

134. Hatch, M. D., Slack, C. R., Johnson, H. S. Further Studies on a New Pathway of Photosynthetic Carbon Dioxide Fixation in Sugar Cane and Its Occurrence in Other Plant Species, Biochem. J. <u>102</u>: 417-422 (1967).

135. Heath, R. L. and Hind, G., The Role of Chloride Ion in Photosynthesis IV. Studies on the Low Temperature Fluorescence Emission Spectrum, Biochim. Biophys. Acta,<u>180</u>: 414-416 (1969).

136. Hew, C.-S and Gibbs, M., Light-Induced O_2-Evolution, Triphosphopyridine Nucleotide Reduction, and Phosphorylation by Chloroplasts of Maize, Sugar Cane and Sorghum, Can. J. Bot. <u>48</u>: 1265-1269 (1970).

137. Homann, P. H., Fluorescence Properties of Chloroplasts from Manganese Deficient and Mutant Tobacco, Biochim. Biophys. Acta 162: 545-554 (1968).

138. Homann, P. H., Fluorescence Studies on Tobacco Chloroplasts Deficient in Photosystem II, Progress in Photosynthesis Research 1: 932-937 (1969).

139. Homann, P. H., Cation Effects on the Fluorescence of Isolated Chloroplasts, Plant Physiol. 44: 932-936 (1969).

140. Homann, P. H. and Schmid, G. H., Photosynthetic Reactions of Chloroplasts with Unusual Structures, Plant Physiol. 42: 1619-1632 (1967).

141. Homann, P. H., Schmid, G. H., and Gaffron, H., Structure and Photochemistry in Tobacco Chloroplasts, Comparative Biochemistry and Biophysics of Photosynthesis (University of Tokyo Press, Japan, 1968).

142. Huber, W., de Fekete, M.A.R., and Ziegler, H., Enzymes of the Starch Metabolism in Bundle Sheath and Palisade Cells of Zea mays Planta 87: 360-364 (1969).

143. Huzisige, H., Usiyama, H., Kikuti, T., and Azi, T., Purification and Properties of the Photoactive Particle Corresponding to Photosystem II, Plant and Cell Physiol. 10: 441-455 (1969).

144. Ikehara, N. and Uribe, E. G., A pH Dependent Alteration of Photosystem II Activity in Tris-Washed Chloroplasts, FEBS (FED. EUR. Biochem. Soc.) Lett. 9: 321-323 (1970).

145. Ikehara, N. and Uribe, E. G., The Relation of the Alteration of Photosystem II Activity to the Inhibition of Energy Transfer and the Proton Pump in Tris-Washed Chloroplasts, Arch. Biochem. Biophys. 147: 717 (1971).

146. Izawa, S., and Good, N. E., Effects of Salts and Electron Transport on the Conformation of Isolated Chloroplasts. 11. Electron Microscope. Plant Physiol. 41: 544-552 (1966).

147. Jensen, R. G. (University of Arizona, Tucson, Arizona), personal communication, August, 1969.

148. Jensen, R. G. and Bassham, J. A., Photosynthesis by Isolated Chloroplasts, Proc. Nat. Acad. Sci. USA 56: 1095-1101 (1966).

149. Johnson, H. S. and Hatch, M. D., Distribution of the C_4-Dicarboxylic Acid Pathway of Photosynthesis and Its Occurrence in Dicotyledenous Plants, Phytochemistry 7: 375-380 (1968).

150. Johnson, H. S. and Hatch, M. D., The C_4-Dicarboxylic Acid Pathway of Photosynthesis, Biochem. J. 114: 127-134 (1969).

151. Johnson, H. S. and Hatch, M. D., Properties and Regulation of Leaf Nicotinamide-Adenine Dinucleotide, Phosphate-Malate Dehydrogenase and "Malic" Enzyme in Plants with the C_4-Dicarboxylic Acid Pathway of Photosynthesis, Biochem. J. 119: 273-280 (1970).

152. Johnson, H. S., Slack, C. R., Hatch, M. D. and Andrews, T. J., The CO_2 Carrier Between Mesophyll and Bundle Sheath Chloroplasts in C_4 Pathway Species, in Photosynthesis and Photorespiration, edited by Hatch (John Wiley and Sons, Inc., New York, 1971), 189-195.

153. Jones, L. W., Two Quantum-Hit Requirement for Delayed Light Emission from Photosynthetic Green Algae, Proc. Nat. Acad. Sci. USA, 58: 75-80 (1967).

154. Karlstam, B. and Albertsson, P., Isolation of Different Classes of Spinach Chloroplasts by Counter-Current Distribution. A Methodological Study, Biochim. Biophys. Acta 255:

539-552 (1972).

155. Karpilov, Y. S., Photosynthesis in Xerophytes, Academy of
     Sciences, Moldavian SSR 1970.

156. Kirk, J. T. O., Chloroplast Structure and Biogenesis, Annu.
     Rev. of Biochem. 40: 161-196 (1971).

157. Knaff, D. B. and Arnon, D. I., Contrasting Requirements for
     Plastocyanin in the Photooxidation of Chloroplast Cytochromes,
     Biochim. Biophys. Acta 223: 201-204 (1970).

158. _____, Photography through the Microscope, Eastman
     Kodak Co., Rochester, New York, (1966), Publication P-2.

159. _____, Kodak Filters for Scientific and Technical Uses,
     Eastman Kodak Co., Rochester, New York, (1971), Publication
     B-3.

160. _____, Applied Infrared Photography, Eastman Kodak Co.,
     Rochester, New York, 1972, Publication M-28.

161. _____, Ultraviolet and Fluorescence Photography,
     Eastman Kodak Co., Rochester New York, 1970, Publication M-27.

162. _____, Medical Infrared Photography, Eastman Kodak
     Co., Rochester, New York, 1969, Publication N-1.

163. _____, Kodak High Speed Infrared Film 2481 (Estar
     Base), Eastman Kodak Co., Rochester, New York, 1970, Publi-
     cation M-9.

164. Kok, B. and Hoch, G., Spectral Changes in Photosynthesis,
     Light and Life, edited by McElroy, W. D. and Glass, B. (John
     Hopkins Press, Baltimore, 1961).

165. Kortschak, H. P., Hartt, C. E., and Burr, G. E., Carbon
     Dioxide Fixation in Sugarcane Leaves, Plant Physiol. 40:
     209-213 (1965).

166. Kortschak, H. P., Photosynthesis in Sugarcane and Related Species, in Photosynthesis in Sugar Cane, Proceedings of an International Symposium, London, England, June 1968.

167. Kortschak, H. P., Sugar Synthesis in Mesophyll Chloroplasts of Sugarcane, in Photosynthesis and Photorespiration, edited by Hatch (John Wiley and Sons, Inc., New York, 1971), 255-258.

168. Kortschak, H. P. and Nickell, L. G., Calvin-Type Carbon Dioxide Fixation in Sugarcane Stalk Parenchyma Tissue, Plant Physiol. 45: 515-516 (1970).

169. Laetsch, W. M., Chloroplast Specialization in Dicotyledons Possessing the C_4-Dicarboxylic Acid Pathway of Photosynthetic CO_2 Fixation, Amer. J. Bot. 55: 875-883 (1968).

170. Laetsch, W. M., Relationship Between Chloroplast Structure and Photosynthetic Carbon-Fixation Pathways, Sci. Prog. Oxf. 57: 323-351 (1969).

171. Laetsch, W. M., Specialized Chloroplast Structure of Plants Exhibiting the Dicarboxylic Acid Pathway of Photosynthetic CO_2 Fixation, Progress in Photosynthesis Research 1: 36-46 (1969).

172. Laetsch, W. M., Chloroplast Structural Relationships in Leaves of C_4 Plants, in Photosynthesis and Photorespiration, edited by Hatch (John Wiley and Sons, Inc., New York, 1971), 323-349.

173. Laetsch, W. M. and Kortschak, H. P., Chloroplast Structure and Function in Tissue Cultures of a C_4 Plant, Plant Physiol. 49: 1021-1023 (1972).

174. Laetsch, W. M., and Price, I., Development of the Dimorphic

Chloroplasts of Sugar Cane, Amer. J. Bot. 56: 77-87 (1969).

175. Laetsch, W. M., Stetler, D. A., and Vlitos, A. J., The Ultra-structure of Sugar Cane Chloroplasts, Z. Pflanzenphysiol. 54: 472-474 (1966).

176. Latzko, E., Laber, L. and Gibbs, M., Transient Changes in Levels of Some Compounds in Spinach and Maize Leaves, in Photosynthesis and Photorespiration edited by Hatch (John Wiley and Sons, Inc., New York, 1971), 196-201.

177. Leech, R. L., The Isolation of Structurally Intact Chloro-plasts, Biochim. Biophys. Acta 79: 637-639 (1964).

178. Levine, R. P., The Mechanism of Photosynthesis, Sci. Am. 221: 58-70 (1969).

179. Lewanty, Z., Maleszewski, S. and Poskuta, J., The Effect of Oxygen Concentration on ^{14}C Incorporation Into Products of Photosynthesis of Detached Leaves of Maize, Z. Pflanzenphy-siol. 65: 469-472 (1971).

180. Lichtenthaler, H. K., and Park, R. B., Chemical Composition of Chloroplast Lamellae from Spinach, Nature 198: 1070-1072 (1963).

181. Lintilhac,P. M. and Park, R. B., Localization of Chlorophyll in Spinach Chloroplast Lamellae by Fluorescence Microscopy, J. Cell. Bio. 28: 582-585 (1966).

182. Litvin, F. F. and Belyaeva, O. B., Sequence of Photochemical and Dark Reactions in the Terminal Stage of Chlorophyll Bio-synthesis, Photosynthetica 5: 200-209 (1971).

183. Liu, Y. and Black, C. C., Glycolate Metabolism in Mesophyll Cells and Bundle Sheath Cells Isolated from Crabgrass, Digi-taria sanguinalis, (L.) Scop., Leaves, Arch. Biochem. Bio-

phys. $\underline{149}$: 269-280 (1972).

184. Ludlow, C. J. and Park, R. B., Action Spectra for Photosystems 1 and 11 in Formaldehyde Fixed Algae, Plant Physiol. $\underline{44}$: 540-543 (1969).

185. Lüttge, U., A Comparative Study of the Coupling of Ion Uptake to Light Reactions in the Leaves of C_3 and C_4 Plants, in Photosynthesis and Photorespiration, edited by Hatch (John Wiley and Sons, Inc., New York, 1971), 394-399.

186. Lüttge, U., Ball, E. and von Willert, K., A Comparative Study of the Coupling of Ion Uptake to Light Reactions in Leaves of Higher Plant Species Having the C_3 and C_4-Pathway of Photosynthesis, Z. Pflanzenphysiol. $\underline{65}$: 336-350 (1971).

187. Lyttleton, J. W., Use of Colloidal Silica in Density Gradients to Separate Intact Chloroplasts, Anal. Biochem. $\underline{38}$: 227-281 (1970).

188. Lyttleton, J. W., Studies of Chloroplasts from Amaranthus and Maize after Isolation in Aqueous Systems, in Photosynthesis and Photorespiration, edited by Hatch (John Wiley and Sons, Inc., New York, 1971). 232-239.

189. Lyttleton, J. W., Ballantine, J. E. M., and Forde, B. J., Development and Environment Studies on Chloroplasts of Amaranthus Lividus, in Autonomy and Biogenesis of Mitchondria. and Chloroplasts, edited by N. K. Boardman, Anthony W. Linnane, and Robert M. Smillie (North-Holland Publishing Co., Amsterdam-London, 1971), 447-452.

190. Machold, O., Meister, A., and Adler, K., Spectroscopical Characteristics of Electrophoretically Separated Chlorophyll-Protein-Complexes of Photosystems 1 and 11 Derived from

Vicia faba and Chlorella pyrenoidosa, Photosynthetica. 5: 160-165 (1971).

191. Mayne, B. C., Edwards, G. E., and Black, C. C., Light Reactions in C_4 Photosynthesis, in Photosynthesis and Photorespiration. edited by Hatch (John Wiley and Sons, Inc., New York, 1971), 361-371.

192. Mayne, B, C., Edwards, G. E. and Black, C. C., Spectral, Physical, and Electron Transport Activities in the Photosynthetic Apparatus of Mesophyll Cells and Bundle Sheath Cells of Digitaria sanguinalis (L.) Scop. Plant Physiol. 47:600-605 (1971).

193. Menke, W., Structure and Chemistry of Plastids, Annu. Rev. Plant Physiol. 13: 27-44 (1962).

194. Michel, J. M. and Michel-Wolwertz, M. R., On the Fractionation of the Photosynthetic Apparatus of Spinach Chloroplasts, Progress in Photosynthesis Research 1: 115-127 (1969).

195. Michel, J. M., and Michel-Wolwertz, M. R., Fractionation and Photochemical Activities of Photosystems Isolated from Broken Spinach Chloroplasts by Sucrose-Density Gradient Centrifugation, Photosynthetica 4: 146-155 (1970).

196. Mohanty, P., Braun, B. Z., and Govindjee, Fluorescence and Delayed Light Emission in Tris-Washed Chloroplasts, [FEBS (FED. EUR. Biochem. Soc.) LETT], 20: 273-276 (1972).

197. Mohanty, P., Braun, B. Z., Govindjee and Thornber, J. P., Chlorophyll Fluorescence Characteristics of System 1 Chlorophyll a - Protein Complex and System 11 Particles at Room and Liquid Nitrogen Temperatures, Plant and Cell Physiol. 13: 81-91 (1972).

198. Mohanty, P., Mar, T., and Govindjee, Action of Hydroxyla-mine in the Red Algae Porphyridium cruentum, Biochim. Biophys. Acta 253: 213-253 (1971).

199. Mohanty, P., Munday, J. C. and Govindjee, Time-Dependent Quenching of Chlorophyll a Fluorescence From (Pigment) System 11 by (Pigment) System 1 of Photosynthesis in Chlorella, Biochim. Biophys. Acta 223: 198-200 (1970).

200. Mohanty, P., Papageorgious, G., and Govindjee, Fluorescence Induction in Red Algae Porphyridium cruentum, Photochem. Photobiol. 14: 667-682 (1971).

201. Murakami, S. and Packer, L. The Role of Cations in the Organization of Chloroplast Membranes, Arch. Biochim. Biophys. 146: 337-347 (1971).

202. Murata, N., Control of Excitation Transfer in Photosynthesis 1. Light-Induced Change of Chlorophyll a Fluorescence in Porphyridium cruentum. Biochim. Biophys. Acta 172: 242-251 (1969).

203. Murata, N., Control of Excitation Transfer in Photosynthesis 11. Magnesium Ion-Dependent Distribution of Excitation Energy Between Two Pigment Systems in Spinach Chloroplasts, Biochim. Biophys. Acta 189: 171-181 (1969).

204. Murata, N., Control of Excitation Transfer in Photosynthesis. 111. Light-Induced Decrease of Chl_a Fluorescence Related to Photophosphorylation Systems in Spinach Chloroplasts, Biochim. Biophys. Acta 190: 182-191 (1969).

205. Murata, N., Effects of Monovalent Cations on Light Energy Distribution Between Two Pigment Systems of Photosynthesis in Isolated Spinach Chloroplasts, Biochim. Biophys. Acta 226:

422-432 (1971).

206. Murata, N., Nishimura, M., and Takamiya, A., Fluorescence of Chlorophyll in Photosynthetic Systems. 111. Emission and Action Spectra of Fluorescence-Three Emission Bands of Chlorophyll a and the Energy Transfer Between Two Pigment Systems, Biochim. Biophys. Acta 126: 234-243 (1966).

207. Murata, N., Tashiro, H., and Takamiya, A., Effects of Divalent Metal Ions on Chlorophyll a Fluorescence in Isolated Spinach Chloroplasts, Biochim. Biophys. Acta 197: 250-256 (1970).

208. Nathanson, B. and Brody, M., Changes in Fluorescence Spectra of Chloroplasts Induced by a Naturally-Occurring Factor, Photochem. Photobiol. 12: 469-479 (1970).

209. O'Brien, T. P. and Carr, D. J., A Suberized Layer in the Cell Walls of the Bundle Sheath of Grasses, Aust. J. Biol. Sci. 23: 275-287 (1970).

210. Ogawa, T., Vernon, L. P., and Mollenhauer, H. H., Properties and Structure of Fractions Prepared From Anabaena variabilis by the Action of Triton X-100, Biochim. Biophys. Acta 172: 216-229 (1969).

211. Ohki, R. and Takamiya, A., Improvement in Separation of System 1 and System 11 Particles of Photosynthesis Obtained by Digitonin Treatment, Biochim. Biophys. Acta 197: 240-249 (1970).

212. Okayama, S., Fluorescence Yield of Chlorophyll a and Photochemical Activities of Isolated Chloroplasts, Plant and Cell Physiol. 8: 47-59 (1967).

213. O'Neal, D., Gibbs, M. and Peavey, D., Photosynthetic Carbon

Metabolism of Isolated Corn Chloroplasts, in Photosynthesis and Photorespiration, edited by Hatch (John Wiley and Sons, Inc., New York, 1971), 240-245.

214. O'Neal, D., Hew, C. S., Latzko, E., and Gibbs, M., Photosynthetic Carbon Metabolism of Isolated Corn Chloroplasts, Plant Physiol. 49: 607-614 (1972).

215. Osmond, C. B., C_4 Photosynthesis in the Chenopodiacea, Z. Pflanzenphysiol. 62: 129-132 (1970).

216. Osmond, C. B. The Absence of Photorespiration in C_4 Plants: Real of Apparent?, in Photosynthesis and Photorespiration, edited by Hatch (John Wiley and Sons, Inc., New York, 1971), 472-482.

217. Osmond, C. B., Troughton, H. G., and Goodchild, D. J., Physiological, Biochemical and Structural Studies of Photsynthesis and Photorespiration in Two Species of Atriplex, Z. Pflanzenphysiol. 61: 218-237 (1969).

218. Paolillo, D. J., The Three-Dimensional Arrangement of Intergranal Lamellae in Chloroplasts, J. Cell Sci. 6: 243-255 (1970).

219. Paolillo, D. J., and Falk, R. H., The Ultrastructure of Grana in Mesophyll Plastids of Zea mays, Amer. J. Bot. 53: 173-180 (1966).

220. Paolillo, D. J., and Reighard, J. A., On the Relationship Between Mature Structure and Ontogeny in the Grana of Chloroplasts, Can. J. Bot. 45: 773-782 (1967).

221. Park, R. B., in Plant Biochemistry, edited by J. Bonner and J. E. Varner (Academic Press, New York, 1965), Second Edition in Press, Chapter 7, p. 124.

222. Park, R. The Architecture of Photosynthesis, in <u>Biological</u> <u>Ultrastructure</u>: <u>The</u> <u>Origin</u> <u>of</u> <u>Cell</u> <u>Organelles</u>, edited by Patricia J. Harris (Oregon State University Press, 1971).

223. Park, R. B., (Botany Department, University of California, Berkeley), Personal Communication, 1971.

224. Park, R. B., (Botany Department, University of California, Berkeley), Personal Communication, 1972.

225. Park, R. B., and Branton, D., Freeze-Etching of Chloroplasts from Glutaraldehyde-Fixed Leaves, Brookhaven Symposia in Biology <u>19</u>: 341-352 (1966).

226. Park, R. B., and Epstein, S. Metabolic Fractionation of C^{13} and C^{12} in Plants, Plant Physiol. <u>36</u>: 133-138 (1961).

227. Park, R. B. and Pfeifhofer, A. O., The Continued Presence of Quantasomes in Ethylenediaminetetraacetate-Washed Chloroplast Lamellae, Proc. Nat. Acad. Sci. USA <u>60</u>: 337-343 (1968).

228. Park, R. B. and Pfeihofer, A. O., The Effect of Ethylenediaminetetraacetate Washing on the Structure of Spinach Thylakoids, J. Cell Sci. <u>5</u>: 313-319 (1969).

229. Park, R. B. and Pon, N. G., Correlation of Structure with Function in <u>Spinacea</u> <u>oleracea</u> Chloroplasts, J. Mol. Biol. <u>3</u>: 1-10 (1961).

230. Park, R. B. and Sane, P. V., Distribution of Function and Structure in Chloroplast Lamellae, Annu. Rev. Plant Physio. <u>22</u>: 395-429 (1971).

231. Park, T. B., Steinback, K. E., and Sane, P. V., Distribution of Variable Fluorescence Among Subchloroplast Fractions, Biochim. Biophys. Acta <u>253</u>: 204-207 (1971).

232. Paulsen, J. M. and Lane, M. D., Spinach Ribulose Diphosphate

Carboxylase. 1. Purification and Properties of the Enzyme, Biochim. $\underline{5}$: 2350-2357 (1966).

233. Polya, G. M. and Osmond, C. B., Photophosphorylation by Mesophyll and Bundle Sheath Chloroplasts of C_4 Plants, Plant Physiol. $\underline{49}$: 267-269 (1972).

234. Poyton, R. O. and Branton, D., A Multipurpose Microperfusion Chamber, Exptl. Cell Res. $\underline{60}$: 109-114 (1970).

235. Pyliotis, N. A., Woo, K. C., and Downton, W. J. S., Thylakoid Aggregation Correlated with Chlorophyll a/Chlorophyll b Ratio in Some C_4 Species, in Photosynthesis and Photorespiration, edited by Hatch (John Wiley and Sons, Inc., New York, 1971), 406-412.

236. Rabinowitch, E. and Govindjee, Photosynthesis (John Wiley and Sons, Inc., New York, 1969).

237. Racker, E., The Reductive Pentose Phosphate Cycle 1. Phosphoribulokinase and Ribulose Diphosphate Carboxylase, Arch. Biochim. Biophys. $\underline{69}$: 300-310 (1957).

238. Radunz, A., Schmid, G. H., and Menke, W., Antibodies to Chlorophyll and their Reactions with Chloroplast Preparations, Z. Naturforsch. $\underline{266}$: 435-446 (1971).

239. Rhoades, M. M. and Carvalho, A., The Function and Structure of the Parenchyma Sheath Plastids of the Maize Leaf, Bull. Torrey Bot. Club $\underline{71}$: 335-346 (1944).

240. Rosenberg, J. L., The Photochemical Events in Photosynthesis, in Abstracts of the Sixth International Congress of Biochemistry, New York, 1964.

241. Sane, P. V., Goodchild, D. J., and Park, R. B., Characterization of Chloroplast Photosystems I and II Separated by a Non-

Detergent Method, Biochim. Biophys. Acta 216: 162-178 (1970).

242. Sane, P. V. and Park, R. B., Detergent Fractionation of Glutaraldehyde-fixed Spinach Thylakoids, Plant Physiol. 46: 852-854 (1970).

243. Sane, P. V., and Park, R. B., Purification of Photosystem 1 Reaction Centers From Spinach Stroma Lamellae, Biochim. Biophys. Res. Commun. 41: 206-210 (1970).

244. Sane P. V. and Park, R. B., Action Spectra of Photosystem 1 and Photosystem 11 in Spinach Chloroplast Grana and Stroma Lamellae, Biochim. Biophys. Acta 253: 208-212 (1971).

245. Sane, P. V. and Park, R. B., Further Properties of Stroma Lamella Photosystem 1, in Second International Congress on Photosynthesis, Stresa, 1971.

246. Satoh, K., Mechanism of Photoinactivation in Photosynthetic Systems 1V. Light-Induced Changes in the Fluorescence Transient. Plant and Cell Physiol. 12 13-28 (1971).

247. Schmid, G. H., Photosynthetic Capacity and Lamellar Structure in Various Chlorophyll-Deficient Plants, J. Microscopie 6: 485-498 (1967).

248. Schmid, G. and Gaffron, H., Chloroplast Structure and the Photosynthetic Unit, Brookhaven Symposia in Biology 19: 380-392 (1966).

249. Schmid, G. H., and Gaffron, H., Light Metabolism and Chlorophyll-Deficient Tobacco Mutants, J. of Gen. Physiol. 50: 563-582 (1967).

250. Schmid, G. H., and Gaffron, H., Quantum Requirement for Photosynthesis in Chlorophyll-Deficient Plants with Unusual Lamellar Structures, J. of Gen. Physiol. 50: 2131-2144 (1967).

251. Schmid, G. H. and Gaffron, H., Photosynthetic Units, J. Gen. Physiol. 52: 212-239 (1968).

252. Schmid, G. H., Price, M. and Gaffron, H., Lamellar Structure in Chlorophyll-Deficient But Normally Active Chloroplasts, J. Microscopie 5: 205-212 (1966).

253. Schoch, E. and Kramer, D., Korrelation von Merkmalen der C_4-Photosynthese bei vertretern verschiedener Ordnungen der Angiospermen, Planta 101: 51-66 (1971).

254. Sestak, Z., Leaf Age and the Shape of the Red Absorption Band of Maize Chloroplasts, Photosynthetica 6: 75-79 (1972).

255. Shepard, D. C., Levin, W. B. and Bidwell, R. G. S., Normal Photosynthesis by Isolated Chloroplasts, Biochem. Biophys. Res. Commun. 32: 413-420 (1968).

256. Shumway, L. K. and Park, R. B., Light-Dependent Reduction of Some Tetrazolium and Ditetrazolium Salts by Chloroplasts, Exptl. Cell. Res. 56: 29-32 (1969).

257. Silayeva, A. M., The Structure and Possible Function of Chloroplasts of the Sheath Cells of Vascular Bundles, Fiziol. Rast. USSR 13: 623-627 (1966).

258. Slack, C. R., Photoactivation of a Phosphopyruvate Synthese in Leaves of Amaranthus palmeri Biochem.Biophys. Res. Commun. 30: 483-488 (1968).

259. Slack, C. R., Localization of Certain Photosynthetic Enzymes in Mesophyll and Parenchyma Sheath Chloroplasts of Maize and Amaranthus palmeri, Phytochemistry 8: 1387-1391 (1969).

260. Slack, C. R., The C_4 Pathway: Assessment, in Photosynthesis and Photorespiration, edited by Hatch (John Wiley and Sons, Inc., New York, 1971), 297-301.

261. Slack, C. R. and Hatch, M. D., Comparative Studies on the Activity of Carboxylases and Other Enzymes in Relation to the New Pathway of Photosynthetic Carbon Dioxide Fixation Tropical Grasses, Biochem. J. 103: 660-665 (1967).

262. Slack, C. R., Hatch, M. D., and Goodchild, D. J., Distribution of Enzymes in Mesophyll and Parenchyma-Sheath Chloroplasts of Maize Leaves in Relation to the C_4-Dicarboxylic Acid Pathway of Photosynthesis, Biochem. J. 114: 489-498 (1969).

263. Slatyer, R. O., Comparative Photosynthesis, Growth, and Transpiration of Two Species of Atriplex, Planta, Planta 93: 175-189 (1970).

264. Smillie, R.M., Andersen, K. S. and Bishop, D. G., Plastocyanin-Dependent Photoreduction of NADP by Agranal Chloroplasts from Maize, FEBS (FEB. EUR. Biochim. Soc.) LETT. 13: 318-320 (1971).

265. Smillie R. M., Andersen, K. S., Tobin, N. F., Entsch, B. and Bishop, D. G., Nicotinamide Adenine Dinucleotide Phosphate Photoreduction from Water by Agranal Chloroplasts Isolated from Bundle Sheath Cells of Maize, Plant Physiol 49: 471-475 (1972).

266. Smith, F. A., Transport of Solutes During C_4 Photosynthesis Assessment, in Photosynthesis and Photorespiration, edited by Hatch (John Wiley and Sons, Inc., New York, 1971), 302-306.

267. Spencer, D. and Unt, H., Biochemical and Structural Corelations in Isolated Spinaeh Chloroplasts under Isotonic and Hypotonic Conditions, Aust. J. Biol. Sci. 18: 197-210 (1965).

268. Sun, A. S. K. and Sauer, K., Pigment Systems and Electron Transport in Chloroplasts 1. Quantum Requirements for the Two

Light Reactions in Spinach Chloroplasts, Biochim. Biophys. Acta <u>234</u>: 399-414 (1971).

269. Szalay, L., Rabinowitch, E., Murty, N. R., and Govindjee, Relationship Between the Absorption and Emission Spectra and the "Red Drop" in the ACtion Spectra of Fluorescence <u>in Vivo</u>, Biophys. J. <u>7</u>: 137-149 (1967).

270. Takebe, I., Otsuki, Y., and Aoki, S., Isolation of Tobacco and Mesophyll Cells in Intact and Active State, Plant and Cell Physiol. <u>9</u>: 115-124 (1968).

271. Thorne, S. W. and Boardman, N. K., Formation Chlorophyll b and the Fluorescence Properties and Photochemical Activities of Isolated Plastids from Greening Pea Seedlings, Plant Physiol. <u>47</u>: 252-261 (1971).

272. Trebst, A. V., Tsujimoto, H. Y., and Arnon, D. I., Separation of Light and Dark Phases in the Photosynthesis of Isolated Chloroplasts, Native <u>182</u>: 351-355 (1958).

273. Tregunna, E. B., Smith, B. N., Berry, J. A., and Downton, W. J. S., Some Methods for Studying the Photosynthetic Taxonomy of the Angiosperms, Can. J. Bot. <u>48</u>: 1209-1214 (1970).

274. Vernon, L. P. and Ke, B., Photochemistry of Chlorophyll <u>in</u> <u>Vivo</u>, in The <u>Chlorophylls</u>, edited by L. P. Vernon and G. R. Seely (Academic Press, New York, 1966).

275. Virgin, H. I., The Physiology of Chlorophyll Formation in Relationship to Structural Changes in Chloroplasts, Photochem. Photobiol. <u>2</u>: 83-91 (1963).

276. Vredenberg, W. J. and Slooten, L., Chlorophyll a Fluroescence and Photochemical Activities of Chloroplast Fragments, Biochim. Biophys. Acta <u>143</u>: 583-594 (1967).

277. Walker, D. A., Physiological Studies on Acid Metabolism IV. Phosphoenolpyruvic Carboxylase Activity In Extracts of Crassulaccean Plants, Biochem. J. 67: 73-79 (1957).

278. Walker, D. A., CO_2 Fixation: Assessment, in *Photosynthesis and Photorespiration*, edited by Hatch (John Wiley and Sons, Inc., New York, 1971), 294-296.

279. Waygood, E. R., Arya, S. K., and Mache, R., Carbon Dioxide Fixation by Maize Chloroplasts Isolated by the "Laceration Technique", in *Photosynthesis and Photorespiration*, edited by Hatch (John Wiley and Sons, Inc., New York, 1971), 246-254.

280. Waygood, E. R., Mache, R., and Tan, C. K., Carbon Dioxide, The Substrate for Phospho-enolpyruvate Carboxylase from Leaves of Maize, Can. J. Bot. 47: 1455-1458 (1969).

281. Weier, T. E., Stocking, C. R. and Shumway, L. K., The Photosynthetic Apparatus in Chloroplasts of Higher Plants, Brookhaven Symposia in Biology 19: 353-374. (1966)

282. Welkie, G. W. and Caldwell, M., Leaf Anatomy of Species in Some Dicotyledon Families as Related to the C_3 and C_4 Pathways of Carbon Fixation, Can. J. Bot. 48: 2135-2146 (1970).

283. Wessels, J. S. C., Separation of the Two Photochemical Systems of Photosynthesis by Digitonin Fragmentation of Spinach Chloroplasts, Biochim. Biophys. Acta 65: 561-564 (1962).

284. Wild, A., Conrad, G. and Zickler, H., Der Gehalt an Plastidenchinonen und Pigmenten von *Zea mays* und *Atriplex rosea* in Abhangigkeit von der Lichtintensitat und dem alter der Pflanzen, Planta 103: 181-187 (1972).

285. Wolman, M., An Optical Artifact in the Microscopic Study of Fluorescent Materials, Histochemie 21: 5-8 (1970).

286. Woo, K. C., Anderson, J. M., Boardman, N. K., Downton, W. J. S., Osmond, C. B., and Thorne, S. W., Deficient Photosystem II in Agranal Bundle Sheath Chloroplasts of C_4 Plants, Proc. Nat. Acad. Sci. USA 67: 18-25 (1970).

287. Woo, K. C., Pyliotis, N. A., and Downton, W. J. S., Thylakoid Aggregation and Chlorophyll a/Chlorophyll b Ratio in C_4-plants, Z. Pflanzenphysiol. 64: 400-413 (1971).

288. Yamashita, T. and Butler, W. L., Photoreduction and Photophos-phorylation with Tris-Washed Chloroplasts, Plant Physiol. 43: 1978-1986 (1968).

289. Yamashita, T. and Butler, W. L., Inhibition of the Hill Re-action by Tris and Restoration by Electron Donation to Photo-system 11, Plant Physiol. 44: 435-438 (1969).

290. Yamashita, T. and Butler, W. L., Photo-oxidation by Photosys-tem 11 of Tris-Washed Chloroplasts, Plant Physiol. 44: 1342-1346 (1969).

291. Yamashita, T. and Butler, W. L., Electron Donation to Tris-Washed Chloroplasts by Artificial Electron Donors, Prog. Pho-tosyn. Res. 111: 1236-1240 (1969).

292. Yamashita, T., Tsuji-Kaneko, J. and Tomita, G., Reactivation of the Hill Reaction of Tris-Washed Chloroplasts, Plant and Cell Physiol. 12: 117-126 (1971).

293. Yamashita, T., Tsuji-Kaneko, J., Yamada, Y., and Tomita G., Manganese Content, Fluorescence Yields and the Effect of Chloride Ion in Hill REaction Activity of Tris-Washed and Reactivated Chloroplasts, Plant and Cell Physiol. 13: 353-364 (1972).

294. Yao, V. J., Sterling, C., and Stocking, C. R., Specific

Structural Alteration of the Chloroplasts of Spinach Leaves

by Neutral Salts, Physiol. Plant. 26: 191-199 (1972).

295.   , Automatic Photomicrographic Camera, Operating In-

structions, Carl Zeiss, Inc., New York, New York.

296.   , Light Filters for the Microscope, Carl Zeiss, Inc.,

New York, New York.

297.   , Photomicroscopy, Carl Zeiss, Inc., New York, New York.

298.   , Fluorescence Microscopy, Carl Zeiss, Inc., New York,

New York.

299.   , Standard Microscope, Carl Zeiss, Inc., New York, New

York.

300.   , Photomicroscope, Carl Zeiss, Inc., New York, New York.

301. Zelitch, I., Photosynthesis, Photorespiration, and Plant Pro-

ductivity (Academic Press, New York, 1971), Chap. IV.